GEOPHYSICAL FLUID DYNAMICS LABORATORY

Princeton, N.J.

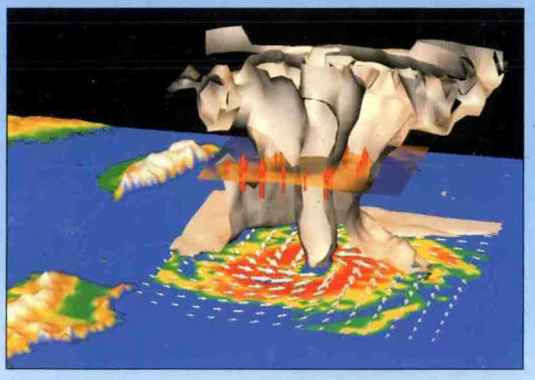

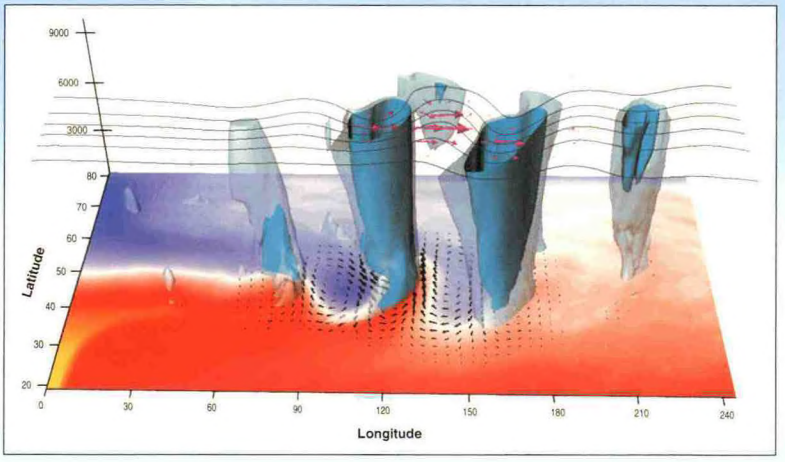

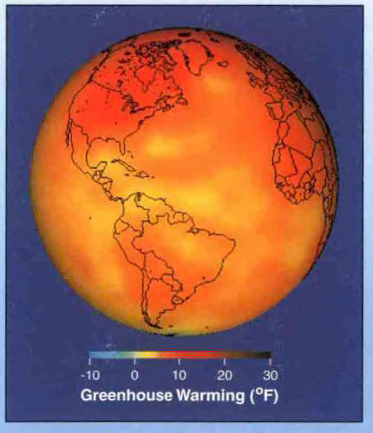

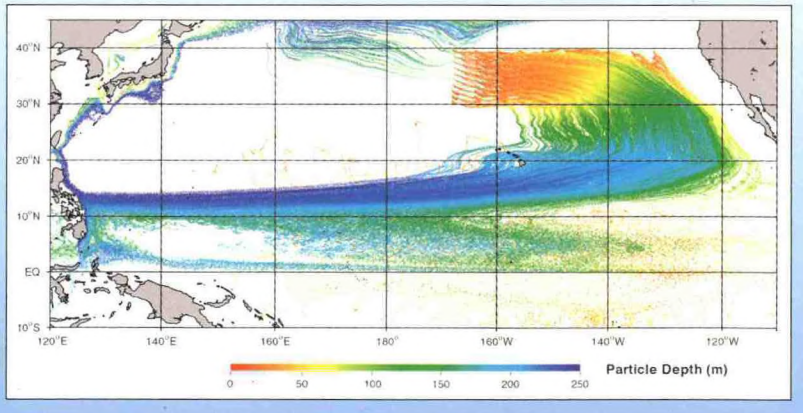

Activities - FY98 / Plans - FY99

U.S. Department of Commerce
National Oceanic and Atmospheric Administration
Environmental Research Laboratories

Front Cover:

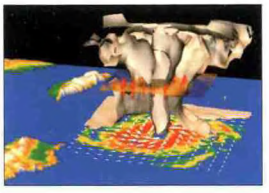

Three-dimensional model view of the simulation of an extremely strong hurricane in a greenhouse-warmed atmosphere. Hurricanes that approach their upper-limit intensity are expected to be slightly stronger in the warmer climate due to the higher sea surface temperatures. In the figure, winds at the surface are indicated by the white arrows, and the color shading at the earth's surface represents the precipitation rate. The grey three-dimensional "cloud-like" feature is the 88% relative humidity surface, cut away on its southern side to reveal the hurricane's interior structure. The horizontal plane and layer of red arrows slicing through the middle of the storm indicates the upward motion in the storm's interior.

(Section 6.3.1)

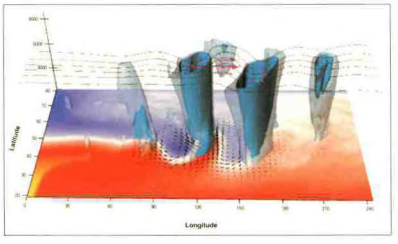

Stages of cyclone evolution within a model-generated storm track. Each stage in a storm's development is depicted by tube-like isosurfaces of cyclonic relative vorticity, complemented by the surface potential temperature (color shading) and flow (black arrows), contours of upper-level geopotential height, and upper-level energy flux vectors (magenta arrows). The vorticity in the westernmost eddy has the westward tilt with height typical of young developing cyclones. As this wave matures, the low level cyclone center moves poleward during its rollup and the upper level center moves equatorward. These features are apparent in the central vortex, which is typical of a mature eddy. Upper level energy fluxes exiting this eddy are quite dispersive with a considerable equatorward component, which produces an upper level disturbance that tends to move equatorward, as shown the third vorticity center. The anticyclonic shear on the equatorward side of the jet shreds the eddy, which breaks anticyclonically.

(Section 7.2.1)

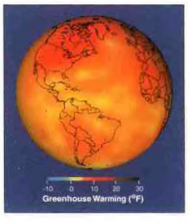

Illustration of the changes in surface air temperature that result from increasing levels of atmospheric carbon dioxide. The colored shading represents the difference in the surface air temperature between a 100-year simulation in which atmospheric carbon dioxide increases at 1% per year from the modern-day level, and a control simulation. Warming is more rapid over the continental regions than over oceanic regions, and is larger in polar regions than at lower latitudes.

(Section 1.3.1)

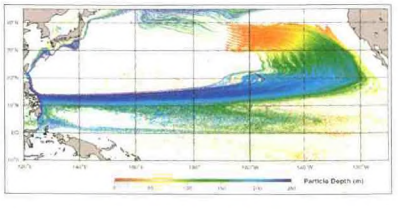

A plot of the trajectories followed by 1000 neutrally-buoyant particles released at the surface in the North Pacific in the GFDL Modular Ocean Model. (Color indicates the depth of the particle in the plot.) The trajectories show that surface waters from the mid-latitudes subduct and flow equatorward below the mixed layer, ventilating the thermocline and maintaining the mean equatorial temperature structure. Energetics studies show that the mean state of the equatorial Pacific is vital in trying to predict the behavior of the Southern Oscillation.

(Section 3.5)

GEOPHYSICAL FLUID DYNAMICS LABORATORY

ACTIVITIES - FY98

PLANS - FY99

OCTOBER 1998

GEOPHYSICAL FLUID DYNAMICS LABORATORY
PRINCETON, NEW JERSEY

UNITED STATES
DEPARTMENT OF COMMERCE

WILLIAM M. DALEY
SECRETARY OF COMMERCE

NATIONAL OCEANIC AND
ATMOSPHERIC ADMINISTRATION

D. JAMES BAKER
UNDERSECRETARY FOR OCEANS
AND ATMOSPHERE

ENVIRONMENTAL
RESEARCH
LABORATORIES

JAMES L. RASMUSSEN
DIRECTOR

NOTICE

Mention of a commercial company or product does not constitute an endorsement by NOAA Environmental Research Laboratories. Use for publicity or advertising purposes of information from this publication concerning proprietary products or the tests of such products is not authorized.

PREFACE

This document summarizes recent research activities at the Geophysical Fluid Dynamics Laboratory (GFDL) and presents a glimpse of the planned direction of this research for the near future. The distribution of this report is intended primarily for GFDL members, Princeton University affiliates, and offices of the National Oceanic and Atmospheric Administration (NOAA), but it is also freely available to other relevant government agencies, national organizations, and interested individuals.

The organization of this document encompasses an overview, project activities and plans for the current and next fiscal year, and appendices. The overview covers highlights of the three major research areas that correspond to Strategic Plan Elements in NOAA's Environmental Assessment and Prediction Portfolio: Advance Short-Term Forecasts and Warnings; Seasonal to Interannual Climate Forecasts; and Predict and Assess Decadal to Centennial Changes, plus a category of topics which cuts across all three time scales: Basic Geophysical Processes. The body of the text describes goals, specific recent achievements, and future plans for the following major research categories: Climate Dynamics; Atmospheric Process; Experimental Prediction; Oceanic Circulation; Planetary Circulations; Climate Diagnostics; Hurricane Dynamics; and Mesoscale Dynamics. These categories, which correspond to the GFDL organization of research groups, are different from the NOAA categories and are far from being mutually exclusive. Interaction occurs among the various groups and is strongly encouraged. The last section of the body is a description of the Laboratory's technical and computational support and its plans for the coming fiscal year.

The appendices contain the following: a list of GFDL staff members and affiliates during Fiscal Year 1998; a bibliography of recent research papers published by staff members and affiliates during their tenure with GFDL (these are referred to in the main body according to the appropriate reference number or letter); a listing of seminars presented at GFDL during Fiscal Year 1998; a list of seminars and talks presented during Fiscal Year 1998 by GFDL staff members and affiliates at other locations; and a list of acronyms.

The editors wish to acknowledge the substantial effort put forth by the GFDL staff and their Princeton University collaborators in preparing this report. Special thanks are extended to all who contributed to this work.

John P. Sheldon, Scientific Editor
Wendy H. Marshall, Technical Editor

September 1998

Geophysical Fluid Dynamics Laboratory/NOAA
P.O. Box 308, Princeton, New Jersey 08542

(609) 452-6500
http://www.gfdl.gov

TABLE OF CONTENTS

AN OVERVIEW

SCOPE OF THE LABORATORY'S WORK

The Geophysical Fluid Dynamics Laboratory is engaged in comprehensive long lead-time research fundamental to NOAA's mission.

The goal of this research is to expand the scientific understanding of the physical processes that govern the behavior of the atmosphere and the oceans as complex fluid systems. These systems can then be modeled mathematically and their phenomenology can be studied by computer simulation methods. In particular, GFDL research concerns the following:

- the predictability of weather on large and small scales;
- the structure, variability, predictability, stability and sensitivity of global and regional climate;
- the structure, variability and dynamics of the ocean over its many space and time scales;
- the interaction of the atmosphere and oceans, and how the atmosphere and oceans influence and are influenced by various trace constituents;
- the Earth's atmospheric general circulation within the context of the family of planetary atmospheric circulations.

The scientific work of the Laboratory encompasses a variety of disciplines including meteorology, oceanography, hydrology, classical physics, fluid dynamics, chemistry, applied mathematics, and numerical analysis. Research is also facilitated by the Atmospheric and Oceanic Sciences Program (AOSP), which is a collaborative program at GFDL with Princeton University. Under this program, regular Princeton faculty, research scientists, and graduate students participate in theoretical studies, both analytical and numerical, and in observational experiments in the laboratory and in the field. The program is supported in part by NOAA funds. AOSP scientists may also be involved in GFDL research through institutional or international agreements.

The following sections describe the GFDL contributions to three major research areas that correspond to Strategic Plan Elements in NOAA's Environmental Assessment and Prediction Portfolio, plus a broader category that supports all three.

HIGHLIGHTS OF FY98

and

IMMEDIATE OBJECTIVES

In this section, some research highlights are listed that may be of interest to those persons less concerned with the intricate details of GFDL research. Selected are items that may be of special significance or interest to this wider audience.

Most of the items in this section have been ordered according to the current NOAA Strategic Plan Elements, which are divided roughly according to time scale:

- Advance Short-Term Forecasts and Warnings
- Seasonal to Interannual Climate Forecasts
- Predict and Assess Decadal to Centennial Changes

Recognizing that much scientific progress has application to phenomena at a wide variety of scales, a number of items have been placed into a category which cuts across the time scales represented by the previous elements:

- Basic Geophysical Processes

This avoids an awkward force-fit of certain topics into a particular time scale and highlights the fundamental role that these topics play as building blocks for progress in multiple research areas.

Note that the categories described above are organized rather differently than the GFDL research project areas presented in the main body of the report. This is but another reflection of the variety and interplay of activities within such a fertile research environment. As an aid in cross-referencing, the number in parentheses following each highlight refers to sections in the main body of the report.

ADVANCE SHORT-TERM FORECASTS AND WARNINGS

The need for short-term warning and forecast products covers a broad spectrum of environmental events which have lifetimes ranging from several minutes up to a month or so. Some examples of these events are tornadoes, hurricanes, tsunamis, and coastal storms, as well as "spells" of unusual weather (warm, cold, wet, or dry). Benefits of these products can be measured in terms of lives saved, injuries averted, and expenses spared. NOAA's vision for improvement in this area involves operational modernization and restructuring, strengthening of observing and prediction systems, and improved applications and dissemination of products and services.

Efforts at GFDL are centered around the development of numerical models which may be used in the prediction of "short-term" atmospheric and oceanic phenomena. Simulations from these models are studied and compared with observed data to aid in the understanding of the processes which govern the behavior of the various phenomena.

With regard to tropical weather systems, efforts are aimed at the genesis, growth, and decay of tropical storms and hurricanes. In extratropical regions, interest includes the development of severe weather systems, the interaction of medium-scale atmospheric flow with that on larger scales, and the influence of the underlying topographic features. Experimental prediction of regional-scale weather parameters weeks to months in advance is being pursued; included in this context is the study of "ensemble forecasting." With regard to the marine environment, forecasts of coastal conditions on a day-to-day basis can be made by coupling of ocean and atmosphere models. Ocean models are also used to simulate coastal bays and estuaries, the response of coastal zones to transient atmospheric storms, and Gulf Stream meanders and rings.

ACCOMPLISHMENTS FY98

Studies of the energy budget of idealized models of radiative-convective equilibrium with resolved moist convection have shown that the dominant source of frictional dissipation in precipitating atmospheres is not the traditional cascade of energy to small scales, but occurs instead in the immediate vicinity of falling hydrometeors. In the global atmosphere this mechanism is estimated to dissipate 1.5 W/m^2, which is comparable to classical estimates of the rate of energy loss from the large-scale atmospheric circulation in the planetary boundary layer (2.2.3).

The GFDL Hurricane Prediction System was upgraded in the 1998 hurricane season. Based on positive test results, the asymmetry of the forecast storm at 12 hours from the preceding forecast cycle is now utilized in the initial storm specification (6.2.3).

Commitment to the WMO-cosponsored COMPARE project was completed with successful application of the GFDL system to the preparation of the initial conditions for a typhoon case study (6.4).

A recently completed study of cyclone wave activity confirms its importance in shaping the large-scale quasi-stationary circulation. It also provides a clear picture of the month-to-month evolution of the storm track during the transition from fall to winter. Consistent with these results, this study also describes the relationship between interannual variability and the ENSO cycle. This may have important implications for the trajectories of winter storms entering the North American continent and improving forecast skill during these events (7.1).

A series of numerical experiments has focused on the life cycle of cyclone-scale eddies in realistic storm track environments. Preliminary analyses of cyclone-scale eddy forcing show encouraging similarities between the velocity correlations that maintain the isolated ridge in the model simulations and the wintertime ridge in the eastern Pacific. These simulations have clarified the mechanisms that predominate in the life cycle of eddies which eventually break anticyclonically, the precursor of establishing the quasi-stationary ridge. This process is strongly interactive since it is the trough-ridge system itself that limits the life cycle of these eddies (7.2).

The hydrostatic terrain-following Zeta model has been used extensively in the ICTP Summer Colloquium on the Physics of Weather and Climate entitled "The Effect of Topography on the Atmospheric Circulation". One outgrowth of this is that the ZETA model is being run at a number of sites worldwide for investigating a wide variety of atmospheric flows (7.4).

PLANS FY99

- The GFDL hurricane model will be improved by increasing the grid resolution of multiply nested meshes. The improved representation of the eye and eyewall of intense hurricanes, as well as of the large-scale environmental flow, should improve both the skill of the GFDL Hurricane Prediction System and accuracy of simulations for numerical research.

- A new methodology will be developed for the initialization of hurricane models in which the initial vortex will be one which is compatible with the environmental conditions. Also, the new scheme will be better able to ingest various types of available data from other observations/analyses.

- The ongoing investigation into the interaction between cyclone wave activity and the large-scale quasi-stationary circulation will be extended to the Southern Hemisphere. Variations in cyclone development at the entrance of the Atlantic-Indian Ocean storm track during the warm and cold phases of the ENSO cycle will be examined. Extended numerical simulations of storm tracks will focus on the mechanisms responsible for the growth, maintenance, and dissipation of the quasi-stationary features in idealized storm tracks.

- Numerical simulations of storm tracks will assess the sensitivity of cyclone evolution to its position within the storm track. In particular, the mechanisms responsible for the poleward progression of low-level eddies and the equatorward progression of upper-level eddies will be further analyzed. The role of cyclone-scale eddies in the growth, maintenance, and

dissipation of the quasi-stationary features in idealized storm tracks will continue to be evaluated.

- The development of limited area models will emphasize the incorporation of moist physics and boundary layer processes into the new, high resolution anelastic hydrostatic and non-hydrostatic models.

SEASONAL TO INTERANNUAL CLIMATE FORECASTS

Seasonal to interannual climate fluctuations have far-reaching consequences for agriculture, fishing, water resources, transportation, energy consumption, and commerce, among others. Short-term climate anomalies which persist from a season to several years affect rainfall distributions, surface temperatures, and atmospheric and oceanic circulation patterns. Reliable climate forecasts may be used to reduce the disruption, economic losses, and human suffering that occur in connection with these anomalies. NOAA's vision for improvement in this area is based on better predictive capability, enhanced observations, greater understanding of climate fluctuations, and assessment of impacts.

The study of seasonal to interannual climate fluctuations at GFDL is based on both theoretical and observational studies. Available observations are analyzed to determine the physical processes governing the behavior of the oceans and atmosphere. Mathematical models are constructed to study, simulate, and predict the coupled ocean-atmosphere, land-surface, sea-ice system.

Simulations based on the numerical models maintained at GFDL, in conjunction with observations, are used to study climate variations on seasonal and longer time scales. Processes under study include large-scale wave disturbances and their role in the general circulation, the effects of boundary conditions such as sea surface temperature and soil moisture, influence of clouds, radiation, and atmospheric convection, and the "teleconnection" of atmospheric anomalies across the global atmosphere. Furthermore, experimental model forecasts are used to evaluate atmospheric predictability and to assess skill in forecasting atmospheric and oceanic climate anomalies, both in general and in connection with the El Niño-Southern Oscillation phenomenon. Also, a more accurate representation of the state of the global ocean is being studied through data assimilation for better initialization of seasonal-interannual forecasts.

ACCOMPLISHMENTS FY98

The tropical intraseasonal oscillations in the R30 atmospheric model have been shown to be very sensitive to the inclusion of a cloud prediction scheme, with some of the effects due to direct interaction of clouds with the oscillation and some due to the change in the structure of the mean tropical atmosphere (1.7.2).

Considerable progress has been made on developing a flexible system for general circulation modeling. Two atmospheric dynamical cores, a B-grid and a spectral model, are essentially complete. Both models have been tested with the same modular physical parameterizations. A flexible framework for coupling component models with arbitrary grids is under development and has been used to create coupled atmosphere-ocean-ice-land surface models (3.1).

A hybrid coupled model with a statistical atmosphere coupled to the MOM ocean general circulation model has been developed. This model provides a powerful and relatively inexpensive framework in which to investigate the impacts of changes to the details of the ocean model. It also provides a good benchmark against which to measure the abilities of more comprehensive coupled prediction models (3.2.2).

A large coupled model ensemble prediction experiment has been conducted to facilitate the investigation of an array of problems in seasonal/interannual prediction and predictability. A set of six 19-year atmospheric simulations and corresponding sets of one year lead coupled model predictions has been produced and formatted for easy analysis (3.3.1).

A series of atmosphere-only GCM simulations has been used to explore the causes of interannual and interdecadal variations in the number of tropical storms over the Atlantic Ocean. On interannual timescales, the primary cause appears to be the impact of tropical Pacific SSTs through an indirect pathway via a modified large-scale atmospheric circulation. On interdecadal timescales, the local tropical Atlantic SST seems to be the major factor impacting the number of Atlantic tropical storms (3.3.2).

A Monte Carlo implementation of a non-linear filter for ensemble data assimilation has been greatly improved. The method has been tested in a variety of low-order models and produced high quality stochastic analyses. Initial tests in global barotropic models suggest that the method may be successfully extended to realistic general circulation models (3.4.1).

An extended suite of experiments on the atmospheric response to sea surface temperature (SST) anomalies in different parts of the World Oceans has been completed using a R30, 14-level climate GCM. This project represents a major commitment of GFDL to the simulation of climate variability using higher-resolution GCMs. The performance of the R30 model is much improved over the earlier R15 version in many respects, including the generation of more realistic precipitation anomalies in response to tropical SST changes, more energetic transient eddies in the middle latitudes, and stronger teleconnections between ENSO-related SST anomalies and the extratropical atmospheric circulation (5.4.1, 5.4.2).

A GCM experiment with interannual SST variations prescribed in the tropical Pacific and with SST changes outside of this forcing region being predicted by a simple mixed-layer ocean model has been analyzed. The results indicate that the remote atmospheric response to the SST anomalies in the tropical Pacific exerts a notable influence on the SST variability in the North Pacific, a large portion of the Atlantic Basin, and parts of the Indian Ocean. These findings illustrate that the "atmospheric bridge" linking the ENSO region with other parts of the

World Oceans is an important contributor to variability of the coupled system on interannual timescales. Considerable agreement exists between the air-sea interactions simulated in this experiment and those inferred from observations (5.4.2).

Satellite observations of temperature, water vapor, precipitation and outgoing longwave radiation have been used to characterize the variation of the tropical hydrologic and energy budgets associated with ENSO. Atmospheric global climate models, forced with observed sea-surface temperatures, accurately reproduced the observed tropospheric temperature, water vapor and outgoing longwave radiation changes. However, the predicted variations in tropical-mean precipitation rate were substantially smaller than observed. The comparison suggests that either the sensitivity of the tropical hydrological cycle to ENSO-driven changes in SST is substantially underpredicted in existing climate models, or that current satellite observations are inadequate to accurately monitor ENSO-related changes in the tropical-mean precipitation (5.2.1).

PLANS FY99

- Modifications to the R30 coupled model will be made, concentrating on a smoother initialization and improved tropical intraseasonal variability. A control integration and various scenario integrations will be initiated with this improved version of the model.

- Complete coupled atmosphere-ocean-ice-land surface models will be constructed in the context of the flexible modeling system. These models will be tested for both climate and seasonal/interannual prediction purposes.

- The newly developed hybrid coupled model will be used to investigate the impact of details of the ocean model on seasonal/interannual prediction. Stochastic forcing will be added to the hybrid model in an attempt to determine the impact of atmospheric noise on the coupled system's dynamics.

- The results of the coupled model ensemble prediction experiment will be analyzed by a number of scientists within GFDL and by members of the GFDL University Consortium. In particular, forecast skill and potential skill will be examined for both tropical and extratropical fields.

- The Monte Carlo non-linear filter data assimilation technique will be applied to the flexible B-grid dynamical core model. If this is successful, further extension to a B-grid model version with realistic physics will be undertaken.

- Multiple experiments with the atmospheric climate GCM coupled to a new mixed-layer ocean model with variable depth will be performed. Particular attention will be devoted to the simulation of the atmospheric and oceanic processes associated with the atmospheric bridge mechanism linking ENSO with SST changes throughout the World Oceans, and the nature of the recurrence of extratropical SST anomalies in consecutive cold seasons.

- The simulated atmospheric circulation changes associated with SST anomalies prescribed in the tropical Atlantic will be analyzed. The mechanisms for the air-sea coupling over the Atlantic will be critically examined using the model output, with special emphasis on the nature of local interactions between the wind field and the underlying SST anomaly, as well as the remote midlatitude atmospheric response to tropical Atlantic SST forcing.

- The relationship between upper tropospheric water vapor and the tropical circulation will be examined on diurnal and seasonal time scales using hourly satellite observations. A tracking algorithm will be applied to analyze the spatial displacement of the patterns of pixel-resolution GOES total precipitable water. Such an application will be used to study the role of moisture transport from the Caribbean Basin and eastern tropical Pacific on precipitation variability over the U.S.

PREDICT AND ASSESS DECADAL TO CENTENNIAL CHANGES

Events such as the Sahel drought, the dust bowls in the Midwest, the Little Ice Age, stratospheric ozone depletion, and global warming may define eras in history. Events such as these have lifetimes of decades to centuries and their causes may be either natural or anthropogenic. An ability to predict such changes and to assess the causes is essential in long-range policy making. Adapting to these changes and reducing the effects of human activities will require enhanced predictive capability. NOAA's vision for improvement in this area is based on a commitment to research in climate and air quality, as well as to insure long-term climate and chemical records.

The related research efforts at GFDL require judicious combinations of theoretical models and specialized observations. The modeling efforts draw on principles from the atmospheric, oceanic, chemical, and biological sciences. One area of focus is long-term climate variability and secular change associated with the atmosphere and oceans. This area encompasses a number of topics, including the effects of changes in the concentration of atmospheric gases such as carbon dioxide, the simulation of past climates, and the variability of the oceanic thermohaline circulation. Another area of focus is the formation, transport, and chemistry of atmospheric trace constituents. This area addresses problems such as: the transport of quasi-conservative trace gases; the biogeochemistry of climatically significant long-lived trace gases; the transport, sources, and sinks of aerosols; the chemistry of ozone and its regulative trace species; the effects of clouds and aerosols on chemically important trace gases; and the impact of anthropogenic chlorofluorocarbons on stratospheric ozone amounts. Yet another area of focus relates to the modeling of the marine environment. It includes the dispersion of geochemical tracers in the world oceans, the oceanic carbon cycle and trace metal geochemistry, and ecosystem structures.

ACCOMPLISHMENTS FY98

A 400-year control integration with a stable climate has been generated with a medium resolution (R30) coupled atmosphere-ocean climate model. The model produces very active ENSO-like variability. The first CO_2+aerosol scenario integrations with this model are

under analysis. Global warming occurs at roughly the same rate as in earlier lower resolution studies (1.3.1).

A 10,000 year control integration of the low resolution, R15 model has been completed which allows climatic variability on time scales up to 1,000 years to be studied. The model generates a singular cooling event in the North Atlantic of several decades duration that is larger in amplitude by a factor of two than any other such events in the entire 10,000 years integration. This result underlines the need for such long integrations in the study of natural climatic variability (1.4.1).

The existence of two stable, climatic equilibria - one with an active Atlantic thermohaline overturning and one in which this overturning is weak and reversed - has been confirmed using a new version of the coupled model. The climate with a weak reversed overturning circulation does not exist if the vertical diffusivity in the model is increased (1.4.2).

An ensemble of nine C02+aerosol scenario integrations of global warming has been completed with the R15 low resolution coupled model. This ensemble has been used to study the emergence of climatic signals from the model's natural variability and to determine the distortions caused by starting the integrations in the late 19th or early 20th centuries, rather than in the pre-industrial era (1.4.3).

The behavior of the R15 coupled model has been simulated by forcing the ocean model in isolation with stochastic heat and freshwater fluxes. Studies of the model's interdecadal variability in the North Atlantic have shown that this variability is not due to coupled air-sea modes, and that the heat fluxes are of greater importance than the freshwater fluxes in generating the coupled model's interdecadal oscillations (1.4.7).

A study of river discharge statistics generated by the R15 CO_2+aerosol scenario integrations suggests that increased frequency of major floods should become significant by the year 2020, but is undetectable at present (1.5.2).

A study with an atmospheric GCM coupled to a mixed layer ocean in the tropics, but with specified surface temperatures in the extratropics, has shown that the effect of cooling in the extratropics of one hemisphere, with respect to the extratropics of the other hemisphere, has a very large effect on the tropical Hadley circulation and the position of the intertropical convergence zone (1.6.1).

A test has been devised, using atmospheric data, to evaluate a method for estimating the diffusivity due to mesoscale eddies in the ocean from altimeter measurements of sea level variability. The results suggest that this method is reliable, implying that altimeter data can be used to constrain eddy flux closure schemes in ocean models (1.7.3).

Sulfate chemistry and transport have been modeled in a high-resolution cloud-system model. Vertical transport of sulfur, nucleation scavenging, and aqueous oxidation result in appreciable sulfate concentrations in upper-tropospheric ice clouds. The presence of sulfate in these clouds alters both their shortwave and longwave radiative properties, exerting an indirect aerosol effect. Earlier studies of indirect effects have focused mostly on boundary-layer clouds and shortwave effects, so these results draw attention to new issues in the cloud-climate problem (2.2.2).

Studies with the cloud-system model have also shown that treatment of ice microphysics and ice radiative transfer plays a central role in both top-of-atmosphere and surface cloud forcing by these systems. Recent observations of the surface radiation balance in the equatorial western Pacific have made possible an evaluation of these important aspects of the cloud-convection-radiation problem (2.2.2).

Simulations of global tropospheric NO_x by the GFDL Global Chemical Transport Model (GCTM) quantitatively capture the observed latitudinal, vertical and seasonal behavior. Detailed analyses of individual natural and anthropogenic sources find that: a) lightning, the primary natural source, dominates in the upper half of the tropical and summertime extratropical troposphere; b) anthropogenic emissions from fossil fuel combustion and biomass burning dominate in the lower half of the troposphere; and c) aircraft emissions have a significant impact on the upper troposphere of the Northern Hemisphere extratropics (2.3.4).

A three-tracer simulation of tropospheric ozone with the GFDL GCTM finds that ozone produced in the background troposphere accounts for 54% of the global tropospheric budget, while ozone transported from the stratosphere accounts for 38%. Ozone directly produced by the complex hydrocarbon photochemistry of the polluted boundary layer plays a minor role outside of that region and only contributes 8% of the global budget (2.3.5).

A control integration using a version of the SKYHI model at 0.33° x 0.4° resolution has continued for over six months. The simulation of the zonal-mean circulation in the extratropical middle atmosphere in this model has been found to be quite realistic over most of the year, even without the inclusion of any parameterized drag on the mean flow (2.4.2). The horizontal spectrum of kinetic energy in this model has been analyzed and found to agree well with available observations (2.4.5).

Simulations using the SKYHI model with enhanced vertical resolution (less than 1 km grid spacing in the stratosphere) display long-period oscillations in the tropical stratospheric mean winds with properties very similar to the observed quasi-biennial oscillation. This represents encouraging progress on a long-standing problem with first-principles simulations of the middle atmospheric circulation (2.5.3).

A long integration has been performed using a moderate-resolution version of the SKYHI model and including a sophisticated treatment of ozone photochemistry. The model displays considerable interannual variability in the circulation and in ozone concentrations. Particularly interesting is the appearance of significant long-period (decadal or longer)

variations in the Northern Hemisphere midlatitudes. These appear with prescribed, seasonally varying SSTs and in the absence of external forcing (such as anthropogenic chemical release, volcanic aerosols, solar variability, etc.) and are apparently driven by internal atmospheric dynamics (2.4.9).

Temperature trends in lower stratosphere are broadly consistent among different datasets, ranging from radiosonde and satellite measurements to analyzed fields. This is particularly so in the midlatitude Northern Hemisphere. Model simulations indicate that the cooling of the lower stratosphere at nearly all latitudes is a consequence of the global ozone depletion (2.5.1).

A simulation of the atmospheric distribution of carbonaceous aerosols from a specified distribution of source strengths has been performed using the SKYHI GCM's tracer transport capability. The aerosols are transported well away from the source regions, both horizontally and vertically. Comparisons with NOAA/CMDL's surface observations at Sable Island and Bondville indicate that the seasonal simulations at these sites compare reasonably well with the measurements (2.3.6).

Benchmark computations reveal that the total solar flux absorbed in overcast atmospheres differs from that in clear-sky. It depends crucially on cloud type, geometrical thickness and location. The benchmark results disagree with recent interpretations from observations concerning both the magnitude and apparent invariance of cloud absorption. This suggests that either the observational inferences are incorrect or the known fundamental radiative transfer principles are at odds with the process in the actual atmosphere (2.1.2).

A new shortwave radiation parameterization has led to a pronounced improvement in the simulation of the stratospheric temperatures, primarily due to a more proper accounting of the solar absorption by CO_2. The warming of the stratosphere due to an increase in the absorption by CO_2 directly alleviates a bias seen in earlier model simulations when compared against recent satellite observations (2.1.3).

The radiative forcing due to tropospheric sulfate (negative) and soot (positive) aerosols, and tropospheric ozone (positive) all have a geographical distribution that is maximized near the source regions in the continental midlatitude Northern Hemisphere. The sum of the forcings due to these three inhomogeneously distributed species has an interesting cancellation in the global-mean, but substantial gradients exist on the regional scale, consisting of positive and negative values, especially in the midlatitude Northern Hemisphere (2.5.2).

Considerable progress has been made on developing a flexible system for general circulation modeling. Two atmospheric dynamical cores, a B-grid and a spectral model, are essentially complete. Both models have been tested with the same modular physical parameterizations. A flexible framework for coupling component models with arbitrary grids is under development and has been used to create coupled atmosphere-ocean-ice-land surface models (3.1).

A series of atmosphere-only GCM simulations has been used to explore the causes of interannual and interdecadal variations in the number of tropical storms over the Atlantic Ocean. On interannual timescales, the primary cause appears to be the impact of tropical Pacific SSTs through an indirect pathway via a modified large-scale atmospheric circulation. On interdecadal timescales, the local tropical Atlantic SST seems to be the major factor impacting the number of Atlantic tropical storms (3.3.2).

An idealized coupled model has been developed which demonstrates that the Atlantic Ocean's meridional overturning circulation can be initiated simply by opening Drake Passage. This result suggests that the formation of deep water in the North Atlantic and the northward heat transport in the Atlantic Ocean are linked to the Antarctic Circumpolar Current in the high latitudes of the Southern Hemisphere (4.1.1).

Results from a new isopycnal-coordinate ocean model indicate that the ocean's density structure is dynamically consistent with low levels of vertical mixing in the open ocean. The warming branch of the thermohaline circulation occurs mainly through wind-driven upwelling in the Southern Ocean and at the equator (4.1.2).

A new sea-ice model has been developed for coupled models. Sea-ice motion in the new model is a product of internal stresses within the ice, in addition to the motions forced by the wind and underlying ocean currents (4.1.3).

A new study of terrestrial and oceanic carbon sinks shows that the North American continent is a significant sink for atmospheric CO_2. The North American terrestrial sink is at least 2/3 of the total terrestrial sink for the Northern Hemisphere and is comparable in magnitude to fossil fuel emissions from North America (4.4.1).

The impact of climate warming on hurricane intensities was investigated using the GFDL hurricane model embedded in a CO_2-induced warm climate derived from the GFDL climate model. For a sea surface temperature increase of about 2.2°C, storms in the northwest Pacific basin were stronger by 3-7 m/s for the surface wind and deeper by 7-20 hPa (6.3.1).

PLANS FY99

- Several R30 coupled climate model CO_2+aerosol scenario integrations will be analyzed to assess the robustness of the climate changes predicted by earlier R15 simulations, with a focus on changes in oceanic circulation.

- An ensemble of R15 scenario integrations will undergo detailed analysis to study the emergence of a variety of climatic signals from the noise of natural variability. The number of members in the ensemble will be increased as needed for this study.

- New versions of the coupled model will be used to study various alternative approaches to the initialization of coupled models for studies of global warming and natural variability.

- The dynamics of the changes in the position and strength of the Southern Hemisphere surface westerlies, produced in a number of global warming simulations, will be studied with a hierarchy of models aimed at clarifying the relationships between changes in meridional temperature gradients and changes in the zonal mean surface winds.

- The R15 atmospheric model, coupled to a mixed layer, will be use to simulate the last 120,000 years of climate history, as forced by prescribed changes in orbital parameters, ice sheets, and greenhouse gas concentrations, by accelerating the evolution of these forcing functions by a factor of 30.

- Working within the new GFDL atmospheric modeling structure, a new T42, 30 level model will be coupled to the MOM3 ocean code using the recently designed coupling software, and tests will be performed on alternative parameterizations of atmospheric physics. New ice and land surface models will be incorporated into this structure as well. A T106 version of the atmospheric model will be developed simultaneously.

- New approaches to ice microphysics and radiative transfer will be implemented in the cloud-system model and evaluated using both surface and top-of-atmosphere observations of radiative fluxes. This should improve our understanding of the role of deep convective systems in the coupled ocean-atmosphere system.

- The chemical and transport mechanisms involved in generating interannual variability in SKYHI ozone photochemistry simulations will be analyzed.

- Computations and analyses of solar radiative benchmark computations for more complex cloud systems, including multi-layered clouds, will be continued. Additionally, longwave benchmarks will be started, for the purpose of developing parameterizations for non-gray absorbers in the thermal infrared.

- Investigation of the chemistry-transport problem leading to the geographical distribution of various kinds of aerosols will continue. Plans call for the simulation of the transport of sulfate aerosols, to be followed by dust, organics and sea-salt. Also, the problems associated with stratospheric aerosol distribution following volcanic events will be pursued, and the accompanying radiative impacts will be evaluated. Climatic effects of radiative forcing due to non-well-mixed trace gases in the troposphere and stratosphere will also be investigated.

- Aerosol-cloud interactions will continue to be investigated from a host of microphysically- and chemically-based perspectives, from micro-scale models to cloud-

resolving models to GCMs. Observational data will be utilized to test and analyze the model simulations.

- Convection-cloud-radiation-climate interactions will be pursued using the cloud resolving model and the laboratory's GCMs. Emphasis will include examination of available observational data on water vapor, clouds and the energy budget in order to test, evaluate and develop each of the physical components that govern these interactions and thus play a role in climate. Additionally, the influence of these interactions for the maintenance of present-day climate and for future climate change will be investigated.

- Temperature trends in the entire stratosphere (extending to the middle and upper stratosphere) derived from observational data will be analyzed. Model simulations will be performed to extend the detection-attribution investigation to the entire stratosphere. Both natural and anthropogenic factors will be considered.

- Complete coupled atmosphere-ocean-ice-land surface models will be constructed in the context of the flexible modeling system. These models will be tested for both climate and seasonal/interannual prediction purposes.

- The interannual variability of oceanic and terrestrial CO_2 uptake will be studied using a new time-varying inverse model for atmospheric carbon sinks. An inverse model will also be applied to the study of steady state fluxes of CO_2 and oxygen between the ocean and atmosphere.

BASIC GEOPHYSICAL PROCESSES

A number of the research topics at GFDL cut across the various time scales characteristic of each of the foregoing sections. Progress on these topics impacts many other research areas which depend critically on the successful representation of numerous lower-level processes which are common to problems at all scales. Topics which fall into this category include hydrological processes, radiative transfer (including the effects of aerosols and clouds), cloud prediction/specification, "teleconnection" of atmospheric anomalies across the global atmosphere, satellite data interpretation, transport processes, gravity wave effects and parameterization, model resolution effects, and many other model enhancement efforts. As these processes become better understood and more accurately represented, benefits will accrue to a multitude of other research efforts.

ACCOMPLISHMENTS FY98

A tool designed to facilitate conversions of models to scalable parallel architectures is under development. A version of the flexible spectral dynamical core has been parallelized using this tool and has demonstrated reasonable performance on parallel platforms (3.1.1.4).

A series of experiments with coupled general circulation models identified a number of shortcomings in the convective and cloud parameterizations in the experimental prediction models. New versions of the Relaxed Arakawa Schubert convection scheme in concert with modifications to the cloud parameterization have led to improved simulations at both the surface and in the upper troposphere (3.2.1).

A new version of GFDL's Modular Ocean Model (MOM 3) has been made available for testing. This version contains an upgrade which allows MOM to be run efficiently on the next generation of parallel computers (4.2.1).

A combination of high-resolution numerical and analytical models have been used to estimate the total mountain drag exerted by the Rocky Mountains down to horizontal scales of 20 km. For summertime flow conditions, fine-resolution numerical experiments indicate that most of the momentum flux reaching the stratosphere is due to linear, hydrostatic gravity waves launched by the smallest resolved terrain features which occur primarily at the upstream and downstream edges of the massif. The parameterized subgrid drag and divergent surface velocity from a coarse resolution experiment are in good agreement with the high-resolution result (7.3).

PLANS FY99

- The spectral kinetic energy budget in high-resolution SKHYI model simulations will be analyzed to determine the dominant excitation and dissipation mechanisms. Such analysis may have implications for designing appropriate subgrid-scale closure schemes for climate and weather models.

- A scalable version of the flexible spectral dynamical core will be improved and a scalable version of the B-grid flexible dynamical core will be written. Work will begin on understanding the problem of parallelizing coupled models.

- New representations of boundary layers at the bottom of the ocean will be implemented in both z-coordinate and isopycnal coordinate models at GFDL.

- GCMs and limited-area model simulations with very high resolutions and realistic temporal and spatial variations of the basic flow will be used to test the linear model of total mountain drag.

PROJECT ACTIVITIES FY98

PROJECT PLANS FY99

1. CLIMATE DYNAMICS

GOALS

To construct mathematical models of the atmosphere and of the coupled ocean-atmosphere system which simulate the global large-scale features of climate.

To study the dynamical interaction between large-scale wave disturbances and the general circulation of the atmosphere.

To identify and elucidate the physical and dynamical mechanisms which maintain climate and cause its variation, and to examine their generality in the context of paleoclimate and the atmospheres of other planets.

To evaluate the impact of human activities on climate.

1.1 BACKGROUND FOR COUPLED CLIMATE MODELING AT GFDL

Two distinct coupled atmosphere-ocean climate models are actively being used in research on global warming and other aspects of climatic sensitivity and variability. This section summarizes the general characteristics of these models and the design of some key experiments using these models.

A low resolution model has provided the basis for much of GFDL's global warming, paleoclimate, and low-frequency variability research for over a decade and continues to yield new insights. This model consists of an R15 atmosphere (with a 7.5° longitude by 4.5° latitude grid) coupled to an ocean model of roughly 4° resolution, a simple free drift ice model, and a "bucket" land hydrology. While the resolution of this model is marginal, and, in some cases clearly insufficient, for the simulation of many atmospheric and oceanic phenomena, the low resolution and simplicity of this model and the flux adjustment strategy it employs are designed to allow integrations that would otherwise be computationally prohibitive. To cite some examples (described more fully below), this model has been integrated for 10,000 years with a stable climate, and an ensemble of nine CO_2+aerosol global warming scenarios has been generated. This model is referred to as the R15 coupled model.

A medium resolution coupled model, designated R30, has been under development for the past several years, and has recently been integrated for 400 years with a reasonably stable climate. It has also been used for global warming simulations. It consists of atmosphere and ocean models with exactly twice the horizontal resolution as R15, with 50% higher vertical resolution in both atmosphere and ocean, and with similar ice and land surface parameterizations. The atmospheric component of this model has been extensively analyzed, most recently by the Observational Studies Group in a series of twelve 40-year experiments with prescribed observed sea surface temperatures (5.4), and has been shown to provide realistic

responses to tropical sea surface temperature anomalies. It has been know for many years that the R30 model provides an atmospheric circulation superior to the R15 model. This is most evident in the simulation of the extratropical storm tracks, the strength of the tropical Hadley circulation and the intertropical convergence zone, and the strength of midlatitude westerlies in the Southern Hemisphere, all of which have important implications for the coupled model and the generation of global warming scenarios. The R30 coupled model is also run with flux adjustments, and the development of this model continues. Results are included in this chapter as a status report, and the reader is encouraged to keep their provisional nature in mind.

Both the R15 and R30 models have been used to simulate the evolution of the Earth's climate due to past changes in greenhouse gases and sulfate aerosols, as well as to project climate change into the 21st century. In these scenario integrations, the format follows that used in a previous R15 model study (1473) which, in turn, is based on Mitchell et al. (1995)[1]. An "equivalent" CO_2 concentration is used to represent changes in all of the trace greenhouse gases, and changes in aerosol loading are modeled by changing the surface albedo. The "standard" scenario integrations begin in 1765 and proceed for 300 years, till 2065 with equivalent CO_2 increasing at a rate of 1% per year after 1990. This projection is clearly uncertain. Some integrations are underway with a 0.5% increase in equivalent CO_2 per year after 1990. Forcing functions for the 20th century are also uncertain, due to uncertainties in aerosol loading, indirect effects of aerosols on clouds, biomass burning, and possible solar insolation changes. Any climate projections must be considered with these uncertainties in mind.

1.2 COUPLED MODEL DEVELOPMENT

T. Delworth *T. Knutson*
K. Dixon *P. Kushner*
S. Griffies *P. Phillipps*
I. Held *M. Spelman*
T. Hughes *R. Stouffer*

ACTIVITIES FY98

While a stable, long integration of the R30 coupled model has been achieved in the past year, research continues on modifying this model to reduce climate drift, minimize the shock of initialization, and generate more realistic tropical interseasonal variability.

A version of the R30 coupled model without flux adjustments has been run for several centuries to help identify any major problems in the model. As anticipated, the subtropical oceans become too warm due to the lack of boundary layer stratus clouds, and the oceanic salinities depart from those observed in several important regions, particularly in regions affected by substantial river runoff. The overturning circulation in the Atlantic is observed to weaken dramatically. Given the R15 model prediction of large changes in this thermohaline circulation in the 21st century, the stability of the overturning is a critical part of the coupled

1. Mitchell, J. H., T. C. Johns, J. M. Gregory, and S. Tett, Climate response to increasing levels of greenhouse gases and sulfate aerosols, *Nature, 376*, 501-504, 1995.

model requiring scrutiny. The conclusion is that the non-flux-adjusted model is not currently usable for global warming studies, even though it produces a realistic climate in many other respects and has little drift in global mean temperature. We continue to use flux adjustments at the air-sea interface, realizing on the one hand that both this procedure and overturning as an alternative are problematic, and on the other hand that the realism of the unperturbed climate is essential to studies of climate sensitivity.

The R30 coupled model with flux adjustments undergoes a shock following the multi-step initialization protocol within which the flux adjustments are computed. In particular, the strength of the thermohaline circulation in the Atlantic weakens by one-third and undergoes several large excursions (of 4-6 Sverdrups) that are unlikely to be characteristic of the final model climate (Fig. 1.1). Most of this shock appears to result from the fact that the coupled model has a somewhat different distribution of precipitation than that used when spinning up the ocean-only model to its climatic equilibrium as part of the initialization procedure. Modest changes in this pattern move rainfall from one drainage basin to another, so that rivers run off into different parts of the ocean, thereby altering oceanic salinities. Experiments are underway to minimize the modest changes in sea surface temperature that appear to be the cause of these shifts in precipitation. Alternative initialization strategies are also under consideration.

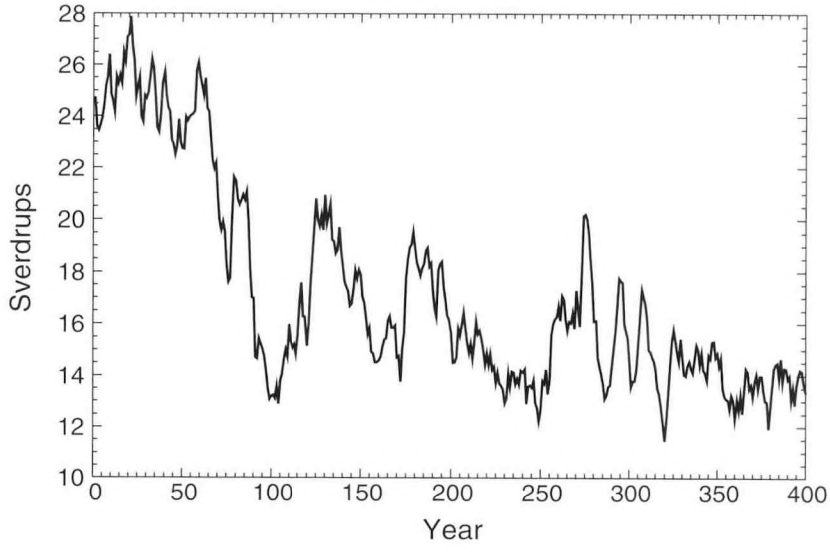

Fig. 1.1 Time series of the meridional overturning stream function in the North Atlantic from the control integration of the R30 coupled model. Annual mean values are plotted in units of Sverdrups (10^6 m^3 s^{-1}). After an initial adjustment period in which the circulation weakened, a stable overturning circulation appears to have been achieved.

The exaggerated ENSO-like variability of the R30 model (1.3.2) has been found to be surprisingly sensitive to the horizontal diffusion in the ocean model. Experiments on this aspect of the R30 model are in progress.

The coupled model has been renovated in the past year to take advantage of upgrades to MOM (the Modular Ocean Model) (4.2.1) in a timely fashion. A version of the model coupled to MOM2 has been tested and found to produce a climate simulation similar

to earlier versions of the model. Testing of a model incorporating the MOM3 code and its new isopycnal mixing schemes is now underway.

A new structure for atmospheric model development is under construction, jointly with the Experimental Prediction and Atmospheric Processes Groups, which will centralize laboratory activities aimed at improving the atmospheric component of the models used for climate studies, as well as for research in extended-range and seasonal forecasting (3.2).

PLANS FY99

The coupled model will make the transition to the new atmospheric modeling framework within the next year. Ongoing research on ice and land surface modeling will be incorporated into this new model in the next year as well. The goal on the one to two year time scale are to build new coupled models at approximately 3° atmospheric resolution and with oceanic resolutions ranging from 3° to 1°, which can be stably integrated for a millennium with less dependence on flux adjustments at the air-sea interface. Simultaneously, a version of the atmospheric model at a resolution of roughly 1° will be built for the study of regional climate change using boundary conditions provided by the lower resolution coupled model, all in a software environment that encourages experimentation by a large number of users inside and outside of GFDL.

1.3 SENSITIVITY AND VARIABILITY STUDIES WITH THE R30 COUPLED MODEL

ACTIVITIES FY98

1.3.1 Control Integration and Global Warming Experiments

T. Delworth *M. Spelman*
K. Dixon *R. Stouffer*
T. Knutson

A reasonably stable control run with the R30 coupled model has been achieved using an initialization and flux adjustment strategy similar to that used in earlier R15 experiments. This integration is currently over 400 years in duration. The drift in global mean sea surface temperatures over the first 400 years is less than 0.1 K.

Five extended integrations of this model with perturbed radiative forcing have been conducted. In the first of these integrations, the CO_2 concentration, meant to represent all of the radiatively active trace gases, increases at a rate of 1% per year until the initial concentration is doubled, and is held constant thereafter. A second integration has the same structure, but the effective CO_2 concentration does not level off until it quadruples.

In addition, integrations for three alternative scenarios are in progress using the standard framework (1.1), but with the integrations starting in 1865. The first two scenarios have CO_2 increasing at 1% per year after 1990, but differ in initial condition with the second integration branching off from the control run 200 years later than does the first. The third

scenario run branches off from the first at year 1990 and has CO_2 increasing at 0.5% per year thereafter.

Shown in Fig. 1.2 are time series of global mean surface air temperature from observations, one of the 1% per year R30 scenario runs, and previously obtained results from the R15 coupled model. The larger variability in the R30 experiment is partially attributable to the model's exaggerated ENSO-like variability in the tropical Pacific (1.3.2). The R15 and R30 atmospheric models have similar equilibrium sensitivities to a doubling of CO_2 when coupled to mixed layer oceans. For both, the global mean surface air temperature increase is close to 4 K, which is at the upper end of the 1.5 K-4.5 K range discussed by the IPCC (Intergovernmental Panel on Climate Change), so they are anticipated to have similar overall sensitivities when coupled to full ocean models as well. Fig. 1.2 is consistent with this expectation. The two models agree on the timing of the warming in these scenario integrations, although there is a hint that the warming in the R30 is delayed by roughly a decade compared to the R15. Despite their high sensitivity, both model integrations are also in relatively good agreement with the observed increase of surface air temperature over the last century. This fit must be interpreted with care, as it is dependent on the cooling effect of the poorly constrained sulfate forcing, and could also be modified by other radiatively important

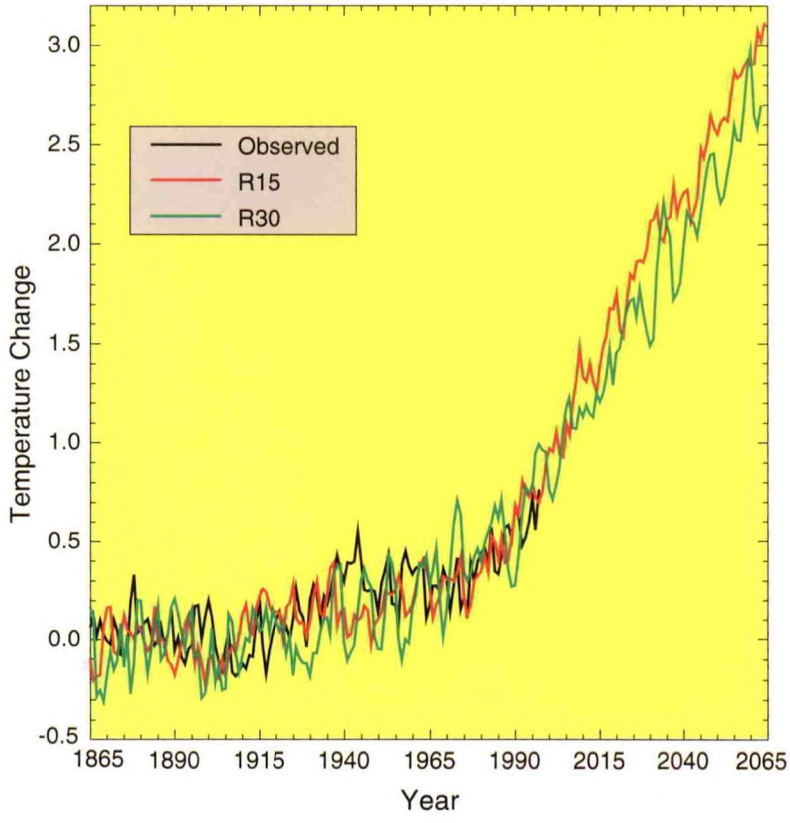

Fig. 1.2 Time series of global mean surface air temperature from observations (black), a simulation using the R15 coupled model (red), and a simulation using the R30 coupled model (green). All time series denote annual mean anomalies relative to the period 1880-1920. The model simulations incorporate an estimate of the radiative effects of changing concentrations of greenhouse gases and sulfate aerosols. The higher resolution R30 model provides a similar fit to the observations as does R15 and warms a bit more slowly in the 21st century.

perturbations to the system (*i.e.*, solar constant changes, biomass burning) unaccounted for in this calculation.

Preliminary results have been obtained regarding changes in the Atlantic overturning circulation in the five transient integrations with varying CO_2 and/or aerosol loading. The overturning eventually weakens in all of these integrations, but indications from the scenario integrations are that this weakening in less rapid in the R30 coupled model than in the R15. Given the large internal variability of the overturning in the R30 model, some of which could be related to the initialization process, additional experimentation will be needed before a more definitive analysis can be completed.

The spatial pattern of surface air temperature changes for years 2030-2050 minus 1976-1995 is shown in Fig. 1.3. Noteworthy features include the slower warming in the Southern Hemisphere compared to the Northern Hemisphere (particularly over the Southern Ocean), and the more rapid warming of the eastern tropical Pacific compared to the western tropical Pacific, which has the effect of decreasing the east-west temperature gradient. Given the large decadal variability in this model, the details in this pattern will undoubtedly differ from one realization to another.

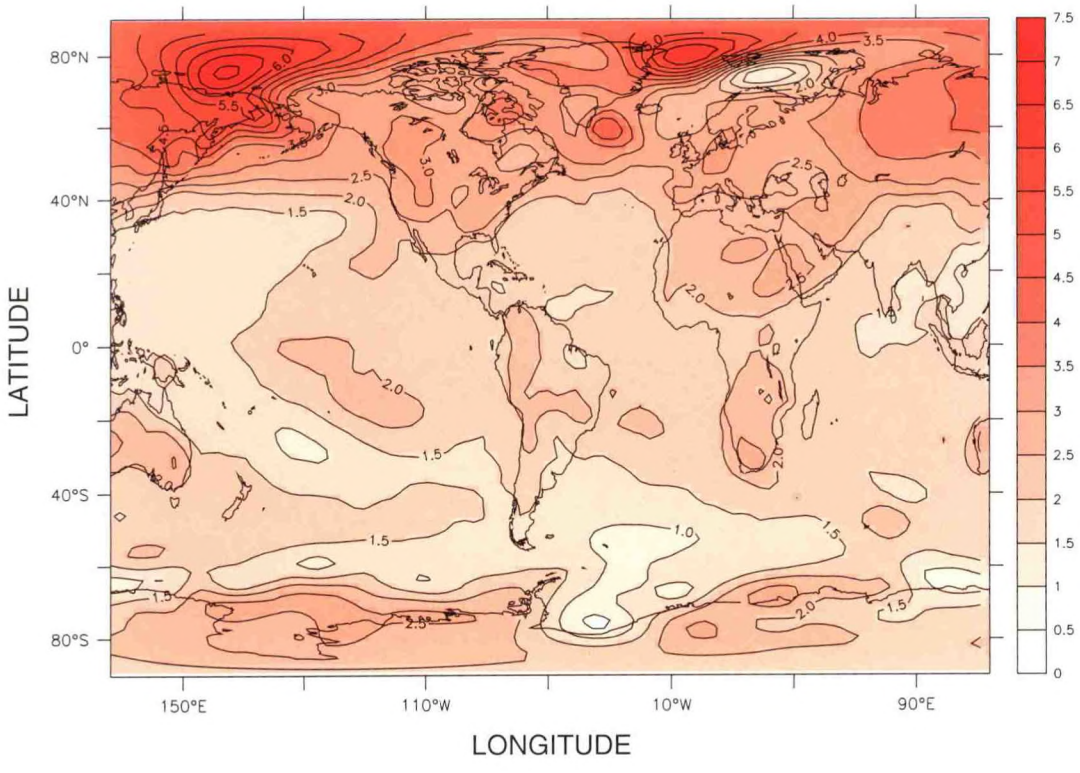

Fig. 1.3 Change in simulated surface air temperature from the period 1976-1995 (20 year mean) to the period 2046-2065 (20 year mean) from the R30 transient aerosol run. Values plotted are annual means. Units are °K. While there is broad similarity with the pattern predicted in earlier R15 integrations, there are differences in detail in the equatorial Pacific and North Atlantic.

1.3.2 Tropical Pacific Variability

T. Delworth *T. Knutson*

An important test of coupled climate models is their simulation of tropical Pacific SST variability on interannual to decadal time scales. The R30 coupled model shows very pronounced ENSO-like (El Niño-Southern Oscillation) variability in the equatorial Pacific. Large magnitude events such as the super El Niños of 1982-1983 and 1997-1998 are common in the model. Indeed, they are too common, and have too long a duration. The model's tropical Pacific has a longer time scale (~8 years) than the observed ENSO (~4 years), and the oscillations are too regular and somewhat too large in amplitude on average, as can be seen in Fig. 1.4. However, preliminary analysis indicates that the dynamics underlying the simulated variability appears to be quite similar to the "delayed oscillator" mechanism to which the observed interannual variability is generally attributed (er).

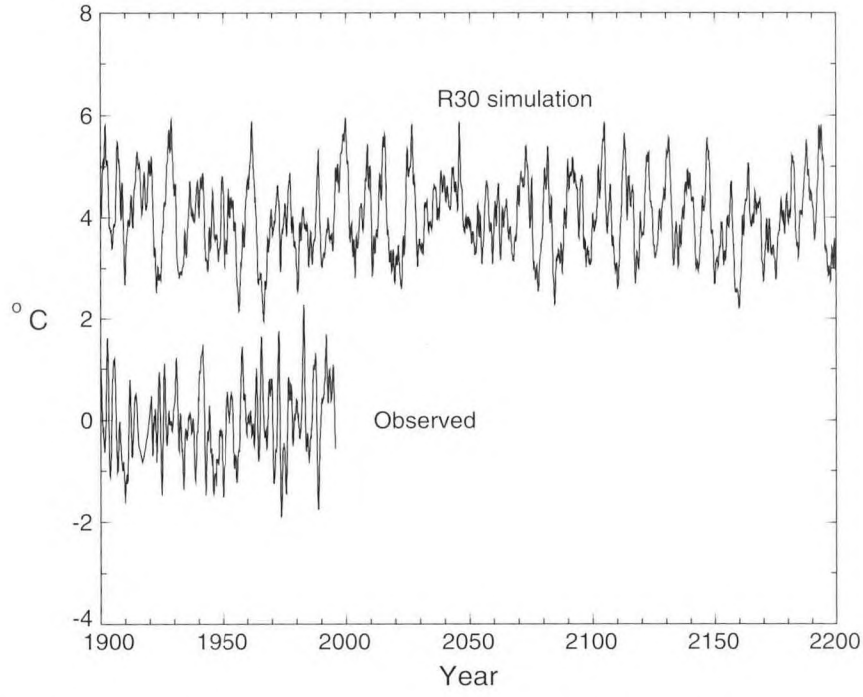

Fig. 1.4 Simulated (top curve) and observed (bottom) SST variability in the equatorial Pacific. The simulated R30 series is for the NINO4 region (6°N-6°S, 160°E-151°W) and is offset by 4°C for clarity. The observed data is for the NINO3.4 region (5°N-5°S, 170°W-120°W) based on the Hadley Centre's MOHSST6 data set. A slightly different region is used for the model and observation due to the fact that the model's center of variability is located west of the observed center of variability. For both model and observed, the seasonal cycle has been removed, and the anomalies have been smoothed using a seven-month running average. The calendar year is arbitrary for the simulated series.

The model's enhanced and relatively low-frequency ENSO-like Pacific variability results in enhanced decadal variability in the extratropical Pacific Ocean, through "atmospheric bridge" effects (1393), making it difficult to isolate extratropical sources of variability on these time scales. It also may create exaggerated decadal variations in global mean temperature, biasing studies of global warming detection. Therefore, it is important to isolate the reason for this larger-amplitude low-frequency ENSO-like variability in the model. One possibility is simply that greater resolution is needed in the ocean model, particularly within the narrow equatorial

waveguide which is thought to play an important role in shaping ENSO dynamics. On the other hand, recently obtained results indicate that the tropical variability in the model appears to become more realistic when the horizontal diffusivity in the ocean is reduced, shifting to higher frequencies and with somewhat smaller amplitudes. Thus, while higher resolution may ultimately be needed to obtain satisfying ENSO simulations, it is possible that the R30 model's distorted variability may be at least partially ameliorated without an increase in resolution.

1.3.3 Southern Hemisphere Atmospheric Response to Global Warming

K. Dixon *P. Kushner*
I. Held

The various transient R30 coupled model integrations produce an interesting response in the surface winds in the Southern Hemisphere. The CO_2-doubling experiment described above (effective CO_2 is increased at 1% annually until doubled at about year 70, after which it is held fixed), provides a particularly clear example, illustrated in Fig. 1.5. The zonally averaged winds become more westerly, by roughly 1 m/s, in a latitude band centered at 60°S, while becoming more easterly near 40°S. This corresponds to a poleward shift and a modest strengthening of the westerlies.

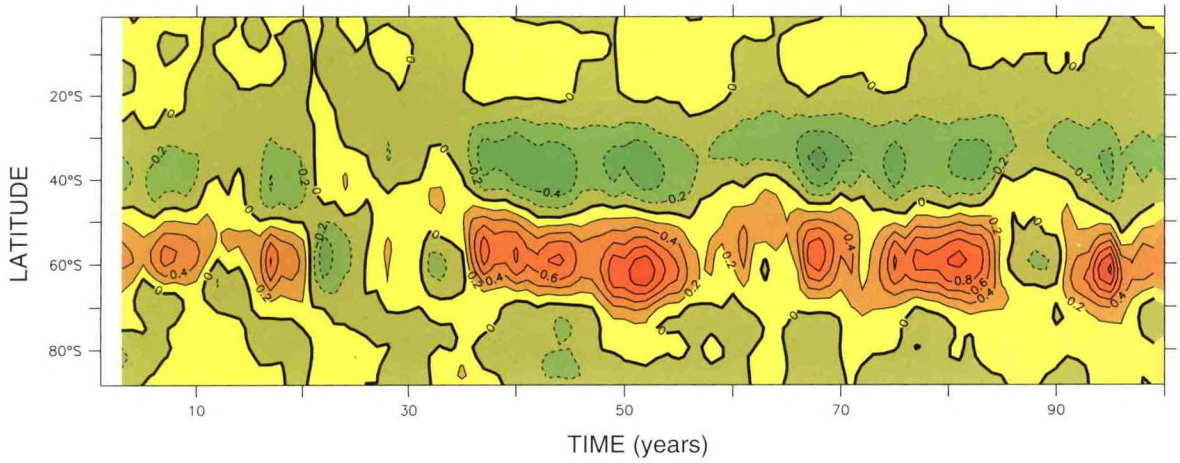

Fig. 1.5 Annual-mean zonally averaged surface zonal wind anomalies (relative to the long-time average of an R30 control integration) for an R30 integration in which CO_2 is increased to doubling (around year 70) and held fixed afterward. Contour interval: 0.2 m/s. A five-year running mean has been applied to the data. Changes in the meridional temperature gradient result in a poleward shift and modest strengthening of the Southern Hemisphere westerlies.

This wind shift is presumed to be related to changes in the north-south temperature gradients that provide the energy source for the storms that maintain this wind distribution through their momentum fluxes. A robust feature of both R15 and R30 coupled model responses to transient greenhouse-gas increase is a significant difference between the hemispheres in the latitudinal pattern of the warming. In the Northern Hemisphere, the warming increases with latitude so that the magnitude of the north-south temperature gradient is always reduced. In contrast, there is initially very little warming of the Southern Oceans, from 50°S to 70°S, while the tropics do warm somewhat, so that the temperature contrast between low and high latitudes in the Southern Hemisphere is increased. The

increase in the temperature gradient is more pronounced in the upper troposphere because the tropical warming increases with increasing height. As the integration proceeds, the polar amplification familiar from equilibrium integrations eventually sets in (as studied in detail in the R15 context in 1.4.5), reducing the temperature gradient near the surface.

Work is underway to better understand the connections between the changes in temperature gradient, both at the surface and in the upper troposphere, and the surface westerlies. This work involves analysis of eddy fluxes and eddy structures in the atmospheric model, experimentation with models with more idealized lower boundary conditions that produce similar responses, and experimentation with modified coupled models to see if these wind anomalies have a significant impact on the evolution of the ocean. The pattern of the wind anomalies in Fig. 1.5 is very similar to the dominant pattern of the month-to-month variability of these winds in atmosphere-only integrations with fixed ocean temperatures. Therefore, one focus of this research is the possibility that one phase of a natural "mode" of variability, akin to the classical "index cycle", is preferentially being excited by changes in oceanic temperatures.

PLANS FY99

Experimentation with incremental modifications to the model will focus on the characteristics of the model's ENSO-like variability and on the problem of initializing the model so as avoid exciting oscillations in the North Atlantic overturning that are not representative of the model's long term climate. Meanwhile, integration and analysis of the existing set of integrations will continue, with the immediate goal of clarifying which conclusions concerning climate sensitivity and variability obtained with the R15 model over the past decade are also supported by R30, and which may need to be modified. A focus on Southern Hemisphere circulation changes will continue. Besides being important in itself, the Southern Hemisphere response to climate change provides a relatively simple test bed for dynamical ideas that should prove useful in interpreting the more complex circulation of the Northern Hemisphere.

1.4 SENSITIVITY AND VARIABILITY STUDIES WITH THE R15 COUPLED MODEL

ACTIVITIES FY98

1.4.1 A 10,000 Year Integration

A. Broccoli *R. Stouffer*

The control integration of the R15 coupled model has now been extended to 10,000 years in order to study natural variability in the model on time scales up to 1000 years. A small drift in the global mean surface air temperature found in the first 1000 years of the integration continued until the year 2000, but the total drift in the global mean is only 0.7 K. After year 4000, there appears to be little or no drift in any part of the coupled system. From preliminary analysis it appears that most of the variability on time scales of 100 years and longer is found in the Southern Ocean. However, one very interesting event occurs near year 3100 in the North Hemisphere. Fig. 1.6 shows the time series of annual mean surface air temperature near the sinking site of the thermohaline circulation in the Northern Hemisphere. In this time period, an

exceptional negative temperature anomaly occurs, reaching a magnitude of 4 K. Except for this event, anomalies in this region never reach significantly beyond 2 K. During this same time period, the Atlantic thermohaline circulation weakens from its normal value of 18 Sverdrups to 14 Sverdrups. The cold anomaly is centered over the sinking region of this circulation and extends, with smaller amplitude, from Northern Canada, across Greenland and the North Atlantic, to Western Europe. This cold anomaly is also associated with changes in sea level pressure which likely act to enhance the cooling in the North Atlantic. This event appears to be a very high amplitude case of the model's dominant mode of interdecadal variability (1428).

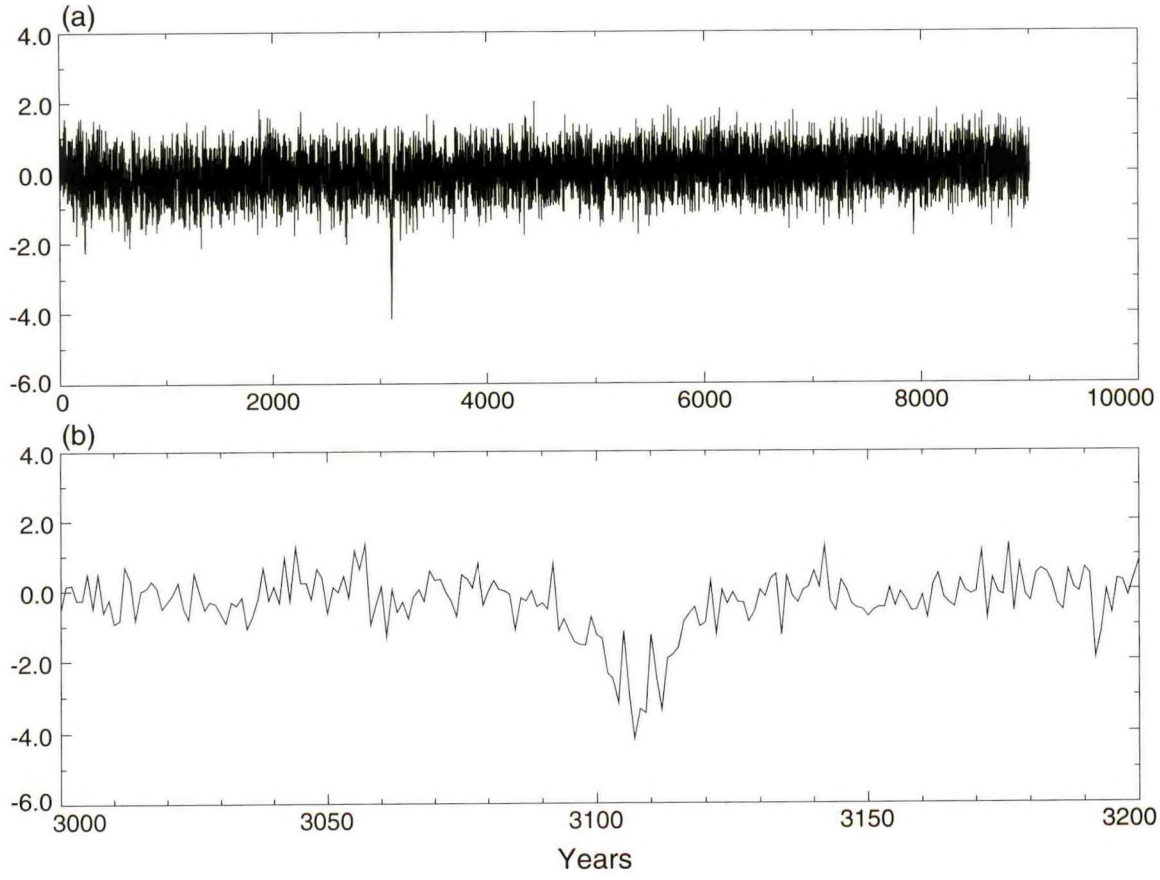

Fig. 1.6 Time series of the annual mean surface air temperature anomaly (°C) from just east of the tip of Greenland (30° to 22.5°W longitude, 64.5°N latitude) (a) a 9000 year time series, and (b) 200 years centered at year 3100.

In the paleo-record, there is a sharp cooling event in the Holocene, near 8,200 years before the present (Alley et al., 1997[2]) with a somewhat longer time scale (≈100 years). This event has been thought to be associated with freshwater discharge from melting glaciers which slows down the thermohaline circulation, cooling the North Atlantic. This model integration suggests that this early Holocene event could be unforced variability of the coupled system that does not require large changes in freshwater input from melting glaciers.

2. Alley, R. B., P. A. Mayewski, T. Sowers, M. Stuiver, K. C. Taylor, and P. U. Clark, Holocene climatic instability: A prominent, widespread event 8200 years ago, *Geology*, 25, 483-486, 1997.

Natural events of this magnitude have the potential to make the detection and attribution of observed local climate change more difficult. The fact that only one such event occurs in this 10,000 year integration serves to underline the need for such long integrations. However, it should be noted as well that this large event has a negligible signature in the global mean temperature.

1.4.2 Two Stable Equilibrium Climates

S. Manabe *R. Stouffer*

An important result obtained in the past with the R15 coupled model is that it supports two distinct climate states with the same boundary conditions and forcing. One state has a realistic and active thermohaline circulation in the Atlantic Ocean. The other has a weak reversed circulation with extremely weak upwelling throughout the North Atlantic, although it maintains substantial sinking in the Southern Ocean. The temperature difference between these two climatic states at the surface in the Polar North Atlantic is as large as 8 K. In order to remove lingering doubts as to whether these two states remain stable on the very long diffusive time scales on which the deep ocean equilibrates, the model in its weak reversed circulation state has now been integrated for 7,000 years, to accompany the 10,000 year control run which is in the active circulation state. As shown in Fig. 1.7a, the results demonstrate unequivocally that this model does have two distinct equilibrium climates.

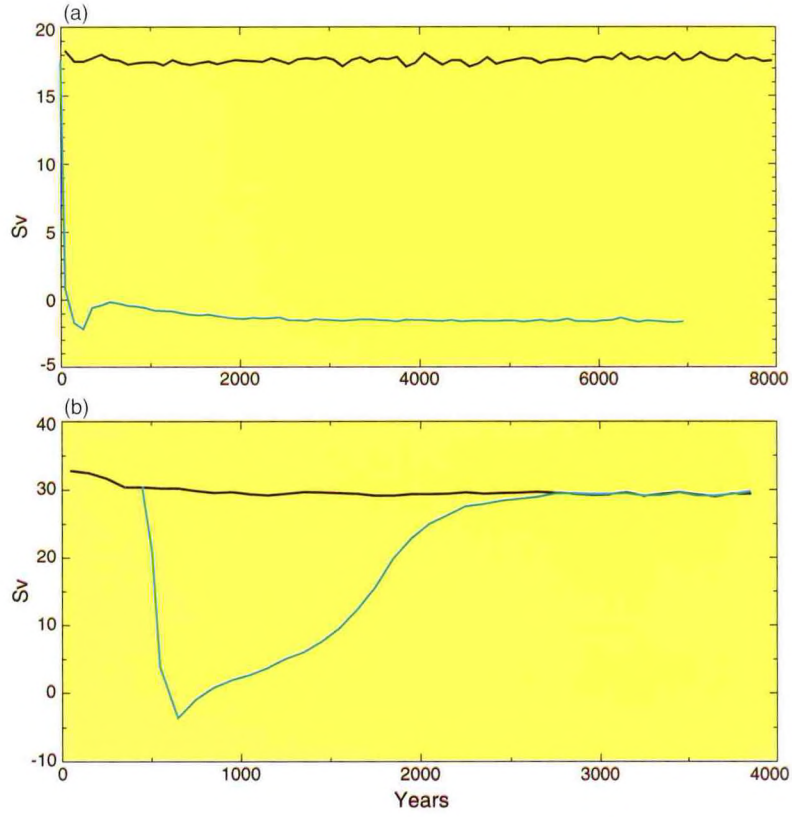

Fig. 1.7 The maximum value of the overturning streamfunction in the North Atlantic Ocean for the model with a) the normal value of the vertical diffusion coefficient and b) a large value for the vertical diffusion coefficient (LVD). The black line represents values obtained from the control integration for each experiment. The perturbation integration is represented by the blue line.

Partly to address questions raised by others concerning the stability of the weak, reversed circulation mode, particularly Schiller et al.[3] using a version of the MPI (Max Planck Institute, Hamburg) coupled model, this simulation has been repeated with another version of the R15 coupled model using a larger vertical subgrid scale diffusion coefficient. A weak reversed thermohaline circulation is induced in the model's Atlantic Ocean by a massive discharge of freshwater, but the circulation eventually returns to its active, direct state (Fig. 1.7b). The implication is that there is a critical value of the diffusivity below which two stable equilibria exist. The behavior of the more diffusive version of the coupled model resembles the response of the model of Schiller et al. Since the MPI model employs a first-order upstream differencing scheme which yields large, implicit diffusion, it appears likely that the difference in behavior of their model and the standard R15 model results from the fact that the former is more diffusive. Even the standard R15 model uses vertical diffusivities that are larger than those measured by direct release of artificial tracers into the Atlantic Ocean, so these results support the hypothesis that the Earth possesses two distinct climatic equilibria.

1.4.3 An Ensemble of R15 Scenario Integrations

K. Dixon *J. Lanzante*

A set of nine CO_2-aerosol scenario integrations has been performed to facilitate studies of the emergence of the global warming signal from the noise of natural variability. The nine scenario experiments are conducted in three groups of three. They are initialized from various points of a long-running control model integration, with successive groups initialized at times separated by 500 model years. Within each group, experiments of 300, 200, and 150 years duration were performed, with radiative forcings starting from years 1765, 1865 and 1915, respectively. One motivation for this experimental design is to help determine whether or not it is important to start integrations of this type in the pre-industrial era, or if mid 19th or even early 20th century initial conditions are adequate. This issue becomes particularly relevant when working with more computationally intensive models. In the 1765 set of experiments, there is a smooth transition from equilibrium conditions, since the aerosol and greenhouse gas forcing for year 1765 are identical to the control model's. Scenario integrations begun in 1865 or 1915 experience initial discontinuities in radiative forcing.

The sensitivity of simulated 21st century global mean surface air temperatures to the choice of radiative forcing starting point (1765, 1865 or 1915) is detectable, but relatively small, and similar in magnitude to the inter-experiment variability that arises from variations in the choice of initial conditions for the coupled model. The range of responses in the global mean surface air temperature among all nine integrations is indicated in Fig. 1.8. Further analysis will be directed at the more slowly evolving parts of the system, such as the thermohaline circulation and sea level, in order to better characterize the systematic errors associated with starting a climate change scenario run in 1865 or 1915 rather than 1765.

---

3. Schiller, A., U. Mikolajewicz, and R. Voss, The stability of the North Atlantic thermohaline circulation in a coupled ocean-atmosphere general circulation model, *Clim. Dyn., 13,* 325-347, 1997.

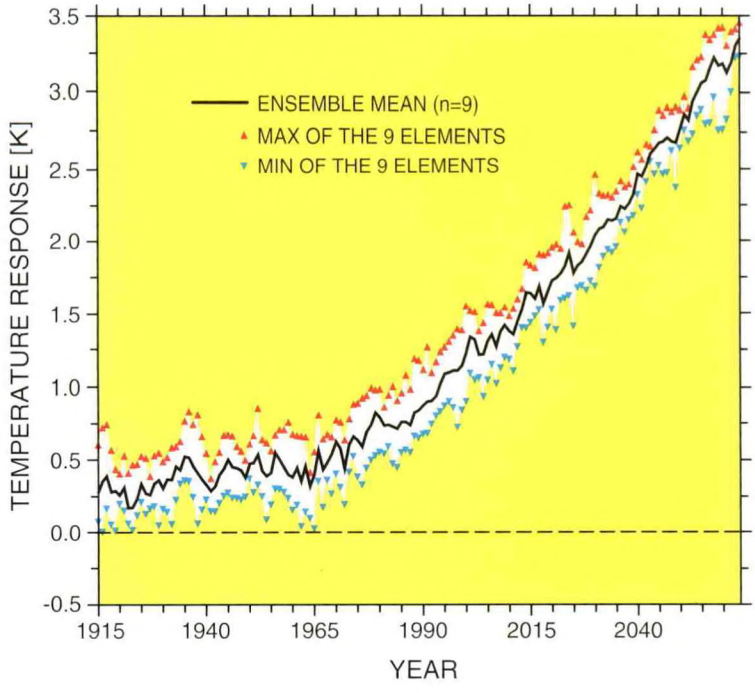

Fig. 1.8 150 year time series of the coupled models' global mean surface air temperature responses to imposed greenhouse gas and sulfate aerosol forcings. Results from the nine members each lie within the white region. The ensemble mean response (solid line) is bracketed by the extremes (greatest warming = red triangle; least warming = cyan triangle).

1.4.4 A Scenario Integration Without Water Vapor Feedback

A. Hall *S. Manabe*
I. Held

A modified version of the R15 coupled model has been constructed in which the water vapor feedback is disabled (the radiative transfer algorithms of the model use a water vapor distribution produced by a control integration, which is fixed when the model is perturbed). The models' response to a doubling of CO_2 is reduced from 3.8°C to 1.05°C when modified in this way. This artificial modification results in a very stable climate with a response which is below the low-end of the plausible range of climate sensitivities suggested by IPCC and others. Previous work has analyzed the reduction in low-frequency variability in this fixed H_2O model (fz), and ongoing work has focused more closely on a surprisingly sharp reduction in this model's ENSO-like variability.

A standard scenario integration (1.1) has been performed with this fixed H_2O model. Fig 1.9 shows the resulting evolution of global mean surface temperature, along with the analogous result for the standard R15 model and observations. The modified model is unable to predict the observed warming during the 20th century with this scenario forcing. Consistency with observations would require much larger radiative forcing. In addition, the natural variability of global mean temperature in this model is reduced by nearly a factor of two on multidecadal time scales, so it is even more difficult for this model than it is for the unmodified model to produce, through natural variability, a temperature trend like that observed.

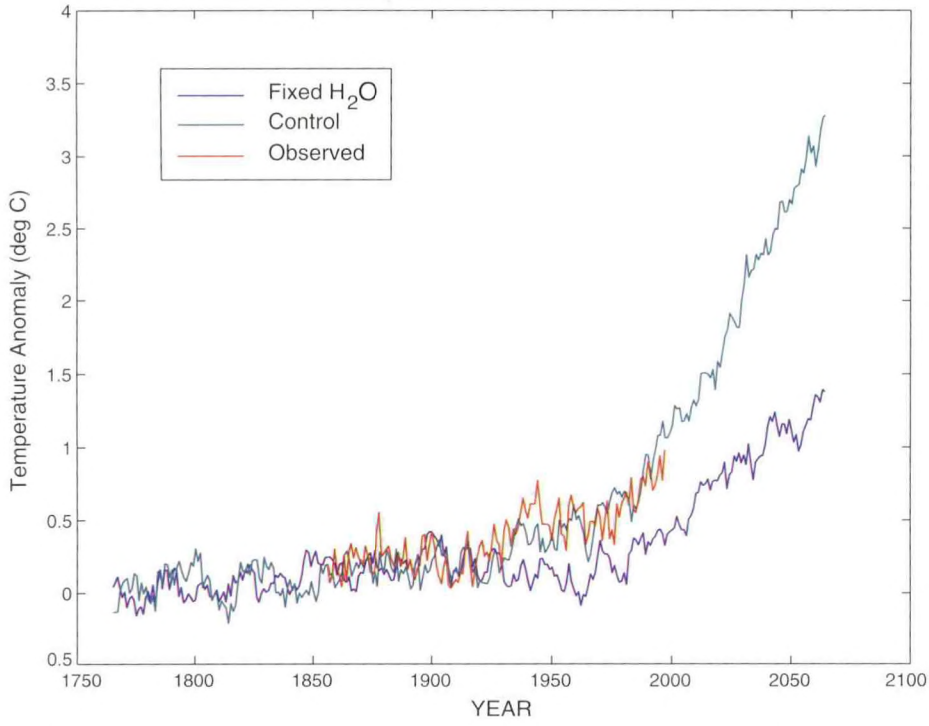

Fig. 1.9 The global-mean surface temperature change that occurs in the "scenario runs" in response to estimated sulfate and greenhouse gas forcings. The dark blue curve shows the fixed H_2O case, while the light blue curve shows the control case. In addition, the observed time series is shown with a red line. The curves were scaled to overlap during the first forty years of the observed time series. The model with water vapor feedback provides a better fit to observations, given the forcing history used in these models.

1.4.5 Comparison of the Fully Coupled and Mixed-Layer Models

S. Manabe *R. Wetherald*
R. Stouffer

A comparison of the equilibrium and transient climatic response to changes in greenhouse gases in fully-coupled and mixed layer ocean models allows one to isolate the role that ocean dynamics plays in shaping these responses. By utilizing flux adjustments, one attempts to produce control climates in the two models which have identical sea surface temperatures. Differences between the climate responses in the two models should then be related to changes in ocean heat transport.

The equilibrium response of the climate to a doubling of the CO_2 concentration in the R15 model has been studied by integrating the model until a true equilibrium is reached. The control is of 10,000 years length. The doubled CO_2 integration is 5,000 years in length. Equilibria are attained after about 4,000 years of integration. The globally averaged equilibrium surface air temperature (SAT) change due to CO_2 doubling in the coupled model is found to be 4.5 K, and 3.7 K for the mixed layer model. While it is tempting to look for changes in ocean circulation responsible for this larger response, it appears instead to be at least partly a consequence of a small drift towards cooler temperatures in the coupled model control run. The cooler climate results in a larger snow-ice-albedo feedback and a larger sensitivity to

increased CO_2. As a result, it is uncertain whether the equilibrium response of the coupled model would be significantly larger than that of the atmosphere-mixed layer model if the control temperatures were more nearly identical.

The spatial pattern of equilibrium SAT response to doubled CO_2 concentration (Fig. 1.10b) in the coupled model is very similar over most regions to that in the mixed-layer model (Fig. 1.10a). The familiar polar amplification is seen in both models. An exception is found in the region southwest of Australia where the warming is at a minimum in the coupled model due to changes in vertical mixing in the ocean. Analysis of the time series indicates that this pattern is robust and does seem to be a feature of this model's equilibrium response. In general, however, the changes in the ocean model's heat transport are not large enough to change the SAT pattern substantially. Whether this will continue to be the case in higher resolution ocean models remains to be seen.

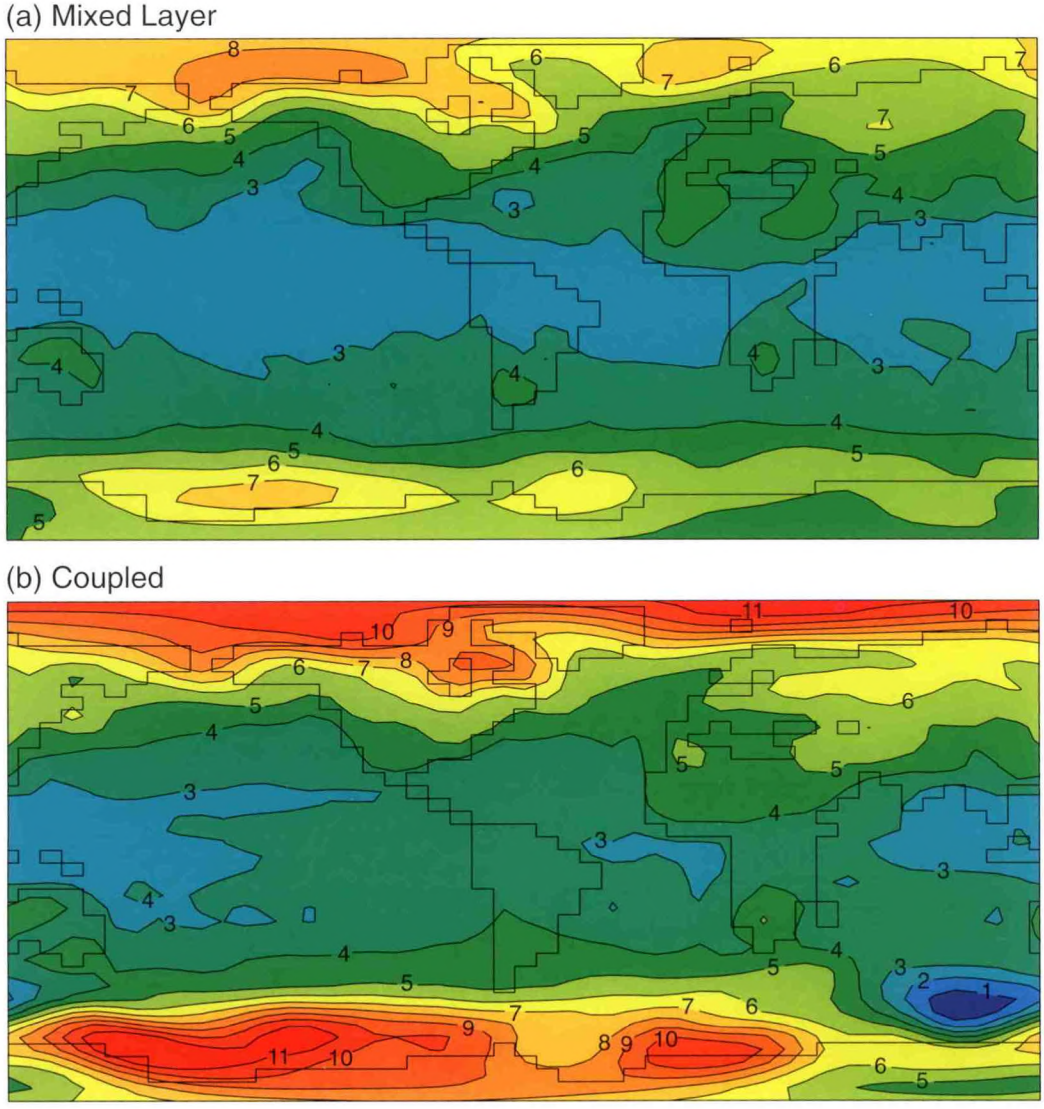

Fig. 1.10 Equilibrium response of surface air temperature (°C) to a doubling of CO_2 in (a) an atmospheric model coupled to a 50 m mixed layer, and (b) a fully coupled atmosphere-ocean model.

A project has also been initiated to compare integrations using the mixed layer and fully-coupled R15 models, following the standard scenario format (1.1). In addition, the mixed-layer ocean-atmosphere model has been integrated to equilibrium for five separate static settings of the total radiative forcing, corresponding to the years 1980, 2000, 2020, 2040 and 2060 of the scenario integrations. As discussed in the previous paragraph, the mixed layer model appears to provide a good estimate of the equilibrium response, at least in the context of this R15 model.

Figure 1.11 summarizes the resulting responses of global mean surface air temperature. Coupling to a full-ocean model delays the global mean warming by 20-30 years as compared to the 50 meter mixed layer results, with a somewhat longer delay near the end of the integration. The delay is primarily caused by the failure of the Southern Ocean and the extreme northern part of the Atlantic to warm appreciably in the coupled model. Other differences in the geographical pattern of the responses are under investigation.

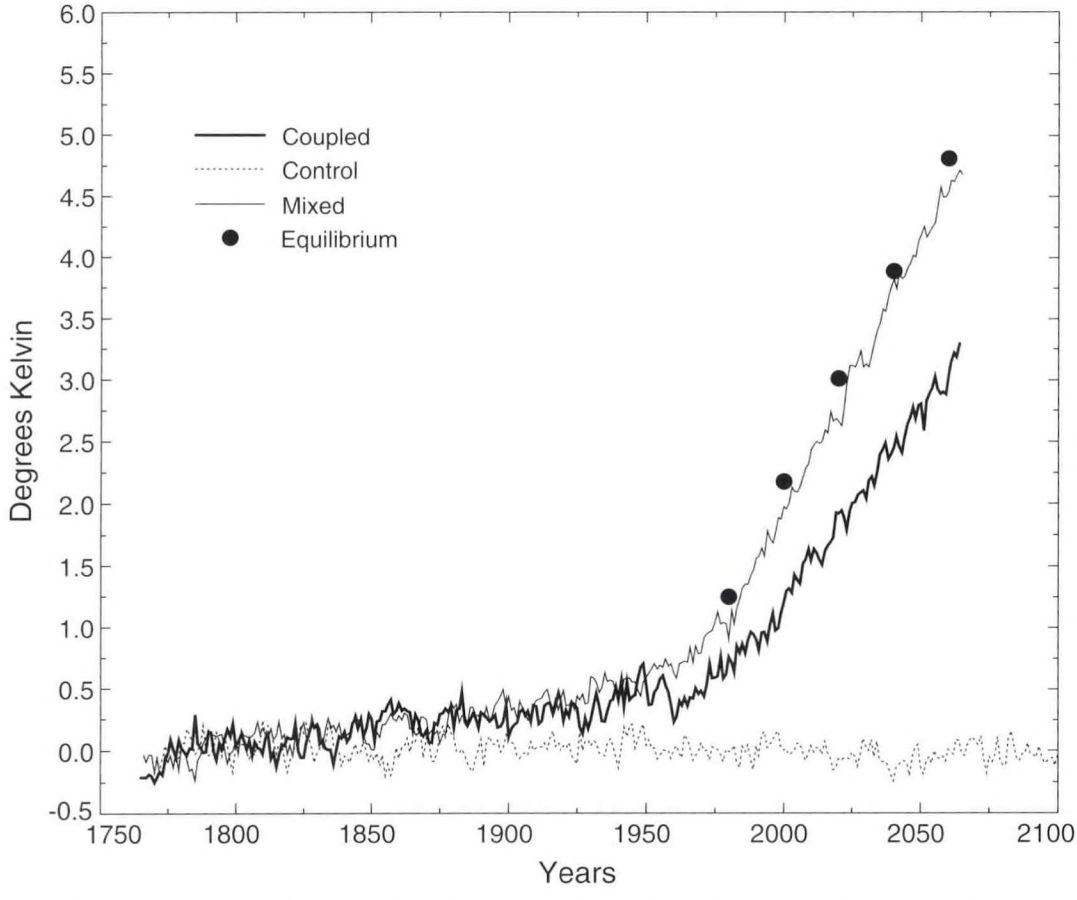

Fig. 1.11 The change in global mean surface air temperature caused by both greenhouse gases and sulfate aerosols for the fully coupled ocean-atmosphere model (1473), the mixed-layer model, and the equilibrium mixed-layer model. For reference, the control run of the fully coupled ocean-atmosphere model is also shown. The equilibrium response in year 2000 is more than 2 K.

Note that the equilibrium responses are close to those of the dynamic mixed layer model, indicating that even if the radiative forcing were somehow to be held fixed at today's value, the global mean SAT would rise by an additional 0.9°C, which is larger than historical

warming since the late 1800s. Differences in the geographical pattern of the responses are under investigation.

1.4.6 Detection of Global Warming Trends

R. Stouffer *S. Tett***
*G. Hegerl**

**University of Washington*
***Hadley Centre for Climate Prediction and Research*

A comparison has been completed of the variability of surface air temperature in 1,000-year coupled model integrations performed at the Hadley Centre (HadCM2), Max Planck Institute (HAML3) and at GFDL, where the R15 simulation was used for this purpose (hn). Integrations of this length are needed to study natural variability on the 100-year time scale that is most crucial when trying to attribute the observed 20th century warming to changes in radiative forcing or to natural variability. Models play an important role in this signal detection problem because the observational record for variability on this time scale is so limited.

The linear trends of surface air temperature in all three models are small over most areas of the globe. Although there are notable differences among the models, the simulated SAT variability is fairly realistic on annual to decadal time scales, both in terms of the geographical distribution and in the global mean, with the exception of the simulation of observed tropical Pacific variability. In the HadCM2 model, the tropical variability is overestimated, as in the GFDL R30 model (1.3.2), while in the GFDL R15 and HAM3L models it is underestimated. 1000-year integrations with models that provide better simulations of ENSO are clearly needed, but are not yet available.

None of the models generate a temperature trend as large as that observed (Fig. 1.12). If the models' simulation of variability on long time scales is realistic, then the observed warming must be due to changes in the radiative forcing of the planet and not the result of internally generated variability.

A question of central importance is, therefore, whether all of these models could be grossly underestimating natural variability on the century time scale. It would be surprising if models that simulate ENSO better would affect this conclusion, since models that actually overestimate ENSO variability produce nothing resembling the observed trend. Mesoscale ocean eddies appear to be the most plausible remaining potential source of variability missing in these models. Such eddies could plausibly energize the variability in the oceans on the gyre scale and within convective regions, at higher levels than the rather diffusive, low resolution ocean models used here. Climate change studies resolving ocean eddies in global models will require greatly enhanced computational resources.

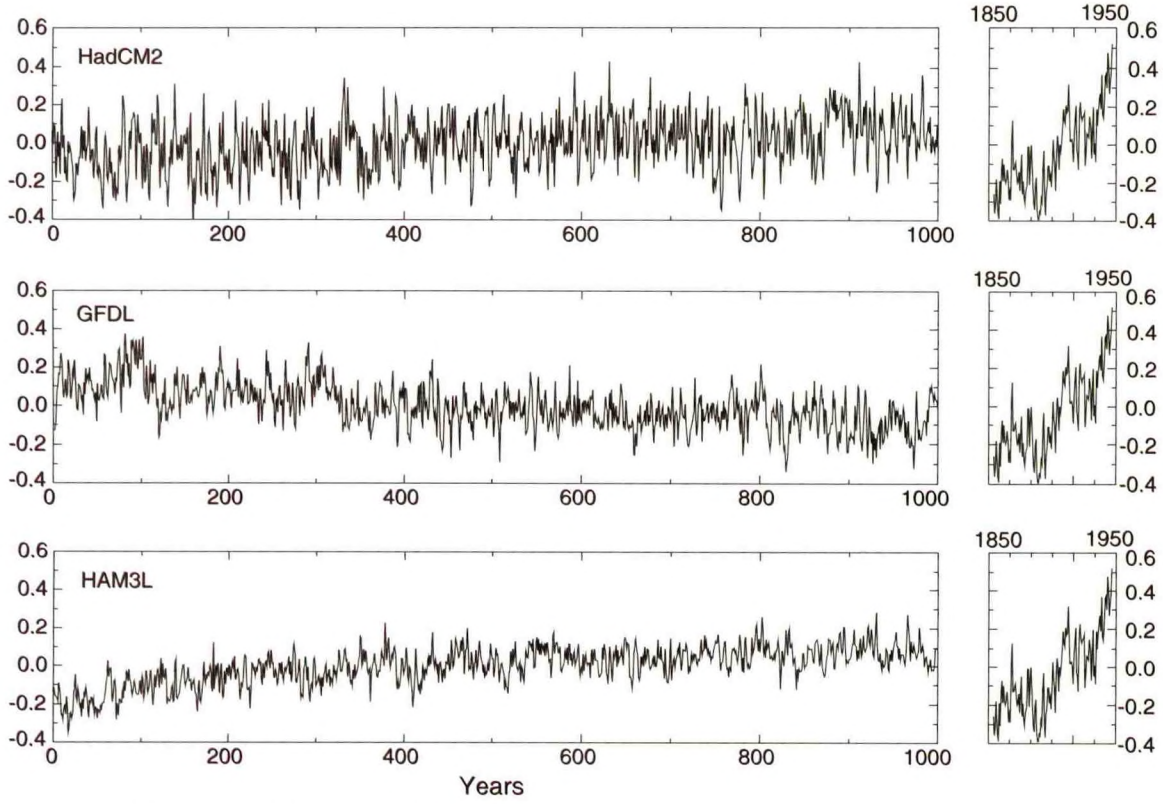

Fig. 1.12 Time series of the globally averaged, annual mean surface air temperature anomaly (°C) from three models (top, left: HadCM2; middle left: GFDL; bottom, left: HAML3). The right column of plots (all the same) represent the globally averaged, annual mean surface air temperature observations compiled by Jones and Briffa (1992). None of the models generate a temperature trend as large as that observed.

1.4.7 Decadal to Multi-Decadal Variability

T. Delworth *V. Mehta***
*R. Greatbatch**

**Dalhousie University*
***University of Maryland*

Previous analyses have documented the existence of multi-decadal variability in the North Atlantic thermohaline circulation of the R15 coupled model (1428). In order to evaluate the role of the atmosphere in this variability, experiments have recently been conducted using only the oceanic component of this model subjected to different time series of surface fluxes. These fluxes were derived both from extended integrations of the coupled model and from integrations of the atmospheric component of the coupled model run with a prescribed seasonal cycle of ocean surface temperatures. A sequence of experiments has been performed in which the nature of the fluxes is systematically altered in order to explore the importance of air-sea coupling for the model's thermohaline variability. This study demonstrates that the thermohaline variability can be fully excited by surface flux forcing which is stochastic in time, implying that the thermohaline variability in this model is not due to feedback between the surface fluxes and the state of the ocean, and rules out

explanations based on coupled air-sea modes. It also demonstrates that variations in surface heat flux are primarily responsible for exciting this thermohaline variability, rather than variations in freshwater flux.

Analyses have also been conducted to assess the higher frequency interannual to decadal variability simulated in the tropical North Atlantic by the R15 coupled model. Spectral analyses of both observed and simulated SST variations over this region show a weak peak on decadal time scales. The dominant spatial pattern of SST variability resembles that from observational analyses, as shown in Fig. 1.13. In the model, fluctuations in the intensity of the atmospheric subtropical high are associated with changes in the intensity of the trade winds, thereby causing changes in the air-sea flux of latent heat and providing the primary mechanism responsible for this model-simulated pattern of SST variability. Changes in oceanic heat advection also contribute to the SST pattern, but these are smaller in magnitude than the surface heat flux variations.

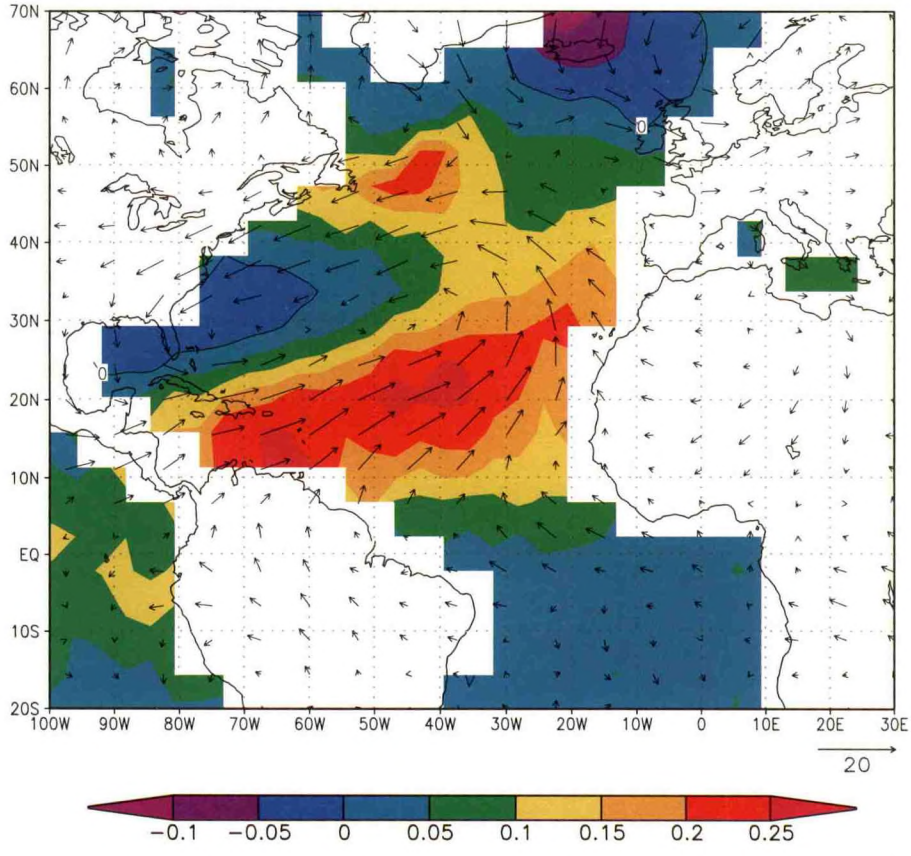

Fig. 1.13 First EOF of annual mean SST from the R15 coupled model computed over the domain from the Equator to 72°N, explaining 11.8% of the spatially integrated variance. The color shading denotes the regressions of the input SST values on the EOF time series, multiplied by the standard deviation of the EOF time series (these therefore represent typical SST anomalies associated with this EOF pattern). Superimposed on this are vectors denoting the regressions of surface winds on the EOF time series, multiplied by the standard deviation of the EOF time series. Units are °C for SST and cm s^{-1} for winds. These patterns are similar to those found in observations.

PLANS FY99

Work in the coming year with the R15 coupled model will focus on those areas in which such a fast, low-resolution model still plays a unique role in climate research. The 10,000 year integration will be analyzed to study natural variability on the 100-1,000 year time scale. Using the new nine-member ensemble of scenario integrations, which will likely be extended to more members, the emergence of the full variety of climatic signals from the noise of natural variability will be studied, and these integrations will be used as a test-bed for statistical methods that will be useful for future integrations with higher resolution models. Comparisons will be made between the multi-decadal thermohaline circulation variability in R15 and in the emerging long control integration with the R30 model. Finally, both the R15 and R30 models will continue to provide a testing ground for new techniques for initializing coupled models, and it will be upgraded as new ocean, atmosphere, land, and ice models are tested and become available.

1.5 HYDROLOGY AND CLIMATE

ACTIVITIES FY98

1.5.1 Summer Dryness in a R15 Scenario Integration

S. Manabe *R. Wetherald*

In a continuation of earlier work on the drying of continental interiors due to global warming (1473), this phenomenon has been re-examined in a R15 coupled model scenario run. Standard scenario forcing is used (1.1) except that three integrations are performed, one with equivalent CO_2 forcing alone and one with aerosol forcing alone, in addition to the standard case of CO_2 + aerosol forcing. The pattern of drying in the presence of CO_2 + aerosols is similar to that found in previous integrations: summer drying and winter moistening in middle-to-high latitudes of North America and southern Europe, but drying through most of the annual cycle in southern North America, where the percentage reduction of soil moisture during summer is particularly large. A similar pattern is seen in other semi-arid regions in subtropical to middle latitudes, such as central Asia and the area surrounding the Mediterranean Sea. An analysis of the central North American region (Fig. 1.14) indicates that the reduction of summertime soil moisture exceeds one standard deviation of the summertime mean soil moisture by around year 2030. The corresponding emergence of the runoff signal is even later. The inclusion of sulfate aerosols delays the reduction of soil moisture by several decades. Using the same measure, the model's temperature response in this region has already emerged from the variability by 1980. Surface air temperature in the model is clearly a better early indicator of global warming than hydrologic quantities, such as precipitation, runoff and soil moisture. The high climatic sensitivity of this model, more than 4 K for the equilibrium response to doubling CO_2, which is at the upper end of the range regarded as probable by the IPCC, should be kept in mind when considering these model responses.

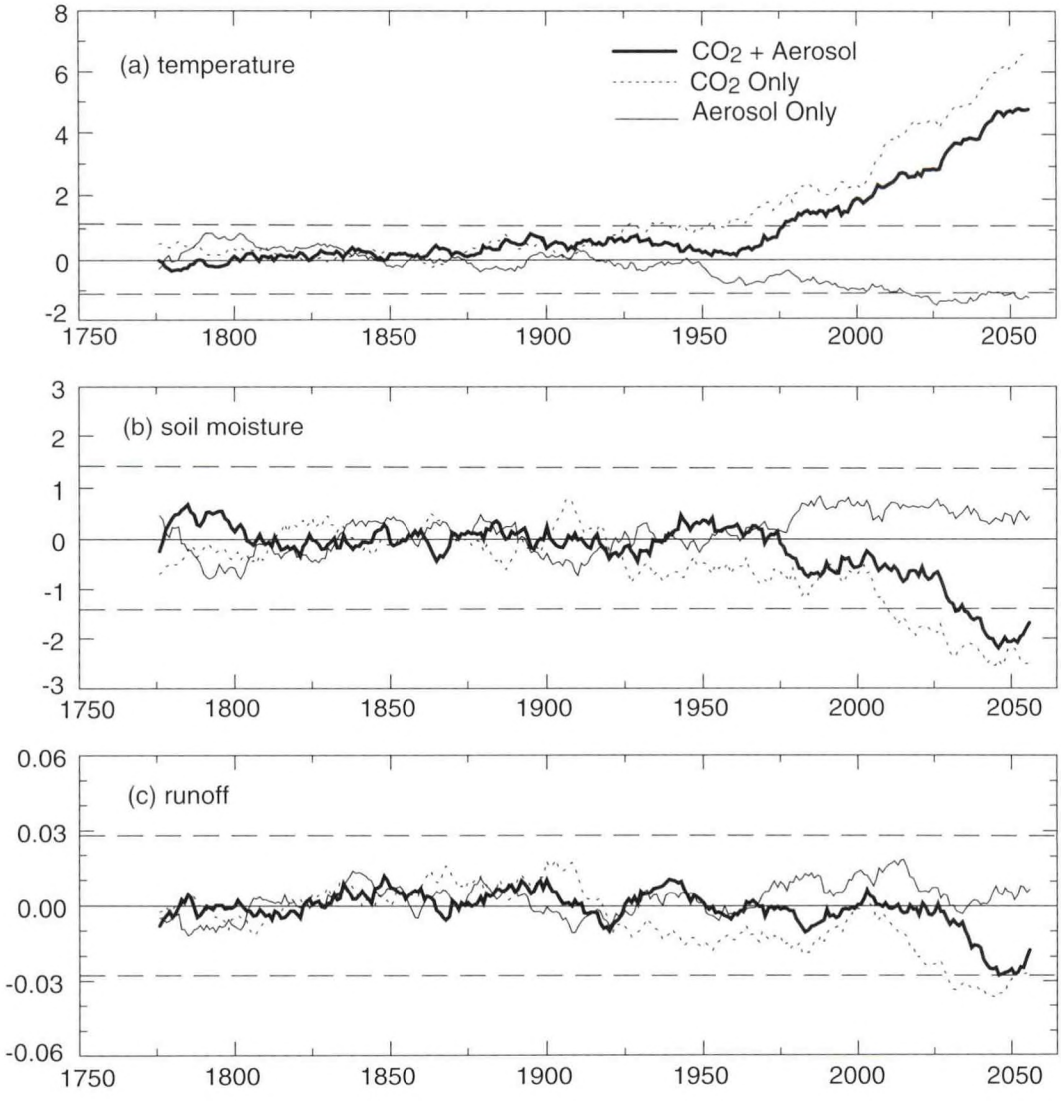

Fig. 1.14 Time series of area-averaged anomaly of (a) soil moisture (cm), (b) surface air temperature (°C) and (c) runoff (cm/day) for the central North American region for each of the three radiative forcings. Each time series consists of differences between the yearly June-July-August averages of the above quantities for each of the three integrations and the corresponding control integration over the entire 1000-year period for June-July-August. Also, each time series has been smoothed by a 20-year running mean. The two horizontal dashed lines denote one standard deviation of the control integrations.

1.5.2 Changes in Flood Frequency and Trends in River Discharge

K.A. Dunne *R.T. Wetherald*
P.C.D. Milly

The detectability of greenhouse-induced changes in extremes of river discharge has been examined using three R15 scenario runs and observational data from 45 large river basins, with periods of record typically 50-100 years. The corresponding model discharges were derived through a simple river-basin storage model, from global runoff fields generated in a 1000-year steady-climate experiment and from three standard scenario experiments (1.1).

Preliminary analyses suggest that changes in flow characteristics of individual rivers could generally not be detected until well into the 21st century. For this reason, and to simplify subsequent analysis, the pooling of discharge measures from multiple river basins was explored. Fig. 1.15 shows the results of such an analysis. It can be seen that the fraction of basins experiencing a 30-year flood (flood whose magnitude is equaled or exceeded, on average, once every 30 years) in any year has fluctuated around the expected value of 1/30 during the past century, with no obvious trend. Additionally, the fluctuations are consistent with those expected from the steady-climate and greenhouse-warming experiments. Only at the start of the 21st century does the climate change signal indicate a significant rise in the incidence of flooding within this set of basins. In general, the analyses to date suggest that any globally-extensive changes in flood frequencies associated with greenhouse warming are too small to be detected at this time.

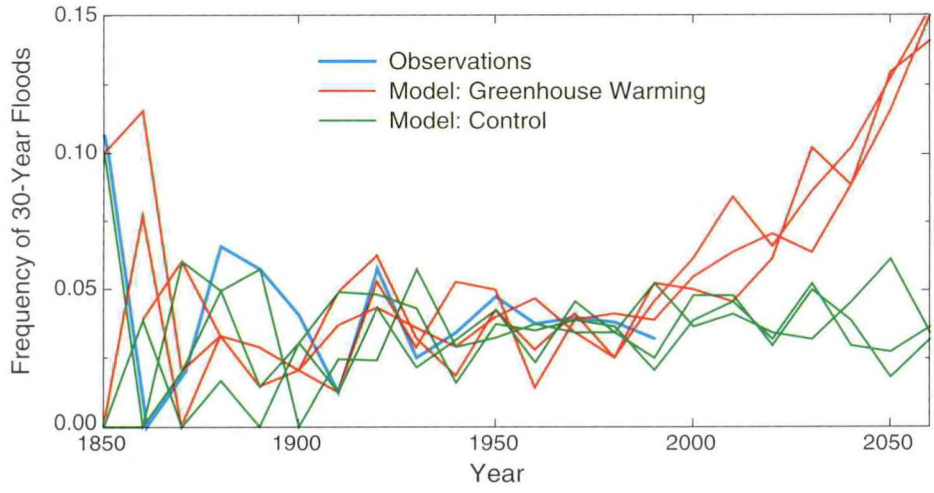

Fig. 1.15 Frequency of 30-year floods as function of time. Data averaged over 10-year periods centered around plotted time. The flood frequency is evaluated as the fraction of total active basins experiencing a 30-year flood. The number of active basins increases from 1 around 1850 to 43 around 1960 and thereafter; this explains the change in natural variability over time. (The three control curves are based on three separate portions of the 1000-year control run.)

Previous studies of 20th-century river discharge revealed an upward trend in combined mean runoff of nine major world rivers (gb). The +8% trend over the century (significant at the 99% level) appears to be too large to be easily explained by natural variability, increased water-use efficiency of ecosystems resulting from heightened atmospheric carbon-dioxide levels, or direct water-balance effects of deforestation. It is also much larger than trends predicted by the R15 scenario runs. Because the Amazon River has the largest mean flow of the nine rivers, and because its individual flow trend has the highest level of statistical significance (95%), it was chosen for further study. Preliminary analyses of precipitation records suggest that precipitation trends were insufficient to explain the flow rise. Furthermore, the largest increases in runoff appear to have occurred during the dry season. These factors point toward decreased dry-season evaporative demand as the cause of the flow rise. Decreased evaporative demand could be driven by increase in cloud cover. An alternative explanation is a reduction in surface solar radiation caused by increased smoke aerosols, transported into the basin from nearby regions of intensive biomass burning.

1.5.3 Sensitivity of the Global Water Cycle to Stomatal Resistance of Vegetation

K.A. Dunne *P.C.D. Milly*

A series of numerical experiments has been conducted with the R-15 climate model with fixed ocean temperatures to assess the sensitivity of the global water cycle to stomatal resistance of continental vegetation. Historically, GFDL climate models have not included any representation of this resistance. Its direct physical effect is to impede evaporation and latent heat flux from the land surface to the atmosphere. Thus, the direct effect of incorporating stomatal resistance into a model should be to decrease mean evaporation and thus increase runoff from land to oceans. An equilibrium climate has been calculated for bulk stomatal conductance equal to 100 m/s, an estimated realistic value. Fig. 1.16 shows the global field of change in annual mean runoff resulting from inclusion of bulk stomatal resistance in the model. In the tropics and south Asia, the computed increase in runoff (5-15 cm over large areas) is qualitatively consistent with the expected direct model response. In contrast, in the middle and high latitudes, the dominant response is a decrease in runoff.

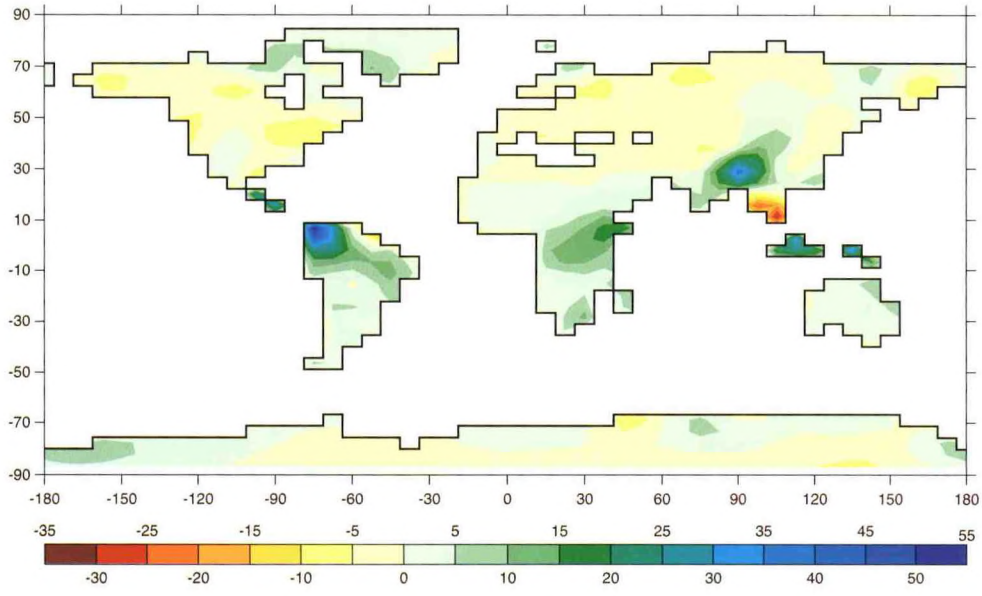

Fig. 1.16 Change in annual mean runoff (cm) induced by incorporating stomatal resistance into model.

PLANS FY99

The summertime drying of continental interiors and changes in river runoff will be studied with the expanding set of scenario integrations being performed with the R15 and R30 coupled models. In addition, the counter-intuitive effect of stomatal resistance on runoff will be analyzed. Work will also begin on a new class of land surface models for inclusion in the developing modular atmospheric modeling framework.

1.6 PALEOCLIMATE MODELING

ACTIVITIES FY98

1.6.1 Tropical Cooling at the Last Glacial Maximum

A. Broccoli

The ongoing investigation of the sensitivity of tropical temperature to glacial forcing continued during the past year. Using specifications of glacial forcing established by the Paleoclimate Modeling Intercomparison Project (PMIP), changes in continental ice, orbital parameters, atmospheric CO_2 and sea level were imposed in the R30 model coupled to a mixed layer ocean. These changes create a global mean radiative forcing of -4.20 W m^{-2}, with the vast majority of this forcing coming, in nearly equal portions, from the changes in continental ice and CO_2. In response, the model's global mean surface air temperature decreases by 4.0°C, with the largest cooling in the extratropical Northern Hemisphere. In the tropics, a more modest cooling of 2.0°C (averaged from 30°N to 30°S) is simulated, but with considerable spatial variability resulting from the interhemispheric asymmetry in radiative forcing, contrast between oceanic and continental response, advective effects, and changes in soil moisture. Analysis of the tropical energy balance reveals that the decrease in top-of-the-atmosphere longwave emission associated with the tropical cooling is balanced primarily by a combination of increased reflection of shortwave radiation by clouds and an increased atmospheric heat transport to the extratropics.

Comparisons with paleodata indicate that the overall tropical cooling simulated by this model is comparable to paleoceanographic reconstructions based on alkenones and species abundances of planktonic microogranisms. The most comprehensive paleotemperature reconstruction of this kind comes from the CLIMAP (Climate: Long Range Investigation Mapping and Prediction) Project, in which statistical transfer functions were used to estimate glacial sea surface temperatures from the abundances of planktonic microfossils in deep sea sediment cores. The zonal mean glacial anomalies simulated by the model are quite similar to those reconstructed by CLIMAP (Fig. 1.17). Other paleotemperature proxies, such as noble gases in aquifers, pollen, snow line depression, and the isotopic composition of corals, indicate a larger glacial cooling than that simulated by the model. The differences in the magnitude of the reconstructed tropical cooling among the different proxies preclude a definitive evaluation of the realism of the tropical sensitivity of the model. Nonetheless, the comparisons with paleodata suggest that it is unlikely that the model exaggerates the actual climate sensitivity in the tropics.

1.6.2 Climate Variations During the Last Glacial Cycle

A. Broccoli C. Jackson

Preparations have begun for an R15 atmosphere-mixed layer ocean model experiment intended to explore the contributions of changes in orbital parameters, continental ice extent, and atmospheric CO_2 content to climate variations during the past 120,000 years. This experiment is intended to investigate the internal workings of the climate system which communicated these three forcings to the paleoclimate record. Because an atmosphere-mixed layer ocean model will be used, mechanisms involving the atmosphere will be the focus. Pathways involving changes to the ocean's circulation will not be included

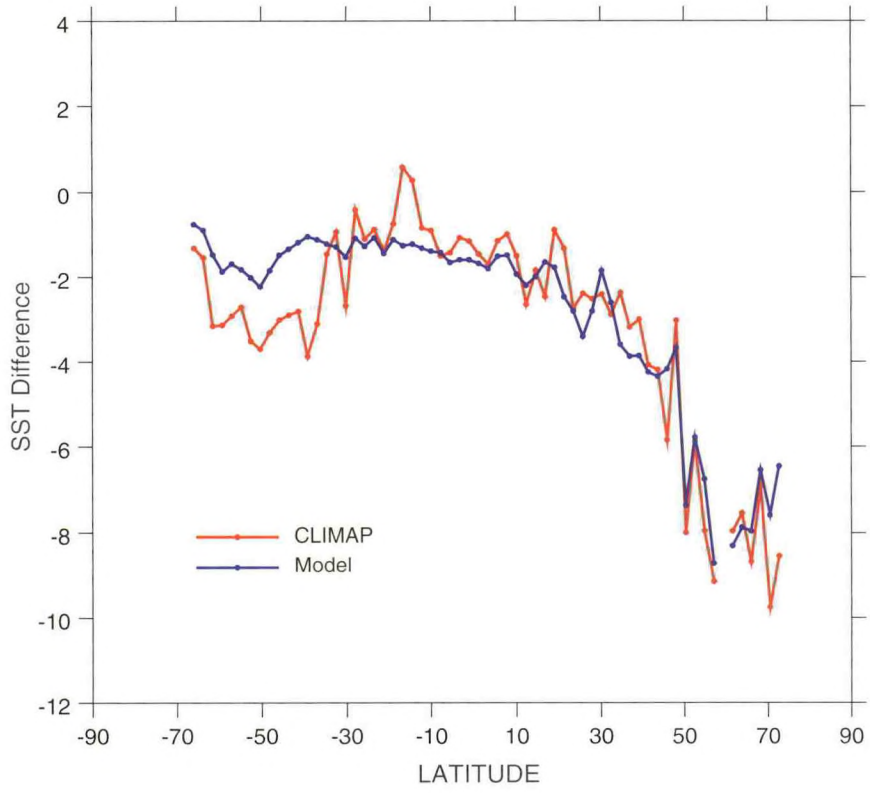

Fig. 1.17 Zonally averaged annual mean difference in sea surface temperature between last glacial maximum and present as reconstructed by CLIMAP (red) and simulated by the atmosphere-mixed layer ocean model (blue). Units are °C. Only model grid points containing CLIMAP data points enter the zonal averages.

because of the large computational cost. To further reduce the computational requirements, the variations in climate forcing will be accelerated by a factor of approximately 30, reducing the integration to a manageable 4,000 years, a strategy that is consistent with the relatively short response time of the atmosphere-mixed layer ocean system. The experimental design will provide time series information that can be directly compared to a variety of paleoclimatic data sets. Most of the work during the past year has dealt with two issues: developing temporally consistent time series for each of the climate forcings (orbital parameters, ice extent, and atmospheric greenhouse gas concentrations) and adapting the existing version of the model to produce suitable output.

1.6.3 Paleohydrological Analysis of the Lake Victoria Basin

P.C.D. Milly

Recent field investigations[4] at Lake Victoria have suggested that the lake was dry prior to 12,800 ^{14}C years ago. Through a simple water-balance analysis, it was subsequently inferred that precipitation in the drainage basin of Lake Victoria must have been smaller than its present value by at least a factor of 4 in order for the lake to remain dry[5]. This inference,

4. Johnson, T.C., C.A. Scholz, M.R. Talbot, K. Kelts, R.D. Rickets, G. Ngobi, K. Beuning, I. Ssemmanda, J.W. McGill, Late Pleistocene desiccation of Lake Victoria and rapid evolution of Cichlid fishes, *Science, 273*, 1091-1093, 1996.

together with the near-simultaneity of large lake-level changes at other locations on the globe, has been used to support the hypothesis of abrupt global climate change near the end of the most recent glaciation. In the present study, the water balance of Lake Victoria has been reconsidered, with attention to various feedbacks that would accompany regional drying. As precipitation decreases, not only does the runoff decrease, but the fraction of the precipitation that runs off decreases also, in response to general drying of the soil. This runoff feedback appears to be a major factor in the history of Lake Victoria. In contrast, the evaporation feedback, whereby lake-area reduction contributes to regional aridity and enhancement of evaporation from land, is apparently only a minor factor. Additionally, possible regional changes in surface radiation add significant uncertainty to the paleohydrologic analysis. Overall, the new analysis suggests a higher sensitivity of lake area to precipitation than previously recognized. A halving of precipitation in the Lake Victoria basin appears sufficient to dry out the lake. This revised estimate of lake sensitivity to precipitation makes it easier to explain the drying of Lake Victoria in terms of orbital forcing, without the need to invoke an abrupt shift in global atmospheric circulation.

PLANS FY99

The 120,000 year accelerated simulation of the last glacial cycle with the R15-mixed layer model will be generated, and the results will be compared to a variety of paleoclimatic time series. The experiment will be repeated forcing the model with only the changes in orbital parameters, ice sheets, or CO_2, in order to study how each of these forcings contributes to the total response.

1.7 LARGE-SCALE ATMOSPHERIC DYNAMICS

ACTIVITIES FY98

1.7.1 Extratropical Forcing of Tropical Interhemispheric Asymmetry

A. Broccoli

Evidence from a variety of climate simulations has been suggestive of a relationship between the latitude of the intertropical convergence zone (ITCZ) and the interhemispheric temperature contrast. An experiment has been performed to address this issue more directly, using a climate model with idealized continental geometry. The model geography includes two continents, symmetric about the equator, which produce approximately the same land fraction as the actual continents. Poleward of 40° latitude, seasonally varying but zonally uniform sea surface temperatures are prescribed in the control run in approximate agreement with observations; elsewhere, a mixed layer ocean is present, with a heat flux adjustment to mimic the poleward transport of heat by the ocean. The resulting climate resembles a more zonally symmetric version of the actual climate, with the tropical ocean temperature maximum and ITCZ migrating from the southern tropics in boreal winter to the northern tropics in boreal summer.

---

5. Broecker, W.S., D. Peteet, I. Hajdas, J. Lin, E. Clark, Antiphasing between rainfall in Africa's Rift Valley and North America's Great Basin, *Quat. Res.*, in press.

To create an asymmetry in extratropical forcing, a second run of the hybrid model was made in which 4°C positive (negative) surface temperature anomalies are imposed in the Northern (Southern) Hemisphere poleward of 40° latitude, in the region in which surface temperatures are prescribed. Any response of tropical climate to this perturbation must be transmitted through the model atmosphere. Dramatic changes in tropical circulation result, with a northward shift of ~6° in the latitude of the ITCZ and the generation of southerly anomalies in the tropical surface winds (Fig. 1.18). These features are most evident over oceanic regions, as monsoonal effects produce a more complicated pattern over the low latitude continents. The symmetric Hadley cell structure of the control experiment is replaced by a much more asymmetric structure in which the southern Hadley cell expands and intensifies at the expense of its northern counterpart.

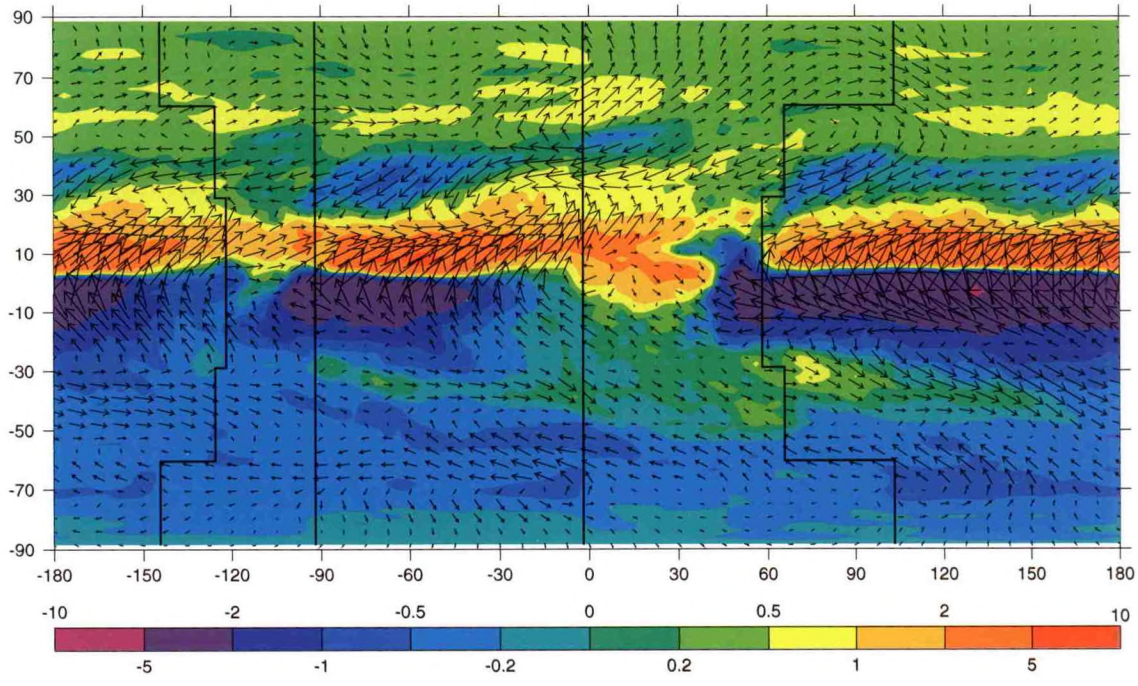

Fig. 1.18 Differences in annually averaged precipitation rate (colors, in mm d^{-1}) and surface winds (vectors) between warm northern extratropics/cold southern extratropics and control simulations with an idealized climate model.

This experiment clearly demonstrates that the ITCZ and the interhemispheric asymmetry of the Hadley circulation can be strongly influenced by extratropical forcing, a process that is likely to play an important role in the tropical response to ice age forcing and also in the transient response to global warming, in which there is substantial interhemispheric asymmetry in the extratropical climatic response.

1.7.2 Tropical Intraseasonal Oscillations

D. Golder *Y. Hayashi*

The sensitivity of tropical intraseasonal oscillations (TIOs) to cloud feedback has been examined using various R30 atmospheric models. The simulation of this oscillation continues to be a severe test of a model of the tropical atmosphere. Two separate modes of variability have

been isolated in analyses of atmospheric models (1118), one at 20-30 days and one at 40-50 days. The observations have power at 40-50 days, but very little at 20-30 days, whereas in some models the 20-30 day peak is as strong, or even stronger than the lower frequency peak. The relative magnitude of these two peaks has been found to be sensitive to cloud feedbacks in the model.

When the distribution of cloud cover is fixed at observed zonal-annual mean values, as in previous work, the model's 40-50-day oscillation has an amplitude comparable to that of the 20-30-day oscillations, contrary to observations. With predicted clouds the 40-50-day oscillation is strengthened and the 20-30-day oscillation weakened, in much better agreement with observations. However, this modification changes the mean tropical climate, which in turn affects the oscillations. By prescribing the distribution of daily values of cloud cover to be that obtained from a one-year run of the predicted-cloud model, the correlation of clouds with other variables can be eliminated while leaving the climatic mean nearly unaffected. This experiment leads to a more complex picture of the effects of the cloud feedback. The direct cloud-oscillation feedback does in fact weaken the 20-30-day oscillation, but does not affect the 40-50-day oscillation. The latter is strengthened in the predicted cloud model through the changes in basic state in the tropics. Space-time regression analysis of radiative damping and amplification rates has been used to help rationalize these results.

One candidate mechanism for exciting the TIO is evaporation-wind feedback (EWF), in which changes in low level winds modify the evaporation field, which then alters the distribution of latent heat release that drives the wind field. This mechanism has recently been studied in both idealized and realistic atmospheric model settings, extending previous idealized studies (1452). The idealized model with globally uniform sea surface temperature has an easterly zonal-mean surface flow in the tropics, which is thought to be conducive to EWF. When the zonal-mean zonal flow in the parameterized surface heat fluxes is replaced with weak westerlies, the TIOs weaken drastically, consistent with the EWF mechanism. Similarly, when the fluctuations in the wind speed of the surface heat fluxes are eliminated, the TIOs weaken drastically, again consistent with the EWF mechanism.

The results are different in the standard R30 model. In this model the surface winds in the tropical western-Pacific region (90°E-180°E, 30°N-30°S) are biased towards being weak easterlies rather than weak westerlies as observed. When the surface winds in the flux formulation are replaced by weak westerlies, the TIO does not weaken dramatically, contrary to the EWF mechanism. Similarly, when the fluctuations of the surface wind in the flux formulation are eliminated from the tropical region (30°N-30°S), the TIOs again do not weaken drastically. While one can create idealized models in which EWF is dominant, the TIOs are generated in other ways in more realistic models (1490).

1.7.3 Atmospheric Test of a Method for Estimating Oceanic Eddy Diffusivities

I. Held *P. Kushner*

G. Holloway[6] has proposed a simple scaling that relates the rms eddy sea-surface height as measured by satellite altimetry to the effective tracer diffusivity of oceanic

6. Holloway, G., Estimation of oceanic eddy transport from satellite altimetry. *Nature, 323,* 243-244, 1986.

mesoscale eddies. This scaling, which could be of importance in the effort to parameterize fluxes due to oceanic eddies, has been tested using atmospheric data, for which the energetic eddies are well resolved. Using NCEP/NCAR reanalysis data, a diffusive estimate for the heat flux, with a diffusivity obtained from the scaled height variance, has been compared to the actual heat flux. At a given height in the lower troposphere, the proposed scaling appears to be successful to within a fairly uniform proportionality factor, as shown in the Fig. 1.19. The results suggest that non-eddy resolving ocean GCMs require highly inhomogeneous diffusivities to match the inhomogeneity of the height variance in the altimeter data, and that the success of an eddy-resolving ocean model at reproducing the observed sea-surface height variability may also be a good measure of its ability to simulate the mesoscale eddy fluxes near the surface.

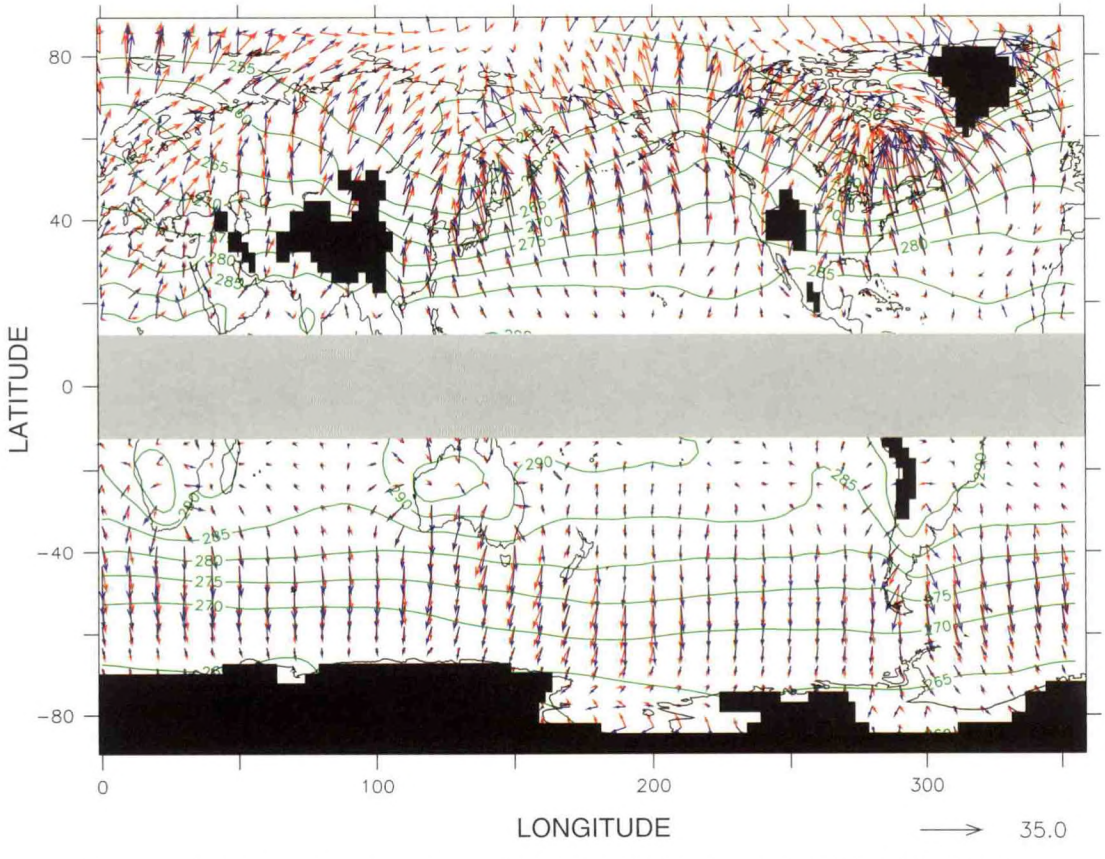

Fig. 1.19 Red arrows: divergent part of 850 mb heat flux for 1979-1995 DJF from NCEP/NCAR reanalysis data, 1979-1995. Blue arrows: divergent part of the 850 mb heat-flux estimate, which uses the diffusivity based on the rms eddy geopotential height, and which includes a best-fit scaling factor based on a linear regression between the meridional components of the two fluxes. Contours: 850 mb temperature; contour interval: 5 K. Equatorial areas are excluded (gray box), and topographic blockages are shown in black. The diffusive approximation simulates the observed fluxes very well.

This atmospheric analysis also confirms that diffusive models can be very useful in emulating eddy heat fluxes in the atmosphere. Despite the success of atmospheric GCMs, replacing the complex dynamics of such models with simple diffusive parameterizations would still be of great value for some applications, such as slow transitions in and out of ice ages. The

credibility of such models for climate studies is dependent on having a theory for the eddy diffusivities.

1.7.4 Linear Stochastic Models of the Midlatitude Storm Tracks

I. Held *Y. Zhang*
P. Kushner

In recent years, a new approach to developing an understanding of the horizontal structure of midlatitude eddy statistics based on linear theory has emerged, in which one attempts to mimic the statistically steady state of the atmosphere with a stable linear operator forced stochastically by white noise (Farrell and Ioannou (1995))[7]. Some success has been achieved recently in simulating a GCM's storm tracks with such a model (gr). This linear model passes the important test of being able to qualitatively simulate the "midwinter suppression" of the Pacific storm track, given the seasonal cycle of the three-dimensional mean flow. It is interesting that in this linear model, changes in the perturbations far upstream over Eurasia can influence the oceanic storm tracks. The extent of this influence is, however, sensitive to the manner in which one perturbs the atmosphere. As shown in Fig 1.20, if one forces the

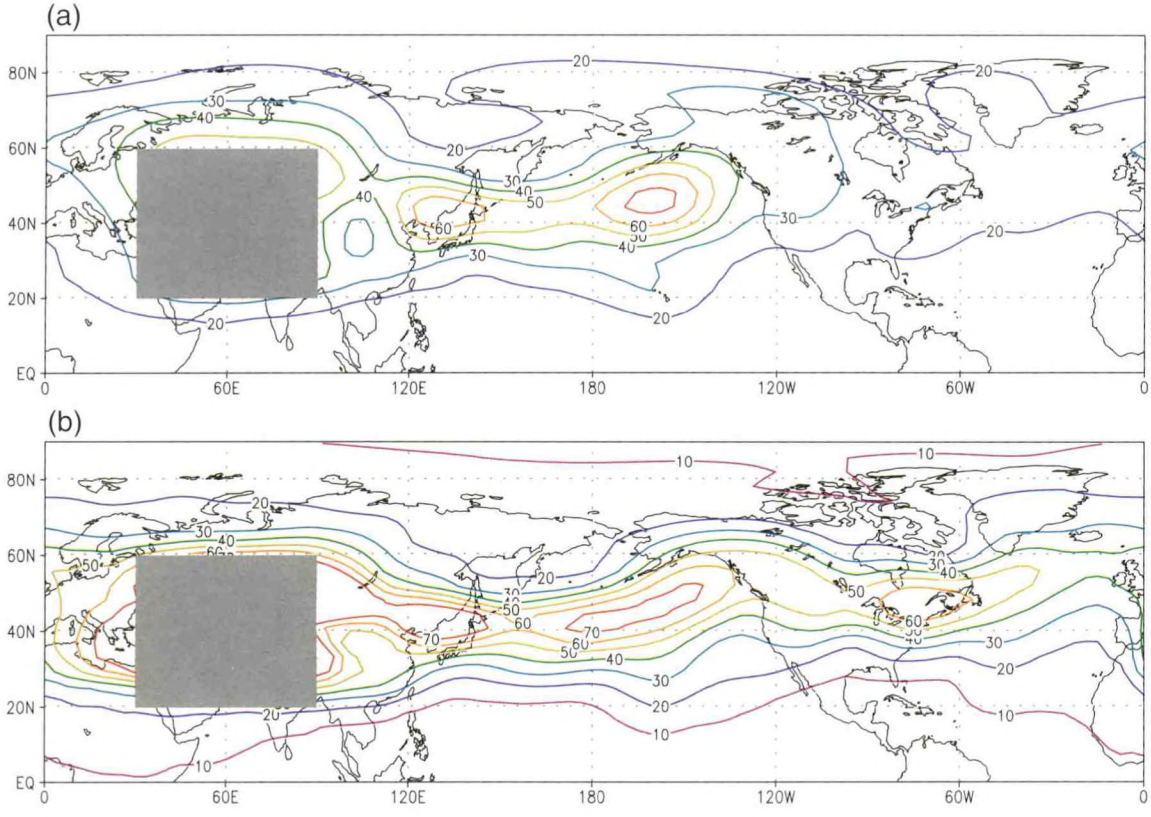

Fig. 1.20 Standard deviation of 300 mb geopotential height predicted by a linear stochastic model when perturbed within the black square in two different ways: (a) low-level temperature perturbations only; (b) temperature and vorticity perturbations throughout the troposphere. The strength of the Atlantic storm track is surprisingly sensitive to the details of the forcing over Asia.

7. Farrell, B., and P. Ioannou, Stochastic dynamics of the midlatitude jet. *J. Atmos. Sci., 52,* 1642-1656, 1995.

temperature equation in the lower troposphere only, within the shaded region over central Asia, as in the upper panel, the Pacific storm track is excited, but the eddies refract rather quickly into the tropics and do not generate an Atlantic storm track of the correct intensity. In contrast, if one perturbs both the temperature and vorticity equations of the linear model throughout the troposphere, within the same central Asian region, the Atlantic storm tracks is simulated more realistically. The dependence of the result on the details of the stirring, given the same linear operator, complicates the interpretation of such models but raises important questions about the factors that control the interaction between the two oceanic storm tracks.

1.7.5 Zonally Asymmetric Wave-Mean Flow Interaction Theory

I. Held *P. Kushner*

A new framework for examining wave–mean flow interaction for zonally asymmetric flows has been developed (fj). A satisfying theoretical foundation has been in place for many years for the analysis of zonally symmetric wave-mean flow interactions in atmospheric models and observations. But it is necessary to generalize this theory to apply to zonally asymmetric flows in order to study the interaction of the oceanic storm tracks with the time-mean flow. The new framework exploits the analogy between the flux of mass between density surfaces in stratified flow, which has played an important role in recent attempts at parameterizing eddy fluxes in the ocean, and the flux of mass between potential vorticity surfaces in two-dimensional horizontal flow. Results include the derivation of a residual-mean circulation formulation for two-dimensional and quasi-geostrophic dynamics, and points of contact with previous results in zonally asymmetric wave–mean-flow interaction theory. This approach helps explain in simple physical terms why there can be no simple "non-acceleration theorem" in the zonally asymmetric problem analogous to the well-known theorem in the zonally symmetric case.

1.7.6 The Surface Branch of the Zonally Averaged Mass Transport Circulation

I. Held *T. Schneider*

The mean meridional mass transport within isentropic layers in the atmosphere is characterized by poleward flow in the upper troposphere and equatorward flow in the lower troposphere. The lower branch of this circulation is difficult to visualize, and has rarely been examined in detail, because much of the equatorward flow occurs in layers that are interrupted by the surface. The structure of this near-surface branch of the overturning mass transport circulation has now been analyzed theoretically, supported by a diagnosis of the circulation in the R30 atmospheric model (gm). This analysis helps explain how the structure of the return flow is related to the probability distribution of the surface potential temperature (Fig. 1.21). In particular, an explanation is given for the fact that much of the equatorward mass transport occurs in isentropic layers that are colder than the mean surface potential temperature. This analysis also leads to an alternative formulation of the transformed Eulerian mean circulation in height-coordinates that corresponds more closely to the isentropic overturning.

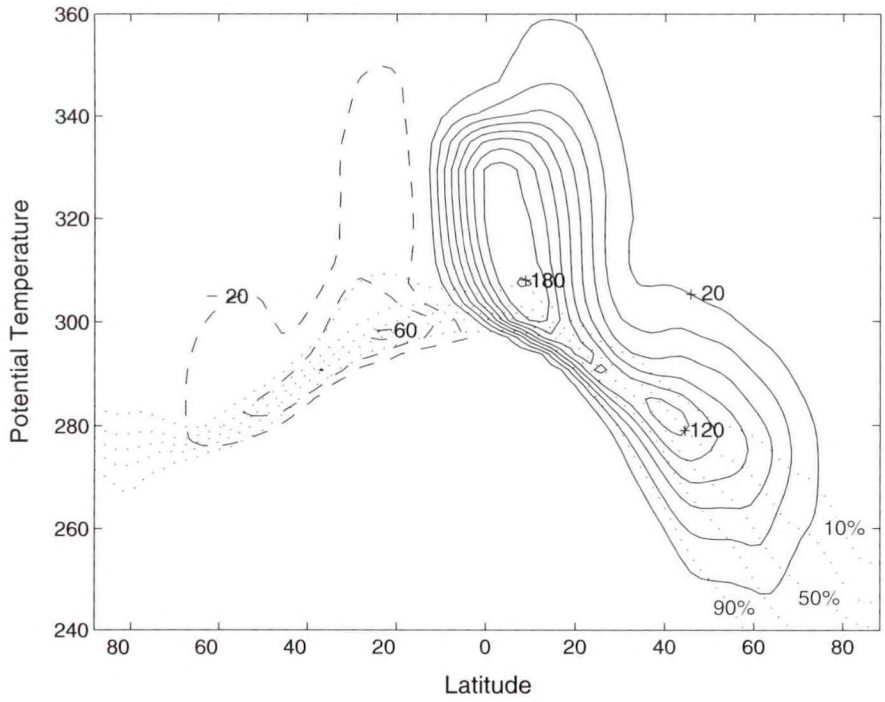

Fig. 1.21 The isentropic mass transport stream function in northern winter as simulated by an R30 atmospheric model (contour interval is 2 x 10^{10} kg/s). Also shown are the 10%, 30%, 50%, 70% and 90% isolines of the surface potential temperature distribution. The major part of the equatorial transport near the surface occurs at potential temperatures colder than the mean surface potential temperature.

1.8 PLANETARY FLUID DYNAMICS

G.P. Williams

ACTIVITIES FY98

Two of the most basic problems in GFD involve trying to understand the role of turbulent cascades and nonlinear coherent balances in the formation and maintenance of jet streams and planetary vortices, respectively. Successful theories for these processes must take into account their manifestation on the Jovian planets. The Jovian atmospheres may have close dynamical ties with Earth's atmosphere and oceans, exhibiting conventional GFD processes in new arrangements under different constraints that could help generalize and clarify theory. Jupiter appears to behave like a larger, faster-spinning Earth, but its unbounded vertical structure makes it behave more like the oceans than the atmosphere.

The main problem in defining Jupiter's meteorology, particularly the character of the jets and vortices, is that the nature and extent of the motions are not generally known for the region below the clouds. To develop a theory for the circulation, 3-D primitive equation models are used to examine the formation of the various turbulent and coherent phenomena for hypothetical vertical structures. The main hypotheses involved - that the atmospheric circulation occurs in a relatively thin layer and is driven by horizontal temperature variations - have been examined with a wide range of meteorological models over the years. Present

studies extend these models by considering the influence of the vertical structure more thoroughly.

The main questions concerning the formation and maintenance of jets and vortices in a planetary context are: 1) why do vortices exist and why do they last so much longer on Jupiter than in Earth's oceans; 2) what processes control the various single and multiple vortex states seen in the various anticyclonic zones; 3) how are the various jets generated in low- and mid-latitudes for unbounded atmospheres in a way that is consistent with vortex stability and genesis; and 4) what causes the onset of the equatorial super-rotation in such a multi jet-vortex system. Preliminary answers to these questions have been found that are mutually consistent and suggest possible vertical forms for the motions. These forms are also compatible with the vertical wind distribution measured by the "Galileo" probe (1454).

The main vortex sets on Jupiter are made up of the single Great Red Spot (GRS) at 22°S latitude, the three Large Ovals at 33°S latitude, and the dozen or so Small Ovals that occur at 41°S latitude; all are visible in Fig. 1.22. Calculations have been made in order to extend the theory for low latitude vortices such as the GRS to the midlatitude Ovals. For these calculations the primitive equation model is subjected to various hypothetical and experimental forms of heating function that are deemed appropriate for the Jovian configuration. Such models permit examination of how vortices are generated and how they are maintained when and if equilibration occurs. They also extend an earlier study of vortex genesis in spindown systems that was used mainly to isolate the preferred vertical structures for vortex longevity.

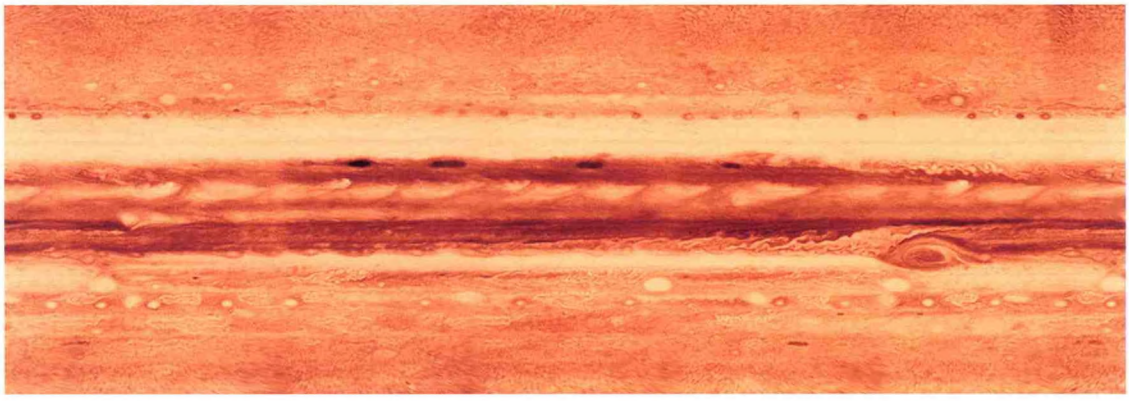

Fig. 1.22 This cylindrical projection of composited images of Jupiter taken by Voyager spacecraft in 1979 shows the three main vortex sets - the GRS, the 3 Large Ovals, the 12 Small Ovals - as they occur in the Southern Hemisphere at latitudes of 22°, 33°, and 41°, respectively. (Some overlap occurs in the longitudinal direction which extends ~400°.)

Realistic sets of equilibrated vortices have been produced in simulations of the three major groups, as shown in the example in Fig. 1.23. Such solutions reveal some similar traits among the three storm sets but also highlight some fundamental differences. For example, the Small Ovals are forms of cnoidal waves whereas the other two sets are more like solitary waves. They all exist, however, under similar physical conditions which support the basic vortex theory and its preferred structures and parameter range as derived earlier (1400).

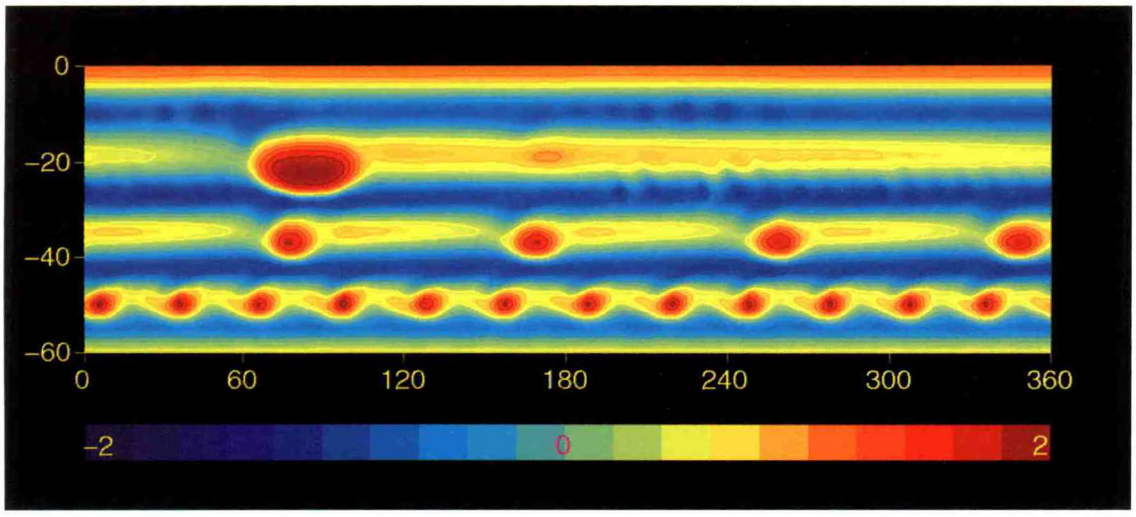

Fig. 1.23 The horizontal temperature field shows the equilibrated form, at 10,000 days, of three steady vortex sets lying in the anticyclonic zones between easterly and westerly jets. The vortices are generated by baroclinic instabilities and occur at similar latitudes and have the same relative sizes, velocities, and phase speeds as those of Jupiter's Great Red Spot, Large Ovals, and Small Ovals, becoming smaller, weaker and more numerous with increasing latitude. The Small Ovals become even smaller when their amplitude is reduced.

The main factors determining the characteristics of the three classes of vortices have been isolated from a wide range of calculations. Thus the dependence of the vortex scale, shape and number upon the jet amplitude and width, the dependence of equilibration and regenesis on the heating and dissipation time scales, and the dependence of migration on the flow depth and strength are now well understood quantitatively. Furthermore, the existence of optimal resolutions and dissipations give an implicit measure of the scale of the small eddies and their role in the overall circulation, which should greatly assist further model development.

PLANS FY99

Additional calculations will be made to produce global circulations that achieve a more complete synthesis of multiple jets and vortex sets in a Jovian context. Additional study of the processes underlying the genesis and equilibration of the different jets and vortices will also be carried out. The primitive equation models and analysis programs will be further developed, as needed.

2. ATMOSPHERIC PROCESSES

GOALS

To develop general circulation models for understanding the interactive three-dimensional radiative-dynamical-chemical-hydrological structure of the climate system from the surface and troposphere to the upper stratosphere and mesosphere on various time and space scales.

To employ meteorological observations in conjunction with models for diagnostic analyses of atmospheric processes, and for evaluating and improving parameterizations employed in weather and climate models.

To model the interactions between clouds, convection, radiation and large-scale dynamics and understand their roles in climate and climate change.

To model the physics, chemistry and transport of atmospheric trace gases and aerosols; to investigate the impact of future emissisions on regional and global air quality; and to investigate the regional and global climatic effects due to changes in natural and anthropogenic radiatively-active species.

2.1 RADIATIVE TRANSFER

S.M. Freidenreich *M.D. Schwarzkopf*
J. Haywood *B.J. Soden*
V. Ramaswamy

ACTIVITIES FY98

2.1.1 Solar Benchmark Computations

Computations of the suite of overcast sky cases initiated in A97/P98 were completed. These cases account for absorption by all the major gaseous constituents and clouds, with the calculations being performed using the "line-by-line + doubling-adding" (LBL+DA) technique. The high cloud case was performed using ice crystal optical parameters based on a formulation developed by Q. Fu of Dalhousie University. Additional benchmark cases were generated for both ice and water clouds, including geometrically thick systems, in order to focus on the absorption effect of large in-cloud vapor contents.

A collaborative research project investigating the direct radiative forcing due to sulfate aerosols, and which utilized GFDL's LBL+DA algorithm, has been completed (1569).

2.1.2 Characteristics of Solar Fluxes

An analysis of the near-infrared flux disposition in plane-parallel overcast sky cases has been completed (ga). Using the updated catalog of benchmark computations, this study has now been extended to include the complete solar spectrum. In particular, analysis has focused on whether the dependence of solar absorption on drop optical properties and location in the atmosphere, seen to be critical for the near-infrared spectrum, is also important for the total spectrum fluxes. This inquiry has particular relevance for notions about the invariance of solar absorption in clear and overcast atmospheres and for proposed methods that seek to obtain surface solar flux from satellite-measured top-of-the-atmosphere flux.

From Fig. 2.1a, it is apparent that the total solar flux absorbed in overcast atmospheres, besides differing considerably from the clear-sky case, is not the same when clouds at different altitudes (*e.g.*, 500-600 mb versus 800-900 mb case), different optical depths (τ_d), different size/shape of particles (CS-stratocumulus, CL-cumulonimbus, FU-ice crystals), and different geometrical thicknesses (*e.g.*, CS 180-900, 300-900 and 500-900 mb cases versus CS 800-900 mb) are considered. An especially interesting consequence is the relationship between cloud forcing at the surface and at the top of the atmosphere (TOA). Observational studies suggest that this ratio is nearly invariant, with an inferred value of ~1.5, while results from some parameterization model studies suggest a value of ~1.0. Fig. 2.1b shows the LBL+DA computed ratio for various model cloud cases, as a function of the drop optical depth, cloud type and location in the atmosphere. Note that the ratio is between 1.0 and 1.5 for all the cases considered. For $\tau_d > 5$, there is little dependence of this ratio on τ_d for a specific cloud type and location. Notable decreases with increasing τ_d are seen to occur for $\tau_d < 5$. Of greater significance is the variation that occurs among the cloud cases for a fixed τ_d, with absorptivity differences > 0.1 possible for the same cloud type located in the middle versus the lower troposphere. The computational results suggest that either the measurements and/or their interpretations leading to the inference of an invariant value are incorrect, or that solar radiative transfer in realistic atmospheres is somehow inconsistent with known radiative transfer principles. The results also suggest that the total solar surface forcing may not be simply estimated from a knowledge of the TOA forcing, without an accompanying knowledge of the properties of the cloud present.

2.1.3 Parameterization

The effect of the increased stratospheric heating associated with the new solar parameterization (A96/P97) was investigated utilizing the latest version of the N30 SKYHI GCM. Fig. 2.2 shows the change in the annual-mean stratospheric temperature obtained from a difference of 10-year runs with the old and the new shortwave schemes. Temperature increases of more than 2 K occur throughout the stratosphere, with increases of more than 4 K occurring in the upper stratosphere, due mostly to an improved accounting of the solar CO_2 heating. This improvement brings the modeled stratospheric temperatures into a better quantitative agreement with satellite observations, thus overcoming a deficiency noted for earlier model results using the older shortwave parameterization, *i.e.*, the long-acknowledged cold bias of the model's middle and upper stratosphere (A97/A98). The changes in high latitudes do not appear to be statistically significant due to the high degree of interannual variability there.

The new shortwave algorithm has now been tested against reference computations for the case of clouds containing ice crystals (in contrast to water drops, as reported in prior

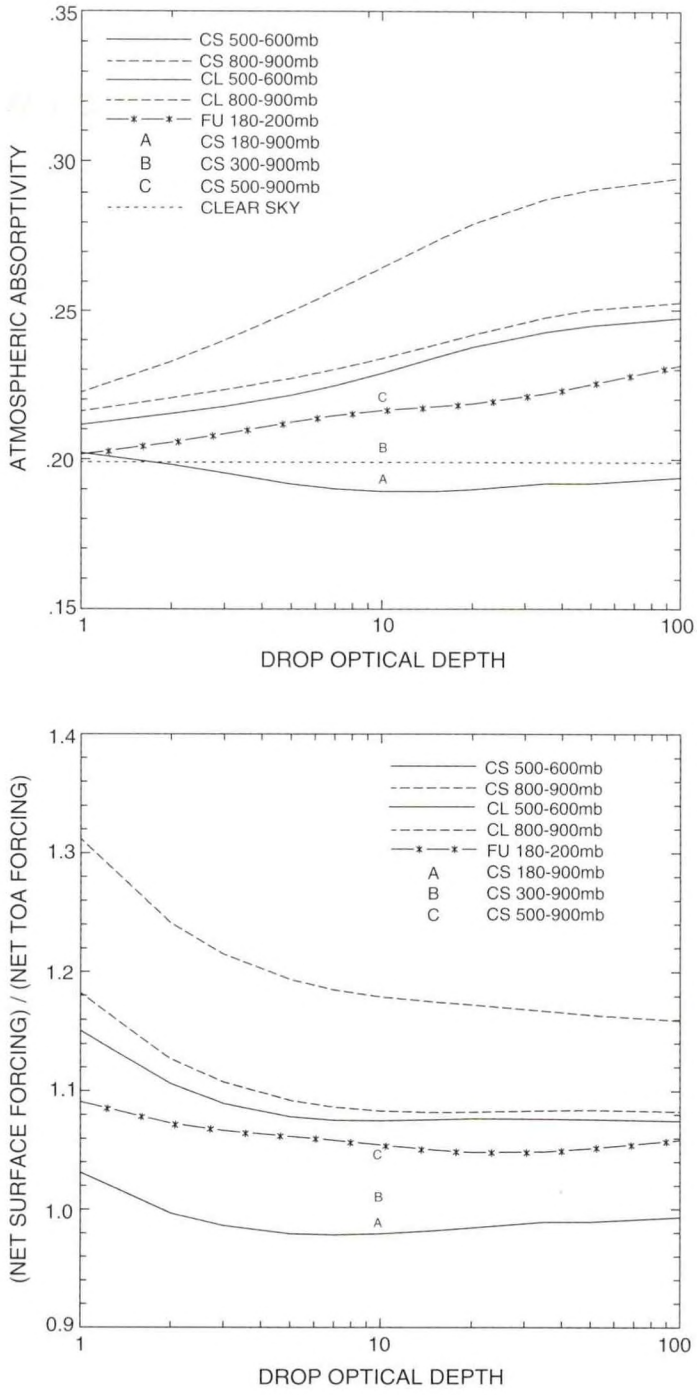

Fig. 2.1 (Top) Fraction of incident solar radiation absorbed in plane-parallel model clouds located at various altitudes in a midlatitude summer atmosphere. Solar zenith angle is 53 degrees. A, B and C denote calculations performed for clouds of different geometrical thicknesses, all having a drop optical depth of 10. Absorption in overcast atmospheres can be substantially different from that in clear skies, and varies considerably depending on cloud type and location. (Bottom) Ratio of the net solar forcing at the surface to that at the top-of-the-atmosphere. A value of 1 would indicate similar absorption as in clear sky. The ratios for model clouds is neither invariant as some studies have suggested nor are they close to 1 as indicated in some recent model investigations. Further, the computed values are not as high as the observed estimate of 1.5, which implies that model cloud atmospheres are not as highly absorbing as interpreted from some observational campaigns.

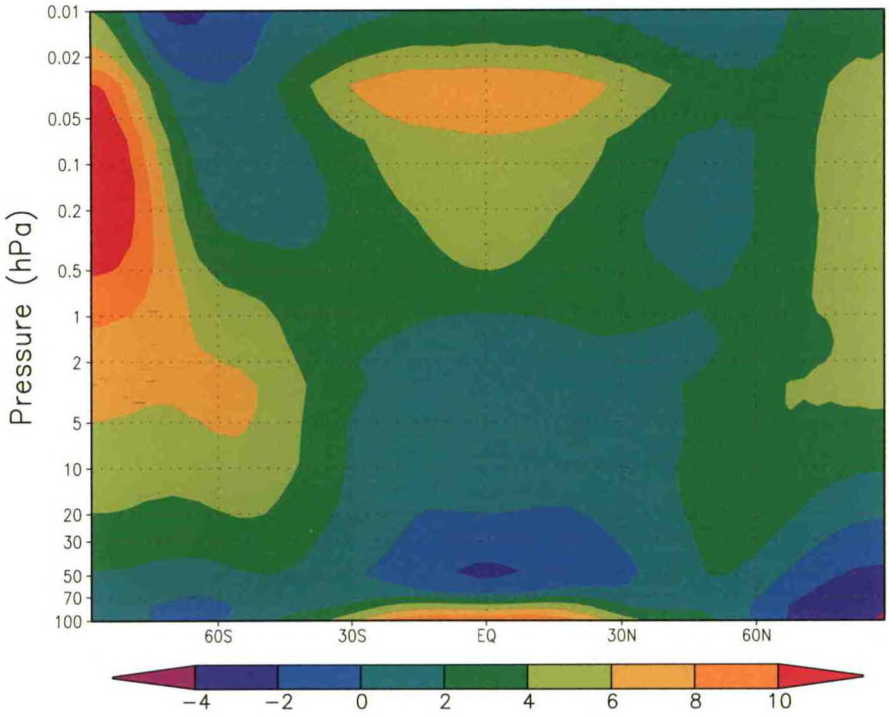

Fig. 2.2 Zonal, annual-mean change in the stratospheric temperature due to improvements in the shortwave radiation scheme. In particular, the improved accounting of CO_2 solar absorption leads to a warming of the middle and upper stratosphere. This alleviates considerably the cold bias noted when earlier model simulations were compared with recent satellite observations.

years). The parameterization reproduces the "exact" results reasonably well and hence should be suitable for application in models that consider ice crystal occurrences explicitly.

2.1.4 Clear-Sky Shortwave Radiative Flux

An investigation of the possible factors involved in accounting for the observed zonal and interannual variations of the clear-sky solar flux has been completed (1547).

Using the new shortwave parameterization, sea surface albedo values, and the known distributions of the atmospheric gases, the top-of-the-atmosphere outgoing solar flux was computed over oceanic regions for clear skies (*i.e.*, devoid of aerosols and clouds). The results were compared with the corresponding ERBE observations. It was found that the computed results underestimate the observed reflected flux by up to 12 W/m^2 in the annual-mean. The most likely reason for this bias is the reflective effects of aerosols in the real atmosphere. Calculations including aerosols suggest that both the naturally occurring sea-salt and anthropogenic sulfate, biomass and dust particles are contributing to the reflected flux in clear skies. Thus, it is concluded that the ERBE clear-sky flux measurements contain signatures of the aerosols' presence over the world's oceans.

PLANS FY99

The "benchmark" cases will continue to be analyzed for complex multi-layer clouds. The longwave radiation algorithm will be modified to account explicitly for non-gray aerosol and cloud absorption. Further computations of the effect of aerosols on the top-of-the-atmosphere and surface fluxes will be performed, and the quantitative roles of natural and anthropogenic aerosols will be analyzed.

2.2 CONVECTION-CLOUDS-RADIATION-CLIMATE INTERACTIONS

2.2.1 Cumulus Parameterization

L. Donner

ACTIVITIES FY98

A major, but elusive goal in parameterizing cumulus convection for general circulation models is to capture the interaction between deep cumulus towers and the mesoscale and synoptic-scale cloud systems in which they are embedded and in whose development they play important roles. The latter, spatially extensive cloud systems are major regulators of the earth's radiant energy system. A new conceptual framework for dealing with this problem has been developed (1133). The frequently used concept of mass-flux cumulus parameterizations was extended to include a statistical treatment of the vertical velocities in cumulus convection. These vertical velocities can be used to drive microphysics at physically appropriate scales, and thereby provide representations of the interactions between cumulus-scale clouds and larger-scale, radiatively important cloud systems (1349).

Preliminary testing of a parameterization built on this new framework in the SKYHI GCM is nearly complete. The parameterization produces plausible distributions for both deep cumulus towers and upper-tropospheric mesoscale circulations associated with deep convection. The mass fluxes associated with these upper-tropospheric stratiform systems are significant fractions of those in the deep cumulus towers, in accordance with observational studies. The vertical penetration of heat and moisture produced by this cumulus parameterization is significantly deeper than that associated with the saturated adiabatic adjustment currently used in SKYHI.

PLANS FY99

Final testing of the parameterization will be completed. The impact of cumulus convection on the climate and climate sensitivity of SKYHI will be evaluated. Cloud-convection-radiation interactions will be examined, including the relationship between deep convective systems and other upper-tropospheric cloud systems (1502).

2.2.2 Limited-Area Nonhydrostatic Models

C. Andronache *T. Reisin*
L. Donner *C. Seman*
R. Hemler

ACTIVITIES FY98

An ongoing study of deep convection and its associated mesoscale circulations using the Lipps-Hemler (885) cloud-system model (fy) focused on the structure of tropical convective systems, the role of these systems as sources of heat and sinks of moisture for larger-scale flows, the relationship of the behavior of these systems to the properties of larger-scale flows, and the transport and transformation of atmospheric sulfate by these systems.

The cloud-system model was used to study deep convection and associated mesoscale circulations for a composite easterly wave in the tropical eastern Atlantic Ocean (fy) and a westerly wind burst in the tropical western Pacific Ocean. The model successfully captures the observed life cycles of deep convection, which begin with deep cumulus towers and end with mesoscale stratiform systems in the upper troposphere. These studies revealed that very strong interactions between radiation and convection can occur under some circumstances. The extent to which these radiative-convective interactions proceed depends strongly on the manner in which ice microphysics is treated in the cloud-system model and, in particular, the rate at which ice crystals are removed by sedimentation.

The cloud-system model was also used to simulate sulfate-cloud interactions in the western tropical Pacific (1537, 1543). The model included a new, detailed sulfate aerosol microphysics scheme, designed to estimate the effects of sulfate on cloud microphysics and radiative properties, and the effects of deep convection on the transport and redistribution of aerosol. Model results showed that the presence of convective clouds has a significant impact on the spatial and temporal distribution of sulfur species. An instantaneous simulated total sulfate concentration in the cloudy domain in the western Pacific is illustrated in Fig. 2.3 for a case with high sulfur from the Pacific Exploratory Mission West B (PEM West B) observations during February-March 1994. Increases in sulfate as observed during PEM West B cause a significant decrease of the effective radius of cloud droplets, an increase in the cloud droplet concentration, and an increase of the shortwave reflection above clouds.

PLANS FY99

Treatments for microphysics and radiation in the cloud-system model will be modified. The current radiative treatment of ice crystals as small, spherical particles will be replaced with an approach in which the ice particles are treated as larger crystals. Techniques such as geometric ray tracing will be used to model radiative transfer through ice (1502). The formulation for ice sedimentation will probably be changed from its current form, in which cloud ice does not fall unless snow is also present (fy). Most likely, an approach will be used in which cloud ice falls at terminal speeds which depend on ice concentration. Shortwave and longwave fluxes at the top of the atmosphere and the surface observed in recent field experiments in the tropical western Pacific, will be used to constrain the radiative and microphysical parameterizations in the cloud-system model.

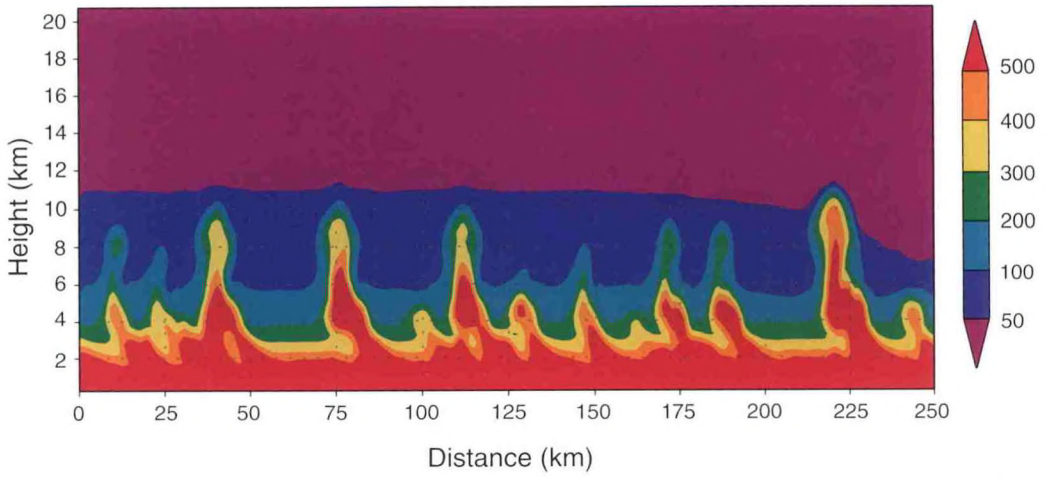

Fig. 2.3 Instantaneous distribution of the model simulated total sulfate concentration in a cloudy domain along an east-west line centered on 2°S-156°E at t=12 hours UT, December 20, 1992. Conditions correspond to a polluted case from PEM West B. Units are ng kg^{-1}. Substantial vertical penetration of sulfate by convective transport and chemical transformation is evident.

The relationships described to date between sulfate concentration and the radiative properties of cloud systems (1537, 1543) are based on empirical data. However, using a new approach to the treatment of particle sizes in the cloud-system model, in which several moments of the size distributions for microphysical species are treated as prognostic variables, a more general approach may be possible and will be investigated. This strategy will be pursued in FY99.

2.2.3 Radiative-Convective Equilibria with Explicit Moist Convection

V. Balaji *O. Pauluis*
I. Held

ACTIVITIES FY98

Simulations of radiative-convective equilibrium in a horizontally homogeneous atmosphere are being conducted with a cloud-resolving nonhydrostatic model. These integrations address fundamental issues in the theory of moist convective turbulence and cloud-radiative feedbacks. The studies are being carried out with both two- and three-dimensional models at various resolutions with a vertically stretched grid and cyclic lateral boundary conditions.

Recent focus has returned to detailed studies of the energy and entropy budgets of the two-dimensional model. This analysis has led to the significant finding that an important way in which kinetic energy is dissipated in the model is through the force exerted by precipitation. From a microscopic perspective, the surprising implication is that a large part of the kinetic energy dissipation occurs in shears in the immediate vicinity of falling hydrometeors and is not a consequence of a turbulent cascade to small scales. A simple theory has been developed that relates the energy dissipation associated with falling hydrometeors to the precipitation rate and the average distance that a hydrometeor falls. The resulting estimate for

the global mean of this term, which has been neglected in all discussion of energy dissipation in the atmosphere, is surprisingly large: 1.5 W/m^2. This is comparable to classical estimates of the frictional loss of kinetic energy from large scales that occurs in the planetary boundary layer.

The entropy budget also has surprising features. In particular, kinetic energy dissipation is not the dominant irreversible source of entropy; rather, the evaporation of water into unsaturated air is the dominant term. This complexity in the entropy budget and in the sources of kinetic energy dissipation cast doubt on the viability of several recent theories that use the entropy budget to constrain convective velocity scales and the average CAPE (convective available potential energy) of the tropical atmosphere.

Insights into the energy and entropy budgets, as well as other features of moist-convective turbulence, has been gained by varying the value of the latent heat of condensation and studying the consequences for radiative-convective equilibria. This series of integrations includes the limit of zero latent heating, in which water vapor is simply a passive tracer in a dry radiative-convective model. Convection in the dry limit is found to penetrate and overshoot radiative equilibrium at the tropopause much more dramatically than in the case with realistic latent heating, forming a sharp inversion at the tropopause.

Preliminary radiative-convective equilibrium calculations have been performed with the three-dimensional model with 2 km resolution and a 128 x 128 grid, fully interactive cloud-radiation feedback with two different values of surface temperature (25° and 30°C) and two different treatments of the ice microphysics. Differences in microphysics cause dramatic changes in the upper level cloud cover and in the dynamics of the convection in the upper troposphere. This sensitivity to the microphysical assumptions is currently the most serious limitation to the utilization of this model for a variety of purposes.

PLANS FY99

The study of radiative-convective equilibria as a function of the strength of the latent heating will be pursued, as well as the energy and entropy budget analyses. Experimentation with the three-dimensional model will continue, as well. In addition, the study of inhomogeneous statistically steady states will begin with a model of a Walker cell in a relatively small domain in which the surface temperature possesses an east-west gradient.

2.2.4 Physical Parameterization Tests in Single Column Models

S.A. Klein *B. Wyman*

ACTIVITIES FY98

The parameterization of cloud microphysics and convection is a source of large uncertainty in simulations by general circulation models. A creative way to test physical parameterizations is to simulate the vertical structure of temperature, water vapor and clouds at a single point. In these so-called "single-column" models (SCMs), the effects of large-scale dynamics must be specified. If they are specified from observations, then the predictions of

the SCM, which are the result of the interaction between the specified forcing and the physical parameterizations, can be compared to observations taken at the same point.

Tests of the model parameterizations in the flexible/modular modeling system (3.1.1) have been carried out with forcing specified by data taken from the Atmospheric Radiation Measurement (ARM) program's Oklahoma site in July 1995. The results of these tests have been submitted to an intercomparison project of SCMs from other major research labs (NCAR, ECHAM, etc.). Results indicate that the GFDL SCM's temperature tends to drift warm in simulations relative to ARM data, but that this error is common to many of the other SCMs.

SCMs can also be used to demonstrate the sensitivity of model simulations to physical parameterizations. An example of this is shown in Fig. 2.4, which shows how the predicted amount of cloud liquid plus ice differs when the convection scheme is changed from the Relaxed Arakawa-Schubert (RAS) parameterization to Moist Convective Adjustment (MCA). The simulated cloud field occurs at a higher altitude (lower pressure) when RAS is used. This reflects the fact that RAS is a significantly more penetrative scheme and detrains water vapor at a higher altitude than MCA.

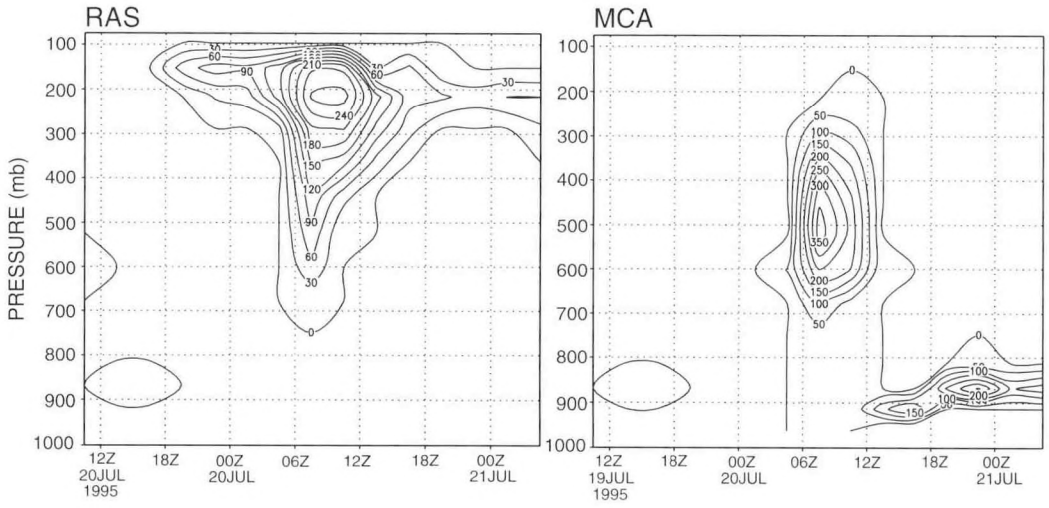

Fig. 2.4 The time evolution of the vertical profile of the amount of cloud liquid and ice from the GFDL Single Column Model (SCM) when forced by data taken at the Oklahoma field site of the Atmospheric Radiation Measurement (ARM) program in July 1995. In the left figure, the GFDL SCM is run with the Relaxed-Arakawa Schubert (RAS) convection scheme, whereas in the right figure, the model is run with the Moist Convective Adjustment (MCA) scheme. The choice of convection scheme has a large impact on the simulated distribution of clouds.

PLANS FY99

Participation in the SCM program of ARM will continue. It is anticipated that tests of the SCM will occur for other seasons using data from ARM. In addition, as new parameterizations become available, they will be evaluated in the SCM with ARM data.

2.2.5 "Predicted" Cloud Distributions in SKYHI

S.M. Freidenreich *V. Ramaswamy*
R. Hemler *M.D. Schwarzkopf*

ACTIVITIES FY98

The SKYHI GCM integration using the new cloud prediction scheme with "part black" high clouds (A97/P98) has been extended to include a period of 10 model years. Comparison of this GCM simulation with a 10-year simulation using the standard prescribed-cloud distribution indicates that the predicted-cloud approach leads to increased diabatic heating in the upper troposphere, and yields significant improvements in the simulation of upper tropospheric temperatures and lower stratospheric water vapor mixing ratios.

Figure 2.5 displays the 10-year average differences in the zonally averaged temperature and fractional change in the mixing ratio between the two simulations. Changes in the zonally averaged fractional cloud amount are similar to January results (A97/P98). The increase in temperatures in the tropical upper troposphere (100-150 hPa) exceeds 4 K, and attains ~8 K near the equator. This confirms the robustness of the results previously reported (A97/P98). The H_2O mixing ratio increases in the stratosphere by at least a factor of 2, with increases of a factor of 4 in much of the lower stratosphere. This moistening represents a significant improvement in the GCM water vapor simulation of this region. The results demonstrate that the global stratospheric water vapor amount depends on cloud-convective-radiative interactions occurring in the troposphere.

PLANS FY99

SKYHI GCM calculations with increased horizontal and vertical resolution are planned. Tests of the effects of modified cloud prediction schemes and boundary layer formulations on the cloud, moisture and temperature distributions will be pursued.

2.3 ATMOSPHERIC CHEMISTRY AND TRANSPORT

ACTIVITIES FY98

2.3.1 Tropospheric Photochemistry

A. Klonecki *H. Levy II*

HO_x radicals are the key to chemical reactivity in the troposphere and acetone is considered to be an important source of them in the upper troposphere, where mixing ratios of water vapor are small. Reactions of acetone and its derivatives were added to the box model that is used to calculate the tables of ozone production and destruction (A97/P98). The GFDL Global Chemical Transport Model (GCTM) ozone simulation run with tables that included the additional source of HO_x from acetone showed that the impact of introducing acetone is greatest at the top tropospheric level of the model (190 mb) and decreases quickly for lower levels. The simulated impact on OH at this level for the month of July varies between 10% in the moist region over southeast Asia to more than 50% in some regions of the

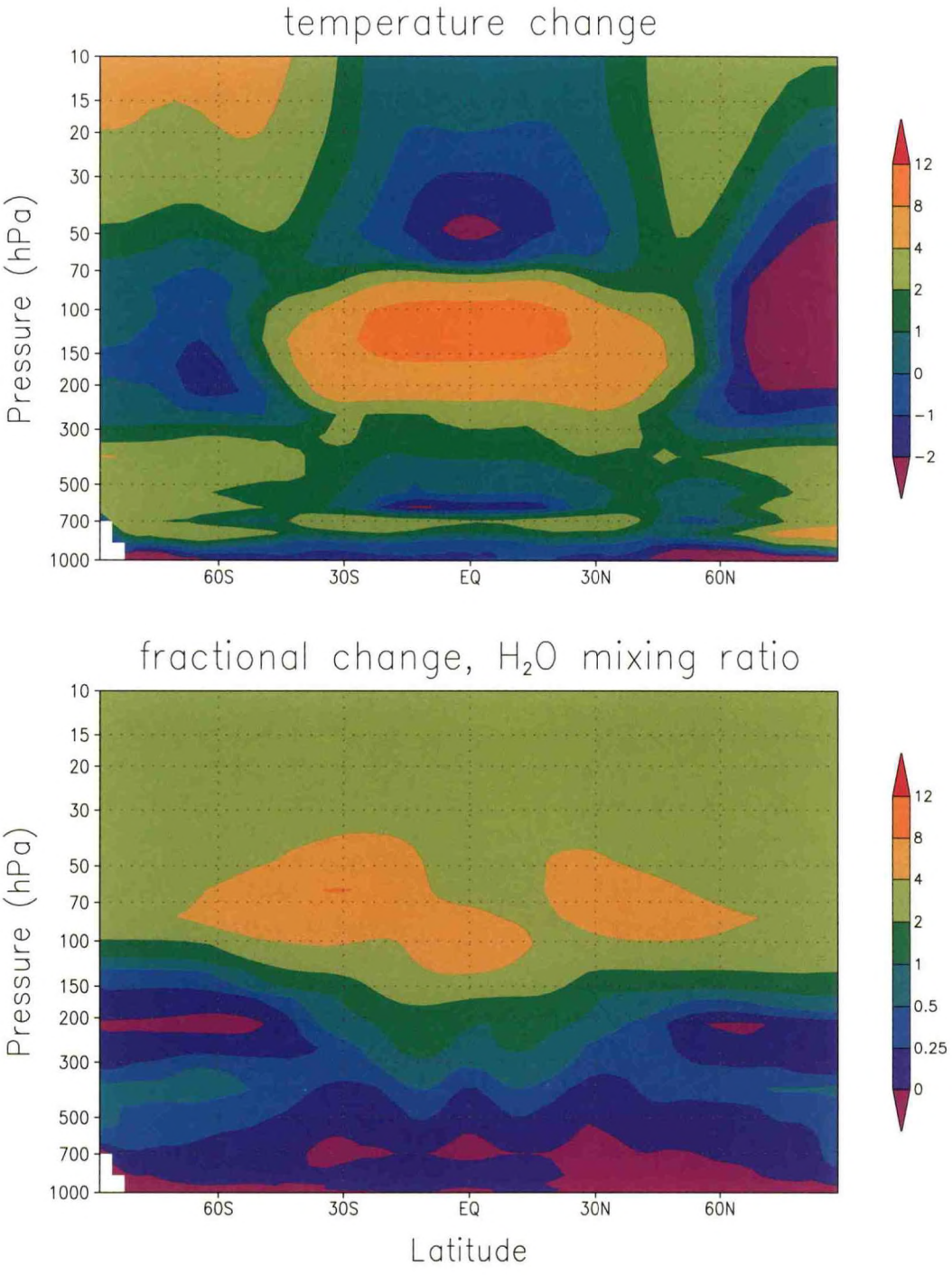

Fig. 2.5 Difference between the SKYHI predicted-cloud and prescribed-cloud temperature (K) (top panel) and fractional change in moisture (bottom panel) simulations for a 10-year annual average. The increase in upper tropospheric temperature and in lower stratospheric moisture makes the predicted-cloud simulation more realistic than the prescribed-cloud case. Differences in polar regions are not statistically significant.

Southern Hemisphere. At lower altitudes, the acetone-induced change in OH is much smaller, generally less than 10% by 315 mb.

The associated changes in the chemical ozone production follow the absolute changes in the concentration of OH, so these changes are also greatest in the tropics and subtropics at 190 mb, where it increases by 0.25 to 1.00 ppbv/day, amounting to a 50 to 100% increase. At 315 mb, the largest increase in ozone production due to acetone is only 10-20%. The influence on ozone itself is much less, with the increased production leading to only 5-10% more ozone in the tropics at 190 mb, and progressively less at lower altitudes. In summary, while acetone plays a major role in HO_x chemistry of the upper troposphere, the resulting impact on ozone levels is minor.

2.3.2 Fast Photochemical Solver Development

A. Klonecki *S.W. Wang*
H. Levy II

In current GCTMs with *in situ* chemistry, 75-90% of the computational time is spent determining the chemical tendency terms for the continuity equations of the transported species. A recent effort has begun to examine an approach whereby, after a one-time off-line expenditure of significant computational resources, on-line chemical tendency terms, which are equivalent to those produced by a full on-line chemistry, can be calculated very rapidly.

The High Dimensional Model Representation (HDMR) method was used to construct the Fully Equivalent Operational Model (FEOM) of $CO\text{-}CH_4\text{-}NO_y\text{-}H_2O$ chemistry for calculating the O_3 chemical tendencies. The HDMR method maps out the relationship between sets of high dimensional input variables and output variables through explicit algebraic equations which can be rapidly evaluated. These explicit algebraic equations constitute the core of the FEOM, in contrast to the ordinary differential equations which normally must be solved to generate the chemical tendencies. The FEOM can then be used in place of the current look-up tables in the GCTM for obtaining the time-dependent chemical production and destruction terms of ozone, as well as OH and the O_3 net chemical tendency, for all model levels, all months, every 10° band of latitude, and all tropospheric values of H_2O, CO, NO_x and O_3. This represents a first step in the development of a FEOM for the complex non-methane hydrocarbon chemistry of the full troposphere, including the polluted continental boundary layer. While calculated off-line, the FEOM is expected to reproduce the chemical tendencies resulting from a fully time-dependent on-line chemical model, while requiring much less on-line computation.

2.3.3 Tropospheric Carbon Monoxide

T.A. Holloway *H. Levy II*
*P.S. Kasibhatla**

**Duke University*

Carbon monoxide (CO) plays both a primary and secondary role in determining air quality. In urban areas with large CO emissions, concentrations can be large enough to cause health problems. However, even far from its emission source, CO affects air quality as part of catalytic ozone production and destruction cycles, and as an important sink for OH radicals.

The lifetime of CO varies from about 15 days to more than one year, which is long enough to transport CO long distances and affect air quality throughout the hemisphere. Thus, the chemistry and transport of CO, as well as its emissions, must be considered when examining air quality globally.

The GFDL three-dimensional GCTM was used to examine the evolution and distribution of carbon monoxide, and to investigate the specific role of each contributing source: fossil fuel emissions, biomass burning, oxidation of biogenic hydrocarbons, and oxidation of methane. An understanding of the global CO budget will aid analyses of tropospheric ozone, evaluations of emission estimates for contributing sources, and should lead to improvements in the calculation of global hydroxyl concentrations. Model results were compared with observations from the 33 CMDL/NOAA global cooperative flask sampling network stations which measure CO. Over most of the globe there is good agreement, with only 14% of seasonal averages differing by more than 25% between model and observations. For all of these outliers (18 points out of 132), the model overestimated CO concentrations, thus revealing a high bias to the simulation. An investigation into the specific causes for model discrepancies is underway. In the Southern Hemisphere, an overestimation of CO from biogenic hydrocarbons is a likely source of error.

2.3.4 Tropospheric Reactive Nitrogen

*P.S. Kasibhatla** *W.J. Moxim*
A. Klonecki *J.J. Yienger***
H. Levy II

**Duke University*
***University of Iowa*

The 11-level GFDL GCTM has been used to simulate the tropospheric fields of NO_x, PAN, HNO_3, NO_y, and NO_3-deposition, which are then evaluated with available observations from surface stations and aircraft missions and analyzed for the contributions of individual natural and anthropogenic sources. This simulation includes all known sources of tropospheric NO_x, transports three families (nitrogen oxides, PAN, HNO_3), and employs pre-calculated chemical conversions among them. With the exception of outliers due to either anomalous local observations or local errors in the GCTM's NO_x source and simulated precipitation, the GCTM's HNO_3 wet deposition is highly correlated with observations and clearly captures the observed spatial patterns of wet deposition. However, there appears to be a significant positive bias (~20%) in the simulated U.S. deposition, though not for the rest of the world. The GCTM's NO_x fields are in reasonable agreement with the large majority of the observations, show no systematic global biases, display the observed vertical profiles, have high levels (~1 ppbv or greater) in the polluted boundary layer (BL), and the very low values in the remote BL. At Mauna Loa Observatory, while summer and fall simulated NO_x is clearly in deficit, the PAN is in surplus and the sum of the two agrees well with observations. In general, the level of agreement between simulation and observation is as good as the agreement between separate, but simultaneous observations of NO, NO_x or NO_y.

The BL sources of NO_x, which are primarily anthropogenic, exceed free tropospheric (FT) emissions, which are primarily natural, by more than 8:1 and completely dominate lower tropospheric NO_x levels (except for very remote regions where BL and FT sources have a comparable impact). At higher altitudes, the smaller FT sources play a larger role and generally

dominate in the upper troposphere. A more detailed analysis of individual natural and anthropogenic NO_x source contributions is shown in Fig. 2.6. Anthropogenic emissions from surface fossil fuel combustion and biomass burning dominate in the lowest layers with a significant contribution from biogenic emissions in remote regions that do not have biomass burning. In the lower troposphere, surface fossil fuel combustion dominates in the Northern Hemisphere (NH) extratropics, while lightning is the primary source in the tropics and biomass burning plays a major role in much of the Southern Hemisphere (SH). In the middle troposphere, lightning dominates in both the tropics and much of the midlatitudes, while transported surface fossil fuel emissions supply the NH high latitudes, and transported emissions from biomass burning do the same in much of the SH. In the upper troposphere, lightning dominance extends farther poleward, while stratospheric injection is the major source in the NH high latitudes. Remnants of biomass burning, along with stratospheric injection dominate in the SH high latitudes. Although seldom dominant, aircraft emissions do play a significant role in the upper troposphere and lower stratosphere of the NH extratropics.

In an effort to assess the impact of pre-calculated, monthly-mean, zonally-averaged (off-line) NO_y interconversion rates, a GCTM simulation of NO_x, HNO_3, and PAN was conducted with an interconversion rate table calculated with the chemical box model for the same set of variables as the rates of ozone production and destruction (3.1.2, A97/P98). The interconversion rates were interpolated at every GCTM time-step using the GCTM's time varying fields of NO_x and O_3, and monthly averaged fields of simulated CO and observed H_2O. An additional source from isoprene oxidation was added to PAN formation, and photolysis was added to PAN loss. The primary impact of the new treatment was higher average OH, due mostly to higher observed values of middle and upper tropospheric water vapor. As a result, the NO_x chemical lifetime was significantly shortened and the global scaling of the lightning source was increased from 4TgN/yr to 10TgN/yr. There was also a significant zonal variation in the NO_x lifetime in the lower troposphere, though there was much less variation in the upper troposphere, as a result of the switch to on-line chemistry. The NO_x and PAN data from this simulation were then compared with the available data from aircraft campaigns and surface sites. The NO_x values were generally lower than observed with approximately 60% of the compared points within ±50% of the observed values. The level of agreement with observations was comparable to the earlier PAN simulation (1372), but not quite as good as it was for the earlier NO_x simulation with the pre-calculated chemical interconversions. In general, the switch to on-line chemistry did not have a major impact, though the improved water vapor fields did increase upper tropospheric OH and lead to a significant increase in the lightning source.

The sensitivities of the NO_x simulations to uncertainties in the observed specific humidities, simulated OH, and simulated ozone were tested in separate GCTM simulations. A 50% reduction in the specific humidities reduced the OH levels by 30-50% in the middle and lower troposphere and by 10-40% at 190 mb. The resulted in NO_x increases of 10-30% in the upper troposphere and 20-40% in the middle and lower troposphere. A 25% reduction in ozone increased NO_x by 15-20% in the upper and middle troposphere and by 5-10% in the lower troposphere. Increasing ozone by 25% lowered NO_x levels by about 10% in the upper and middle troposphere, and by 5-10% in the lower troposphere. The NO_x simulations were significantly less sensitive to uncertainties in ozone than to uncertainties in specific humidity and OH.

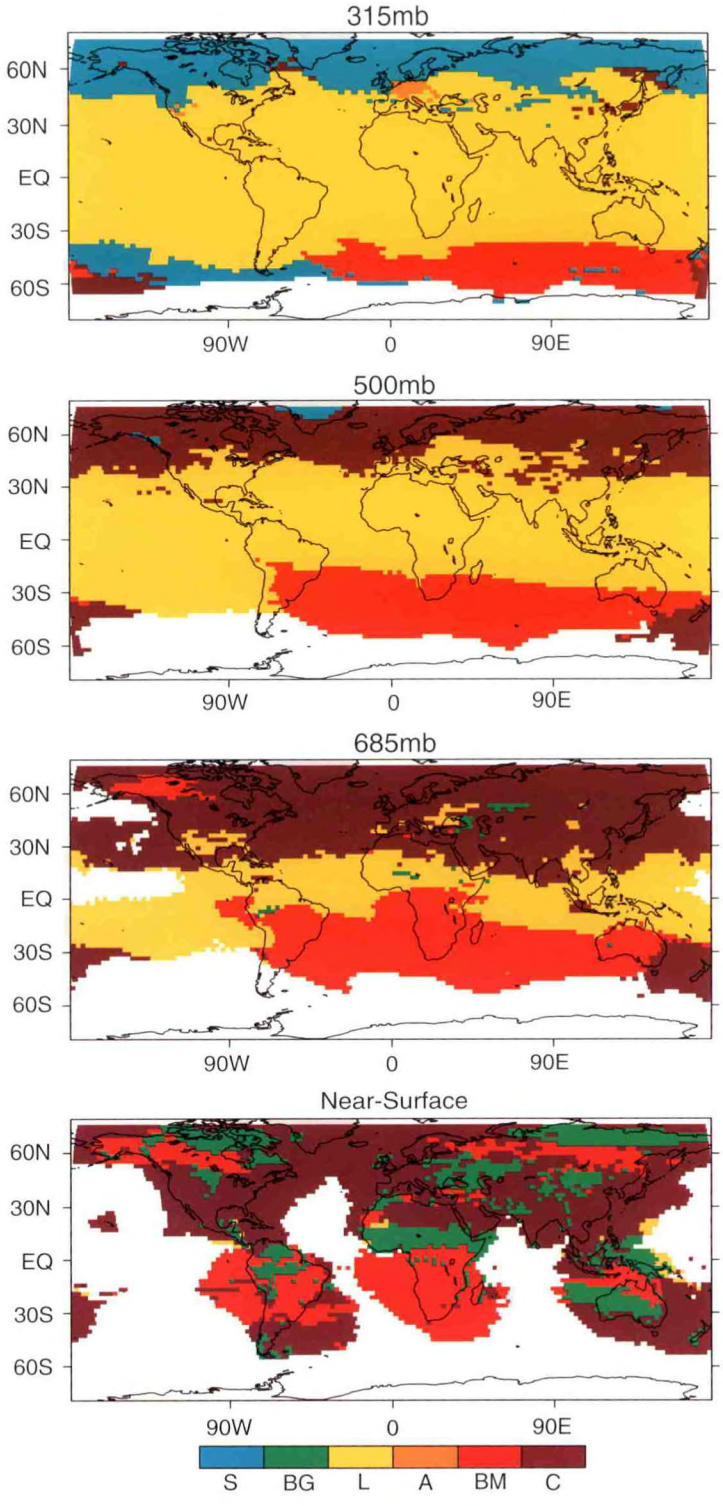

Fig. 2.6 Six-color tropospheric maps of the largest single NO_x source contribution during June through August for the GCTM's upper troposphere (315 mb), mid-troposphere (500 mb), lower troposphere (685 mb) and surface level (~ 80 m). The color code is Blue (S = stratospheric injection); Green (BG = soil biogenic emission); Yellow (L = lightning emission); Orange (A = aircraft emission); red (BM = biomass burning); Brown (C = surface fossil fuel combustion).

2.3.5 Tropospheric Ozone

*P.S. Kasibhatla** *W.J. Moxim*
A. Klonecki *S. Oltmans***
H. Levy II *J.J. Yienger****

**Duke University*
***Climate Monitoring and Diagnostics Laboratory/NOAA*
****University of Iowa*

A previous GFDL GCTM simulation of ozone (A97P98), which agrees well with ozone observations, has been further improved by the inclusion of acetone in the HO_x chemistry (3.1.1), and by an improvement in the seasonality of ozone production in the polluted lower troposphere. The GCTM was then employed to study two of the key issues in tropospheric chemistry: a) the relative roles of stratospheric injection and tropospheric chemical production in the ozone budget; and b) the nature of tropospheric chemical production. A three-tracer experiment was designed to assess the fractional contributions to tropospheric ozone from stratospheric ozone (Blue), ozone produced in the background troposphere (Green), and ozone produced in the polluted lower troposphere (Red). The source of Blue ozone was direct injection across the model's tropopause. Green ozone was produced by $CO\text{-}CH_4\text{-}NO_y\text{-}H_2O$ chemistry in the background ($NO_x < 200$ pptv) troposphere, and Red ozone was produced by a NO_x dependent parameterization in the polluted boundary layer ($NO_x >$ 200 pptv). All three ozone loss processes, photochemical destruction, nighttime NO_x based loss, and dry deposition, were partitioned among the three tracers in each grid-box according to their individual mixing ratios. Globally, Green ozone from the background troposphere is the largest single component (54%), while Blue ozone transported from the stratosphere is next in importance (38%), with Red ozone from the polluted continental contributing only 8%. However, Red ozone does dominate in its source region, the polluted continental boundary layer, and also accounts for ~30% of the ozone in the summertime boundary layer over the North Atlantic. Generally, Blue ozone dominates in the extratropical Southern Hemisphere, with Green ozone dominating in the tropical troposphere. Both Blue and Green have comparable roles in the extratropical Northern Hemisphere. Red ozone and its associated complex hydrocarbon photochemistry do not play major roles in most of the troposphere.

The GFDL GCTM simulation of tropospheric ozone previously used to study the impact of human activity on tropospheric ozone (1445; 3.1.6, A97/P98) has also been used to investigate the role of photochemistry in the winter-spring ozone maximum in the NH midlatitude free troposphere (770 mb-240 mb; 30°N-60°N). Free tropospheric ozone mass slowly builds up in the winter and early spring, with net chemistry and transport playing comparable roles. Winter and early spring conditions are favorable to net ozone production for two reasons. First, winter conditions (cold, low sun angle, and dry) reduce HO_x and lower the level of NO_x needed for chemical production to exceed destruction. Second, throughout the winter, NO_x increases above normally net-destructive levels in the remote atmosphere. As a result, net production in the midlatitude NH free troposphere maximizes in early spring while NO_x is still relatively high, while the ozone chemical balance point is still relatively low, and while increasing insolation is speeding up photochemistry. Conceptually, the net ozone production is associated with an annual atmospheric "spring cleaning" in which accumulated winter-time NO_x is removed via sunlight driven OH oxidation. Furthermore, human activity was found to have a major impact on both the simulated levels of

tropospheric ozone and the role of chemistry in the NH midlatitude where anthropogenic NO_x emissions dominate. In that region, modern ozone levels increased by ~20% in the winter and ~45% in the spring. At the same time winter-spring chemistry switched from net destructive to net productive, the winter-spring balance between transport and chemistry switched from transport dominance in pre-industrial times to the present parity, and the pre-industrial February maximum progressed to March-April. Estimated 2020 levels of NO_x emissions were found to lead to even greater net production and to push the O_3 spring maximum later into April-May.

2.3.6 GCM Simulation of Carbonaceous Aerosol Distribution

*W.F. Cooke** *P. Kasibhatla**
V. Ramaswamy

**Duke University*

ACTIVITIES FY98

A model of the carbonaceous aerosol cycle has been implemented in the GFDL SKYHI model. The fossil fuel emissions of carbonaceous aerosol (both black and organic) have been calculated on the GFDL SKYHI GCM N30 (3° x 3.6°) grid. These emissions have been derived from a 1° x 1° database of black and organic carbon emissions[1] using a simple linear interpolation scheme.

Tests have been performed to determine the best transport scheme for use with aerosols. A comparison has been made between the 4th-order and Lin-Rood transport schemes and the Lin-Rood scheme was found to be more appropriate in cases where the emission fields have large gradients. Since this is the case for the emission of carbonaceous aerosol, the Lin-Rood transport scheme has been utilized for the model integrations.

The carbonaceous aerosol model that has been implemented is similar to that of Cooke and Wilson [2]. Briefly, the scheme uses two tracers for each carbonaceous aerosol component. These represent, respectively, the hydrophobic and hydrophilic parts of the carbonaceous aerosol. The sinks for these aerosols are dry and wet deposition, respectively. In addition, there is also a transformation from hydrophobic to hydrophilic aerosol with a time constant of 1 day. This can be thought of as a representation of the aging of the aerosol, which causes it to become more hydrophilic with time.

The SKYHI model was run for 15 months and the results for the final 12 months were compared to surface concentration and wet deposition measurements. Initial comparisons indicate a reasonable agreement between the modeled and measured concentrations of the BC aerosol. Fig. 2.7 shows the monthly mean global distribution of black carbon (BC) ($ng\,m^{-3}$) in July as simulated by the model. The distribution of BC near the surface is similar to that of sulfate[3] with large concentrations near the major source regions of northeast United

---

1. Cooke W.F., C. Liousse, H. Cachier, and J. Feichter, Construction of a 1° x 1° fossil fuel emission dataset for carbonaceous aerosol and implementation in the ECHAM-4 model, submitted to *J. Geophys. Res.*, 1998.
2. Cooke W.F., and J.J.N. Wilson, A global black carbon aerosol model, *J. Geophys. Res., 101*, 19395-19409, 1996.

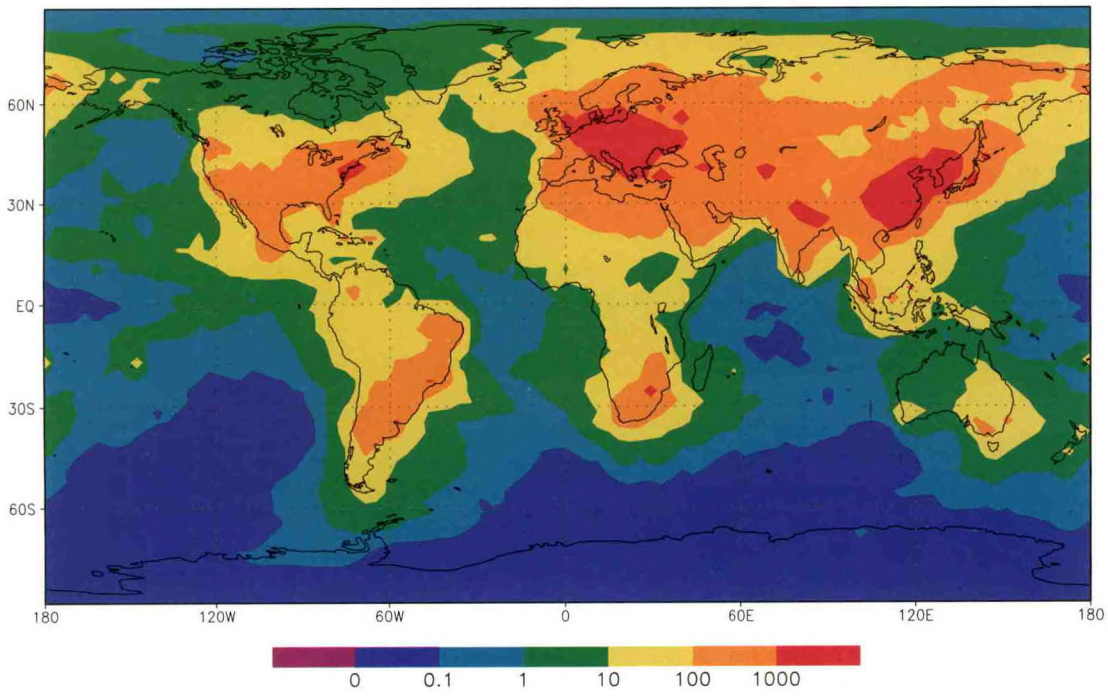

Fig. 2.7 Global mean monthly distribution of black carbon aerosol at the surface for July as simulated by the GFDL SKYHI N30 GCM. The black carbon concentrations are in ng m^{-3}. There is a fairly widespread distribution of the aerosols in the northern midlatitudes away from the source areas.

States, eastern Europe and China. It is also apparent that the entire Northern Hemisphere is affected by this aerosol species, with plumes of aerosol advecting off the east coasts of North America and Asia, and northward from Europe. The Southern Hemisphere is not impacted as severely, although there are areas with significant amounts of black carbon in the atmosphere.

The seasonality of the modeled BC concentrations has been compared with inferred BC concentrations from long-term measurements of light absorption at the CMDL/NOAA sites of Sable Island, Bondville, Barrow and Mauna Loa. The concentrations of this aerosol type are reproduced fairly well for most of the year at Sable Island. At Bondville, the modeled BC concentrations do not account for all of the light absorption in the fall. This may be due to non-carbonaceous absorbing aerosols present at this time of year. The modeled and measured seasonal cycles at Barrow and Mauna Loa agree fairly well, although the model's peak values at these sites are too low. This may be due to stratified transport in the Arctic in the case of Barrow, which is not well represented in models, and to long-range transport of dust from Asia in the case of Mauna Loa. Longer term model runs will be needed to determine whether the differences are due to interannual variability in the atmospheric transport.

---

3. Kasibhatla P., W.L. Chameides, and J. St. John, A three-dimensional global model investigation of seasonal variations in the atmospheric burden of anthropogenic sulfate aerosols, *J. Geophys. Res.*, 102, 3737-3759, 1997.

PLANS FY99

The contributions to tropospheric ozone from stratospheric ozone, ozone produced in the relatively clean troposphere and ozone produced in the polluted boundary layer will be quantified, and the dependence of each source of ozone on season and location will be analyzed.

The GFDL GCTM simulated tropical distribution of tropospheric ozone will be analyzed, coincident with existing observational programs in three remote regions: the tropical South Atlantic, the Indian Ocean, and the South Pacific Ocean near Samoa.

The GCTM study of carbon monoxide will be completed, with an investigation into the pre-industrial distribution. The GCTM simulations will be used to examine cross-border air pollution in Asia, with a focus on possible changes into the next century.

GCTM simulations of NO_x, CO and O_3 resulting from Indonesian fires will be compared with available observations from the region for both normal and El Niño years, and the impact of the extensive fires in 1997 on local, regional and global air quality will be quantified.

Sensitivity of the global distribution of NO_x and O_3 to rapidly changing emissions in Asia will be investigated with the GFDL GCTM. Specific goals include quantifying the export of NO_x and ozone from Asia's polluted BL to the free troposphere, and investigating the impact of this export on the balance of ozone production and destruction in the Central Pacific.

A five-tracer simulation with interactive NO_x, HNO_3, PAN, O_3, and CO will be conducted with the GFDL GCTM using a FEOM representation of the fully coupled *in situ* CO-NO_x-O_3-H_2O chemistry. The resulting fields will be compared with available observations and previous independent simulations of NO_y , O_3 and CO.

Development of the Fully Equivalent Operational Model (FEOM) for the complex non-methane tropospheric chemistry will be initiated. Specifically, the FEOM development will focus on the carbon-bond mechanism (CBM-IV).

Sulfate emissions will be integrated into the SKYHI model in the coming year. Global-scale calculations of the distribution of this aerosol component will be compared to measured global distributions. In addition, a comparison of the relative abundance of sulfate and carbonaceous aerosols will be conducted and the direct radiative forcing of both these aerosols will be calculated. Sensitivity studies with respect to various microphysical and hydrologic assumptions will also be performed.

2.4 ATMOSPHERIC DYNAMICS AND CIRCULATION

2.4.1 SKYHI Model Development

R. Hemler *J.D. Mahlman*

ACTIVITIES FY98

The development of the new standard SKYHI model has continued. A preliminary version of this model containing all of the code upgrades from the last two years (including new long- and short-wave radiation, surface albedo, prognostic cloud and unstable vertical mixing packages) was produced and made available to users. This version is now being used by all SKYHI investigators who are developing and testing additional new model features, so that intercomparison of results between developers may be more easily performed. Some deficiencies still present in the new parameterizations have been identified and efforts are underway to remedy them. Computational upgrades to the model continue, as does the development of generalized initialization and analysis programs.

The parcel trajectory and stratospheric chemistry packages which had been available with older versions of SKYHI are now included in this new release, providing investigators with access to the latest physics parameterizations and model upgrades.

The new SKYHI source has been run on both the Cray T90 and Cray T3E systems. Evaluation of the performance and scaling characteristics of SKYHI on the T3E has identified some model design features which may need modification in order to obtain better performance on distributed memory architectures. Efforts are underway to test the effects of making these changes.

PLANS FY99

Work will continue on the evaluation and improvement of the new scientific parameterizations. The major focus of code development will shift to the task of incorporating the essential functionality of SKYHI into the new GFDL grid-point model, currently under development.

2.4.2 SKYHI Control Integrations and Basic Model Climatology

K. Hamilton *J.D. Mahlman*
R. Hemler *R.J. Wilson*

ACTIVITIES FY98

Control integrations were continued with various versions of the SKYHI model. These now include a 10-year integration of the 3° x 3.6° 40-level model, two years with the 1° x 1.2° 40-level version, two years with the 1° x 1.2° 80-level version, two months with the 1° x 1.2° 160-level version, and seven months with the 0.33° x 0.4° 40-level version. The 160-level and the 0.33° experiments represent integrations at unprecedented spatial resolution (at least for global climate simulation models). Preliminary analysis of these new integrations has concentrated on the simulation of the large-scale circulation in the middle atmosphere.

Overall, the extratropical simulation appears to improve with finer grid spacing, but the effects of increasing horizontal resolution are more significant than vertical resolution. Comparing the 40-level versions, the SH winter polar temperature near 1 mb (~50 km) has a cold bias relative to observations of ~70°C in the 3° version of the model, ~35°C in the 1° version and less than 10°C in the 0.33° version. By contrast, the change from 40 levels to 80 or 160 levels seems to improve this cold bias in the 1° model by only a few °C. In the tropics, however, the changes in vertical resolution were found to lead to much more significant effects on the simulation. In particular, the 80-level and 160-level models develop very strong shear zones in the tropics which descend with time, rather like the observed QBO (Quasi-Biennial Oscillation) shear zones (2.4.3).

Results from the long integration of the 3° x 3.6° version of the model have been incorporated in the middle atmospheric GCM intercomparison organized by the SPARC (Stratospheric Processes and their Role in Climate) initiative of the WCRP (World Climate Research Program) .

PLANS FY99

Analysis will continue of the high-resolution integrations, including an attempt to compare some of the small-scale and high-frequency variations in the simulated middle atmosphere with available observations.

2.4.3 Spontaneous QBO-like Tropical Wind Oscillations in SKYHI Simulations

K. Hamilton *R.J. Wilson*
R. Hemler

ACTIVITIES FY99

As noted earlier, a strong sensitivity of the tropical circulation to the vertical resolution in SKYHI has been discovered. The top panel of Fig. 2.8 shows the height-time evolution of the equatorial zonal-mean zonal wind during two years of the control integration with the 40-level 1° version of SKYHI. The winds near the stratopause undergo a semiannual oscillation with somewhat realistic features, but the winds in the tropical lower stratosphere are nearly constant (typical behavior in most GCMs). The bottom panel of this figure shows the equatorial wind in the 80-level version of the model, in which the equatorial winds and the vertical shears are much stronger. Above about 1 mb, the semiannual variation still dominates, but in the lower and middle stratosphere a longer period oscillation is evident. The mean wind evolution in the lower and middle stratosphere displays both the downward propagation of wind regimes and the concentration of vertical shear into narrow zones that are characteristic of the QBO in the real atmosphere. However, the period of the wind oscillation appears to be about one year, which is much shorter than that of the real QBO. From the limited two-year simulation available, it is not clear whether the period of the lower stratospheric wind variations is exactly one year or not. The model was rerun with fixed equinoctial conditions, and the mean wind evolution in the lower and middle stratosphere was found to be quite similar to that in the seasonally-varying run, showing that this oscillation is indeed a spontaneous "QBO-like" variation rather than being forced by the annual cycle. Detailed analysis of the momentum budget in these experiments has shown that the main driver for the mean flow accelerations in the QBO-like oscillation comes from vertically-propagating waves.

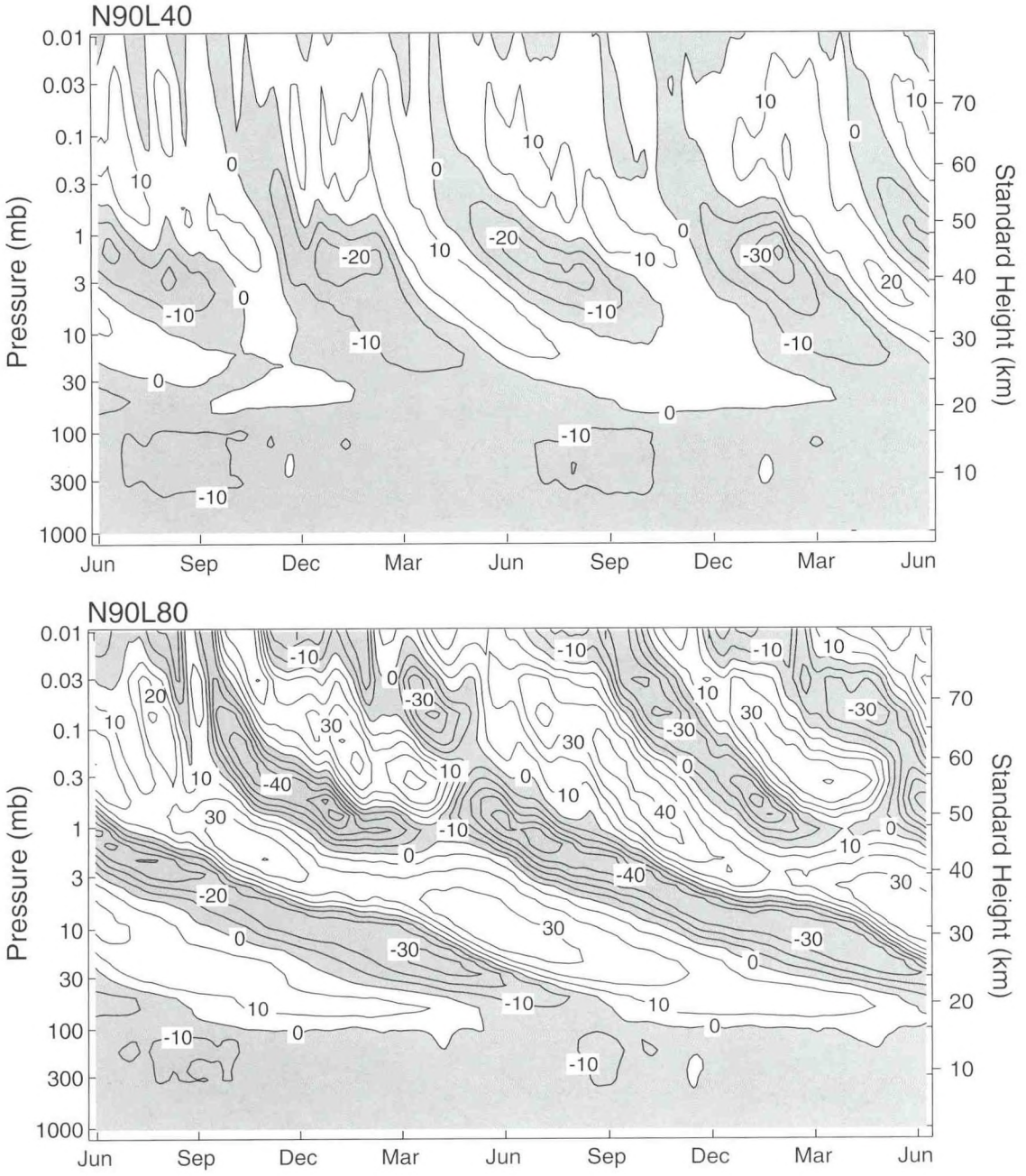

Fig. 2.8 Height-time evolution of the zonal-mean zonal wind in control SKYHI integrations. Results for the 40-level model (top) and for the 80-level version (bottom). The contour interval is 10 m s^{-1} and shading denotes easterly winds. With higher vertical resolution, the circulation in the lower stratosphere exhibits a long-period oscillation similar in many respects to the observed quasi-biennial oscillation.

PLANS FY99

Further analysis of the tropical wind variations in the fine vertical resolution models will continue. Additional experiments will be carried out to examine the dependence of the strength and period of the equatorial wind oscillation on the model resolution, subgrid-scale dissipation and cumulus parameterization scheme.

2.4.4 Low-Frequency Variability of Simulated Stratospheric Circulation

K. Hamilton

ACTIVITIES FY98

Long control integrations of the 40-level 3° x 3.6° SKYHI model have revealed an impressive degree of interannual variability in the NH winter middle atmospheric circulation. The standard deviation of the monthly-mean zonal-mean temperature compares quite well with observations (1275). A striking aspect of the variability is the significant degree of quasi-decadal variation produced by the model. This occurs even in the absence of interannual variations in the prescribed sea surface temperatures or in external forcings (solar flux, volcanic aerosols, etc.). These results are interesting in light of recent claims of significant quasi-decadal variations in the real NH stratosphere, and caution against automatically attributing such long-period variability to effects of external forcing or decade-scale variations in sea surface temperatures.

Some recent studies with simplified models suggest that the zonal-mean zonal momentum in the subtropics may provide some effective interannual memory for the high-latitude stratospheric circulation. To investigate the role of this effect in producing interannual variations in the SKYHI model, the long integrations are being repeated with an arbitrary constraint on the zonal winds in the tropical and subtropical stratosphere.

PLANS FY99

Further analysis of the control and constrained integrations will continue.

2.4.5 Horizontal Spectra from High-Resolution SKYHI Integrations

K. Hamilton *J.D. Mahlman*
*J.N. Koshyk**

**University of Toronto*

ACTIVITIES FY98

The horizontal kinetic energy spectra from the high horizontal resolution SKYHI runs have been analyzed in detail. The spectra at tropospheric levels show two distinct regimes with relatively steep spectral slopes for scales larger than ~500 km and significantly shallower at smaller scales. This corresponds well with observations which demonstrate the existence of a shallow "mesoscale" spectral regime in the troposphere. Fig. 2.9 shows a comparison between one-dimensional power spectra in the midlatitude upper troposphere in the 0.33° SKYHI simulation and results of observations taken from many thousands of commercial aircraft on long flights. The agreement is quite good over most of the range and it appears that the 0.33° SKYHI model is the first global climate model to successfully simulate a significant portion of the mesoscale regime.

Analysis of the detailed spectral kinetic energy budget is proceeding. At each wavenumber the contributions to the energy from horizontal advection, vertical advection, pressure gradient and dissipation terms are being computed. An interesting finding is that, at

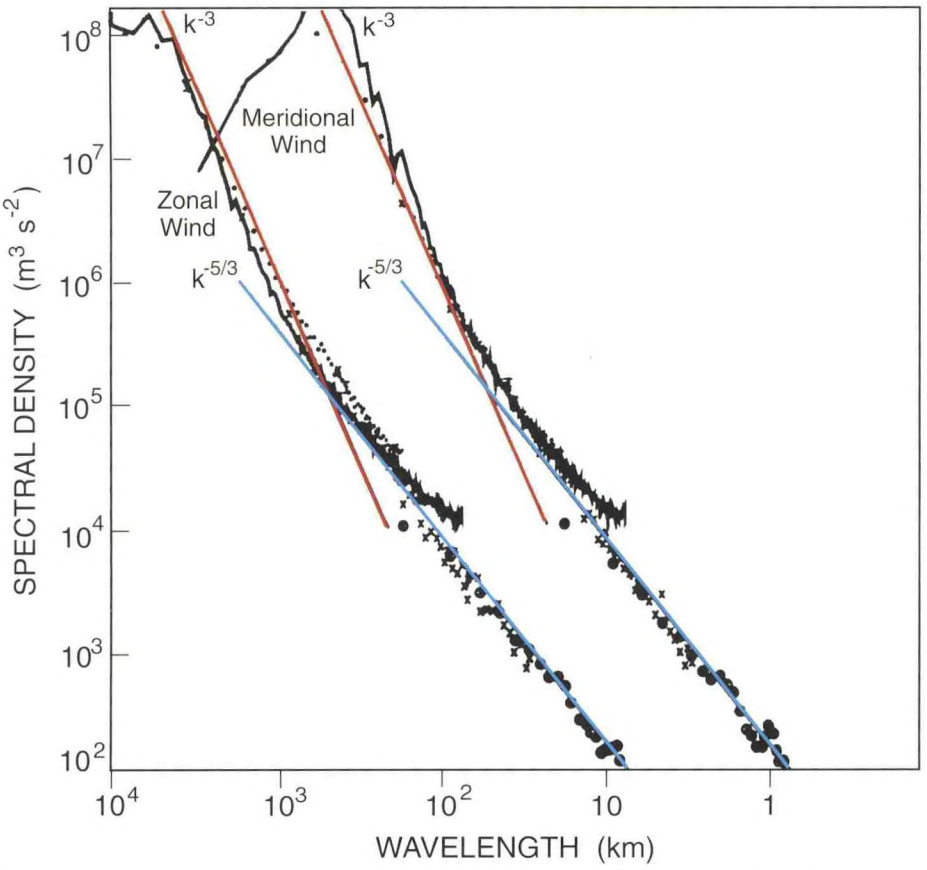

Fig. 2.9 Horizontal power spectra of the zonal and meridional wind components in the upper troposphere. The dots show actual observations based on data from commercial aircraft flights. The solid curve is for the 0.33° SKYHI simulation. The thin lines are drawn for reference and have slopes of -5/3 and -3. The results for the meridional wind have been arbitrarily displaced by one decade to the right.

the 0.33° resolution, the dissipation of kinetic energy by the vertical subgrid-scale diffusion actually dominates that from the horizontal diffusion for most of the spectral range.

PLANS FY99

The analysis of the kinetic energy budget will continue, along with analysis of the available potential energy and tracer variance budgets. A key issue to be addressed is whether the dominant energy cascades in the mesoscale regime are upscale or downscale.

2.4.6 Parameterized Gravity Wave Drag in the SKYHI Model

M.J. Alexander L. Perliski***
K. Hamilton

**University of Washington*
***CMDL/NOAA*

ACTIVITIES FY98

A version of the Alexander-Dunkerton gravity wave drag parameterization scheme has been tested in the 3° 40-level version of SKYHI. Earlier simplified relaxation experiments (1441) have been repeated using the current version of the model to provide a comparison for some preliminary off-line tuning of the parameters.

PLANS FY99

Work towards the efficient implementation and appropriate tuning of the gravity wave scheme will continue. The sensitivity of the residual circulation and the large-scale tracer distribution to the incorporation of the gravity wave drag will be examined.

2.4.7 Effect of Advection Schemes in Simulating Stratospheric Transport

J. Eluszkiewicz L. Perliski***
R. Hemler R.J. Wilson
J.D. Mahlman

**AER*
***CMDL/NOAA*

ACTIVITIES FY98

The age of stratospheric air has been computed in the 3° x 3.6° version of the SKYHI model by three methods: 1) integrating particle trajectories initialized at the tropical tropopause; 2) employing a Green's function approach; and 3) simulating a passive tracer with a linearly increasing source at the surface. Trajectories have been computed using both the model "sigma" levels and potential temperature as vertical coordinates. In the Green's function and the linear source experiments, four gridded advection schemes have been used: the SKYHI 2nd and 4th order centered-difference schemes, the Lin-Rood upstream scheme, and the NCAR semi-Lagrangian (SLT) scheme. This is the first time that such a wide variety of transport schemes (ranging from Eulerian through semi-Lagrangian to fully Lagrangian) have been simultaneously employed in a GCM. Besides computing the age spectrum, the Green's function experiments, in which a passive tracer is advected from a concentrated source in multi-year integrations, constitute a more stringent test of the various advection schemes than the usual tests involving idealized one- or two-dimensional flows and short integrations of three-dimensional simulations of tracers with chemical sources or sinks.

The experiments have demonstrated that a wide range of mean age distributions can be obtained within the same GCM depending on the choice of the advection scheme. Sigma coordinate trajectories exhibit spurious cross-isentropic motions and, as a result, lead to ages

younger than those produced by potential temperature coordinate trajectories. Except in the lowermost tropical stratosphere, the ages computed using gridded advection schemes are too young compared with measurements, most likely as a result of diffusion errors inherent in all Eulerian and semi-Lagrangian advection schemes. This conclusion is supported by the fact that the longest ages overall are obtained using potential temperature coordinate trajectories, which suffer from minimal numerical diffusion. The SLT scheme produces the youngest ages as a result of spurious vertical motions akin to those produced by the sigma-coordinate trajectories. Since the calculation of these trajectories forms the essence of the SLT scheme, this finding, and the contrast between these two trajectory schemes, suggest that the performance of this scheme might be improved if its trajectories were calculated in theta coordinates. Among the gridded schemes, the centered-difference schemes produced the longest ages (and closest to those observed), suggesting that their lack of numerical diffusion outweighs their dispersion errors in this application. The large sensitivity of the computed ages to the model numerics calls for caution in interpreting features of model-generated mean age distributions solely in terms of the model simulation skill.

2.4.8 GCM Chemical Simulation with an Imposed Tropical Quasi-biennial Oscillation

K. Hamilton *L. Perliski**

**CMDL/NOAA*

ACTIVITIES FY98

A 48-year simulation using the 3° x 3.6° SKYHI model with an imposed QBO zonal momentum source (A97/P98) has been analyzed (ex). More than 16 years of this experiment have now been repeated in a version of the model with a detailed prognostic photochemical code. This model produces a simulation of the QBO in ozone near the equator that compares very well with observations (A97/P98). Recent analysis has focussed on the details of the transport and chemical response in the subtropics and midlatitudes. One crucial feature apparent in the observations of stratospheric ozone is the tendency for the annual cycle of ozone and the QBO to be strongly coupled. The power spectrum of total ozone variations near the equator has a strong peak at the QBO frequency (1301), but there is also a strong peak in the subtropics near ~20 months which corresponds to one of the beat frequencies between the QBO and the annual cycle. Fig. 2.10 shows the spectrum of zonally averaged total column ozone at 19.5° latitude computed from 14 years of Nimbus-7 TOMS (Total Ozone Mapping Spectrometer) data. The results are shown separately for the components of the ozone symmetric and antisymmetric between the NH and SH. The symmetric component is dominated by a peak centered near 27 months, but the antisymmetric component has a more prominent peak near 20 months. Also shown is the same analysis applied to the ozone in the SKYHI QBO experiment. The agreement with observations is quite impressive and this is an indication that the model is able to capture the QBO modulation of the annual cycle of trace constituent transport in the subtropics.

PLANS FY99

Analysis of the transport and chemical effects of the QBO in the integration will continue. The SKYHI model experiment will be repeated using a prescribed zonal-mean flow evolution based on detailed radiosonde and satellite observations.

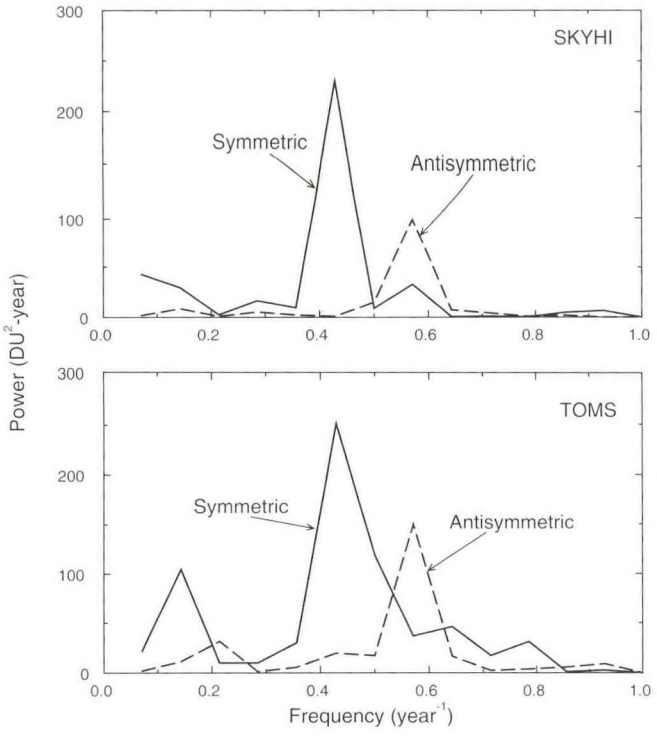

Fig. 2.10 Power spectra of the zonal-mean deseasonalized total column ozone at 19.5° latitude determined from 14 years of SKYHI model simulation (top) and 14 years of TOMS satellite data (bottom). Results are presented separately for components symmetric between Northern and Southern Hemispheres (solid curve) and the component antisymmetric between hemispheres (dashed).

2.4.9 GCM Simulation of Long-Term Variations in Stratospheric Tracer Concentration

K. Hamilton *L. Perliski**

**CMDL/NOAA*

ACTIVITIES FY98

Analysis of the results for the ozone concentration in the SKYHI integration with an imposed QBO has revealed the occurrence of long-period variations, particularly in the NH mid and high latitudes. Fig. 2.11 shows the least-squares linear trend of the zonal-mean total column ozone in the SKYHI simulation. Values are shown for 14 years (omitting the first two years of the experiment as spinup period) and also for just the last 10 years. The results reveal a positive total ozone trend which is particularly pronounced in the NH midlatitudes. The magnitude of the trend in the NH midlatitudes turns out to be more than 50% of the magnitude of the (decreasing) trend actually seen in the 14-year (1979-92) TOMS dataset. This suggests that natural internally-generated transport variability may be able to generate decade-length trends that are of comparable magnitude to those that have been observed, and thus that natural variability might possibly account for a significant portion of the trends seen in NH midlatitude ozone data. Somewhat similar long-period variability is seen in the lower stratospheric N_2O field in the 48-year simulation (ex).

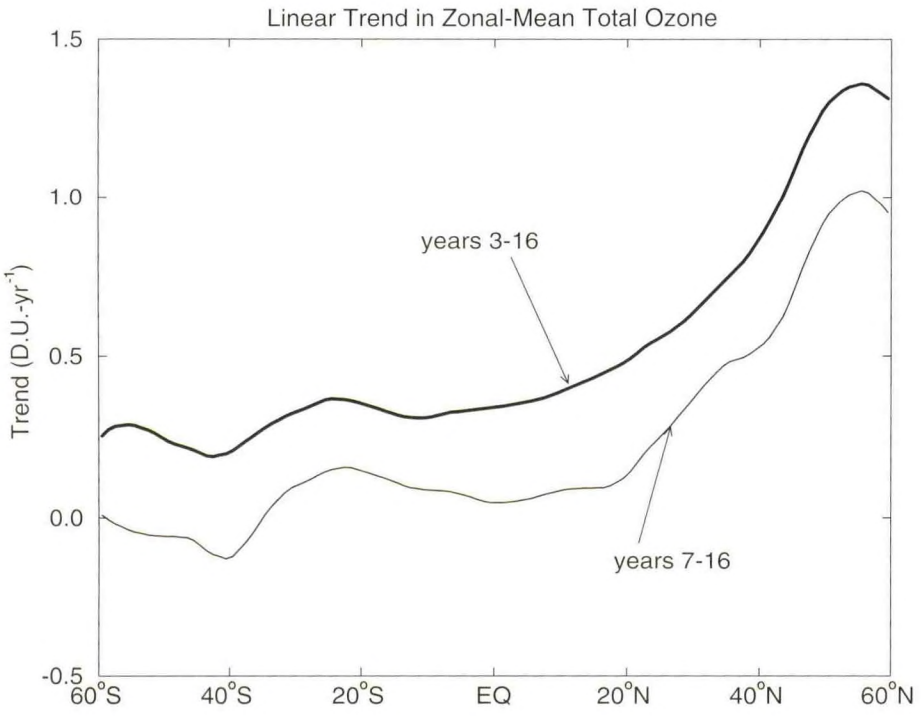

Fig. 2.11 Linear least-squares trend in the zonal-mean total ozone column simulated by the SKYHI model in a control run with no long-term changes in chemical inputs. Results shown for the trend over years 3-16 of the simulation (heavy curve) and for years 7-16 (light curve).

PLANS FY99

The full chemistry version SKYHI simulation will be continued in order to see how the long-period ozone variations develop. The transport mechanisms contributing to the long-period trace constituent variations will be analyzed in detail.

2.4.10 Observational Studies Using Radiosonde Data

K. Hamilton

ACTIVITIES FY98

Six years of high-resolution radiosonde data at Payerne in Switzerland have been obtained. These data are now being analyzed for gravity wave signals as part of a worldwide project (coordinated by SPARC) to establish a gravity wave climatology for the lower stratosphere. In addition, a study has commenced of the statistics of cold extremes in the winter lower stratosphere temperature data. This will be useful in determining how much mesoscale temperature variations might contribute to activation of low temperature heterogeneous chemistry that is thought to be responsible for significant mid- and high-latitude ozone loss.

A review of pre-1950 balloon observations of stratospheric winds at near-equatorial sites was undertaken (1566). Scattered observations exist as early as 1908, and these data

strongly suggest that the QBO has been a fairly stable feature of the equatorial circulation for at least the last century.

PLANS FY99

The analysis of high-resolution radiosonde data will continue and the results will be incorporated into the worldwide SPARC gravity wave analysis project.

2.4.11 Review Papers on Middle Atmospheric Dynamics

K. Hamilton

ACTIVITIES FY98

Two review articles on aspects of middle atmospheric dynamics have been prepared. One is a historical survey of the development of the field with a focus on the period before about 1975 (gl). The other is a review of the state-of-the-art in observations and theory of the general circulation of the tropical stratosphere and mesosphere (gt).

2.4.12 Dynamics of the Martian Atmosphere

R.J. Wilson

ACTIVITIES FY98

Viking Infrared Thermal Mapper (IRTM) data provide the foundation for much of the knowledge of the current martian climate. The IRTM data were collected over a period in excess of two Mars years and contain a wealth of information on the spatial and temporal variation of surface and atmospheric temperatures on diurnal to seasonal time scales. In particular, the 15 μm channel radiance measurements have provided brightness temperatures (T_{15}) for a deep layer of atmosphere centered at the 0.5 level (~25 km). The latitude and seasonal variation of T_{15} is shown in Fig. 2.12. The T_{15} data have indicated a prominent seasonal modulation of global mean temperature that is the result of a large seasonal variation in atmospheric dust loading. The effect of aerosol heating is also indicated by the large diurnal variation in martian T_{15} temperatures, particularly during global dust storm periods. Episodic global dust storms, such as the two observed in 1977, represent a significant interannual component in the climate description.

Work has continued in comparing the IRTM T_{15} observations with Mars GCM simulations of diurnal and seasonal variability. The recent effort to reconcile the spatial pattern of diurnal variability evident in the T_{15} data with that predicted by the GCM has resulted in the identification of a systematic error in the retrieved 15 μm radiances which were evidently additionally sensitive to radiation from the surface. The surface emission resulted in a 15 K temperature bias in the estimate for midday tropical temperatures for relatively clear sky conditions when the contrast between atmosphere and surface temperature was largest. The downward revision of IRTM temperatures during the Northern Hemisphere spring and summer seasons also implies a lower water saturation level and thus, an increased possibility for water ice cloud/dust aerosol interaction. This interaction may be an important aspect of the seasonal variation in atmospheric dust opacity, as has been suggested by one-dimensional

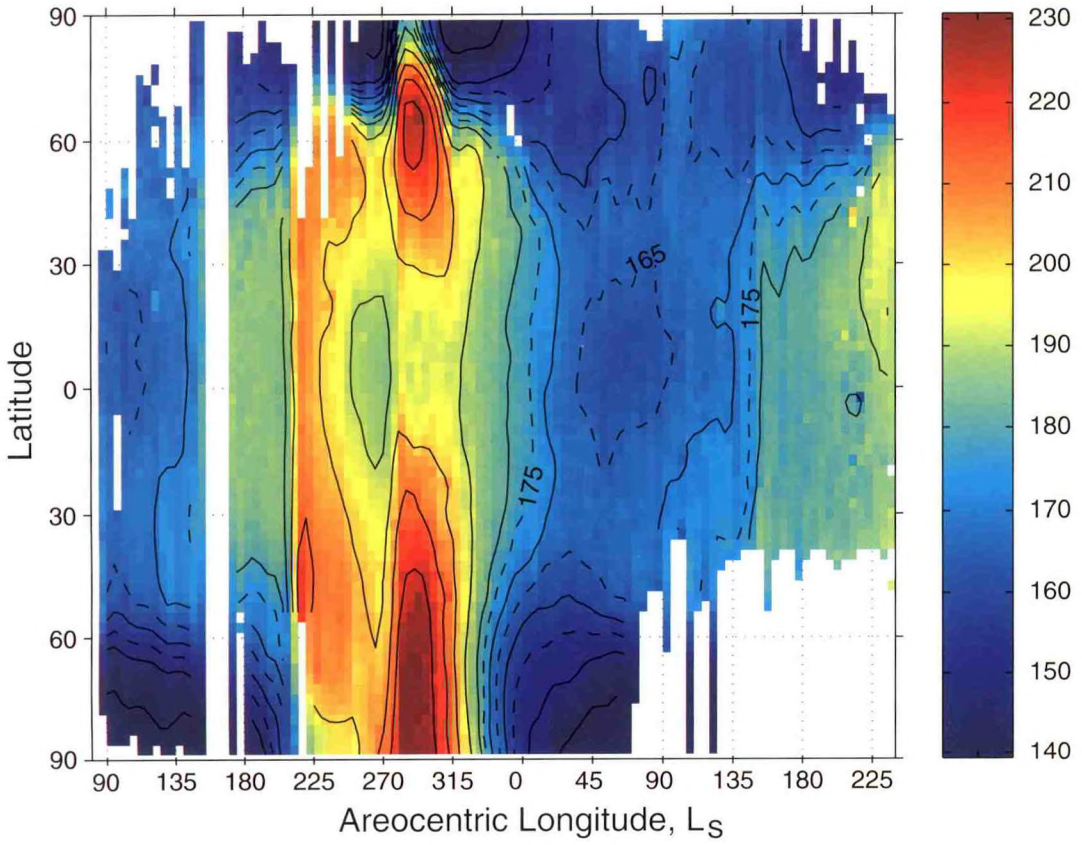

Fig. 2.12 The evolution of IRTM T_{15} temperatures over the course of the Viking mission. The areocentric longitude (L_s) is the Mars seasonal index, running from 0 to 360 degrees with 0 corresponding to vernal equinox, 90° to Northern Hemisphere summer solstice, etc. The bias due to surface radiance has been removed. The large seasonal temperature variation and the two global dust storms (at L_s=204 and L_s=274) are clearly evident.

model simulations employing coupled microphysics, radiative transfer, and turbulent mixing of aerosol (hl).

PLANS FY99

Ice cloud microphysics and improved radiation parameterizations will be incorporated in the Mars GCM in order to examine the influence of microphysical/thermal/dynamic feedback mechanisms on martian climate.

2.5 CLIMATIC EFFECTS DUE TO ATMOSPHERIC SPECIES

M-L. Chanin[*] *J. D. Mahlman*
M. Gelman[**] *V. Ramaswamy*
J. Haywood *M.D. Schwarzkopf*
J-J. R. Lin[**]

**CNRS/ SPARC, France*
***Climate Prediction Center/NOAA*

ACTIVITIES FY98

2.5.1 Lower Stratospheric Ozone and Temperature Trends

Model and observational results indicate that the observed loss of ozone in the global lower stratosphere since ~1980 has led to a cooling of that altitude region (1193, 1394). In recent years, the WCRP SPARC Program has initiated a project to obtain a thorough quantitative assessment of the temperature trends in the entire global stratosphere. This project seeks to: a) assess the temperature change in the stratosphere from a variety of available measurements; and b) evaluate the degree to which these can be attributed to changes in atmospheric species and/or natural variations. Fig. 2.13 shows the 50 and 100 hPa trends over the 1979-1994 period drawn from radiosonde and analyzed datasets, and those derived from satellite data. The Berlin, Angell, Russia and UK/Raob plots represent different radiosonde-based datasets, while the rest of the non-satellite data come from analyses that either do not involve a GCM (NOAA/ Climate Prediction Center or CPC) or that do involve a GCM (NASA's Goddard Space Flight Center; NOAA/NCEP's re-analyses, or "Reanl"). The satellite data consists of the Microwave Sounding Unit (MSU Channel 4) and the thermal infrared Stratospheric Sounding Unit (SSU 15X channel, labelled here as Nash). The MSU senses signals from a region ~50-150 hPa with a peak at ~90 hPa, while the SSU peaks at 50 hPa and has a broad span encompassing ~20-250 hPa.

In the northern midlatitudes, all the datasets exhibit coherence with regard to the magnitude of the cooling. They are also coherent with respect to the statistical significance of the cooling (not shown). In the low latitudes, there is some divergence between the various datasets with regard to the magnitude of the cooling. In the Southern Hemisphere, which does not have as dense a radiosonde monitoring network, the datasets do not exhibit the same degree of agreement. In addition, the annual-mean results for the Southern Hemisphere are not statistically significant at any latitude for most of the datasets, although the Antarctic springtime and the midlatitude Southern Hemisphere during the early part of the year do exhibit a statistically significant cooling (1394). At the high southern latitudes, warming is found at the 50 hPa level, with cooling at 100 hPa. (Note that the lower stratosphere, where considerable ozone loss occurs, is at a higher pressure level at this latitude.) The satellite data contains a signal not only from the lower stratosphere, but also non-negligible components from the region above the lower stratosphere and, more particularly, the upper troposphere. In general, the satellite trend at the NH midlatitudes agrees well with the other datasets in terms of the magnitude and with respect to statistical significance. However, at low latitudes, the satellite trends are smaller than for the radiosonde, likely due to signals from upper troposphere which mask the pure lower stratospheric trend. In the high southern latitudes, the satellite results yield a cooling that is similar to the 100 hPa trend shown in panel (b). At the high northern latitudes, the entire 50-100 hPa layer undergoes a large cooling in contrast to the non-satellite

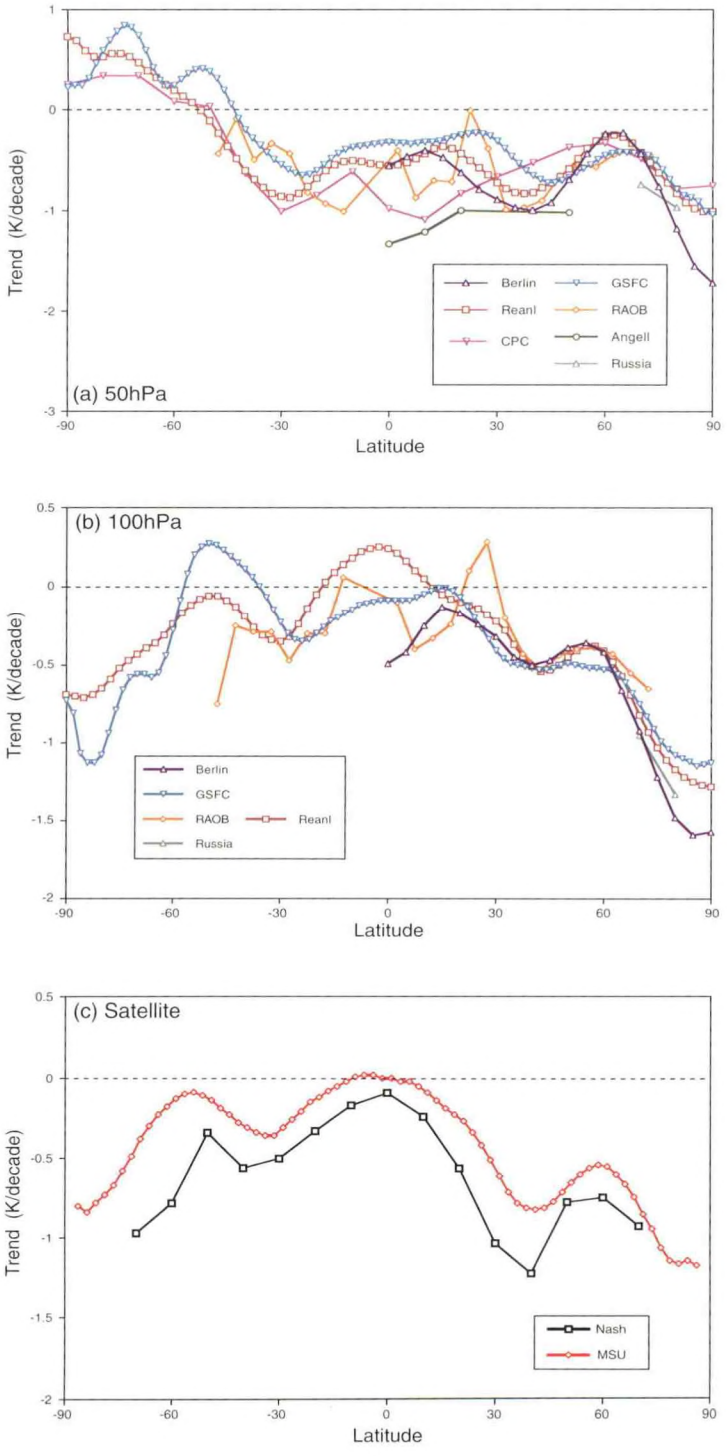

Fig. 2.13 Decadal temperature trends for the period 1979-1994 as computed using different datasets: (a) for 50 hPa level, (b) for 100 hPa level and (c) thermal infrared (Nash) and microwave (MSU) satellite measurements which contain signals from a wide altitude span encompassing the lower stratosphere (*i.e.*, including the 50-100 hPa levels). Panels (a) and (b) include radiosonde data, as well as data derived from analyses (viz., CPC, GSFC and Reanl). A cooling of the lower stratosphere at most latitudes is apparent from all the datasets, with a reasonable degree of coherence among the different datasets, especially in the midlatitude Northern Hemisphere.

data estimates for the high southern latitudes. Model studies of ozone depletion effects (1193, 1394) indicate a warming trend above the region of cooling in the lower stratosphere at high southern latitudes due to dynamical changes. This differs from the high northern latitudes, where the warming tendency is quite weak and cooling occurs over a deeper vertical extent. The fact that the 50 and 100 hPa trends are of opposite sign in the high southern altitudes, and that the low latitude satellite signature may well contain a substantial input from the upper troposphere, illustrates the necessity of extra care in quantitative intercomparisons of radiosonde and satellite trends in the lower stratosphere. It should be noted that the current results regarding lower stratospheric temperature trends constitute a principal highlight of the recently concluded WMO/UNEP 1998 Ozone Assessment.

Simulations of the effects of stratospheric ozone loss (A97/P98) were analyzed further. When ozone losses are distributed over a broader vertical extent than just the lower stratospheric region, the cooling of the lower stratosphere is altered only modestly in magnitude. However, the strength of the warming seen above the ozone depletion regions can be considerably reduced, especially in the high southern latitudes (a result of the change in the stratospheric residual circulation).

The net radiative flux changes at the tropopause due to depletion of lower stratospheric ozone, computed using the SKYHI GCM and Fixed Dynamical Heating (FDH) method, have been compared. Differences in the longwave flux for the two approaches are considerable and arise due to the fact that: a) the GCM's lower stratospheric temperature change differs from the FDH; and b) the troposphere is not held fixed in the GCM, as in the FDH approximation. Thus, caution must be exercised in comparing FDH-computed radiative flux changes with those observed. This is because flux observations already incorporate a measure of the altered dynamics (and thereby the climate system's response to the ozone losses) and thus cannot be simply related to a FDH computation.

2.5.2 Radiative Forcing Due to Tropospheric Aerosols and Ozone

The global radiative forcing features due to sulfate and black carbon aerosols have been examined (1529). A review has been conducted (1523) of the state-of-the-art models used to compute the forcing due to scattering and absorption by atmospheric aerosols, as well as the present methods used to estimate the absorption ability of these aerosols, *e.g.*, single-scattering albedo. It is concluded that it is not possible to generalize the range of the single-scatter albedo at present. Further, most of the measurement techniques suffer from a lack of calibration checks and a systematic overestimation of light absorption coefficients. On the modeling side, the necessity of including humidity-dependent effects on light extinction cannot be overemphasized.

The radiative effects of changes in tropospheric ozone since pre-industrial times has been examined (1555) and the results are illustrated in Fig. 2.14. The forcing due to ozone has been found to be as important as that due to sulfate and carbonaceous aerosols (A97/P98). The requirement of a radiative-dynamical equilibrium in the stratosphere for the determination of the tropospheric ozone radiative forcing, as demanded by the strict FDH definition, is not found to be a significant factor, unlike the case of the lower stratospheric ozone changes.

The radiative forcing due to an external mixture of sulfate and soot aerosols (A97/P98), combined with that due to tropospheric ozone, is shown in Fig. 2.15 which reveals substantial

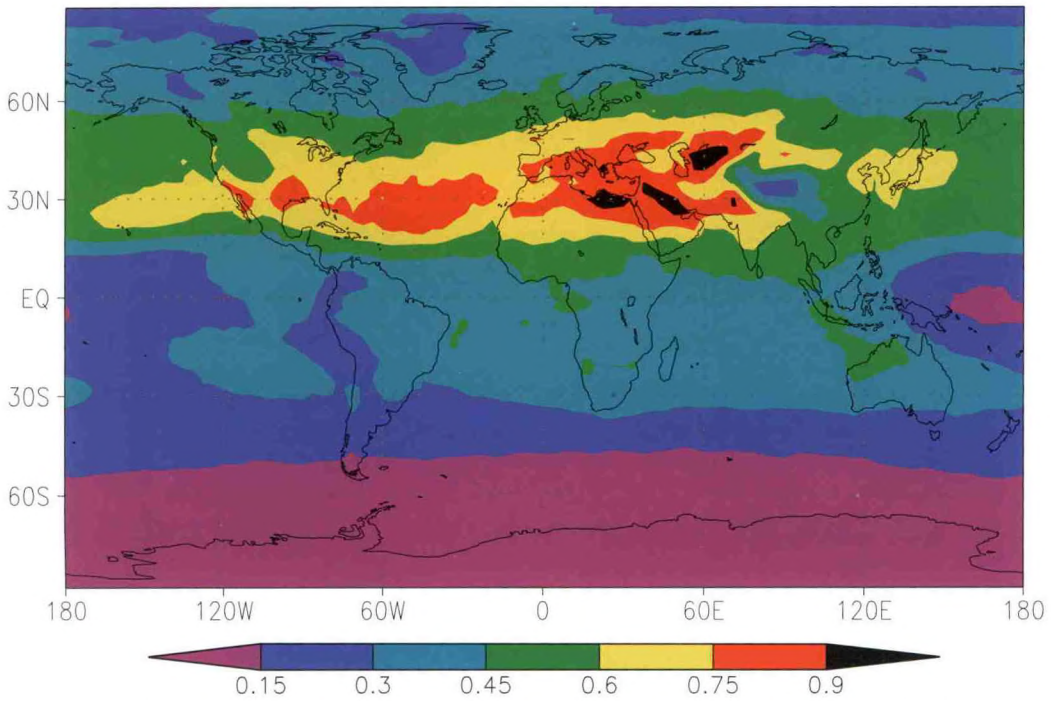

Fig. 2.14 Global distribution of the Instantaneous tropopause radiative forcing due to increases in tropospheric ozone (*i.e.*, present minus pre-industrial). The locations of the maxima in midlatitude NH continental regions are similar to those shown in A97/P98 for soot aerosol forcing and for the direct sulfate aerosol effect (with opposite sign).

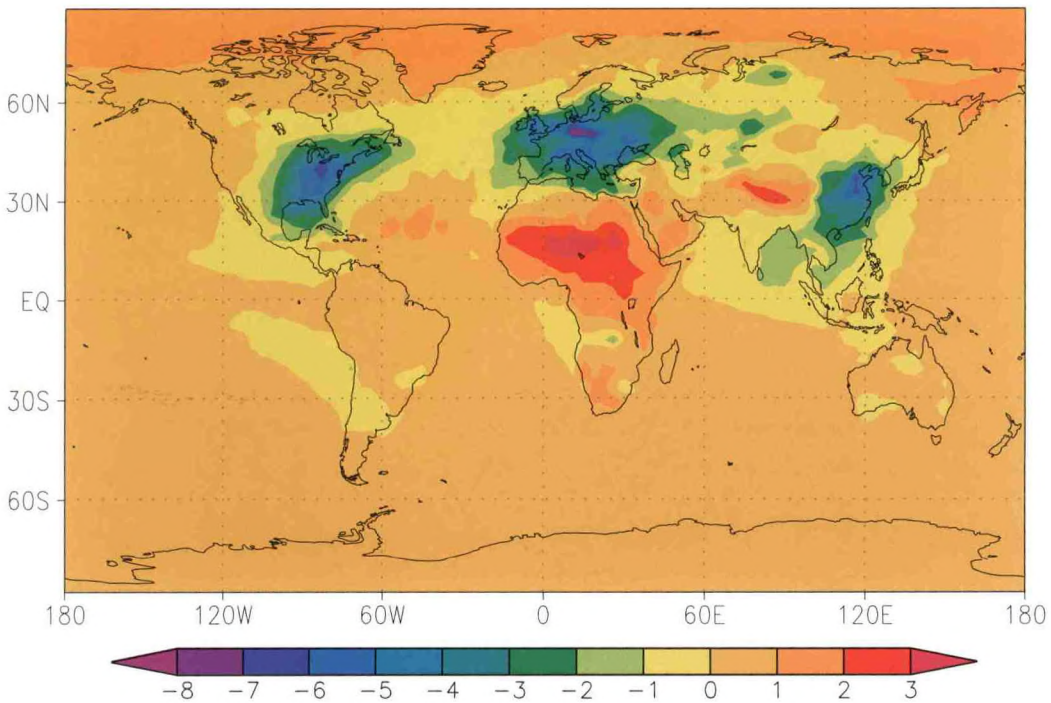

Fig. 2.15 Global distribution of the tropopause radiative forcing (present minus pre-industrial) due to direct tropospheric sulfate aerosols, soot aerosols and tropospheric ozone. Note that there is a considerable geographical gradient of the forcing with positive and negative values occurring on continental scales, even though the global-mean forcing is quite small.

gradients in the geographical distribution of the climate forcing. It is interesting to note that while the forcing from each of the three species has been deemed by the IPCC to be important in its own right, the global-mean is a small residual (-0.12 W/m^2). Nevertheless, the large positive and negative values occurring in the geographical distribution are relevant when considering regional climate effects.

PLANS FY99

The effects due to stratospheric ozone changes will be studied further, with emphasis on middle and upper stratospheric temperature trends. As part of the SPARC investigation of temperature trends, observational records will also be analyzed. Investigations concerning the global radiative forcing due to trace gases and aerosols will continue.

2.5.3 Radiative Effects of Aerosol-Cloud Interactions

C. Erlick *L.M. Russell**
V. Ramaswamy

**Department of Chemical Engineering, Princeton University*

ACTIVITIES FY98

Aerosol and water drop size distributions in clean maritime, continentally influenced maritime, and polluted clouds were modeled using data from the Monterey Area Ship Track Experiment (MAST) and a size- and composition-resolved externally-mixed aerosol model[4]. These results were used to compute the corresponding Mie scattering parameters, which then act as an input to a delta-Eddington exponential-sum-fit solar radiation algorithm (A96/P97). The resulting radiation quantities are analyzed to investigate, on a microphysical level, the corresponding changes in albedo, absorption, and transmission as a consequence of cloud evolution.

Analysis of a clean maritime cloud influenced by a ship track plume reveals an almost order of magnitude increase in cloud optical depth at 550 nm wavelength, with drops in the > 7 micron size range (derived from the plume particles that are activated) making the largest contribution. The increase in optical depth translates into a near doubling of the otherwise clean maritime cloud's visible albedo.

The influence of a clean maritime cloud on atmospheric absorption above and inside the cloud as a function of wavelength has also been investigated. The results show a 17 W/m^2 increase in above-cloud absorption at wavelengths less than 2.0 microns due to reflection by the cloud and absorption by ozone and water vapor above the cloud. There is a 26 W/m^2 increase in the in-cloud absorption at wavelengths greater than 0.7 microns due to scattering by the cloud drops and absorption by water vapor inside the cloud, and to absorption by the cloud drops themselves.

---

4. Russell, L.M., and J.H. Seinfeld, Size- and composition-resolved externally-mixed aerosol model, *Aerosol Sci. Technol., 28,* 403-416, 1998.

PLANS FY99

Analyses and comparisons of the results for the clean maritime cloud with those for continentally influenced clouds will be conducted. An emphasis will be placed on distinguishing the contributions to the cloud radiative properties by particles of different sizes and compositions. These results, plus additional idealized simulations, will be used to assess parameterizations of supersaturation, aerosol activation, and the "Twomey effect." An attempt will be made to extend the study toward an evaluation of the aerosol-cloud interaction and the "indirect" aerosol effect in one-dimensional radiative convective and three-dimensional general circulation models.

2.5.4 Radiative Forcing due to Stratospheric Aerosols

S.M. Freidenreich *V. Ramaswamy*
S. Ramachandran *M.D. Schwarzkopf*

ACTIVITIES FY98

Using the new shortwave parameterization (A96/P97) code (which includes stratospheric aerosols), calculations of changes in the downward and upward fluxes and heating rates were performed for volcanic aerosol size distributions typical of those observed after the El Chichon and Pinatubo eruptions. Line-by-line (LBL) calculations were also performed for these size distributions for the entire shortwave spectral range (1-50,000 cm^{-1}). The LBL calculations enable a quantitative evaluation of the contributions from different spectral regions and for stratospheric aerosols of different sizes. Downward and upward fluxes and the heating rates obtained from the parameterization were compared with the LBL results for the near IR, visible, and UV spectral regions, separately. The net and the spectral upward and downward fluxes obtained from the parameterization are about 5-10% larger than the LBL results. The heating rates obtained from LBL calculations were found to be consistently higher than the parameterized values, with most of the bias coming from the near IR and visible spectral regions.

Volcanic aerosols in the stratosphere can produce significant long-term solar and infrared radiative perturbations, producing a radiative and dynamical response in the climate system. A spectral-, space-, and time-dependent set of zonally monthly averaged aerosol parameters for two years after the Pinatubo eruption (June 1991-May 1993) was obtained[5] and formatted for the SKYHI latitude grids and for the 26 spectral bands of the new shortwave parameterization. Two sets of SKYHI GCM integrations were performed with predicted clouds and monthly varying SSTs, one with aerosols and the other without ("control"). Differences between these runs illustrate the warming of the stratosphere due to the aerosols and the evolution of this warming over the two-year period.

A simple one-dimensional model was developed to study the time evolution of a volcanic aerosol layer and its associated particle size distribution based on the microphysical processes of growth, coagulation, diffusion and sedimentation. The simulated size distributions

5. Stenchikov, G.L., I. Kirchner, A. Robock, Hans-F. Graf, J.C. Antuna, R. Grainger, A. Lambert, and L.W. Thomason, Radiative forcing from the 1991 Mount Pinatubo volcanic eruption, *Report no. 231*, MPI, 1-40, 1997.

for the Pinatubo volcanic event compare reasonably well with available observations. Using the shortwave parameterization code, the changes in the fluxes and heating rates were obtained for the aerosol size distributions simulated at various times. These changes are larger during the initial stages following the eruption, and decrease with time. Since the aerosol size distribution contains more large particles and higher number concentrations initially, the evolution of the radiative changes is consistent with the simulated microphysics.

Using a newly developed radiative-convective model (RCM) with a mixed layer ocean, and incorporating typical volcanic stratospheric aerosol parameters, equilibrium runs have been performed with and without aerosols, and the changes in the global, annual-mean surface and stratospheric temperatures have been determined. Results show a peak stratospheric warming of about 3 K (for a $\tau_{aerosol}$ = 0.1) for a Pinatubo type aerosol size distribution located between 15 and 30 km, which is quite consistent with other model estimates.

PLANS FY99

Efforts are underway to incorporate the non-gray longwave radiative effects due to particulates in eight longwave bands from 560 to 1400 cm^{-1}. This will be implemented in both the RCM and SKYHI GCM radiation codes and used to study the infrared radiative perturbations due to the presence of volcanic aerosols. Using the time-dependent Pinatubo aerosol dataset, an ensemble of runs will be performed to estimate the changes in the net radiative fluxes, temperatures in stratosphere and troposphere, and their temporal variations and other changes in tropospheric climate. The volcanic aerosol effects will be compared with responses due to other types of forcings, such as the lower stratosphere cooling in mid- and high latitudes due to ozone depletion. Further study of the microphysical and radiative impacts of volcanic aerosols is planned by coupling the aerosol microphysical model to the RCM. Also, the aerosol microphysical model will be incorporated into the SKYHI GCM, and the evolution and transport of Pinatubo aerosols at various stratospheric altitudes will be studied.

3. EXPERIMENTAL PREDICTION

GOALS

To develop methods of stochastic-dynamic prediction capable of extracting as much useful forecast information as possible from numerical prediction models given imperfectly observed initial conditions.

To develop and improve numerical models of the atmosphere-ocean-land system in order to produce useful forecasts with lead times of several weeks, months, seasons or years.

To understand the limits of predictability of the ocean-atmosphere system with emphasis on quantifying the amount of useful forecast information that could be available at lead times of several weeks, months, seasons or years.

To develop methods for the assimilation of observations into dynamical models in order to improve predictions of the ocean and atmosphere.

3.1 FLEXIBLE/MODULAR MODELING SYSTEM

ACTIVITIES FY98

3.1.1 Atmospheric Model Development

3.1.1.1 Global Atmospheric Grid Point Model

B. Wyman

A highly flexible and modular version of the B-grid dynamical core (1351) with more user-friendly interfaces has been developed using Fortran-90 enhancements. This code has been optimized on the GFDL Cray T90 with a reduction of about 20 percent in CPU time. The code has been incorporated into the full Atmospheric General Circulation Model (AGCM) and modular physics (3.1.1.3) and has been used in developing the framework for the new flexible coupled models (3.1.2).

3.1.1.2 Flexible Spectral Model

J. Anderson *I. Held*
V. Balaji *P. Phillipps*

The flexible spectral dynamical core has undergone continued development to improve efficiency on the Cray T90 and to make the spectral model interfaces consistent with those of the B-grid model (3.1.1.1). Tests with various physical parameterizations originally developed in the B-grid context have been completed. Extensions to incorporate a semi-

Lagrangian advection scheme are being considered; initial tests with such advection schemes in simple models have been completed.

3.1.1.3 Modular Physics Parameterizations

J. Sirutis

A modular version of the SiB (Simple Biosphere Model) land surface parameterization has been created and tested in off line runs. Development of a modular version of the full Arakawa-Schubert cumulus parameterization scheme has been completed.

3.1.1.4 Spectral Model Parallelization

V. Balaji

The design of GFDL codes is evolving apace with computer architectures and compiler technologies. In particular, codes are now in transition from an era dominated by vector supercomputers to one where massively parallel processing architectures may dominate. The new spectral core is likely to be of vital importance to GFDL in coming years, and will be a key component of a coupled ocean-atmosphere model now under development. Substantial effort has been devoted to its parallelization for distributed memory architectures.

The relevant feature of spectral models is that each model field has a spectral and a grid representation, and operations are performed on each representation at each timestep. Linear terms are treated in the more succinct spectral representation, while physical parameterizations are applied on the grid representation. The problem arises with non-linear terms, such as in advection, which, if explicitly expanded, result in a sum of terms quadratic in the order of the expansion. The transform method is used to convert spectral fields to grid space for the computation of non-linear terms and then back. Since this method involves frequent transformations between grid fields and spectral fields, efficient numerical transform methods have been developed, including parallel methods.

In keeping with the modular approach, a data decomposition and communication tool called "mpp_mod" has been developed for the spectral core. This module has a flexible interface for specifying decompositions of the global grid among processors. Conceptually, the module distinguishes the "computational domain" (the set of grid points for which computations are to be done on any processor in a distributed environment) and the "data domain" (the set of points whose values need to be available in order to carry out the computation). If points in the data domain have been altered, the data domain must be updated, by acquiring data as required from other processors, before the computation can go forward. The "mpp_mod" module maintains the processor map as a linked list, and contains routines for managing these communications with a straightforward interface. Internally, communication is carried out on the GFDL Cray T3E using either the MPI standard (http://www.mcs.anl.gov/mpi) or the Cray-native SHMEM library, which is faster, but proprietary. The domains described here are conceptually general, and can be used to specify computational domains with halo regions for distributed grid-point models as well.

The spectral core is now being parallelized using the approach above. Scaling studies have been carried out at various resolutions (R30, T42, T63, T106, T213) using a one-dimensional decomposition where spectral fields are distributed along the Fourier wavenumber and grid

fields along latitude, requiring a data transposition between the Legendre and Fourier transforms, which are carried out on-processor. The code is now under modification to be run in a shared-memory parallel mode as well.

3.1.2 Coupled Model Development

J. Anderson *B. Wyman*
I. Held

In order to support coupled modeling in a flexible framework, it is desirable to eliminate, as much as possible, the impacts of decisions made in one component model, say the ocean, on another component model, for instance the atmosphere. A coding framework for allowing the coupling of component models with arbitrary grids is under development. One result of this effort that is new to GFDL is that models of the land surface can be developed on their own grid and mostly independently of atmospheric models. The framework also minimizes the impact of design choices in atmosphere, ocean and ice models on each other.

To support this coupled model coding framework, a tool for conservative interpolation between arbitrary grids has been developed. In its present form, this tool accepts information describing the grids of various component models and creates an interpolation mapping that can be used to transfer information between the different model grids. The module has been developed so as to isolate the impacts of parallel computer architectures in a small portion of the interpolation code. Initial versions of atmosphere-ocean-ice-land models coupled with this tool have been completed and successfully integrated. The interpolation tool is relatively efficient on vector architectures and efforts to produce efficient MPP implementations are underway.

3.1.3 Support Tools for Modular Models

J. Anderson *B. Wyman*

Work has continued on a number of software tools to support the development of flexible models of components of the climate system (atmosphere, ocean, land, ice). The time and calendar manager completed last year has been incorporated successfully into the MOM ocean model and into the grid point and spectral model cores. A flexible interface using the facilities of Fortran-90 to read and write NetCDF format files has been completed and incorporated into the atmospheric dynamical cores and physics packages. An improved version of the modular model compilation tool has been developed and is in use to create complete modular models from separately developed and managed components on both the Cray T90 and the SGI workstations. This system allows a single copy of a module's source code to be used to build a variety of models on either computing platform and does not require the creation of any additional files (such as Makefiles). An HTML-based system for documenting flexible modeling components is under development. In addition to documenting individual component modules, this system interacts with output of the compilation tool to produce a set of graphical analyses of the components of a particular model configuration.

PLANS FY99

Complete atmosphere-land-ice-ocean coupled GCMs using both B-grid and spectral dynamical cores and the coupling tool will be developed and integrated.

Atmosphere and coupled integrations with flexible GCM dynamical cores will be performed as the flexible modeling system becomes the operational tool for experimental prediction at GFDL. Climate versions of these models will be developed in parallel and evaluated by GFDL climate groups.

New physical parameterizations, for clouds in particular, will be completed and tested in the flexible modeling system.

Work will continue on producing scalable versions of the spectral dynamical core that can be run efficiently on a variety of architectures. The B-grid dynamical core will be converted to a scalable form.

3.2 MODEL DEVELOPMENT FOR SEASONAL/INTERANNUAL PREDICTION

ACTIVITIES FY98

3.2.1 Sensitivity to Subgrid-Scale Parameterizations

C.T. Gordon *J. Sirutis*

Removal of an upper troposphere-lower stratosphere cap on convection in the RAS cumulus convection scheme yielded a more realistic coupled model simulation of the ITCZ and a reduced SST cold bias in the western tropical Pacific (cl) (Fig. 3.1). Conversely, the model's tropical tropopause rose to 50 hPa, while the 100 and 200 hPa levels warmed by approximately 10K and 6K, respectively. These unrealistic responses had adverse consequences for the atmospheric general circulation. In an attempt to have the best of both worlds at the surface and near the tropopause, the high cloud component of the atmospheric model's cloud prediction scheme was re-tuned. Two modifications produced rather dramatic results. First and foremost, the quadratic, temperature-dependent parameterization of optical depths of cold, cirrus clouds (based upon a scheme of Harshvardhan) was re-activated for the non-anvil class of high clouds. This modification reduced the emissivity of high clouds in convectively inactive regions, including those in the tropics. Second, the bases of high clouds were permitted to reside one sigma layer beneath their tops, if warranted by the local vertical profile of relative humidity. This modification altered the vertical profile of long wave radiative heating/cooling generated by the model's high clouds. Hence, the spatial pattern of outgoing longwave radiation (OLR) improved and the warm bias at 100 hPa and 200 hPa decreased at least to the levels experienced in the previous version of RAS, while the ITCZ and SST improvements were retained.

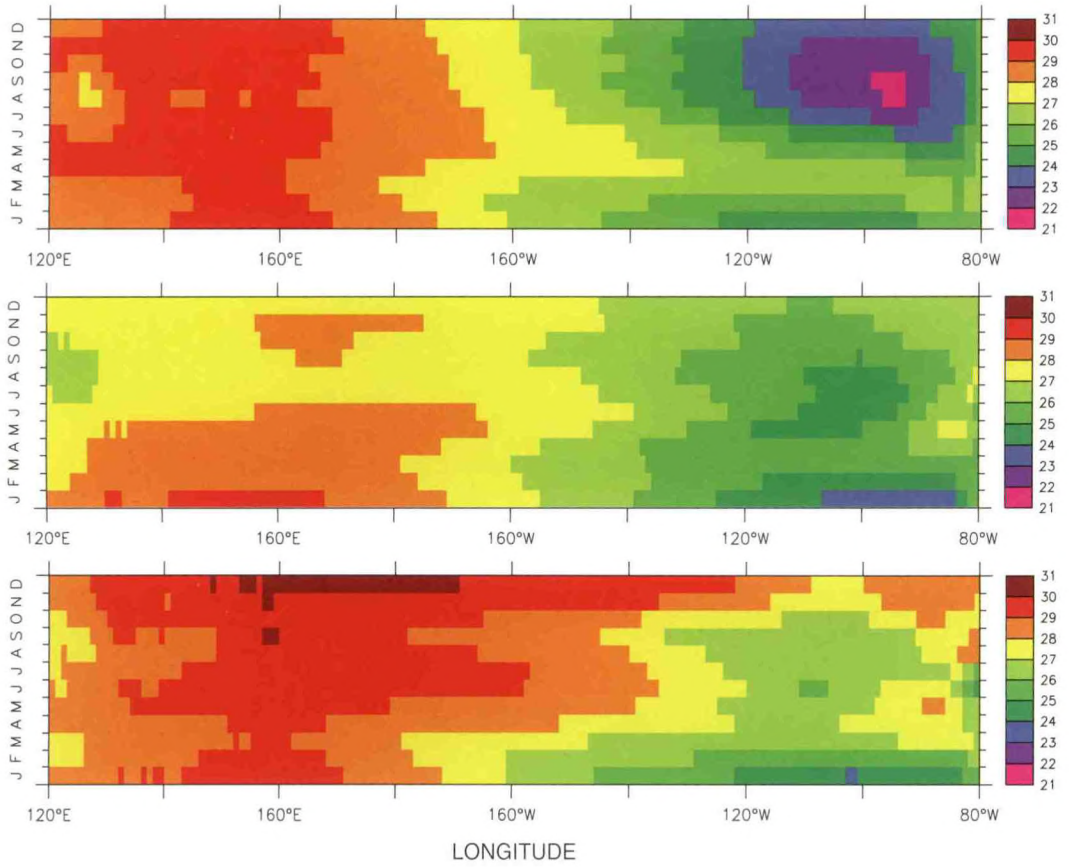

Fig. 3.1 Climatological SSTs on the equator from observations (top), from a set of coupled model one-year forecasts starting on 1 January (middle), and from a set of coupled model forecasts after the removal of the cap on convection in the RAS cumulus convection scheme. The cold bias in the western tropical Pacific has been eliminated by this parameterization change.

3.2.2 Ocean Model Simulations

M. Harrison *A. Rosati*

The verification of the ocean model is complicated by the strong dependence of the model solution on surface forcing. This is a dilemma for tropical ocean modeling in particular due to the strong interaction between planetary wave dynamics in the thermocline and surface mixed layer processes. In order to study the ocean model response to surface forcing, subgrid scale parameterization, and variation of model grid resolution, several experiments were run. The model domain covered the Pacific basin and the simulation period was 1979-1997. Some of the more notable sensitivity tests were:

- horizontal mixing - harmonic, bi-harmonic, non-linear
- vertical mixing - PP (Pacanowski Philander), KPP (K-profile parameterization)
- horizontal resolution - 1x1 degree, .25 x .25 degree
- vertical resolution - 15, 50 levels
- wind forcing - NCEP (daily,monthly,climatology), Florida State University (monthly)

Evaluation of these experiments was performed in the context of comparisons to observed data, *i.e.*, TAO (Tropical Atmosphere Ocean) moorings, TOPEX altimetry, and COARE data. Some of the current phenomenological studies using these simulation runs are:

- *Impact of tropical instability waves (TIW)* - MOM has had a long-standing bias in producing a cold tongue in the eastern Pacific that is too cold. These studies show that the 1/4 degree model produced more intense TIWs, increasing equatorward heat transport. This additional heat is important in controlling the equatorial cold tongue region by balancing the strong upwelling.
- *Warm pool dynamics* - The Pacific basin comprises several current systems that interact on seasonal and interannual time scales. Current modeling efforts are finding this complicated structure a challenge, posing several questions: What is the role of Indonesian throughflow? How is the equatorial thermocline maintained? What determines the depth and source of the equatorial undercurrent?
- *Differences between the '80s and '90s* - The '80s have been found to be more predictable than the '90s. An effort is underway to determine why the delayed oscillator, which seemed to apply in the '80s, did not work in the '90s. The role of the westerly wind bursts is also being investigated.

3.2.3 Hybrid Coupled Model

M. Harrison *A. Rosati*

Traditional ocean model development has involved using a prescribed boundary condition for momentum and a constraint on sea surface temperature (SST) and salinity (SSS) values through linear damping terms. Such constraints on the ocean do not allow for a complete evaluation of the ocean model in the context of a fully coupled GCM. A statistical atmosphere has been implemented to help further ocean model development for seasonal to interannual tropical forecasts. A singular vector decomposition of the observed wind vector and SST covariance matrix is performed in order to extract patterns of covariance in these fields. The issue of the SST and SSS constraints are addressed through the use of linear damping terms using empirically derived heat flux/SST relationships.

Surface heat fluxes are not well observed and are quite sensitive to closure assumptions for the near-surface atmospheric boundary layer, as well as assumptions about the impact of clouds on the surface radiation budget. As a result, drift is inevitable due to imbalances in the ocean/atmosphere heat flux requirements. By running the component models uncoupled, but tied to observed temperatures near the ocean surface, the corresponding heat fluxes can be compared and will, in the absence of perfection, differ. Such imbalances are the basis for "flux adjustments" used in some climate simulations. One can imagine that the climate system is somehow tied to a climatological state at the surface (*i.e.*, a mean annual cycle) and a damping restoring force exists which leads the system back to the climatological state. This is, in fact, verifiable in the tropics owing to the influence of the Clausius-Clapeyron relation, which means the saturation vapor pressure of air immediately above the ocean surface increases with rising SST and leads to an increase of turbulent latent heat transport to the atmosphere, thus reducing SST. While cloud and wind feedbacks can mitigate this process, such a constraint seems to be justified in the tropics. This is not the case in higher latitudes where, in general, circulations are more complicated owing to the variability associated with synoptic disturbances. Local regressions of surface heat flux anomalies (with the mean annual cycle

removed) to interannual SST anomalies are performed using the NCEP reanalysis and the experimental prediction group atmospheric model. These regressions are used in the hybrid coupled model runs in addition to the wind SST relationship. Regression values for SSS are set to a constant value since a clear relationship between SSS and evaporation/precipitation anomalies is not observed.

The hybrid coupled model allows for a free coupled system, not constrained too strongly to climatology, which can mimic to some extent the behavior of a fully coupled GCM (with a flux adjustment). This allows for a more complete assessment of the impacts of ocean sub-grid parameterizations and resolution on tropical variability.

3.2.4 Correction of Systematic Errors in Coupled GCM Forecasts

J. Anderson X.-Q. Yang

A method called the prognostic tendency (PT) correction is used to reduce systematic errors in coupled GCM forecasts with realistic initial conditions. The idea is simple: assess the systematic prognostic tendency error (STE) of the coupled model and subtract it from the discrete prognostic equations. The STE can be estimated by calculating a climatologically-averaged tendency between the forecast value at a very short lead time and the observed initial value and discarding the part associated with the mean seasonal cycle. The STE may be defined as a function of season or as a climatological annually-averaged constant. The PT correction is currently only applied to the three-dimensional ocean temperatures, for which the STE is computed using a very large ensemble of very short forecasts with the coupled GCM. Large values of the STE are found in the subsurface as well as at the surface, in the high latitudes and in the tropical regions. In the tropical Pacific, the dominant pattern for the STE from the surface through the subsurface is characterized by a warming tendency error in the east and cooling error in the west, while in the high latitudes the STE is confined to the surface with a cooling tendency error in the winter hemisphere and warming in the summer hemisphere. The three-dimensional STE structure assessed from the very short forecasts for the oceanic temperature is roughly consistent with the drift behavior of the uncorrected coupled model. The PT correction was incorporated into the coupled GCM system, and two sets of 12-month forecasts with January initial conditions were produced. One uses the annual cycle correction which subtracts the STE defined as a function of season, and the other uses the annual mean correction with the STE defined as a constant. These were compared to a set of forecasts without any correction. The results are summarized in Fig. 3.2, and show that both corrections can greatly reduce the drift of the coupled model and maintain a more realistic mean seasonal cycle in the oceanic temperature field, especially the annual cycle in the eastern Pacific. The impact of the PT correction on the ENSO-related interannual variability and forecasting skill was also examined. The annual mean correction tends to be more helpful in producing a higher skill of ENSO prediction with a longer lead time. The feedback mechanisms responsible for the improvement of mean annual cycle due to corrections and possible impact of corrections on the extratropical seasonal forecasts were also investigated.

PLANS FY99

Ocean simulation runs will be used to explore further the phenomena mentioned in 3.2.2 through the analysis of heat and momentum budgets. The sensitivity studies will be used

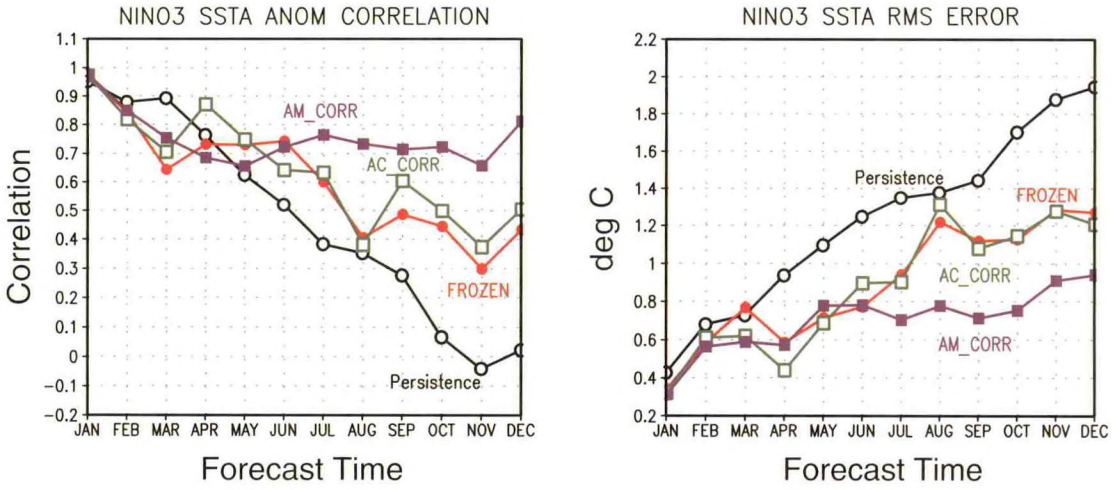

Fig. 3.2 Nino-3 region SST anomaly correlation and rms error as a function of forecast lead time for a set of 17 coupled model forecasts. The red curves are for uncorrected forecasts while the blue and green curves have had annual mean and seasonally varying systematic tendency error corrections applied. The black curves show the skill of persistence forecasts as a control. Both corrections reduce the drift of the coupled model and maintain a more realistic mean seasonal cycle.

in an attempt to configure coupled GCMs so that mean bias is reduced and forecast skill is improved.

Investigation of ocean model development and prediction issues using the hybrid coupled model will continue. External stochastic forcing will be included for the coupled model simulations. Stochastic forcing (1339), for the 1997 event in particular, has been discussed as an important factor in warm event development.

The inter-decadal sensitivity of ENSO forecast skill to realistic marine stratus clouds will be further examined, using the ensemble of model simulations and forecasts (3.3.1). New coupled model ENSO forecasts will be made with the modified RAS cumulus convection scheme and re-tuned cloud prediction scheme. The analysis of the sensitivity of the coupled model's annual cycle and its inter-annual response to various treatments of low cloud forcing (1403) will continue, using additional analysis techniques such as singular value decomposition (SVD) analysis.

The equatorial temporal variability of surface fluxes and other variables from long term coupled and uncoupled GCM integrations will be analyzed. Results from the latter (with specified SSTs) will be compared with NCEP re-analyses and COADS analyses.

3.3 ATMOSPHERIC AND OCEANIC PREDICTION AND PREDICTABILITY

3.3.1 Coupled Model Ensemble Prediction Experiments (CMEP)

J. Anderson *A. Rosati*
C.T. Gordon *J. Sirutis*
R. Gudgel *R. Smith*
M. Harrison *W. Stern*
J. Ploshay

A large set of experiments consisting of ocean data assimilation, atmosphere-only integrations, and coupled model forecasts using a frozen version of the atmosphere (version V197) and ocean (MOM II) models has been completed. The experiments were motivated by a number of goals designed to improve seasonal-interannual prediction, including:

- Assess the seasonal prediction capabilities of the current fully coupled model (he)
- Examine potential predictability of the coupled model (1300)
- Explore the internal variability of the coupled model and its impact on prediction capabilities
- Examine the impact of systematic bias corrections on predictive skill and internal variability
- Compare forced atmospheric simulations to coupled predictions (1449)
- Explore the validity of AMIP-type predictability experiments (gq)
- Identify areas in which the coupled model system may be improved
- Evaluate the use of observed atmospheric initial conditions for seasonal prediction (1450)
- Assess the impact of ocean initial condition details on predictions
- Prepare a set of diagnostics for evaluating coupled model ensembles
- Evaluate the impact of two-tiered and anomaly coupled models

The core of the experiments is an ensemble of simulations and predictions with the atmosphere and coupled models. Each member of an ensemble is composed of an atmosphere-only integration (each starting from slightly perturbed initial conditions) for the duration of the ocean data assimilation period (currently 1979 to 1997), plus a set of coupled model forecasts started every six months (1 January and 1 July) with initial ocean conditions from the assimilation and initial atmosphere conditions from the atmosphere-only integration. An initial ensemble of six members has been completed. One coupled run from the first ensemble member has been extended to several decades to examine the internal variability of this coupled model.

A number of auxiliary experiments have also been completed. These include a set of coupled predictions with observed atmospheric initial conditions from the NCEP reanalysis, a large suite of single timestep coupled runs to derive the systematic error tendency (3.2.4), a limited ensemble of coupled predictions with systematic error correction (3.2.4), an extended coupled integration with systematic error correction, and a number of atmosphere-only and coupled runs from different ocean assimilations.

Output from the coupled model ensemble prediction experiments is available in a standard NetCDF format and has been made available to members of the GFDL University Consortium, as well as to researchers within GFDL for analysis.

3.3.2 Interannual and Interdecadal Predictability of Tropical Storms

J. Anderson F. Vitart

Tropical storms simulated by a nine-member ensemble of GCM integrations forced by observed SSTs have been tracked by an objective procedure for the period 1980-1988 (1455). Statistics on tropical storm frequency, intensity and first location have been produced. Statistical tools (Chi-Square or Kolmogorov-Smirnov tests) indicate that there is significant potential predictability of the interannual variability of tropical storm frequency, intensity and first location over most of the basins. This implies that SSTs play a fundamental role in model tropical storm interannual variability. An EOF analysis of local SSTs over each ocean basin and a combined EOF analysis of vertical wind shear, 850 mb vorticity and 200 mb vorticity have been performed. Over some basins like the western North Atlantic, the impact of SSTs on simulated tropical storm statistics is an indirect effect through the large scale circulation, as in observations.

It has been observed that the number of Atlantic tropical storms was higher in the 1950s than in the 1970s. To test the ability of the GCM to simulate such decadal change, a 10-member ensemble of atmospheric GCM integrations forced by observed climatological SSTs from the 1950s has been performed. The results are summarized in Fig. 3.3, which shows a significantly (99% significance) higher number of tropical storms compared to similar integrations using climatological SSTs from the 1970s. Further examination indicates that it is the

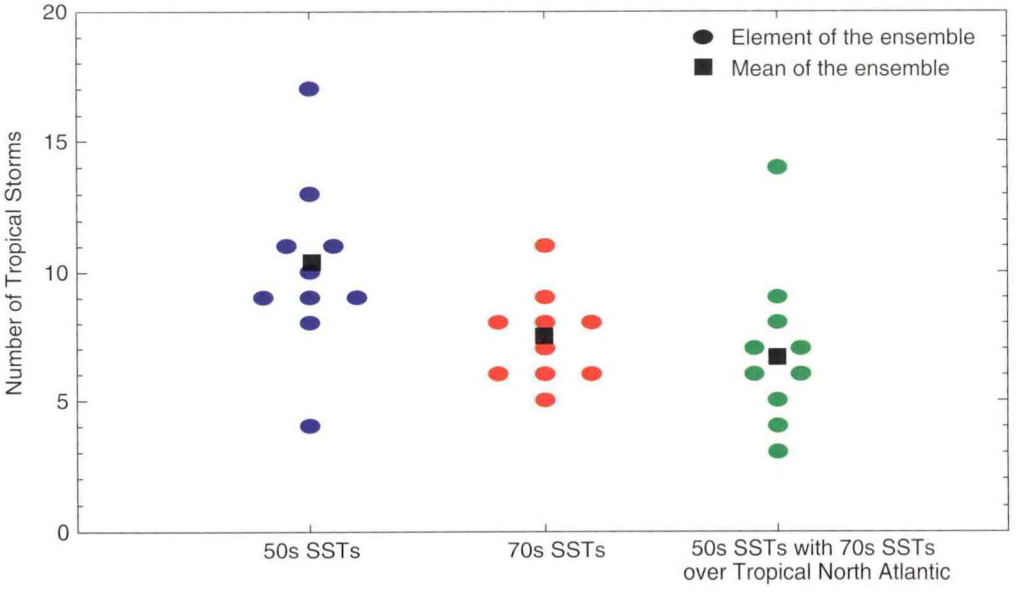

Fig. 3.3 Number of tropical storms produced over North Atlantic in ensemble of 10 AGCM simulations with 1950's SSTs everywhere (blue), 1970's SSTs everywhere (red), and 1950's SSTs everywhere except over the tropical North Atlantic where 1970's SSTs are used (green). Ensemble means are marked by black square. The model is able to capture the decadal change in storm frequency and attribute this change to cooling of the tropical North Atlantic.

local cooling of tropical North Atlantic SSTs that is responsible for the decrease of simulated tropical storm activity in the 1970s.

3.3.3 Tropical Intraseasonal variability

A. Rosati *W. Stern*
R. Smith

Space-time power spectra for the 850 mb velocity potential from a five-case ensemble of integrations with the current (v197) atmospheric GCM (AGCM) configuration show a dramatic improvement relative to earlier AMIP I ensemble results (cj), with the main difference being attributed to changes in the convection scheme (*i.e.*, Relaxed Arakawa-Schubert in v197 versus moist convective adjustment in the AMIP I). These AGCM ensemble mean space-time spectra, along with v197 coupled GCM ensemble mean spectra, are plotted in Fig 3.4. It is evident that the dominant modes for tropical intraseasonal oscillations (TIO) in the v197 AGCM ensembles have more than twice the amplitude of the dominant TIO modes in AMIP I and the period is shifted to the 40-60 day range as compared to approximately 30 days. In addition, tropical intraseasonal oscillations (TIO) from the (five case) ensemble of v197 coupled GCM predictions appear to be of somewhat stronger amplitude and somewhat slower speed (approximately 60 days versus approximately 50 days) when compared to the v197 AGCM ensemble results. This is presumably an impact of the interactive ocean. Studies are currently underway to investigate the potential predictability of TIO by looking at the significance of interannual TIO fluctuations.

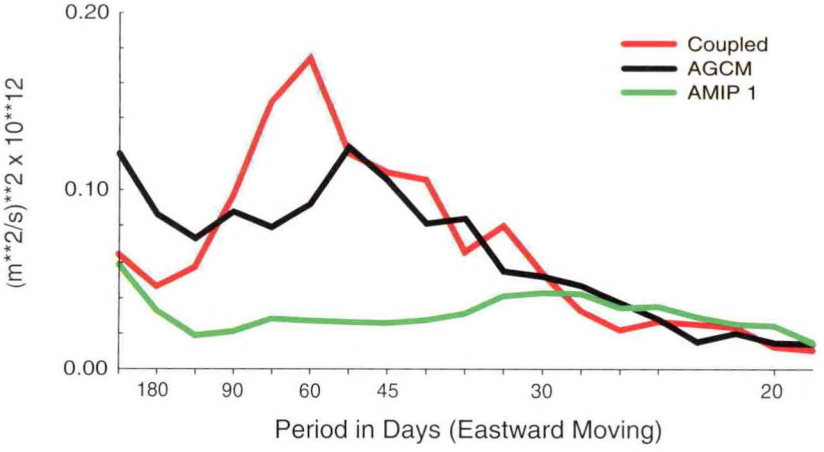

Fig. 3.4 1980-88 time mean, ensemble mean wave number 1 χ_{850} power spectra for: v197 coupled GCM predictions (red curve), v197 AGCM integrations (black curve) and AMIP I ensemble integrations (green curve). Tropical intraseasonal oscillations are much improved in amplitude and phase in v197 versus AMIP I and somewhat stronger and slower in the coupled GCM versus the AGCM.

3.3.4 Relationship Between Tropical Convection and SST

R. Gudgel *A. Rosati*

This study examines the relative roles of the large-scale circulation and SST on the relationship between tropical convection and SST. The SST, outgoing longwave radiation

(OLR), and wind divergence fields from the atmosphere-only, coupled model predictions, and coupled model long run of the CMEP experiment (3.3.1) have been compared to each other and to observations in order to understand better the complex relations between these fields. The comparisons to observed fields showed significant bias in the convection scheme, a problem now under investigation (3.2.1).

3.3.5 Coupled Model Equatorial Response to Different Specifications of Low Clouds

C.T. Gordon *M. Harrison*
R. Gudgel *A. Rosati*

In a previous multi-year coupled model sensitivity experiment, the seasonal cycle of SSTs in the eastern equatorial Pacific was found to improve substantially when the model-predicted low clouds over the ocean were replaced with a specification from the ISCCP (International Satellite Cloud Climatology Project) database. This result was attributed to the fact that the ISCCP clouds quasi-realistically simulated the marine stratus regime. Now, an additional suite of multi-year sensitivity experiments has been performed to help elucidate cloud feedbacks upon the equatorial dynamics in the context of the annual mean SST and its seasonal cycle in the equatorial Pacific, as well as SST variability on the ENSO time scale. All members of the suite of experiments may be viewed as employing specified low clouds over the oceans based upon ISCCP multiplied by a scale factor SF. The distinguishing characteristic of each experiment amongst the suite is the value of SF: 1.0 (full ISCCP), 0.8, 0.5, 0 (zero low clouds), and a hybrid specification corresponding to full ISCCP (SF = 1.0) in the tropical Pacific, east of longitude 120W, and no low clouds (SF = 0) elsewhere. In all experiments, low clouds over land as well as high and middle clouds over both land and sea are predicted by the atmospheric model's empirical cloud prediction scheme.

A modified view of the feedback of clouds upon coupled model equatorial dynamics has emerged from the above suite of sensitivity experiments. The presence of marine stratus leads to an intensification of the trade winds and upwelling. In turn, the strength and westward extent of the eastern equatorial Pacific affects the SSTs in the western equatorial Pacific. However, the efficiency of this circulation is modulated by the sign of the SST and heat content biases in the western equatorial Pacific cold tongue on a somewhat delayed time scale. More specifically, a cold bias (warm bias) in the western equatorial Pacific reinforces (opposes) the positive feedback of the marine stratus upon the equatorial dynamics. Meanwhile, the temperature bias in the western tropical Pacific itself can change sign due to a relatively modest change in low cloudiness and short wave radiation at the ocean surface. Overall, the SF = 0.8 simulation is perhaps the most realistic, as it retains most of the strength of the seasonal cycle of the simulation with the impact of ISCCP low clouds, while exhibiting a reduced cold bias in the western tropical Pacific and somewhat stronger interannual variability on the ENSO time scale. The results also suggest that the SST simulation across the tropical Pacific is very sensitive to cloud amount and cloud optical properties. The 0.8 ISCCP vs. 1.0 ISCCP differential low cloud amount field is quite small in the western tropical Pacific, and may be difficult for cloud parameterization schemes to predict.

3.3.6 Predictable Component Analysis

S. Griffies *T. Schneider*

A conceptual framework has been developed for a unified treatment of issues arising in a variety of predictability studies. The predictive power (PP), a predictability measure based on information-theoretical principles, lies at the center of this framework. The PP is invariant under arbitrary linear coordinate transformations and applies to multivariate predictions without making assumptions about the probability distribution of prediction errors. For univariate Gaussian predictions, the PP reduces to the conventional predictability measure that is based on the ratio of the rms prediction error over the rms error of a "prediction" drawn randomly from the climatology.

Climatic variability on intraseasonal to interdecadal time scales follows an approximately Gaussian distribution. For multivariate Gaussian predictions, the predictability measure PP makes it possible to discriminate a system's predictable components from its unpredictable components. Predictable components can be extracted by predictable component analysis, a procedure derived from discriminate analysis: seeking components with large PP leads to an eigenvalue problem, whose solution yields uncorrelated components that are ordered by PP from largest to smallest.

The application of the PP and the predictable component analysis in different types of predictability studies has been described. Studies are being considered that use either ensemble integrations of numerical models or autoregressive models fit to observed or simulated data.

PLANS FY99

A number of studies using the results from the CMEP experiments will be performed to address the goals listed in 3.3.1. In particular, forecast skill and potential skill will be examined for both tropical and extratropical fields. The impacts of ocean and atmosphere initial conditions on skill and potential skill will also be studied.

Experiments will continue, using the CMEP experiments as a baseline, to evaluate possible improvements to coupled models for seasonal/interannual prediction. Of particular interest will be improvements to atmospheric and ocean model physical parameterizations, especially cloud and convective parameterizations. An effort to understand methods for reducing initial drift of coupled model forecasts will begin.

Efforts to explore the relationship between SST and convection in model runs and observations will continue, with a focus on seasonal and interannual variability of the ITCZ.

Predictable component analysis will be applied to atmosphere-only and coupled model integrations from the CMEP experiments.

3.4 DATA ASSIMILATION

ACTIVITIES FY98

3.4.1 Nonlinear Filter for Ensemble Data Assimilation

J. Anderson

Knowledge of the probability distribution of initial conditions is central to almost all practical studies of predictability and to improvements in stochastic prediction of the atmosphere. Traditionally, data assimilation for atmospheric predictability or prediction experiments has attempted to find a single "best" estimate of the initial state. Additional information about the initial condition probability distribution is then obtained primarily through heuristic techniques that attempt to generate representative perturbations around the "best" estimate (1509). However, a classical theory for generating an estimate of the complete probability distribution of an initial state given a set of observations exists. This non-linear filtering theory can be applied to unify the data assimilation and ensemble generation problem and to produce superior estimates of the probability distribution of the initial state of the atmosphere (or ocean) on regional or global scales. A Monte Carlo implementation of the fully non-linear filter has been developed and applied to several low order models. The method is able to produce assimilations with small ensemble mean errors while also providing random samples of the initial condition probability distribution. The Monte Carlo method can be applied in models that traditionally require the application of initialization techniques without any explicit initialization. Fig. 3.5 demonstrates the application of the Monte Carlo filter in the simple 3-variable Lorenz-63 dynamical system. Initial application to larger models is promising, but a number of challenges remain before the method can be extended to large realistic forecast models. The method has been applied successfully in a spectral barotropic model at T42 resolution. An effort is underway to apply the data assimilation algorithm in the context of the flexible B-grid model (3.1.1.1) with simple physics.

3.4.2 Ocean Data Assimilation

M. Harrison *A. Rosati*

Perhaps the main utility of Ocean Data Assimilation (ODA) is to help correct for the mean bias of both the ocean model and atmospheric forcing (1457). However, continued improvements of the type discussed earlier (3.2.3) are needed. Naturally, efforts at improving the ODA are intimately related to ongoing model development efforts.

In order to produce ocean initial conditions that are more consistent with the coupled model, the ODA system was run from 1979-1997 forced by daily winds from the atmosphere-only runs. This is a first attempt to address the issue of initialization shock. While the forecast runs indicate a sensitivity to the ocean initial conditions using different wind forcing, the forecast results were comparable to those ocean initial conditions from the ODA forced with NCEP reanalysis winds.

PLANS FY99

The Monte Carlo Filter will be applied to the B-grid model to determine if the method is capable of scaling to realistic prediction models.

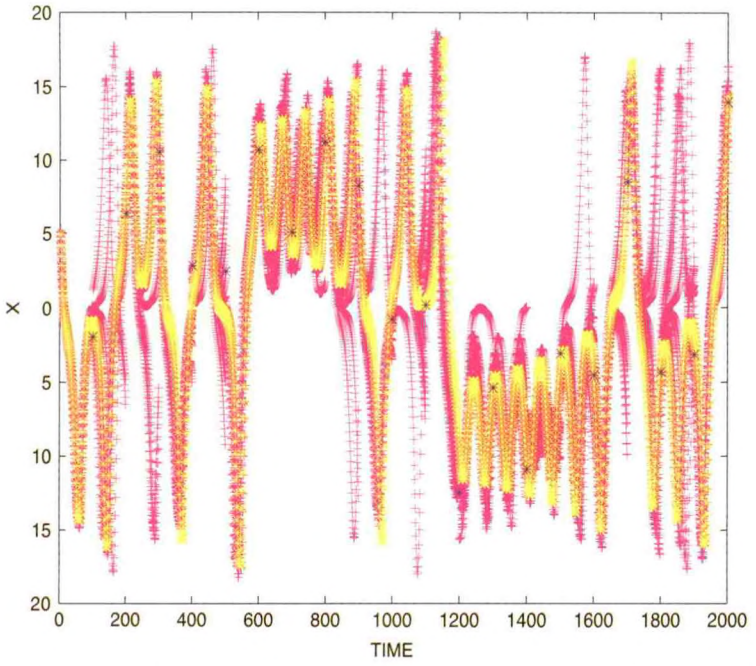

Fig. 3.5 Time series of control integration (yellow), 10 members of a 40 member Monte Carlo assimilation (magenta) and observations (blue) with standard deviation 2.0 available every 100 timesteps, for x variable of Lorenz-63 model. At certain times, such as around timestep 400, the assimilation produces an ensemble with small spread, while at others, such as time step 1100, there is considerable uncertainty in the assimilation.

Aspects of the ODA scheme that improve initialization of the coupled model with regard to a reduction of shock and improved forecast skill will be investigated. In particular, the sensitivity to forcing, the first guess and observational statistics, and data coverage will be examined.

3.5 OCEAN-ATMOSPHERE INTERACTIONS

A. Fedorov *B. Winter*
S. Harper *A. Wittenberg*
S.G.H. Philander

ACTIVITIES FY98

Although much progress has been made in our understanding of El Niño during the 1980's -- no one anticipated the event of 1982, but by 1987 there were coupled ocean-atmosphere models capable of skillful predictions -- the 1990's brought surprises. First there was the unexpected persistence of unusually warm surface waters over the eastern tropical Pacific after El Niño of 1990, then there was El Niño of 1997 which the models predicted with mixed success. Has there been a change in the properties of El Niño between the 1980s and 1990s? Analyses of long time-series indicate that El Niño is subject to decadal modulations (dw), energetic up to the early 1930s, then practically disappearing for a few decades before reappearing in the late 1950s. The possible causes of these changes are being investigated via analysis of data from the TOGA-TAO array, analyses of gridded data sets provided by a GCM that assimilates the available measurements, and through modeling studies.

A change in the mean state of the tropics is one possible explanation for the decadal modulation of El Niño. (Simple coupled ocean-atmosphere models in which the mean depth of the thermocline is specified show that the amplitude of the simulated Southern Oscillation is very sensitive to changes in that depth.) The processes that maintain the thermocline include a shallow, wind-driven meridional circulation that involves the subduction of surface waters in the subtropics off the western coasts of the Americas, Africa, and Australia. Studies with a realistic ocean GCM indicate striking differences between the three oceans. Whereas water parcels can reach the equator from either hemisphere in the Pacific, this is possible only from the Southern Hemisphere in the much smaller Atlantic and Indian Oceans. The implications of this result, which suggests that low frequency variability in low latitudes can have very different origins in the three oceans, have been explored for the case of the Pacific by means of a simple coupled model of self-sustaining decadal oscillations (bo).

The continual exchange of surface waters between the tropics and extratropics means that a change in high latitude conditions will, in due course, affect the tropics. The manner in which the unusually low surface temperatures of the polar regions during the Last Glacial Maximum (LGM) affected low latitudes has been a matter of much debate. At first, it was believed that, during the LGM, the tropics were only slightly colder than they are today. However, recent data indicate that the tropics were significantly colder. Calculations with coupled GCMs show that, because of the shallow meridional circulation that links the tropics and extratropics, a cooling of the polar regions caused the tropical thermocline to shoal. The resultant decrease in sea surface temperatures were then amplified by local interactions between the ocean and atmosphere, interactions of the type that characterizes El Niño.

The importance of the mean state to interannual fluctuations emerges from a study of the energetics of the Southern Oscillation. Data from a realistic simulation over a prolonged period indicate that the surface winds do positive work on the ocean and create available potential energy during half the cycle, and destroy that available potential energy during the other half. If the work done is represented by the terms $u' \overline{\tau^x} + \overline{u}\ \tau^{x'}$ where bars indicate a time average, and primes indicate the departure from a time-average, then the first term is found to be dominant by a large margin. This result suggests that the background state that supports El Niño as part of an interannual oscillation is characterized by certain time-averaged winds with which are associated a certain zonal temperature gradient, and a zonal slope of the thermocline. Current research is focussed on determining whether there were changes in these fields between the 1980s and 1990s.

PLANS FY99

Studies planned for the coming year include the effect of warm and cold extratropical surface anomalies on the tropical thermocline, and the dependence of the spectrum of interannual, coupled ocean-atmosphere modes of oscillation on the mean state (time-averaged climate) of the tropics. A principal question will be whether the time-averaged zonal component of the wind has to exceed a certain value before interannual oscillations are possible. These studies are part of a long-term effort to develop realistic coupled ocean-atmosphere models.

4. OCEANIC CIRCULATION

GOALS

To develop a capability to predict the large-scale behavior of the World Ocean in response to changing atmospheric conditions, through detailed three-dimensional models.

To identify practical applications of oceanic models to human marine activities by the development of a coastal ocean model.

To incorporate biological effects in a coupled carbon-cycle/ocean GCM.

To study the dynamical structure of the ocean through detailed analyses of tracer data.

4.1 WORLD OCEAN STUDIES

4.1.1 The ACC and the Ocean's Large-Scale Circulation

B. Samuels *J.R. Toggweiler*
I. Held

ACTIVITIES FY98

Northward heat transport by the Atlantic Ocean's conveyor circulation maintains a relatively mild climate in the high latitudes of the North Atlantic region. The ocean's ability to transport heat into this region is generally attributed to the formation of North Atlantic Deep Water (NADW) north of Iceland and to the thermohaline processes which give rise to NADW. Diapycnal mixing in the interior and the Atlantic's salt balance are thought to be critical factors. However, recent work (1313, 1562) has suggested that the conveyor circulation is linked to the Antarctic Circumpolar Current (ACC) in the Southern Hemisphere. This work challenges the idea that thermohaline processes are as important as generally believed. A simple coupled model has now been built to evaluate these claims (if).

The new model consists of a fully three-dimensional ocean GCM coupled to an energy balance model of the overlying atmosphere. It describes a nearly water-covered earth in which land is limited to two small polar islands and a thin barrier which extends from one polar island to the other ("water planet model"). The model makes it easy to illustrate the climatic effect of opening Drake Passage and switching on the ACC. All temperatures in the ocean and atmosphere are internally determined and there is no hydrological cycle or salinity forcing. A simple latitudinally varying wind stress is applied to the ocean in lieu of interactive winds.

Figure 4.1 compares the meridional overturning for a full barrier version in which the thin barrier between the polar islands is complete (top), and the Drake Passage gap version

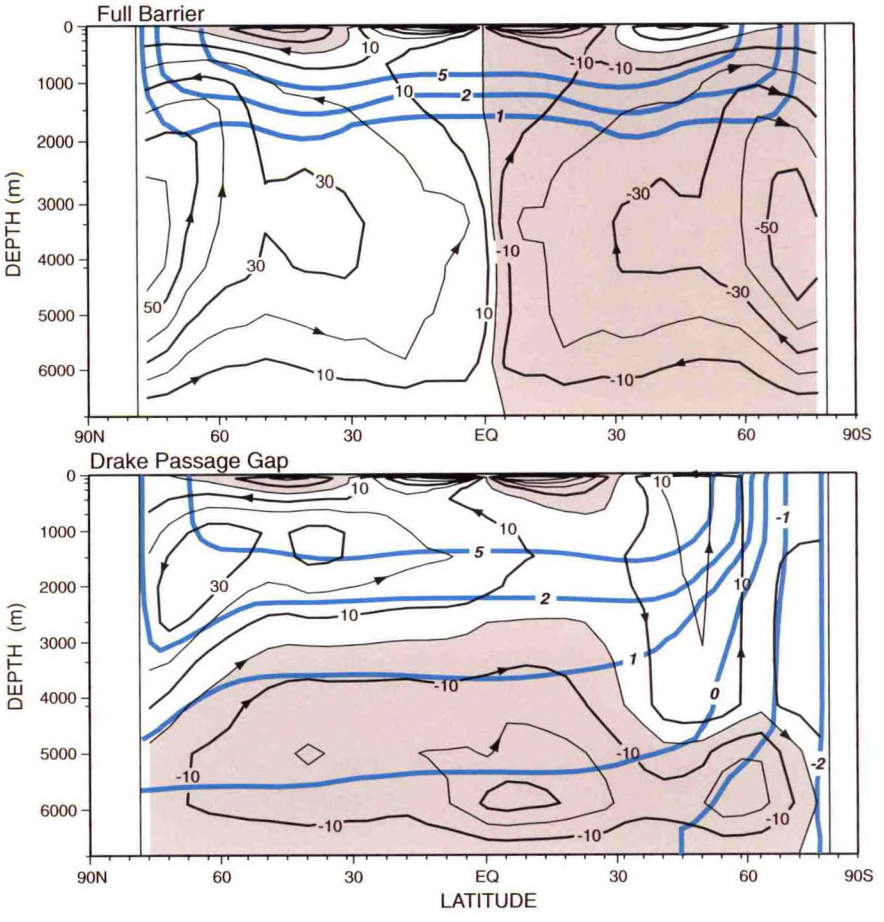

Fig. 4.1 Stream function of the meridional overturning in the ocean for the full barrier (top) and Drake Passage gap (bottom) versions of the water-planet model (units Sv). Blue contours show positions of model isotherms colder than 5°C (zonally averaged). All deep water below 2000 m in the full barrier model is between 0.5° and 1.0°C. Opening Drake Passage initiates a conveyor circulation which warms the high latitudes of the Northern Hemisphere and cools the high latitudes of the Southern Hemisphere.

in which a segment of the barrier is removed in the latitude band of the Southern Hemisphere westerlies (bottom). Positions of the coldest model isotherms are superimposed in blue. With Drake Passage closed, the overturning consists of two large thermally-driven cells in each hemisphere. Water with a temperature of about 0.5°C sinks at both polar islands and fills most of the interior. When Drake Passage is opened, the Southern Hemisphere cools and the Northern Hemisphere warms. Two-degree water sinks at the north polar island and flows southward across the equator above colder bottom water from the south polar island. The formation of deep water at the north polar island draws warm upper-ocean water from the Southern Hemisphere all the way up into the high latitudes of the Northern Hemisphere. This response duplicates to an extraordinary degree the conveyor circulation and thermal structure seen in more comprehensive models.

The stress from winds over the open channel pushes circumpolar surface waters northward, raising the sea surface on the north side of the channel and depressing the surface on the south side. Ekman divergence in the south causes water to upwell from great depth. Surface waters pushed out of the channel to the north reconnect with the water upwelled in the south by traveling all the way up to the north polar island, sinking to middle depths, and

then traveling south again as part of a deep western boundary current along the barrier. This interhemispheric response turns out to be an efficient way for the circulation system to maintain mass and momentum balances in the ACC.

PLANS FY99

The water planet model will be modified to include "Atlantic" and "Pacific" basins where the Atlantic basin extends to a higher latitude. A simple hydrological cycle and salinity variations will also be introduced. It is anticipated that the opening of Drake Passage will cause salty water to be concentrated in the Atlantic basin. The water planet model will also be coupled to an atmospheric GCM in order to include interactive winds.

4.1.2 Thermohaline Circulation in Isopycnal Coordinates

R.W. Hallberg J.R. Toggweiler

ACTIVITIES FY98

The sinking branch of the thermohaline circulation has long been known to consist of relatively few regions of deep convection. The traditional view of the upwelling branch of the thermohaline circulation is a widely distributed upwelling through the thermocline, but measured diapycnal diffusivity is about an order of magnitude less than would be required. Recent studies have suggested that much of the upwelling is actually the result of Ekman pumping in the Southern Ocean (1313).

Isopycnal-coordinate ocean models are ideally suited for studying the thermohaline circulation. Numerical diapycnal diffusion can be eliminated entirely, and all diapycnal mass fluxes are explicitly parameterized. A series of 2° resolution isopycnal-coordinate ocean model simulations are being used to test the hypothesis that interior diapycnal mixing rates of order 0.1 $cm^2\ s^{-1}$ are suitable for the ocean's thermocline. These studies attempt to reproduce both the observed density structure and the meridional heat transport. These simulations use real bathymetry, ECMWF climatological wind stress, and a mixed flux and restoring surface buoyancy forcing that enforces approximately the observed oceanic meridional heat transport. The preliminary indication is that the observed thermocline density structure is in fact recovered with this weak diffusivity, while a larger (0.5 $cm^2\ s^{-1}$) diffusivity leads to an excessively broad thermocline. A larger diffusivity is required at depth to yield a realistically strong meridional circulation in the abyssal Pacific Ocean. This study indicates that the ocean's density structure is dynamically consistent with the observed levels of open ocean mixing, and that the warming branch of the thermohaline circulation largely occurs through wind-driven upwelling in the Southern Ocean and at the equator.

PLANS FY99

Once the global simulations with enforced heat transports have more fully spun up, sensitivity studies will explore the relative importance of the diapycnal diffusivity and the strength of the wind stress in the Southern Ocean in determining the thermocline structure and the strength of the thermohaline circulation. The effect of new parameterizations of mixing in the bottom boundary layer will also be tested.

4.1.3 Sea Ice Studies and Model Development

M. Winton

ACTIVITIES FY98

Sea ice cover is sensitive to the gravitational stability of the near-surface ocean which modulates the upward flux of heat at polar latitudes where a fresh cold surface layer overlies warm salty water below. However, the sea ice can also be considered a component of that stability, in addition to the water column stratification, by virtue of its role as a surface reservoir of fresh water. For example, the enhanced upward flux allowed by weak stratification can melt ice, thereby reducing surface salinities and strengthening the stratification. An analytical expression combining the sea ice cover and stratification into a "bulk" stability has been developed. This allows the stability of observed ice/temperature/salinity profiles to be easily visualized (hk).

Coupled climate models (1286) show that the sea ice response to greenhouse warming provides much of the character of the global response. The arctic winter warming is predicted to be the largest of the transient warmings in any season over the globe and is traceable to thinner sea ice there. In the Southern Ocean, sea ice increases as the ocean becomes more salinity-stratified and so provides less heat to the surface (gs). The satellite record of sea ice concentration over the past two decades contains hints of this modelled asymmetric response.[1]

The sea ice component of the coupled climate model used for the greenhouse predictions is very simple and lacks a proper representation of potentially important dynamical and thermodynamical processes. An alternative model, intended for inclusion in the coupled model, has been developed to address these criticisms, to improve comparability with observations, and ultimately to improve the representation of sea ice in climate simulations. The model is dynamical in that sea ice motion is the product of the forces which act upon the ice. The internal ice stresses are calculated according to a viscous-plastic rheology, and ice-free areas within the ice pack are predicted using standard techniques.

PLANS FY99

The new sea ice model will be incorporated into a coupled ocean-atmosphere model. Values of the tunable parameters and a series of refinements to the basic model will then be considered. Prominent issues for the representation of thin Southern Ocean sea ice include the representation of drag on the upper and lower surface of the ice and interaction with the weakly stratified water column. For thick arctic ice, the representation of internal ice stresses, surface and internal melting, and representation of the ice heat capacity will require investigation.

---

1. Cavalieri, D.J., P. Gloerson, C.L. Parkinson, J.C. Comiso, and H.J. Zwally, Observed Hemispheric Asymmetry in Global Sea Ice Changes, *Science, 278*, 1104-1106, 1997.

4.1.4 Bottom Boundary Layers in Coarse-Resolution Ocean Models

A. Gnanadesikan *R.C. Pacanowski*
R.W. Hallberg *M. Winton*

ACTIVITIES FY98

Dense overflows play an important role in ventilating the deep ocean. The representation of these overflows in different ocean models has been limited by the model architecture. It has recently been demonstrated (et) that level-coordinate models have trouble maintaining the density signal in such flows. This is because as a water mass moves from a shallow water column to a deeper one, it must pass through all intervening levels in the deep water column. This numerical entrainment keeps dense water at the top of shelves unless the slope is resolved by the model grid, a prohibitive constraint for global models. By contrast, isopycnal-coordinate ocean models easily maintain such dense flows, but have problems parameterizing the way in which such flows mix with the interior fluid and are affected by nonlinearities in the equation of state. Sigma-coordinate models are very good at representing dense overflows, but have problems with pressure gradient errors when the water column is stably stratified.

Recently, major progress has been made in improving both the level-coordinate and isopycnal-coordinate models. A bottom-following layer has been added to the level-coordinate model (ez). This layer turns the model into a sigma-coordinate model in regions where there is unstable stratification along the slope, but retains the advantages of a level-coordinate model in regions of stable stratification. The model has been incorporated into the MOM 3 code, and testing is proceeding.

Additionally, a diapycnal mixing scheme for an isopycnal-coordinate model has been developed. This scheme allows for a gravity current to entrain lighter interior fluid, either as the result of stratified shear instability or because of turbulent kinetic energy generated at the bottom. Fig. 4.2 shows the development of such a layer. One interesting feature is the ability of this model to simulate periodic entrainment due to inertial oscillations.

PLANS FY99

Both the isopycnal and level-coordinate models will be tested in regional and global models. The global models will be used to investigate whether resolution of the bottom boundary layer is an important ingredient in allowing for a realistic North Atlantic overturning circulation, and in permitting the Antarctic shelves to communicate with the deep Weddell Sea. Some idealized cases will be run, as well.

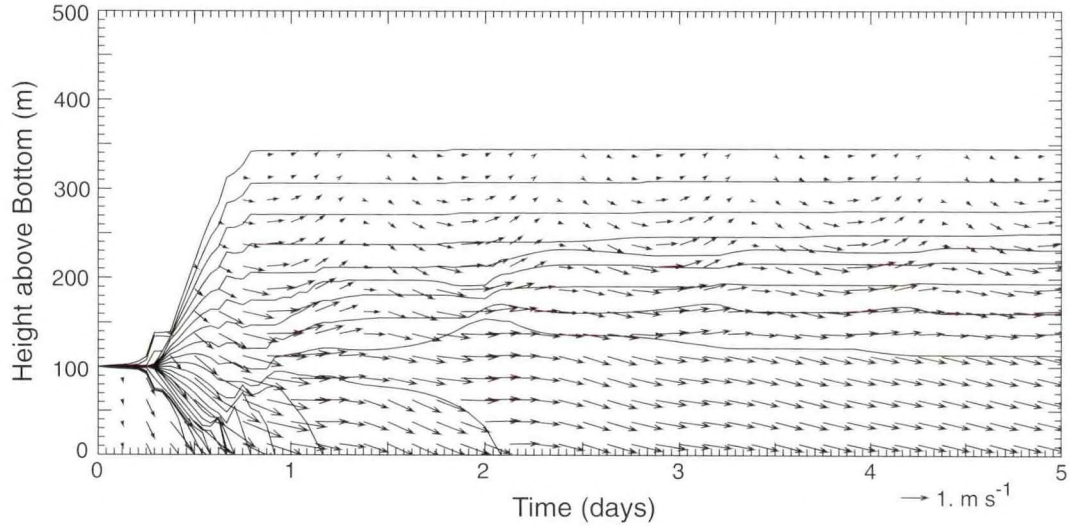

Fig. 4.2 Isopycnal depths and along- and downslope-velocities (right and down in this figure) as a function of time in a one-dimensional isopycnal-coordinate column model of an entraining gravity current. Entrainment is parameterized as a function of the shear Richardson number. The bottom layer is initially 2 kg m^{-3} denser than the interior water, with 20 intervening layers. The water accelerates due to a pressure gradient (isopycnals are assumed to be parallel to a 1% bottom slope), Coriolis acceleration and bottom drag. The parameters here are similar to those in the Strait of Gibraltar overflow, and the amount of entrainment is similar to that observed and occurs with a realistically short time scale of only a few days. A new numerical technique makes this possible (le) with a time step of 1 hour.

4.1.5 Thermally Driven Circulations from a Level Model (MOM) and a Layer Model

K. Bryan *Y.-G. Park*

ACTIVITIES FY98

Thermally driven circulations in an idealized basin are compared using results from a level model with vertical layers of fixed depth (MOM 2) and a layer model based on discrete isopycnal layers (4.2.2). In the interior and away from the side boundaries, both models show very similar flow patterns. Studies of source-driven flows suggest a two-layer flow structure, but both models show a three-layer structure. The eastward surface flow, which has not been recognized in earlier studies, is due to surface boundary conditions. The northeastward deep flow is due to water mass formation as explained[2]. The southwestward subsurface flow compensates for the deep flow and the surface flow, consistent with studies of source-driven flows.

The layer model produces an eastern boundary current that carries warm water to the polar region. There is no equivalent feature in the level model, so the two models produce very different air-sea heat exchange patterns. The lack of an eastern boundary current in the level model is compensated by a stronger western boundary current, making the total meridional mass and heat transports from the two models the same. In the level model, the stronger

2. Stommel, H., and A.B. Arons, On the abyssal circulation of the world ocean, II. An idealized model of the circulation and amplitude in oceanic basins, *Deep-Sea Res.*, *6*, 217-233, 1960.

western boundary current supplies warmer water to the polar region, and the convective adjustment makes vertical mixing stronger. The level model produces warmer deep water.

4.1.6 High-Resolution North Atlantic Studies

W. Hurlin

ACTIVITIES FY98

The Labrador Sea is subject to freshening events that inhibit convection in the center of the basin and suppress the formation of deep water. The best-known event, the Great Salinity Anomaly (GSA) of the late 1960s/early 1970s, is usually attributed to a pulse of fresh Arctic water which entered the Labrador Sea via the East Greenland Current. A set of model simulations was carried out 1) to determine whether a volume of freshwater of the same magnitude as the GSA inserted into the East Greenland Current could, in fact, inhibit convection in the center of the basin, 2) to determine the extent to which the salinity anomaly could alter the circulation patterns (important for sea ice and biology), and 3) to see how model resolution influenced the extent of freshening. The potential for freshening by a change of winds was also evaluated.

At 1° resolution, the prescribed salinity anomaly in the East Greenland current penetrates the central Labrador basin and inhibits convection, but it does so mainly because of poor representation of the Labrador Current. At higher resolution, the entire mass of low-salinity water remained trapped in boundary currents circling the central basin. At 7-km resolution, the model develops more active eddies and some freshening and interruption of convection occurs. Convective activity along the continental slope was reduced at all resolutions.

Figure 4.3 illustrates how salinity anomalies enter the Labrador Basin in the 7-km model. The top panel shows how a salinity anomaly might spread into the Labrador Basin if it were simply a passive tracer carried along with the climatological flow. The passive anomaly is found mainly in the open basin and over shelf break and slope regions. The bottom panel shows the spreading of a more realistic anomaly which interacts dynamically with the flow. A dynamically active anomaly intensifies the flow and causes the boundary currents to move into shallower water up on the shelves. Tighter, more active currents tend to prevent the anomalously fresh water from being carried into the central basin. Inserting a dynamically active tracer also causes the West Greenland Current to flow more strongly into the ice-covered Baffin Bay. This results in significant freshening on the Labrador Shelf due to an increased expulsion of Baffin Bay water.

Experiments were also performed with weaker winds from the low-index phase of the North Atlantic Oscillation (NAO). Low-index winds tend to induce much greater freshening in the Labrador basin than a fresh water anomaly in the East Greenland Current. Because the overall level of freshening is still less than the observed freshening, it is likely that an increased flow of Arctic water through Baffin Bay plays an important role.

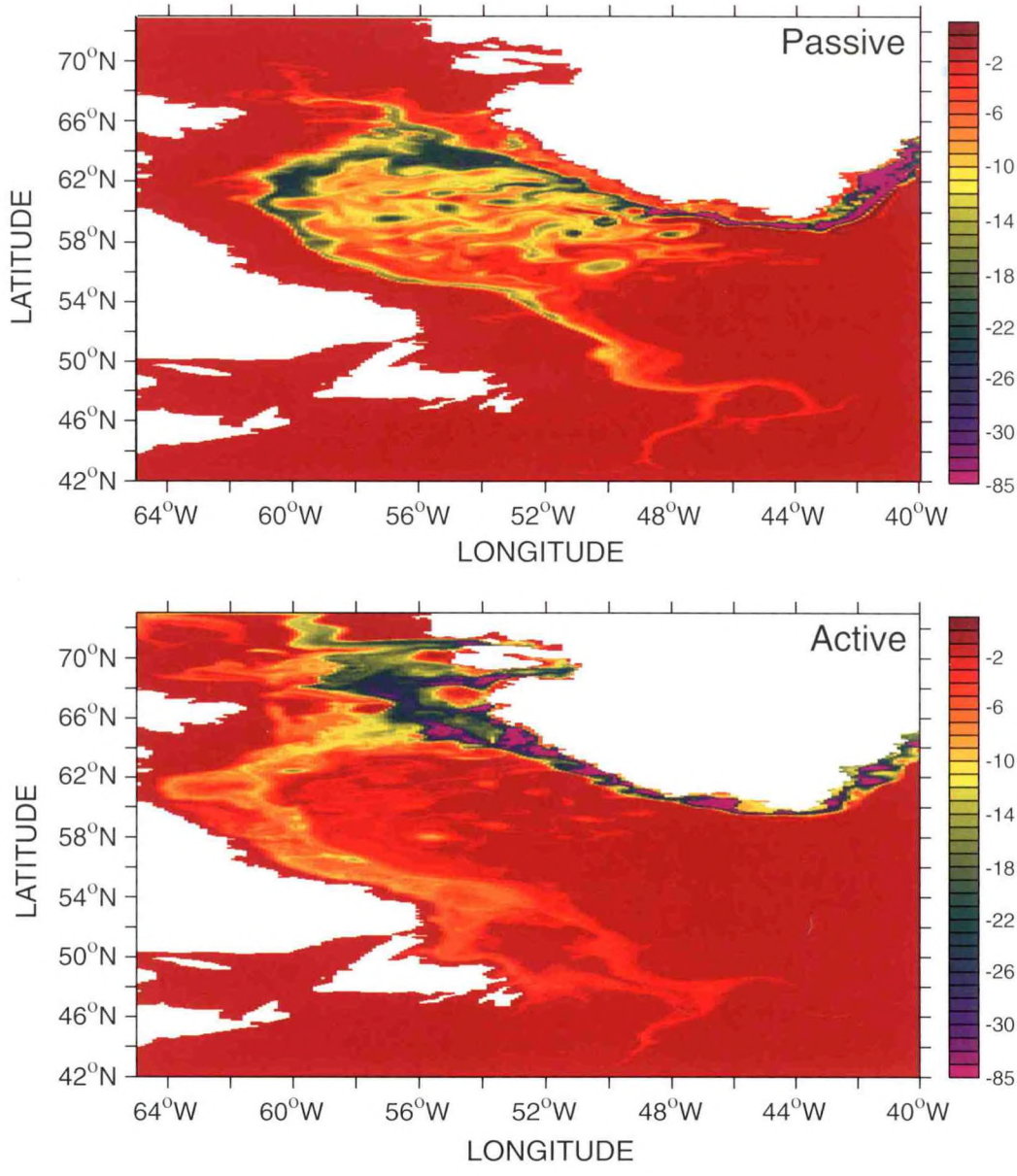

Fig. 4.3 Anomaly tracer in the Labrador Sea 12 months after insertion in the East Greenland Current. In the top panel, a negative salinity anomaly is inserted into the East Greenland Current (right-hand side of figure) as a simple passive tracer. In the bottom panel, a dynamically active salinity anomaly of the same magnitude is added in the same location. Tracer magnitude is in ppt x 1000, and is depth averaged.

PLANS FY99

The model domain will be expanded to investigate the effects of direct fresh water contributions through Baffin Bay. A conversion to MOM 3, suitable for experiments on parallel machines, is under way. Mixing by topographic waves along slope/open ocean boundaries will be investigated. This mixing may be responsible for some of the tracer distributions over the shelf regions in the cases discussed above.

4.1.7 Biogeochemistry in the Water-Planet Model

S. Carson *J.R. Toggweiler*

ACTIVITIES FY98

Atmospheric measurements show that the ocean gives up oxygen in the high latitudes of the Southern Hemisphere and takes up oxygen in the North Atlantic. A similar transfer took place for CO_2 during pre-industrial time. This effect is closely linked to the northward transport of heat by the Atlantic conveyor and is an important part of the natural carbon cycle. Recent studies (fo, Stephens et al.[3]) show that carbon-cycle models based on coarse-resolution ocean GCMs are not able to reproduce this effect at all. The models tend to outgas large quantities of oxygen and CO_2 near the equator and to take up these gases again in the high-latitude regions of both hemispheres. The interhemispheric fluxes predicted by the models are small and tend to have the wrong sign, *i.e.*, net outgassing in the north, uptake in the south.

Interhemispheric oxygen fluxes have been determined for the water planet model (4.1.1). This model produces a net oxygen source to the atmosphere in the south and a sink in the north of $3x10^{13}$ moles per year, close to the observed amount. The key difference between the water planet model and more realistically configured GCMs stems from the temperature difference between the water flowing northward and southward in the conveyor circulation. NADW flowing out of the Atlantic at 30°S should be 7° or 8° colder than the water flowing in at thermocline and intermediate depths. Colder water flowing south at depth is able to carry more oxygen and CO_2 than the water moving northward above. The realistically configured models cited by Stephens et al. do not produce this kind of temperature difference, mainly because the NADW being formed in the north is not cold enough.

PLANS FY99

A full carbon cycle will be introduced into the water planet model. A number of geochemical problems will be revisited, including the formation of the oxygen minimum, and the partitioning of carbon between the ocean and atmosphere via the Southern Ocean.

4.2 MODEL DEVELOPMENT

4.2.1 MOM 3

S. Griffies *A. Rosati*
R.C. Pacanowski

ACTIVITIES FY98

An early version of MOM 3, which runs only under Fortran 90, has been made available for testing in 1998. The new code has been modified to run on parallel computer architectures

3. Stephens, B.B., R.F. Keeling, M. Heimann, K.D. Six, R. Murnane, and K. Caldeira, Testing global ocean carbon cycle models using measurements of atmospheric O_2 and CO_2 concentration, *Glob. Biogeochem. Cycles, 12*, 213-230, 1998.

by allocating individual latitude rows or bundles of adjacent rows to separate processors. Special communication calls exchange data between processors and allow the model to run efficiently on shared memory as well as distributed memory machines. Distributing the computational load by latitude rows limits the number of processors to the number of latitude rows. Two-dimensional domain decomposition is being explored for future applications where the number of available processors may exceed the number of latitude rows. A collaboration with Lawrence Berkely (NERSC) has been initiated to work out a strategy for efficient parallel I/O using Net CDF.

Scaling tests indicate that the baroclinic and tracer portions of MOM 3 scale linearly with the number of processors (up to 128 processors have been tested), but the barotropic portion does not scale as well. Improvements within the implicit free surface and explicit free surface methods are an ongoing area of research. Overall, the code scales reasonably well if there are at least 4-8 latitude rows per processor.

New options in MOM 3 include: a new Fortran 90 time manager, the KPP vertical mixing scheme[4], partial bottom cell topography (fd), the Gent-McWilliams skew-flux (1536), new closure schemes for along-isopycnal diffusion, the explicit free surface[5], and a Robert time filter to replace the backward Euler time step. The meridional stream function diagnostic has been expanded so that the stream function can be computed using potential density as a vertical coordinate. A diagnostic has also been added which outputs all terms affecting the evolution of locally referenced potential density. The model topography can now be changed by simply editing a text input file. An option has also been added for an isotropic grid in which the meridional resolution changes with latitude to compensate for the convergence of meridians. A parameterization for mixing tracers between disconnected regions of ocean has also been added (*e.g.*, to handle the tracer exchange between the Mediterranean and the Atlantic).

PLANS FY99

Future plans include testing the above options, as well as the implementation of fresh water fluxes into the implicit and explicit free surfaces, rather than virtual salt fluxes. Also, a more realistic detrainment is also being explored for the bottom boundary layer. Faster methods of communication between processors are ongoing areas of research, as are more efficient methods for parallel I/O.

4.2.2 Isopycnal-Coordinate Model Development

R.W. Hallberg

ACTIVITIES FY98

Isopycnal-coordinate ocean models offer several potentially important advantages over traditional level models. Isopycnal models avoid numerical diapycnal diffusion. Arbitrary topography can be accurately represented, since the bottom boundary can be treated as a

---

4. Large, W.G., J.C. McWilliams, and S.C. Doney, Oceanic vertical mixing: a review and a model with nonlocal boundary layer parameterization, *Rev. Geophys., 32*, 363-403, 1994.
5. Killworth, P.D., D. Stainforth, D.J. Webb, and S.M. Paterson, The development of a free-surface Bryan-Cox-Semtner ocean model, *J. Phys. Oceanogr., 21*, 1333-1348, 1991.

coordinate surface. Also, with a Lagrangian vertical coordinate, resolution automatically migrates to the locations with the highest stratification and vertical shear, so that flow is represented more accurately with an isopycnal model than a *z*-level model with the same number of layers. However, some aspects, such as the treatment of vertical mixing, are numerically more difficult to implement in isopycnal models than they are in *z*-level models. Accurate and efficient numerical discretizations of the primitive equations in isopycnal coordinates are being developed.

Isopycnal-coordinate models have no inherent diapycnal diffusion, but explicit diapycnal diffusion is difficult to implement numerically. An implicit, vertically iterative technique for incorporating diapycnal diffusion in isopycnal-coordinate ocean models has been developed (Ie). This technique also permits inclusion of Richardson number dependent mixing, which generates vigorous entrainment in the gravity currents downstream of dense flows over sills. These gravity currents are largely responsible for setting the deep watermass properties in the ocean, and accurate inclusion of this entrainment should enhance the realism of numerical ocean models.

One great difficulty with isopycnal models is treatment of a detraining mixed layer. If a bulk mixed layer is coupled to an isopycnal interior, water being detrained from the mixed layer does not generally match the density of one of the isopycnal layers. A variable density buffer layer has been used to couple a variable density bulk surface mixed layer with the isopycnal-coordinate primitive equation model. The combined model has been successfully demonstrated in three-dimensional simulations of the North Pacific circulation.

PLANS FY99

The bulk mixed layer will permit use of the isopycnal-coordinate model for climate simulations, since the model will have a well defined, continuously varying sea surface temperature field, and it will facilitate appropriate heat flux and fresh-water flux boundary conditions even in ocean-only simulations. The ocean's nonlinear equation of state greatly complicates the numerical representation of the ocean's dynamics in isopycnal coordinates. Accurate treatment of nonlinearities in the equation of state with be explored. The isopycnal-coordinate ocean model will be fully implemented on parallel computers.

4.3 COASTAL OCEAN MODELING AND PREDICTION

4.3.1 Princeton Ocean Model Development

T. Ezer *G.L. Mellor*

ACTIVITIES FY98

Support for the growing numbers of users of the sigma coordinate Princeton Ocean Model (POM) has continued (as of July 1998, about 350 users are registered in the POM users group). The second POM users group meeting was held in February 1998 in Miami, and a POM meeting organized by European users is planned for the fall of 1998 in Malta. Meeting proceedings and other information on POM related research activities can be found at http://www.aos.princeton.edu/WWWPUBLIC/htdocs.pom.

A major model development effort was the conversion of the POM code to a generalized coordinate system. This conversion has been completed and the new code is now being tested. This new code can use either z-level, sigma-level or a combination between the two systems; this will give users more flexibility in setting up grids for different topographies and will allow comparison studies between z-level and sigma models using otherwise identical numerics.

In another study, the sigma coordinate pressure gradient error problem has been revisited. An earlier study that showed that, in a two-dimensional (x,z) case with zero diffusivity, the initial velocity error disappeared (1251). The new study shows that in three-dimensional cases there is also a vorticity error that, while tolerably small, does not disappear (1548). This error is significantly lessened with the reduction of the along-sigma diffusion, while keeping the viscosity at high values. Further sensitivity studies with a North Atlantic domain with a non-eddy resolving grid show that the model can tolerate almost zero horizontal diffusion (hi).

PLANS FY99

The generalized POM code will be tested with different grids and different configurations. It will then be made publicly available to users.

4.3.2 Data Assimilation and Model Evaluation Experiments

T. Ezer *G.L. Mellor*

ACTIVITIES FY98

The Data Assimilation and Model Evaluation Experiments (DAMEE) project, which involves a collaboration between several research groups, was concluded in the past year with a comparison of six North Atlantic models: two z-level models, two sigma level models, and two isopycnal-coordinate models; the results were submitted to a special issue of Deep-Sea Research. Princeton's contribution to this project includes the development of a North Atlantic POM configuration which has been used in sensitivity experiments and data assimilation studies. The sensitivity of the model climatology and variability to different parameters and configurations (*e.g.*, lateral boundary conditions, horizontal diffusion and grid resolutions) have been evaluated (hi). The results show decreasing sensitivity to the choice of horizontal diffusion and viscosity with increasing resolution. Assimilation of three years of Topex/Poseidon altimeter data into the same model, using an optimal interpolation approach shows considerable skill in nowcasting mesoscale variabilities in the Gulf Stream and the Gulf of Mexico (hj).

Figure 4.4 compares results from models with and without data assimilation. The assimilation uses altimeter data to update the subsurface temperature fields via vertical correlations (1475). Surface elevation data itself is not assimilated. Also shown is an objective analysis of the altimeter data interpolated into the model grid. While the unassimilated model (top) has a fairly realistic eddy field, some features are not correctly simulated. The vertical projection method works very well and enables the assimilated model (middle) to produce most of the observed features (bottom). Use of the model dynamics in the assimilation produces a better nowcast than the objective analysis by itself which, for example, produces an unrealistic and overly diffusive surface elevation in the Florida Straits.

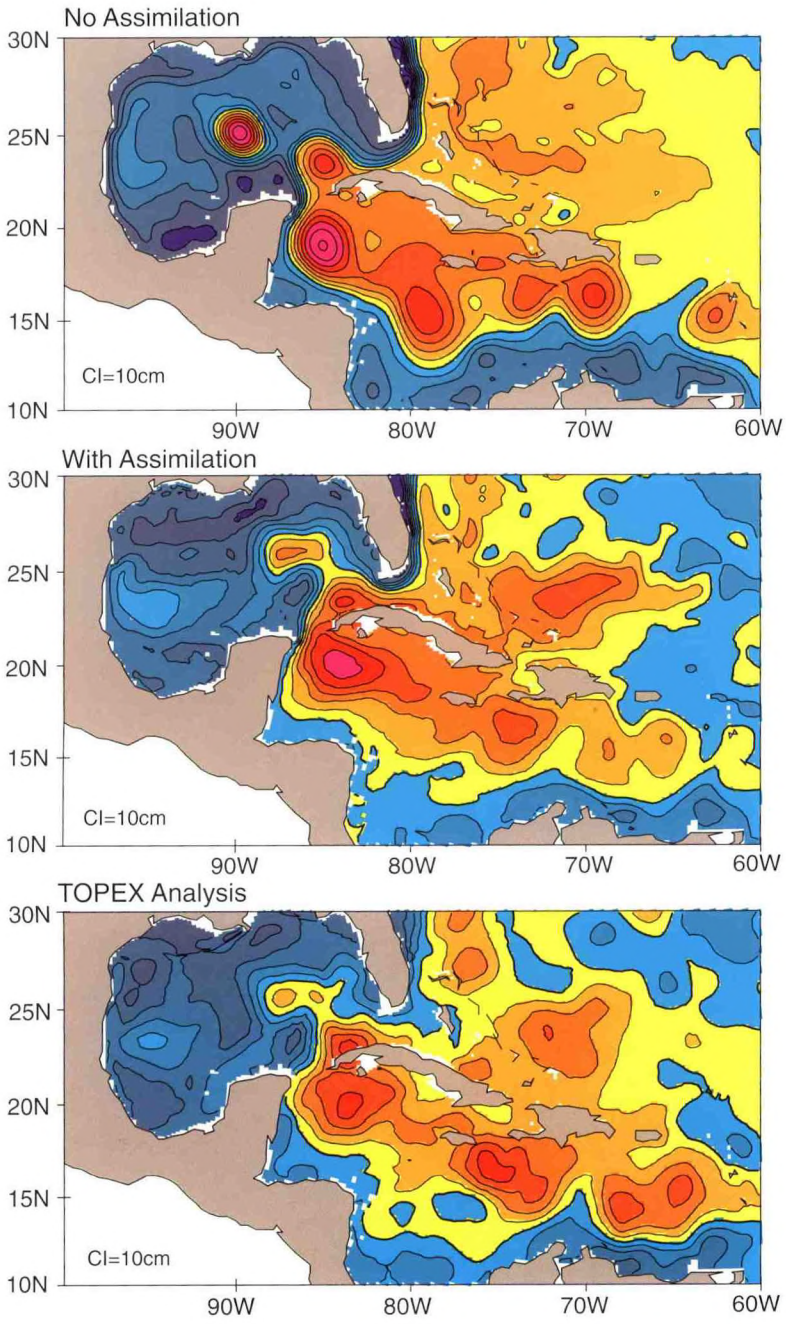

Fig. 4.4 Surface elevation over the Gulf of Mexico and the Caribbean Sea on 10 August 1994 for part of a basin-scale North Atlantic model domain. Top: Model prediction without assimilation; Middle: model hindcast with assimilation; and Bottom: Topex/Poseidon analysis. Contour interval is 10 cm; shades of blue indicate negative values. Predicted surface elevation in the middle panel has more of the features seen in the observed field (bottom) and has a more realistic Gulfstream.

PLANS FY99

The focus of the coming year's research will be on the transfer of data assimilation methods to operational systems and the development of nesting techniques for coastal prediction models.

4.3.3 The Coastal Ocean Forecast System

T. Ezer *G.L. Mellor*
H.-C. Lee

ACTIVITIES FY98

The Coastal Ocean Forecast System (COFS) has been in operation since 1993, producing daily 24-hour forecasts for the U.S. east coast (1406, 1477). The operational system, forced by the mesoscale ETA atmospheric model, is running at the National Centers for Environmental Prediction (NCEP), while parallel systems at the National Ocean Service (NOS), and at Princeton are used for evaluation and development tests. During the past year, data assimilation has been implemented for the first time in the operational system using satellite-derived SST data. Work is in progress to include the assimilation of the Gulf Stream frontal position data and altimeter data. Recently, COFS became part of a new initiative under the support of the National Oceanographic Partnership Program (NOPP) which involves several federal laboratories, universities, and a private weather forecasting company. Under the new initiative, potential users will be provided with real-time forecasts that will be evaluated for their usefulness, timeliness, and accuracy.

PLANS FY99

The first marine demonstration forecast experiment is planned for the summer of 1999. An extended forecast system which also includes the Gulf of Mexico is now being tested and will replace the current operational system.

4.3.4 Atlantic Ocean Climate Variability Studies

T. Ezer *G.L. Mellor*

ACTIVITIES FY98

While previous POM applications include mostly regional and coastal regions, recent studies with a configuration of POM for the entire Atlantic Ocean and the Greenland Sea has shown promising results (1476). In particular, intense deep western boundary currents, and fairly realistic meridional heat fluxes are obtained even in relatively coarse resolution grids. Simulations of decadal climate variabilities compare well with observed variabilities, such as the sea level change at Bermuda and changes in subsurface temperature records. A recent analysis of the model results (cp) found correlations between the decadal changes in the subtropical gyre and wind-driven long Rossby waves, and indicate the feasibility of predicting some climatic oceanic changes.

PLANS FY99

The past research under the support of the Atlantic Climate Change Program has been completed. New initiatives are under consideration.

4.4 CARBON SYSTEM

4.4.1 Anthropogenic CO_2

D.F. Baker
*M. Bender**
S.-M. Fan
E. Gloor
N. Gruber
*G. Hurrt***
J.D. Mahlman
*P. Moorcroft***
*S. Pacala***
J.L. Sarmiento
*P. Tans****

**Dept. of Geosciences, Princeton University*
***Dept. of Ecology and Evolutionary Biology, Princeton University*
****CMDL/NOAA*

ACTIVITIES FY98

The Carbon Modelling Consortium (CMC) completed its third year in 1997/1998, with major progress towards identification of major sinks of anthropogenic CO_2. The consortium has two major goals: 1) To characterize the present-day sources and sinks of carbon; 2) To provide an integrated carbon system model capable of providing assessments for future changes in the carbon system. The consortium has made important progress in both of these areas over the past year.

The existence of a significant Northern Hemisphere sink of carbon has been known for many years. The location of this sink, however, has not been clear. Over the past year, efforts have been directed toward localizing the CO_2 sink by running an inverse model of atmospheric CO_2 concentrations (ih). Using two GFDL general circulation models, CO_2 perturbations due to fossil fuel burning, cement production, air-sea exchange and terrestrial uptake by biota are advected and mixed throughout the atmosphere in a dynamically consistent manner. The results are then compared with observations, as the strengths of various sinks are varied. It is found that the best fit to observations occurs when at least 2/3 of the Northern Hemisphere sink is a terrestrial sink located in North America. A terrestrial sink of this magnitude is comparable to fossil CO_2 emissions from North America. Additional work indicates that this uptake has existed through much of this century (ii). Extensive work has been done to test the sensitivity of this result to the choice of models (ig), as well as to the particular observing network used.

As part of the effort to refine terrestrial carbon models, a forest dynamics model for coupling with climate models is currently under development. This model will be used to look at how a range of processes, including forestry, fire, and disease, interact with climatic processes to produce changes in carbon sequestration. This model complements the results of the inverse model by providing a process-based picture of the terrestrial sink implied by the inversion.

In addition to localizing the primary Northern Hemisphere terrestrial sink, the CMC has made major progress in identifying the oceanic distribution of anthropogenic CO_2. Using methods to correct for biological cycling (1485), it has become possible to estimate the distribution of anthropogenic carbon within the world ocean and to compare inventories of anthropogenic carbon to that predicted from various atmospheric measurements. The measurements seem to be converging on a mean oceanic sink of 2 Gt/yr during the 1980s. Fig. 4.5 shows a comparison between the estimated anthropogenic carbon in the Atlantic and that modelled by the Princeton Ocean Biogeochemistry Model (1551).

PLANS FY99

Large interannual variability in carbon uptake is known to occur, but the processes responsible for this variability are not understood. Time-varying inverse models are under development to examine interannual variability in carbon fluxes, and to show whether this variation arises from changes in the seasonal cycle of carbon fluxes. Measurements of atmospheric oxygen and its isotopic composition will also be used to constrain the sizes of various sources and sinks.

Collaborative work is being undertaken with other institutions to use additional transport models to determine the sensitivity of the current results (ih) to the specific choice of model. Additionally, the design of optimal networks for inversion will continue, providing a framework for monitoring net national emissions of greenhouse gasses.

4.4.2 Modelling Ocean Biology

R. Armstrong
A. Gnanadesikan
T. Hughes
G. Hurtt
N. Gruber
J.L. Sarmiento
R. Slater

ACTIVITIES FY98

Many response strategies for mitigating increasing concentrations of carbon dioxide within the atmosphere assume that the response of the ocean will remain constant. A recent study (1561) demonstrates that this is not the case. Using a coupled atmosphere-ocean model with an embedded carbon cycle, this study shows that, as the model climate changes as a result of global warming, substantial changes could occur in the magnitude of carbon uptake in the Southern Oceans. In the absence of biology, decreased vertical exchange in the Southern Ocean as a result of surface freshening sharply reduces uptake of anthropogenic CO_2. However, if biological production remains constant, the decreased supply of carbon-rich deep water to the surface Southern Ocean results in a decrease of surface carbon concentrations and an increase in net carbon uptake. In cases where the biota become more efficient at taking up nutrients, the model ocean is able to take up even more carbon. The results highlight the importance of understanding the biological and physical response of the Southern Ocean to climate change.

Development work has continued on the oceanic general circulation models used to predict oceanic biology and its response to changes in climate. The carbon cycling code used in a number of previous studies (1320, 1486, fn) has been updated to work in the MOM 2.2

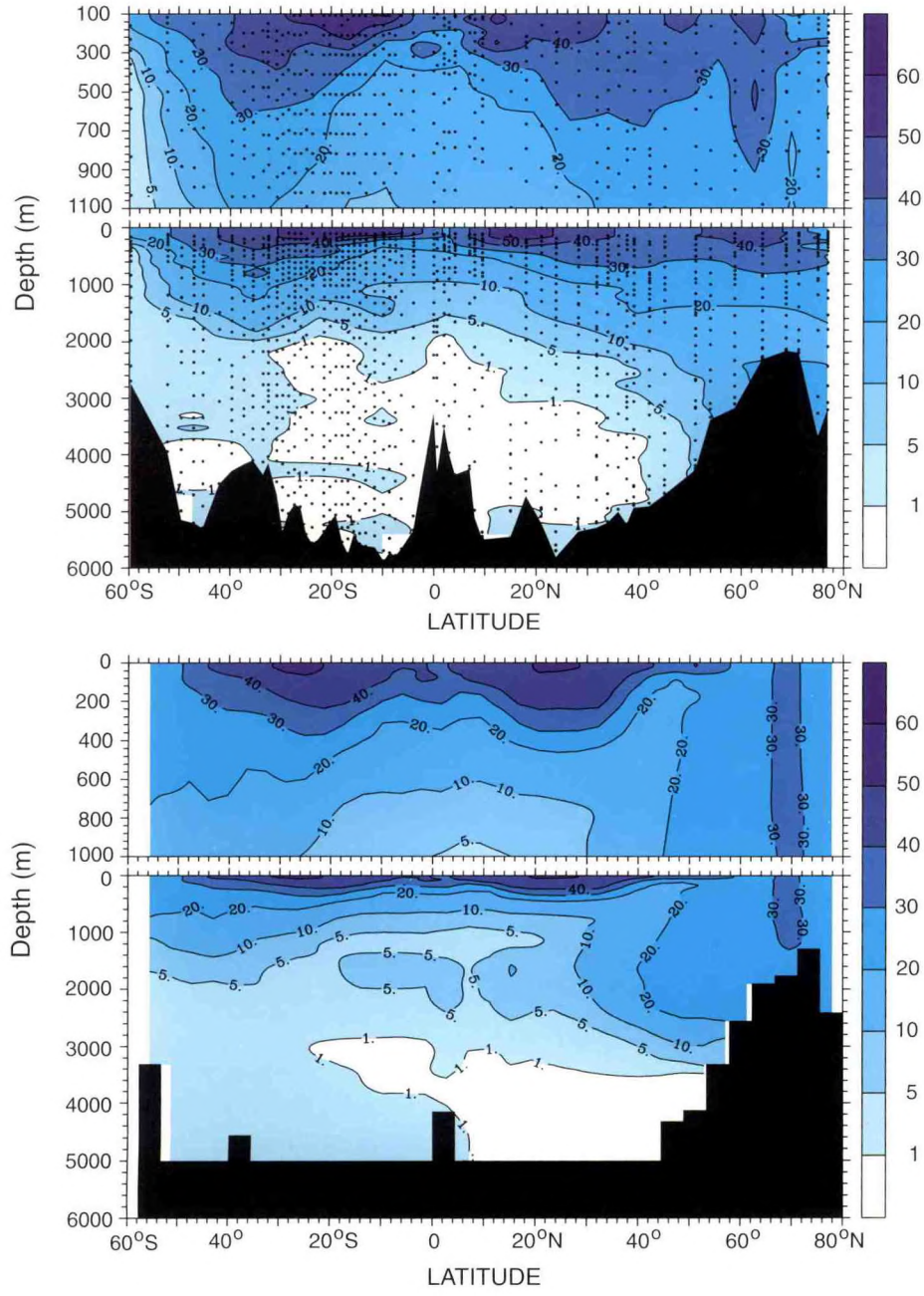

Fig. 4.5 Comparison between observed uptake of CO_2 (top) and that modelled using the Princeton Ocean Biogeochemistry Model (bottom) along a section in the Atlantic Ocean (1551). The dots in the top figure mark locations where observations were made. The signature of Northern Hemisphere overturning, which brings high concentrations to depths of more than 2000 m can be seen in both plots, as can the concentrating effect of the subtropical gyre.

model. Simultaneously, the older version of the model has been compared with a number of other carbon models in the United States and Europe. These studies show similarities in the overall structure of carbon uptake predicted by the models, despite large differences in the Southern Ocean.

Studies of the cycling of silica (gv, id) reveal that the parametrization of mesoscale eddies can have a profound impact on the distribution and production of nutrients within the model. Models with horizontal mixing underpredict the silica concentrations in the Southern Ocean, while models with isopycnal mixing alone overpredict these values. Both models greatly overestimate the vertical exchange of silica, yielding Southern Ocean productions far higher than justifiable from observations. Current estimates of global biogenic silica production require 88 Tmol/yr of export from the mixed layer, of which about half occurs in the Southern Ocean and 1/3 in tropical latitudes.

Development work has continued on models of biological cycling. A particular area of progress is the development of a physiology-based model in which the uptake of nitrate can be limited by light, nutrient, iron or some combination of all three (ik), providing a unified framework for explaining the existence of high-nutrient low-chlorophyll (HNLC) regions. In the model, cells take up ammonia when it is available and in such cases use iron for energy-related functions, such as photosynthesis and electron transport. When ammonia ceases to be available, the cells divert some of the iron supply to reduce nitrate. The iron partition function is assumed to be altered dynamically by the cells in order to maximize the growth rate. This simple picture allows for complex interactions between nutrient supply, light and iron. For example, when the iron and ammonium supply become low, phytoplankton may not have enough iron for photosynthesis and so may become more easily susceptible to light limitation. It is hoped that this model will provide a framework for examining complicated problems associated with climate change. An example is the polar freshening of the Southern Ocean, which would reduce the supply of iron to the mixed layer, but potentially increase the amount of light available to phytoplankton as the mixed layer depth becomes more shallow.

The predictive ability of biological cycling models will be limited by the ability of such models to capture the physical exchanges responsible for providing nutrient to the upper ocean. A method has been developed for characterizing mismatches between satellite observations of ocean color and simulations made with general circulation models. A state-of-the-art algorithm is used to predict primary productivity from satellite color and other environmental data. A simple remineralization/export model is then used to predict the fraction of productivity that is "new production," *i.e.*, the fraction of production that creates a nitrate demand. This demand is then compared to nitrate delivery to the surface by the GCM on a per-grid-square basis. The resulting map highlights areas of mismatch between satellite-derived demand and GCM-delivered nitrate; this information will be used to diagnose which changes to the GCM or other components of the system (*e.g.*, the productivity algorithm) are most effective in reducing mismatches between these data sets.

Development work has continued on more complicated models of marine food webs (fq, ij). A simple approach has been presented to modelling predation due to zooplankton in marine food webs, which eliminates oscillatory behavior associated with previous approaches by allowing zooplankton community structure and predation strategy to adjust smoothly to phytoplankton community structure.

PLANS FY99

The carbon model will be incorporated into the newest version of the Modular Ocean Model (MOM 3) which includes continuous bottom topography (fd), a bottom boundary layer (ez), a stable isopycnal mixing scheme (1535), and more sophisticated advection schemes.

The biological cycling scheme within the carbon model will be altered so as to produce blooms at the appropriate times of the year by making the productivity dependent on light and stability. Higher resolution studies will be made with the biogeochemistry model to look at interannual variability of carbon production. A prognostic version of the ocean color model will be developed and used to evaluate mismatches between model output and satellite data.

The model including silica cycling will be merged with the carbon model to help locate regions where diatom production is most important. This will then be compared with data from the U.S. JGOFS program. The inclusion of iron cycling into the model will also be investigated.

The models of biological cycling which have been developed over the past year will be included in more realistic (possibly eddy-permitting) models of various regions, including the equatorial Pacific and the North Atlantic. Collaborations are also being developed to look at biogeochemical cycling in the Southern Ocean.

4.4.3 Observational Studies

R. Key *C. Sabine*
R. Rotter *J.L. Sarmiento*

ACTIVITIES FY98

From 1990 to the present, the Ocean Tracer Laboratory (OTL) has been involved in the World Ocean Circulation Experiment, assuming principal responsibility for coordinating radiocarbon measurements (1486,1487,1488). More recently, the laboratory has begun making measurements of carbon system parameters such as total CO_2, pCO_2 and alkalinity (1499, 1563). The last of these surveys was completed during 1997 and synthesis work has begun. At present, most of the radiocarbon data in the Pacific has gone through quality control, and samples from the Indian Ocean are being analyzed. One of the key problems in gathering oceanographic data is that different cruises may measure offsets in various parameters due to different onboard instrumentation and personnel. Such systematic offsets are being checked for in both the radiocarbon and carbon system data by looking at places where cruise tracks overlap. In the past year, the radiocarbon data has been used to evaluate the penetration of radiocarbon, produced as the result of nuclear explosions, into the Pacific thermocline, providing a strong constraint on model vertical exchange (1564). Radiocarbon data from the deep Pacific has also been used to examine the rate at which deep waters are formed in the Southern Ocean (1565).

The carbon system data in the Indian Ocean has been analyzed in detail and compared with the output of numerical models. Preliminary results indicate that the models have far too much uptake of anthropogenic carbon in the southern Indian Ocean, about the right amount in the southern subtropics, and too little in the northern Indian Ocean.

An exhaustive analysis has been made of the constants used to derive various components of the carbon system (such as pCO_2) from other species of the system. This work has revealed systematic differences between different calculation methods. A "best-fit" set of constants for carbon modelling has been chosen.

PLANS FY99

Processing of radiocarbon data from the Indian Ocean will continue, and studies will be made of the distribution of radiocarbon within the Pacific. An area of particular interest is the location and structure of the flows which return North Pacific Deep Water to the Southern Ocean.

Comparisons between data and models will continue as part of the Ocean Carbon Model Intercomparison Project (OCMIP). As part of this project, the new set of constants governing carbonate chemistry will be included in the carbon models.

4.4.4 Ocean Inverse Models

A. Gnanadesikan *T. Hughes*
E. Gloor *J.L. Sarmiento*
N. Gruber

ACTIVITIES FY98

As ocean general circulation models continue to improve, some of the techniques used in the atmosphere to estimate fluxes based on the distributions of tracers may be useful for the ocean as well. Preliminary work has begun in this area, using a 4° OGCM similar to that used in other studies (gv). Unit fluxes have been applied to various regions of the model, which was then run out for 6000 years to allow the distributions of various tracers to come to an equilibrium. (Although the concentrations at individual points increase in time, the pattern produced by a particular flux reaches a steady state.) The observed distribution of a tracer can then be inverted for the fluxes. The inversion is yielding promising results for heat and oxygen fluxes.

PLANS FY99

Inverse calculations will be extended to a wider range of ocean models. Oxygen flux estimates will be compared with measurements made by Ralph Keeling at Scripps and Michael Bender at Princeton. Pulsed inversions will be developed to examine the uptake of anthropogenic CO_2 and CFCs.

4.4.5 Global Nitrogen Cycle

C. Deutsch *J.L. Sarmiento*
N. Gruber

ACTIVITIES FY98

Oceanic nitrogen fixation and denitrification represent the major pathways for nitrogen, one of the limiting nutrients for photosynthesis. A novel approach for investigating the global patterns of these two important processes has been proposed on the basis of observations of nitrate and phosphate (1497). These two nutrients are combined linearly to form a quasi-conservative tracer, N*, which reflects the combined effects of nitrogen fixation and denitrification. N* is low in the Arabian Sea and in the eastern tropical North and South Pacific, consistent with the observation of intense water column denitrification in these anoxic

waters. High concentrations of N* indicative of prevailing nitrogen fixation are found in the thermocline of the tropical and subtropical North Atlantic and the Mediterranean. This suggests that on a global scale these basins are acting as sources of fixed nitrogen, while the Indian Ocean and parts of the Pacific Ocean are acting as sinks. Nitrogen fixation has been estimated in the Atlantic on the basis of N* and information about the water age, and a fixation rate of 28 Tg yr^{-1} has been calculated, about three times larger than the most recent global estimate. Extrapolation of this North Atlantic estimate to the global ocean suggests that the present-day budget of nitrogen in the ocean may be in approximate balance.

PLANS FY99

Investigation of N* in the Pacific Ocean has been seriously limited by the small number of available observations. This situation has, however, vastly improved with the increasing availability of WOCE data for this ocean basin. Preliminary analysis of N* in the Pacific indicates that the northwestern Pacific also acts as a major source for oceanic nitrogen. An investigation of this potential nitrogen fixation site is planned, along with the known denitrification sites, with the goal of finally providing a nitrogen budget for the Pacific Ocean. Also planned is an examination of the possible link between marine nitrogen fixation and the atmospheric input of iron. Should iron turn out to be a major control for oceanic nitrogen fixation, this may have significant implications for understanding the glacial-interglacial changes in atmospheric CO_2.

4.4.6 Carbon-13 Cycle

S.-M. Fan *R. Slater*
N. Gruber *J.L. Sarmiento*

ACTIVITIES FY98

The CO_2 emitted to the atmosphere by anthropogenic activities is depleted in the rare isotope ^{13}C. This is because the plants that originally produced the fossil fuels preferentially take up the light isotope ^{12}C during the photosynthetic fixation of CO_2. As a consequence of fossil fuel combustion, the $^{13}C/^{12}C$ ratios of atmospheric CO_2 and inorganic carbon dissolved in the oceans have decreased. This secular decrease is often referred to as the "^{13}C Suess effect". Observations of the ^{13}C Suess effect have recently received much attention, because they constrain the redistribution of anthropogenic CO_2 within the global carbon system, most importantly the uptake of anthropogenic CO_2 by the oceans. These observations, therefore, provide an important crosscheck on the CO_2 uptake estimates based on the inventory methods described above.

A synthesis of the $^{13}C/^{12}C$ ratio of dissolved inorganic carbon (DIC) has been completed by summarizing high-precision data obtained from 1987 to 1997 by C. D. Keeling of Scripps Institution of Oceanography. Secular decreases over time have been identified at two time series locations in the subtropical North Atlantic and subtropical North Pacific, as well as in repeated transects of the Indian Ocean and of the tropical Pacific. A tentative extrapolation of these estimates to the global ocean yields an average oceanic ^{13}C Suess effect of approximately -0.018 permil/yr for the period from 1980 to 1995. The oceanic ^{13}C Suess effect is about equal to that observed in the atmosphere over the same period. This is in contrast to expectations, since the ^{13}C Suess effect in the surface ocean is believed to lag

that in the atmosphere. This apparent inconsistency can be explained by a damping of short-term changes in the atmospheric ^{13}C Suess effects by the oceans on time scales up to several decades caused by the long characteristic time scale for the air-sea gas exchange of the ^{13}C isotope relative to the time scales for exchange of CO_2 gas.

PLANS FY99

The constraints provided by the Scripps data for the uptake of anthropogenic CO_2 will be explored. In addition to the ^{13}C Suess effect, the disequilibrium of the ^{13}C isotope between the atmosphere and the ocean will be estimated on a global basis. Two approaches are envisioned. First, this air-sea disequilibrium will be estimated from a global extrapolation of the $^{13}C/^{12}C$ ratio data. Alternatively, results from the Princeton ocean biogeochemistry model will be used in combination with the observations to yield an "optimized" extrapolation and an estimate of the ^{13}C disequilibrium. The atmospheric distribution of ^{13}C will also be examined, using the inversion techniques developed for CO_2, to evaluate the global distribution and transport.

5. CLIMATE DIAGNOSTICS

GOALS

To determine and evaluate the physical processes by which the earth's climate and the atmospheric and oceanic general circulations are maintained in the mean, and by which they change from year to year and from decade to decade, using all available observations.

To compare results of observational studies with similar diagnostic studies of model atmospheres and model oceans developed at GFDL and thereby develop a feedback to enhance understanding of both observed and simulated climate systems.

5.1 DEVELOPMENT AND ANALYSIS OF DATASETS BASED ON RADIOSONDE OBSERVATIONS

ACTIVITIES FY98

5.1.1 Archiving of Atmospheric General Circulation Statistics

J.R. Lanzante A.H. Oort

A version of the Oort (599) monthly atmospheric radiosonde station statistics has been reclaimed from the old GFDL tape library and has been transferred to the Data Support Section of the Scientific Computing DIvision at NCAR for permanent archiving. These statistics can be used to compute the monthly means of the primary meteorological variables (horizontal wind, temperature, geopotential height, specific and relative humidity) from 1958-89 for individual standard synoptic times, and should prove useful to many researchers.

5.1.2 Enhancing the Information Content of Radiosonde Temperature Data

*D. Gaffen** *J.R. Lanzante*
*T. Habermann***

**Air Resources Laboratory*
***National Geophysical Data Center*

A collaborative effort led by Dian Gaffen of the Air Resources Laboratory (ARL) and also involving Ted Habermann of the National Geophysical Data Center (NGDC) has progressed. This project utilized both a unique compilation of meta-data describing historical changes in global radiosonde instruments (created at ARL) and advanced statistical methods (developed at GFDL and NGDC). Adjustments were made to radiosonde temperature data to account for the effects of instrumental changes. A suite of trial computations were performed in order to assess the relative importance of various factors to the adjustment process. The greatest uncertainty is related to the adjustment for abrupt

changes in the time series. The most liberal adjustment scheme removes most of the trends (both artificial and natural) while the most conservative has but a modest impact. Separation of the variability due to natural causes from those due to human errors and procedural or instrumental changes remains a formidable problem. The findings illustrate the difficulties in estimating local long-term trends based on the radiosonde station network.

5.1.3 Development of a Temporally Homogeneous Tropical Radiosonde Temperature Dataset

S.A. Klein *J.R. Lanzante*

A small network of radiosonde stations covering the tropics was assembled for studies of interannual as well as longer-term variability in the vertical structure of temperature. The concern of this effort was that abrupt artificial changes (related to changes in instrumentation and procedures) may seriously contaminate the temporal variability. A long record of temperatures for more than a dozen stations, using data for seven mandatory levels in the troposphere has been carefully examined. A unique compilation of metadata (5.1.2) was utilized along with "change-points" determined by an objective statistical method (1419) and the Southern Oscillation Index as an indicator of primary tropical variability. In view of the ambiguous nature of the decisions on whether a particular abrupt change is natural or artificial, several parallel sets of adjusted data were produced depending on the level of confidence required to declare changes as being artificial. For each declared artificial "change-point", the time series for a given station were adjusted to remove the discontinuity.

5.1.4 Comparison of the Hadley Circulation Inferred from Reanalysis and Radiosonde Datasets

J.R. Lanzante *Z. Shi*
A.H. Oort *D. Waliser**

**SUNY/Albany*

In a collaborative effort (hv) led by Duane Waliser at The State University of New York (SUNY), and also including Zhixiong Shi (SUNY) and Abraham Oort, a comparison was made between the Hadley circulation inferred from the NCEP/NCAR reanalysis and that from an *in situ* radiosonde-only station analysis (1425). The reanalysis utilizes a variety of non-radiosonde data sources, which are blended by a modern data assimilation system. This model-based approach suffers from potential biases of the numerical model being used. On the other hand, the *in situ* analysis is subject to biases due to the irregular and limited spatial extent of the radiosonde network.

In order to delineate the above-mentioned biases, each of the two products was compared to a third product which was generated from the reanalysis sub-sampled at just the radiosonde station locations. By comparing these products it has been found that the reanalysis and *in situ* products share the same gross features. However, several deficiencies have been noted in the radiosonde-only product. These include a more limited vertical extent into the upper troposphere in some regions, less consistency of poleward limits in certain seasons, excessive strength or weakness of some features and an overestimate of the effects of the El Niño-Southern Oscillation (ENSO) on the Hadley circulation. These deficiencies are all attributed to the sparsity of observations in oceanic regions, particularly in the Pacific. On the

other hand, the model bias in the reanalysis is seen to produce an excessively strong Hadley circulation, by as much as 25-30% in some seasons.

PLANS FY99

An effort to improve the quality of upper air temperature measurements, and subsequently to evaluate interannual variability and long-term temperature trends, will continue. Emphasis will be placed on reducing the uncertainty in separating artificial from natural changes and in assessing the sensitivity to the details of the adjustment procedure.

The sets of tropical radiosonde temperature data, which have been adjusted to remove abrupt artificial (instrumental) changes will be examined in order to relate changes in vertical temperature structure to ENSO variability.

5.2 ANALYSIS OF DATASETS BASED ON SATELLITE OBSERVATIONS

M.W. Crane *R.T. Wetherald*
B.J. Soden

ACTIVITIES FY98

5.2.1 Sensitivity of the Tropical Hydrological Cycle to ENSO

Satellite observations of temperature, water vapor, precipitation and outgoing longwave radiation were used to characterize the variation of the tropical hydrologic and energy budgets associated with ENSO (hw). As the tropical oceans warm during an El Niño event, the precipitation intensity, water vapor mass and temperature of the tropical atmosphere were observed to increase, reflecting a more vigorous hydrologic cycle. The enhanced latent heat release and resultant atmospheric warming led to an increase in the outgoing longwave radiation. Atmospheric global climate models, forced with observed sea-surface temperatures, accurately reproduced the observed tropospheric temperature, water vapor and outgoing longwave radiation changes. However, the predicted variations in tropical-mean precipitation rate were substantially smaller than observed. The comparison suggests that either the sensitivity of the tropical hydrological cycle to ENSO-driven changes in SST is substantially underpredicted in existing climate models, or that current satellite observations are inadequate to accurately monitor ENSO-related changes in the tropical-mean precipitation. Either possible explanation would have important implications for current efforts to monitor and predict changes in the intensity of the hydrological cycle.

5.2.2 Interannual Variations in Upper Tropospheric Moisture and Circulation Patterns

Hourly observations of 6.7 micron "water vapor" radiances from geostationary satellites were used in conjunction with an objective pattern-tracking algorithm to trace upper tropospheric water vapor features from time-lapse satellite imagery (ff). The displacements of water vapor patterns were then used to quantitatively describe the circulation of the upper troposphere. To examine the contrasting circulation and moisture conditions between warm and cold ENSO events, GOES-7 radiances were analyzed for both El Niño (June-August 1987) and La Niña events. For both warm and cold periods, changes in

the distribution of upper tropospheric relative humidity closely coincide with regional variations in the water vapor pattern displacements. Comparison of the warm and cold events revealed coherent differences in the spatial distribution of the upper tropospheric circulation which reflect interannual variations in the Hadley and Walker circulations over the tropical east Pacific and west Atlantic Oceans. The altered pattern of the tropical atmospheric circulation is qualitatively consistent with a tropical atmospheric "bridge" that connects SST anomalies in the central Pacific with those in the tropical Atlantic (fv). Previously, these circulation changes were inferred indirectly from moisture and cloud cover changes. Hence, the presence of this altered circulation in the satellite-derived upper level winds provides more direct evidence of the existence of this phenomenon.

PLANS FY99

The relationship between upper tropospheric water vapor and the tropical circulation will be examined on diurnal and seasonal time scales. A tracking algorithm similar to that used for upper tropospheric water vapor features will also be applied to pixel-resolution GOES total precipitable water. If successful, such an application will be used to study the role of moisture transport from the Caribbean Basin and eastern tropical Pacific on precipitation variability over the U.S.

5.3 ATMOSPHERIC VARIABILITY

N.-C. Lau *M.J. Nath*
J.R. Lanzante

ACTIVITIES FY98

5.3.1 Westward Traveling Atmospheric Patterns

The essential characteristics of westward propagating high-latitude fluctuations with typical periods of approximately three weeks have been documented (is). The datasets for this study include the output from a 100-year integration of the R30 GFDL climate GCM with no interannual SST forcing, as well as the NCEP/NCAR reanalyses for the 1972-1995 period. It has been demonstrated that the GCM provides a realistic simulation of the spatial structure, timescale and preferred site of occurrence of these circulation features. The passage of these fluctuations over certain regions is seen to have notable effects on the local weather. Analysis of the various terms contributing to the vorticity tendency of these waves indicates that the beta-effect (advection of planetary vorticity) is the primary mechanism for the westward propagation. The prominent episodes are accompanied by considerable reorganization of the storm track activities. The latter, synoptic-scale features tend to feed back positively on the more slowly-varying fluctuations.

5.3.2 "Step-Function Like" Nature of the Extratropical Seasonal Cycle

The tendency for the evolution of atmospheric seasonal changes to occur in a discontinuous fashion has been examined. Initial efforts were focused on the evolution of daily surface temperature over the conterminous United States using a network of 80 stations covering the time period of 1961-90. Examination of these data have confirmed an earlier, more limited analysis based on a single station. Namely, abrupt changes of ~10-15°F occur a

few times per year during the spring and autumn transition seasons, typically with precedent and subsequent periods of two to three weeks during which the temperature fluctuates about a nearly constant level. While such behavior displays some degree of interannual variability, it has been found throughout the historical record. Furthermore, these changes occur in a regionally coherent manner.

The discontinuous nature of the seasonal changes calls for the development of a new methodology for analyzing the observations. In order to capitalize on the multivariate nature of these fluctuations, an EOF (Empirical Orthogonal Function) analysis of the spatial distribution of a signal-to-noise measure has been used. This new adaptation of EOF analysis seeks abrupt jumps which are spatially coherent. This new technique will allow for super-posed epoch analysis of a variety of potentially related variables. One such variable is snow cover, for which initial efforts have focused on assembling a suitable daily database over North America.

PLANS FY99

Analysis of the "step-function like" nature of the extratropical seasonal cycle will be expanded to include additional variables in the free atmosphere, as well as surface boundary conditions such as snow cover. If results appear promising, similar phenomena will be sought in simulations from GCMs.

5.4 AIR-SEA INTERACTION

ACTIVITIES FY98

5.4.1 Completion of SST Sensitivity Experiments with R30 Climate GCM

N.-C. Lau *M.J. Nath*

A full suite of GCM experiments aimed at delineating the atmospheric responses to SST variability at different sites has been completed. These experiments differ in the choice of maritime domain for prescription of interannual SST forcing, and in the treatment of the lower boundary condition outside the region of variable SST forcing. Near-global SST variations were prescribed in the "GOGA" experiment. Only SST changes in the tropical Pacific and tropical Atlantic were prescribed in the "TOGA-Pacific" and "TOGA-Atlantic" experiments, respectively, with the SST at maritime sites outside of these forcing regions being fixed at their climatological values. The fourth "TOGA-Pacific-ML" experiment is similar to the TOGA-Pacific experiment, except that the SST changes at oceanic gridpoints outside of the tropical Pacific were predicted using a static, 50-m deep mixed-layer model. All model runs were conducted using a R30, 14-level GCM for the period extending from 1950 to 1995. Four parallel runs initiating from independent atmospheric conditions were conducted for each of the four experiments described above.

The completion of the current series of experiments using the R30 model represents a major commitment of GFDL to the simulation of climate variability using higher-resolution GCMs. The performance of the R30 model is much improved over the R15 version in many

respects, including the generation of more realistic precipitation anomalies in response to tropical SST changes, and more energetic transient eddies in the middle latitudes.

5.4.2 Midlatitude Responses and the Atmospheric Bridge Mechanism in R30 Experiments

N.-C. Lau *M.J. Nath*

The midlatitude responses to near-global and tropical Pacific SST forcings in the R30 experiments (*i.e.*, GOGA and TOGA-Pacific, 5.4.1) have been compared in detail. The results are consistent with earlier findings based on the R15 model (1256). The atmospheric response pattern in the Pacific and North American sectors can mostly be attributed to SST variability in the tropical ENSO region alone. The R30 runs also yield more realistic teleconnection patterns than the R15 runs, both in terms of amplitude and spatial structure.

The preliminary results from the TOGA-Pacific-ML experiment (5.4.1), with the SST changes outside of the tropical Pacific being predicted by a mixed-layer model, indicate that the atmospheric bridge mechanism (1393) plays an important role in linking SST variability in the ENSO region to that in the North Pacific (Fig. 5.1). The R30 simulations illustrate that this mechanism might also explain the covariability of the SST changes in the Atlantic and Indian Ocean Basins with ENSO. Some of the model processes linking the SST anomalies in different oceanic sites are consistent with those deduced from observational data (fv).

5.4.3 Ocean-Atmosphere Interaction in the Atlantic Basin

T. Delworth *M.J. Nath*
N.-C. Lau

The coupled modes of ocean-atmosphere variability in the Atlantic Basin have been examined using output from the TOGA-Atlantic experiment (5.4.1). Analysis of the SST forcing field itself revealed the presence of two characteristic monopolar patterns, one of which resides mainly in the South Atlantic, and the other in the North Atlantic. These individual SST patterns are related to notable changes in precipitation over South America and Africa in the model atmosphere, and in the near-surface atmospheric flow. The simulated response of the surface wind appears to reinforce the imposed SST anomaly, thus indicating that positive feedback mechanisms may contribute to the variability of the coupled ocean-atmosphere system in the tropical Atlantic.

5.4.4 Analysis of the Global Precipitation Variability Associated with ENSO

M.W. Crane *B.J. Soden*
N.-C. Lau

Using a combination of *in situ* and satellite observations, global patterns of interannual precipitation anomalies were compared to the GCM simulations described in 5.4.1. Many previous studies have documented coherent changes in global precipitation patterns that are associated with the oscillation between warm and cold conditions in the equatorial Pacific. While these precipitation changes tend to be largest within the tropical Pacific, significant changes in precipitation are also observed throughout the tropics and extend well into the middle latitudes. Comparison of precipitation anomalies in the GOGA experiment (5.4.1)

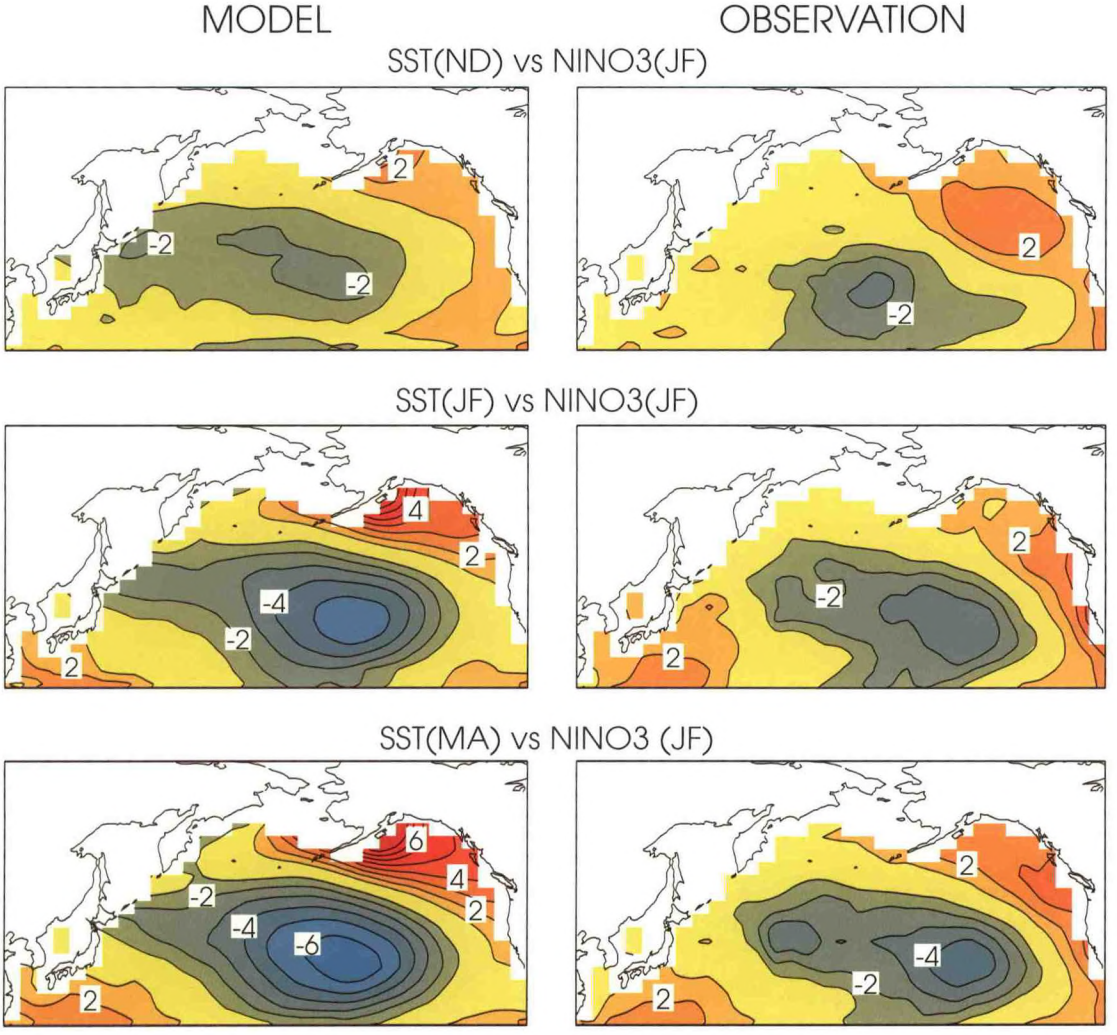

Fig. 5.1 Regression coefficients of the sea surface temperature (SST) in November-December (top panels), January-February (middle panels) and March-April (bottom panels) versus the NINO3 index in January-February. Results from the TOGA-Pacific-ML experiment and the observations are shown in the left and right columns, respectively. Contour interval: 0.1°C. The zero-contour is not plotted. All contour labels are in units of 0.1°C. The NINO3 index is defined as the standardized SST anomaly averaged over the central equatorial Pacific (5°S-5°N, 90°W-150°W). Note that the ENSO events in the tropical Pacific are accompanied by a SST anomaly pattern in the central North Pacific which strengthens from late autumn to early spring. Note also the general agreement between the model and observed patterns.

shows that the model is able to reproduce many of the ENSO-related precipitation changes both within the Pacific as well as in remote regions (Fig. 5.2). The agreement between the observations and model simulations lends confidence in the model's skill at predicting regional precipitation changes associated with ENSO. The agreement suggests that the GCM can be used to study the physical processes responsible for the remote precipitation changes.

Most of the precipitation changes in the TOGA-Pacific experiment (5.4.1) remain very similar to those from the GOGA experiment. This suggests that it is primarily the tropical Pacific SST anomalies that are responsible for the precipitation variations, including those over remote

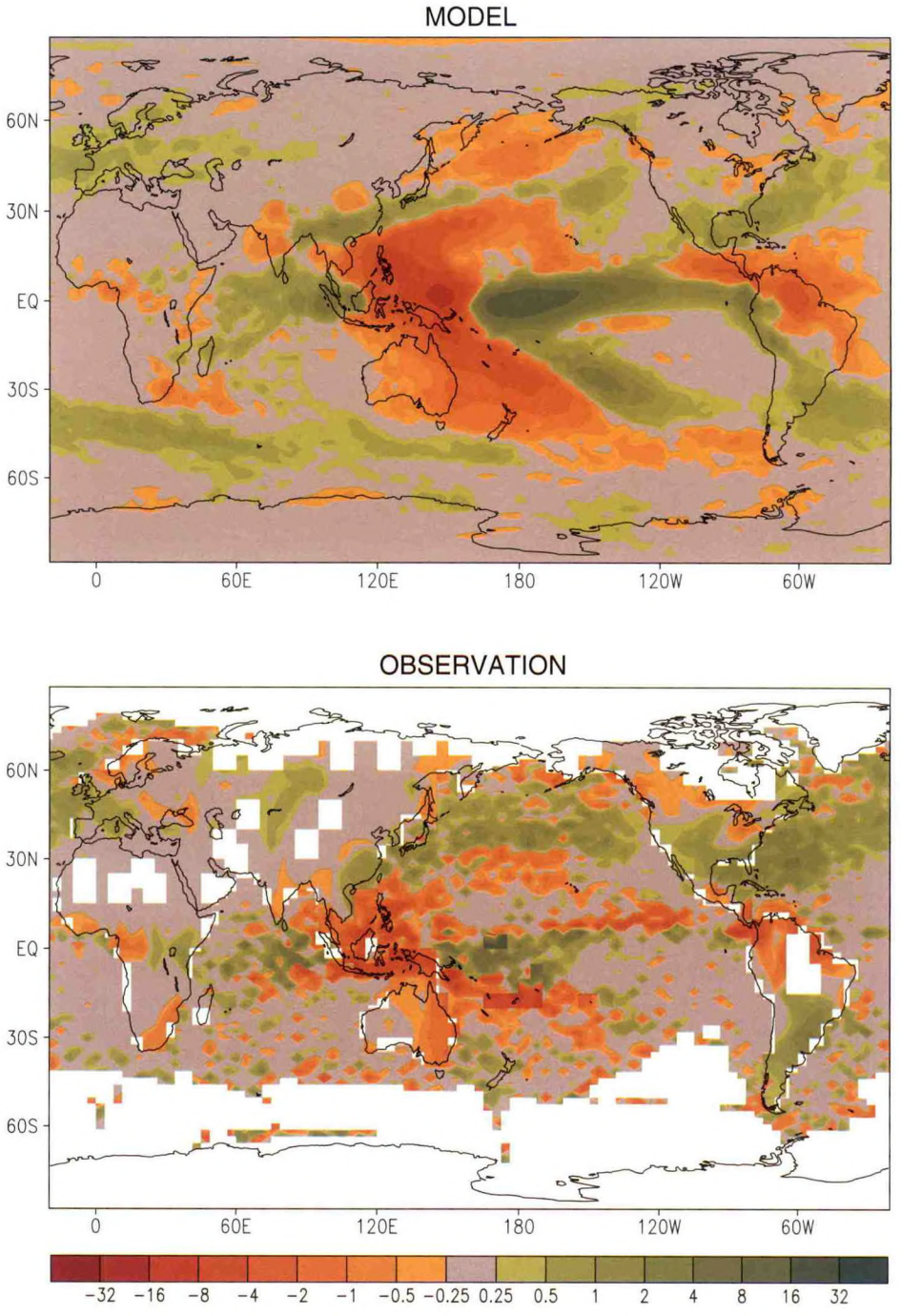

Fig. 5.2 Distribution of the least-absolute deviations slope (in units of 10^{-1} mm/day/°C) computed by regressing the annual mean precipitation in the GOGA experiment (top panel) and the observed atmosphere (bottom panel) versus the NINO3 index. The NINO3 index is defined as the SST anomaly averaged over the central equatorial Pacific (5°S-5°N, 90°W-150°W). Precipitation observations over land are obtained from a gridded network of rain gauge measurements while those over ocean are estimated from ship-reported weather codes. Areas of missing data are unshaded. The agreement between the observations and model simulations lends confidence in the model's skill at predicting regional precipitation changes associated with ENSO.

continental regions such as India, North and South America, and Eastern Europe. Interestingly, the primary region where the TOGA-Pacific experiment fails to reproduce the observed changes is Africa, where previous studies have suggested a connection between regional precipitation changes and SST anomalies in the tropical Atlantic. The GCM simulations hence also suggest that the ENSO-related precipitation variations over Africa cannot solely be attributed to changes in SST over the equatorial Pacific.

5.4.5 Coupling a New Ocean Mixed-Layer Model with an Atmospheric GCM

*M. Alexander** *N.-C. Lau*
J.L. Lanzante *J. Scott**

**Climate Diagnostics Center/NOAA*

In a collaborative effort involving Michael Alexander and James Scott of the Climate Diagnostics Center/NOAA (CDC), a coupled model has been developed utilizing a one-dimensional ocean model developed at CDC and the atmospheric R30 GCM at GFDL. The oceanic component simulates temperature and salinity variations at 31 levels in the vertical and includes fluxes through the air-sea interface and vertical re-distribution in the column, but excludes any horizontal communication in the ocean. The large number of vertical levels in the ocean model allows for a precise determination of the mixed-layer depth. The atmospheric component is a full GCM with horizontal resolution of R30 and 14 levels in the vertical.

Initial efforts have involved software development and testing both at CDC and GFDL. A trial run of this coupled model has been performed at GFDL by adopting a design similar to that of the TOGA-Pacific-ML experiment (5.4.1). Experimentation with the new mixed-layer model complements the existing collection of ensemble integrations aimed at diagnosing the nature of the variability of the global coupled system on interannual time scales.

PLANS FY99

The seasonal modulation of the atmospheric bridge mechanism, as well as the relative importance of wind forcing, air-to-sea temperature/moisture gradients, and cloud radiative processes in generating SST anomalies in the remote oceans will be investigated using data from the TOGA-Pacific-ML experiment. Extensive comparison with observational data on various forms of heat fluxes across the air-sea interface will also be performed.

The simulated circulation changes associated with SST anomalies in the TOGA-Atlantic experiment will be compared in detail with observations. The mechanisms for the air-sea coupling over the Atlantic will be critically examined using the model output, with special emphasis on the nature of local feedbacks between the wind field and the underlying SST anomaly in the tropical Atlantic sector, as well as the remote midlatitude atmospheric response to tropical Atlantic SST forcing.

Further research will be performed to evaluate the ability of the GCM to reproduce the seasonal dependence of the observed precipitation anomalies, and to examine the differences in the precipitation pattern for various ENSO episodes. The role of Atlantic SST variations in generating precipitation anomalies, particularly in the U.S., will also be examined.

Experimentation with the atmospheric GCM coupled to the new mixed-layer ocean model with variable depth will continue and analyses of the output will be conducted. Particular attention will be devoted to the simulation of the atmospheric and oceanic processes associated with the atmospheric bridge mechanism, and the nature of the recurrent extratropical SST anomalies in consecutive cold seasons.

5.5 DIAGNOSIS OF CLOUD PROPERTIES IN OBSERVED AND MODEL ATMOSPHERES

M.W. Crane *B.J. Soden*
S.A. Klein *R.T. Wetherald*

ACTIVITIES FY98

5.5.1 Comparison of Simulated Cloud Patterns in Extratropical Cyclones with Observations

The ability of the forecast model of the European Centre for Medium-Range Weather Forecasts (ECMWF) to simulate the typical organization of clouds surrounding low-pressure centers in the northwestern Atlantic has been evaluated by comparison with the composite of satellite-observed clouds of the International Satellite Cloud Climatology Project (ISCCP) (1309, ho). The model quite accurately simulates the general positioning of clouds relative to a low pressure center (Fig. 5.3). However, the optical depths of the model's high (low) clouds are too small (large) relative to the satellite observations, and the model lacks the midlevel topped clouds observed to the west of the surface cold front.

A subset of 10 cyclones were chosen for sensitivity studies. The error in high-cloud optical depths in the ECMWF composite is more sensitive to the assumptions applied to the ice microphysics than to the inclusion of cloud advection or a change of horizontal resolution from 0.5625° to 1.69° latitude. This may be attributed to the dominant role of gravitational settling in the ECMWF model in controlling the abundance of ice in the high-clouds of midlatitude cyclones. These results underscore the need for careful evaluation of the parameterizations of microphysics and radiative properties applied to ice in large-scale models.

5.5.2 Simulation of Frontal Cloud Patterns in Very High Resolution Models

In a continuation of the study of frontal clouds simulated by the ECMWF forecast model, a high resolution version of the model was run for a case of a rapidly deepening cyclone in the Northeast Atlantic. For this case study, a 18-hour forecast was made with the ECMWF model at T639 resolution (equivalent to 0.28125° latitude or 30 kilometer resolution). Comparison of this simulation to the observed satellite data (taken from the ISCCP project) indicates that the model simulates much of the synoptic scale and mesoscale structure of the cyclone. On the large-scale, the cold front is well-positioned relative to the classic comma-shaped high-topped clouds. Some smaller scale features such as the secondary development of high clouds to the west of the cold front are also well simulated. However, the longitudinal width of the cold frontal clouds is underestimated when compared with satellite data. This discrepancy again reflects the deficiency of the model identified in 5.5.1, namely, that the high clouds of the ECMWF model are optically too thin.

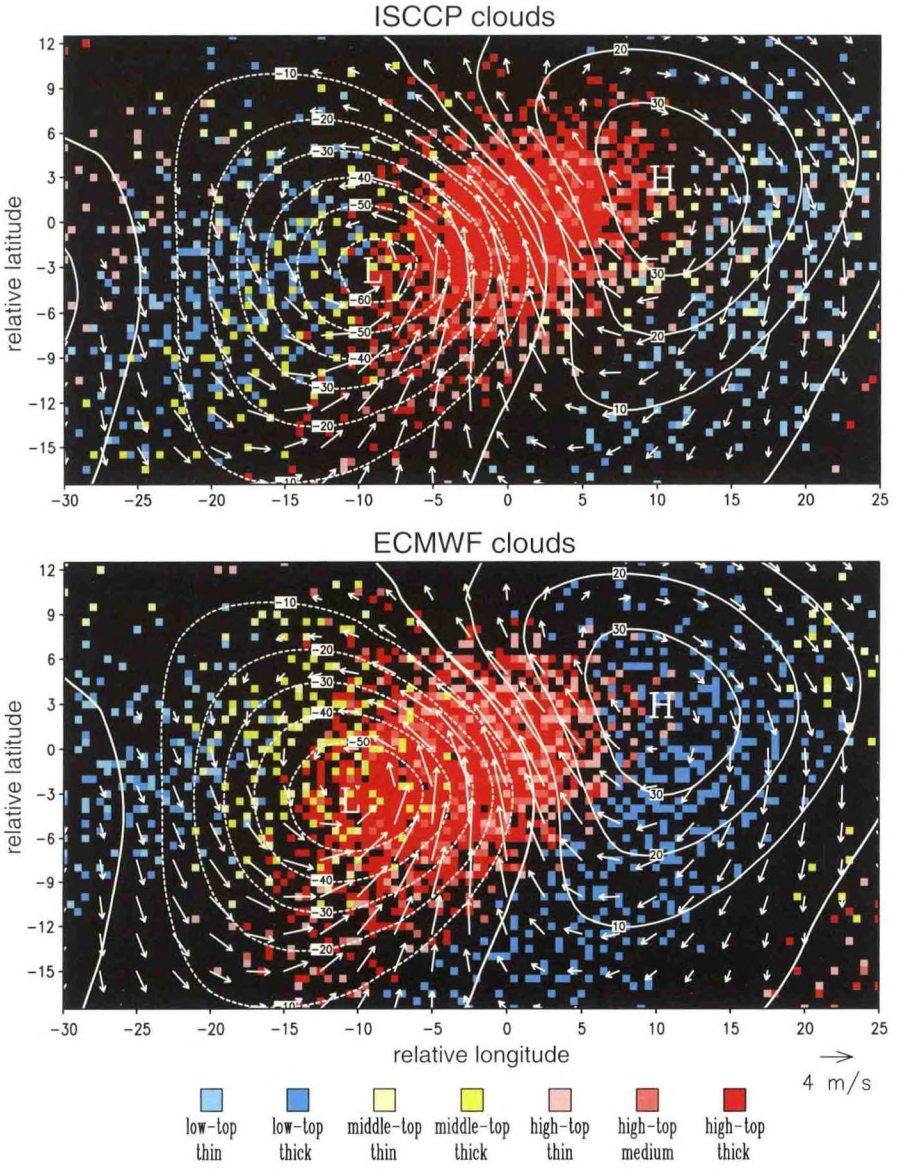

Fig. 5.3 Composite of cloud types (color pixels), 1000 mb geopotential height (contours) and 1000 mb wind anomalies (vectors) for midlatitude baroclinic cyclones in the northwestern Atlantic. The cloud types are deduced from satellite observations (top panel) and simulation by an ECMWF forecast model (lower panel). The altitude of the cloud-top is indicated by color and the optical thickness is indicated by color intensity (see legends at bottom). For example, pink pixels indicate high-topped clouds which are optically thinner than those portrayed by deep red pixels. Note how high-topped thick clouds are organized to the east of the 1000 mb low-pressure center (indicated by the letter "L") in the satellite observations and the forecast model. The model accurately simulates the position of the clouds relative to the cyclone, though the optical depth of the simulated high (low) clouds is too small (large). The amount of middle-top clouds west of the surface cold front is relatively less in the model pattern.

5.5.3 Coupling Between Low Cloud Type and Vertical Motion

Meteorological observations from volunteer observing ships and observations of low cloud types from Ocean Weather Station (OWS) C in the western midlatitude North Atlantic and OWS N in the eastern subtropical North Pacific were used to establish representative

relationships between low cloud type and the surface synoptic environment (hm). Results for OWS C during summer show that bad-weather stratus occurs with strong convergence associated with a surface trough to the northwest, in agreement with an earlier study (1514). Cumulus-under-stratocumulus and moderate and large cumulus occur with divergence in the cold sector of an extratropical cyclone. Both sky-obscuring fog and no-low-cloud typically occur with southwesterly flow from regions of warmer sea surface temperature. Values of divergence and estimated subsidence at OWS C and OWS N during summer and winter are large for ordinary stratocumulus, less for cumulus-under-stratocumulus, and least for moderate and large cumulus.

These observational results confirm and extend previous theoretical understanding that near surface wind divergence is an important large-scale parameter determining low cloud type and therefore low cloud amount and other cloud properties. In particular, decreasing divergence and subsidence, in addition to increasing sea surface temperature, may promote the transition from stratocumulus to trade cumulus observed over low latitude oceans.

5.5.4 Sensitivity of a GCM to Observed Cloud Properties

Monthly climatologies of cloud amount and cloud optical properties were created using ISCCP data, and were then adjusted to develop cloud optical properties that were consistent with the top-of-atmosphere fluxes measured from the Earth Radiation Budget Experiment. The method of producing the climatology was designed so that the results could be easily incorporated into different GCMs utilizing a variety of vertical and horizontal resolutions. A R30 climate GCM was then run using prescribed cloud properties from the ISCCP climatology in place of model-predicted quantities. The largest differences between the ISCCP-prescribed cloud distribution and that predicted by the model's parameterizations occurred for low-level clouds, particularly in the subtropical stratocumulus and midlatitude storm track regions. This has a large impact on the solar radiation absorbed at the surface and highlights the potential importance of accurately simulating low-level clouds in a fully coupled ocean-atmosphere model. In particular, differences between the observed and model-predicted low-level cloud field coincide with areas of large flux adjustments in the coupled ocean-atmosphere model.

PLANS FY99

The prescribed cloud optical properties in both the shortwave and longwave bands will be explicitly linked to provide a consistent set of optical properties at all wavelengths. The impact of the prescribed clouds upon surface radiative fluxes will be further examined within the context of coupled ocean-atmosphere models.

5.6 GFDL/UNIVERSITIES COLLABORATIVE PROJECT FOR MODEL DIAGNOSIS

J.L. Anderson *M.J. Nath*
I.M. Held *P.J. Phillipps*
N.-C. Lau

ACTIVITIES FY98

The primary goals of this collaborative effort are to involve the university community in the analysis and design of numerical model experiments at GFDL for identifying the effects of anomalies in surface boundary conditions on interannual and interdecadal variability of the atmosphere, and to develop procedures for insightful analysis and comparison of GCM predictions of regional climate anomalies. The insights gained from these research activities will be used to improve the physical realism of GCMs at GFDL. The efforts of this collaboration are focussed on the mutual interactions between stationary eddies, low-frequency variability and storm tracks, the maintenance of regional climates and their sensitivities to ocean surface temperature, and the applications of these results to atmospheric predictability. These goals and activities are consistent with the designation of this project as an Applied Research Center (ARC) of the Office of Global Programs/NOAA. In order to forge a more direct connection with NOAA efforts on seasonal-to-interannual prediction and the development of global warming scenarios, a call for new proposals from extramural investigators has been made, and the review process of these proposals has been completed. This round of competition for the available funding has resulted in the participation of new members from M.I.T., University of Wisconsin at Milwaukee and Pennsylvania State University. Continuing support has been offered to existing members at University of Washington, University of Illinois and the Climate Diagnostics Center/NOAA. An annual workshop was held in July 1998 at GFDL, at which the research progress of various participating groups was presented, and the future plans of this joint effort were formulated.

Significant achievements by GFDL investigators associated with this collaborative project during the past year include the completion of a large suite of experiments on the atmospheric sensitivity to anomalous SST forcings in different ocean basins using the R30 climate GCM (5.4.1), identification of the global influences of the atmospheric bridge mechanism in linking SST variability in the tropical Pacific to thermal conditions throughout the World Oceans (5.4.2), successful coupling of the atmospheric climate GCM to a new mixed-layer model of the ocean with variable depth (5.4.5), and detailed description of westward propagating circulation patterns in high latitudes with approximately three-week periods in observed and model atmospheres (5.3.1).

PLANS FY99

The suite of SST sensitivity experiments will be extended to include the recent 1997/98 ENSO episode. Multiple runs will be conducted using the atmospheric GCM coupled to the new mixed-layer ocean model. The nature of the North Atlantic and Arctic Oscillations will be investigated using steady-state models and new sensitivity experiments.

6. HURRICANE DYNAMICS

GOALS

To understand the genesis, development and decay of tropical disturbances by investigating the thermo-hydrodynamical processes using numerical simulation models.

To study small-scale features of hurricane systems, such as the collective role of deep convection, the exchange of physical quantities at the lower boundary and the formation of organized spiral bands.

To investigate the capability of numerical models in predicting hurricane movement, precipitation, and intensity, and to facilitate their conversion to operational use.

6.1 HURRICANE PREDICTION SYSTEM

ACTIVITIES FY98

6.1.1 Performance in the 1997 Hurricane Season

M.A. Bender *R.E. Tuleya*
Y. Kurihara

In the 1997 hurricane season, the tropical cyclone activity in the Atlantic basin was unusually low, coinciding with an extremely strong El Niño phenomenon. Only 30 forecasts from the GFDL Hurricane Prediction System were included in official performance statistics of the National Hurricane Center (NHC). The mean 24-hour forecast position error of the GFDL system was 153 km. In the eastern Pacific, the 24-hour position error was 159 km for 72 cases. The examination of track forecast errors and the comparison against other National Weather Service track models used at NHC indicate that the track forecast with the GFDL system in the Atlantic continues to be more skillful than the other models, particularly after 36 hours. However, the superiority of the GFDL system was not evident in the eastern Pacific where many strong storms developed over the unusually warm waters to the west of Mexico. Storm intensity predictions from the GFDL system exhibited skill only after 36 forecast hours, reflecting problems with both the sparseness of data and the accuracy of the initialization in that region.

6.1.2 Analysis of the Forecast Results

M.A. Bender *R.E. Tuleya*
Y. Kurihara

The track forecast error at 24 hours for the 1997 Atlantic season was comparable to the error during the extremely active 1995 season (165 km for 219 cases). On the other hand, the error at 24 hours in the eastern Pacific was somewhat larger than for the 1995 season (135 km for 86 cases). The database for GFDL forecasts is the global analysis made at the National

Center for Environmental Prediction (NCEP) and the storm message from the NHC. During the 1997 season, the NCEP global model occasionally produced strong spurious tropical vortices, which probably adversely affected the GFDL performance.

During the 1997 hurricane season, the data from dropsondes released over the Atlantic from a new high altitude Gulfstream aircraft became available for use by the NCEP global data assimilation system. There are indications that these additional observations had some positive impact on the GFDL hurricane forecasts. However, the number of cases was very limited.

The forecast skill of the GFDL system was examined with respect to the distribution of the wind and precipitation. It appears the model is capable of simulating first order patterns of these quantities after 12 hours or so. This implies that realistic structure can evolve in the model starting from an initial symmetric structure. However, such a transition of vortex structure in early forecast stages may be detrimental to accurate prediction of storm intensity.

6.1.3 The 1998 Hurricane Season

M.A. Bender *R.E. Tuleya*
Y. Kurihara

The model initialization methodology of the GFDL Hurricane Prediction System has been upgraded. Based on an analysis of the structure of forecast storms (6.1.2) and the test results of a new initialization scheme (6.2.3), it was decided to extract the asymmetric component of the forecast storm at 12 hours from the preceding forecast cycle and use it in the vortex specification for the new run cycle. Test results indicate that inclusion of this additional component will yield improvement in both track and intensity predictions.

The NCEP global analysis on which performance of the GFDL system is heavily dependent was upgraded near the beginning of the 1998 Atlantic hurricane season. The horizontal and vertical resolutions of the global model were increased and model physics was extensively modified. It became known in late June that strong erroneous tropical vortices tended to develop in the new global model, resulting in difficulty on the part of the GFDL system in identifying a synthesize vortex. Moreover, the analyzed environmental flow was not accurate, reducing the forecast skill of the GFDL model in at least some cases in the eastern Pacific.

PLANS FY99

Performance of the GFDL system in the remaining 1998 season will be monitored. Special attention will be given to the environmental flow derived from the NCEP global analysis, as well as the evolution of the asymmetric structure in the GFDL model.

6.2 HURRICANE PREDICTION CAPABILITY

ACTIVITIES FY98

6.2.1 Extended Prediction

M.A. Bender R.E. Tuleya

The operational GFDL model/system has been modified to allow a two-day extension of the standard three-day forecast. Extended prediction of hurricane tracks up to 120 hours was made semi-operational and results obtained in a parallel run mode have been utilized at NHC.

6.2.2 Ensemble Forecast

S.D. Aberson R.E. Tuleya*
*M.A. Bender Y. Zhang***

**Hurricane Research Division/AOML*
***Scientific Visitor*

A study of ensemble forecasts of hurricane tracks using the GFDL model has continued. Ensemble forecasts may be used in planning of adaptive observations. In this case, the locations of fast growing modes are detected from a set of ensemble forecasts performed during a previous forecast cycle.

An ensemble forecast approach was used in a study of the benefit of additional wind observations at high levels. The analysis showed little impact of such observations on storm track prediction. It seems that operational benefit of enhanced wind observations may be very much dependent on how the model ingests the wind data.

6.2.3 Improvements in Initialization

M.A. Bender R.E. Tuleya
Y. Kurihara

A basic guideline used in developing the previous methodology for the GFDL hurricane model initialization was that the initial vortex be consistent with the prediction model. From an analysis of the performance of the GFDL system in the past three years of operational use, it became clear that the initial vortex must also be sufficiently adapted to the environmental conditions. It was found that the time scale for this adaptation is approximately 12 hours. Since the storm structure which evolved in the GFDL model during this period resembled the actual storm to first order, it was considered reasonable to utilize some characteristics of the forecast storm in the initialization.

As a first step, the initial vortex was specified by adding the asymmetric component of the forecast storm to the axisymmetric vortex generated using the original scheme. In this case the asymmetry was recognized as a sub-vortex scale deviation from the azimuthal running mean. Fig. 6.1 shows the positive effects (lower values indicate more skill) of inclusion of asymmetry in both the track and intensity forecasts averaged for 43 test cases, particularly

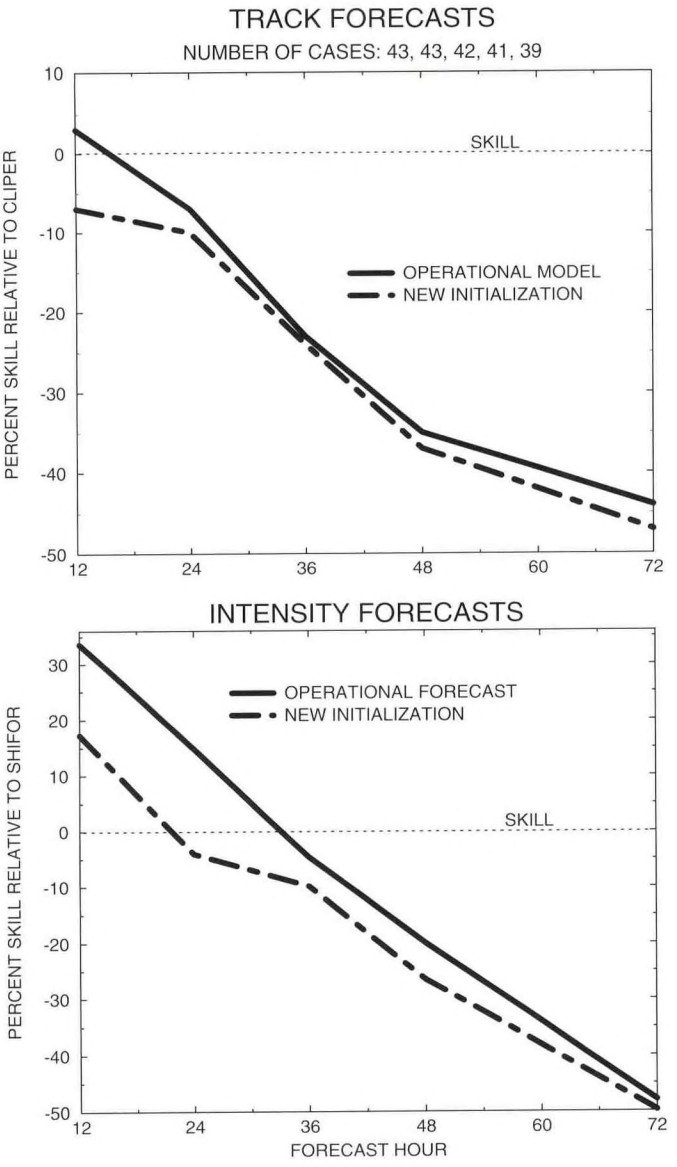

Fig. 6.1 Comparisons of forecast skill using previous operational and new initialization methods. Average errors of the forecast storm position relative to CLIPER (top) and storm intensity relative to SHIFOR (bottom) for 43 test cases. Negative values indicate higher skill than these standard measures.

during the 12- to 24-hour time period. The revised scheme was implemented into the GFDL system in time for the 1998 hurricane season.

An intensive study is under way to further improve the initialization methodology. In the new scheme, the three resources are combined to prepare an initial condition: (a) the environmental fields of the global analysis; (b) the entire forecasted storm consisting of both axi- and asymmetric components; and (c) available observation/analysis data of the storm. The forecast storm, which is assumed to be model consistent and well adapted to the forecasted environmental conditions, is first implanted into the environment specified by the

global analysis. Next, the state thus obtained is adjusted through ingestion of available information on the storm structure, using reformed balance formulas (6.5).

A study was undertaken to investigate the impact of a more accurate positioning of the model storm at the initial time. A systematic bias in the initial position of the circulation center was found for weak, fast moving storms.

PLANS FY99

Experiments of extended forecasts will continue. Developmental work on the initialization methodology will proceed with evaluation of past cases. In addition, work to upgrade the GFDL system by increasing the grid resolution of the model will be given higher priority. Higher resolution is essential for more accurate representation of not only the eye and eyewall of the intense storm, but also the surrounding environmental conditions.

6.3 BEHAVIOR OF TROPICAL CYCLONES

ACTIVITIES FY98

6.3.1 Hurricane Intensity in a High-CO_2 Climate

*I. Ginis** *W. Shen**
T.R. Knutson *R.E. Tuleya*
Y. Kurihara

**University of Rhode Island*

The potential impact of a greenhouse gas-induced global warming on the intensity of hurricanes was investigated in a series of case studies in which a global climate model was used to generate conditions representing both the present climate (control) and a high CO_2 scenario (1527). These conditions were then used as initial conditions for 5-day integrations of the high-resolution GFDL Hurricane Prediction System used operationally at NCEP (1533, hz). The climate model conditions are from a medium resolution (R30) version of the GFDL global coupled climate model (1042, er).

The geographical distribution and magnitude of maximum surface wind speeds for a series of storm cases is illustrated in Fig. 6.2. Under simulated present day conditions in the northwest Pacific (Fig. 6.2b), the maximum wind speeds are fairly realistic compared to the observed distribution (Fig. 6.2a). In particular, the model successfully simulates lower maximum winds over higher latitudes (with cooler SSTs), near the equator, and over land regions. The distribution for high CO_2 conditions (Fig. 6.2c) has more areas of very intense (>70 m/s) wind speeds than does the control (Fig. 6.2b), which suggests modest increase in maximum surface winds in response to CO_2-induced warming. The high CO_2 storm sample was derived from years 71-120 of a +1%/yr CO_2 increase experiment using the R30 global model, in which northwest Pacific basin SSTs were about 2.2°C warmer than for the control.

A statistical comparison of 51 control storm cases and 51 cases under high CO_2 conditions indicates that the high CO_2 storms are more intense than the control storms by

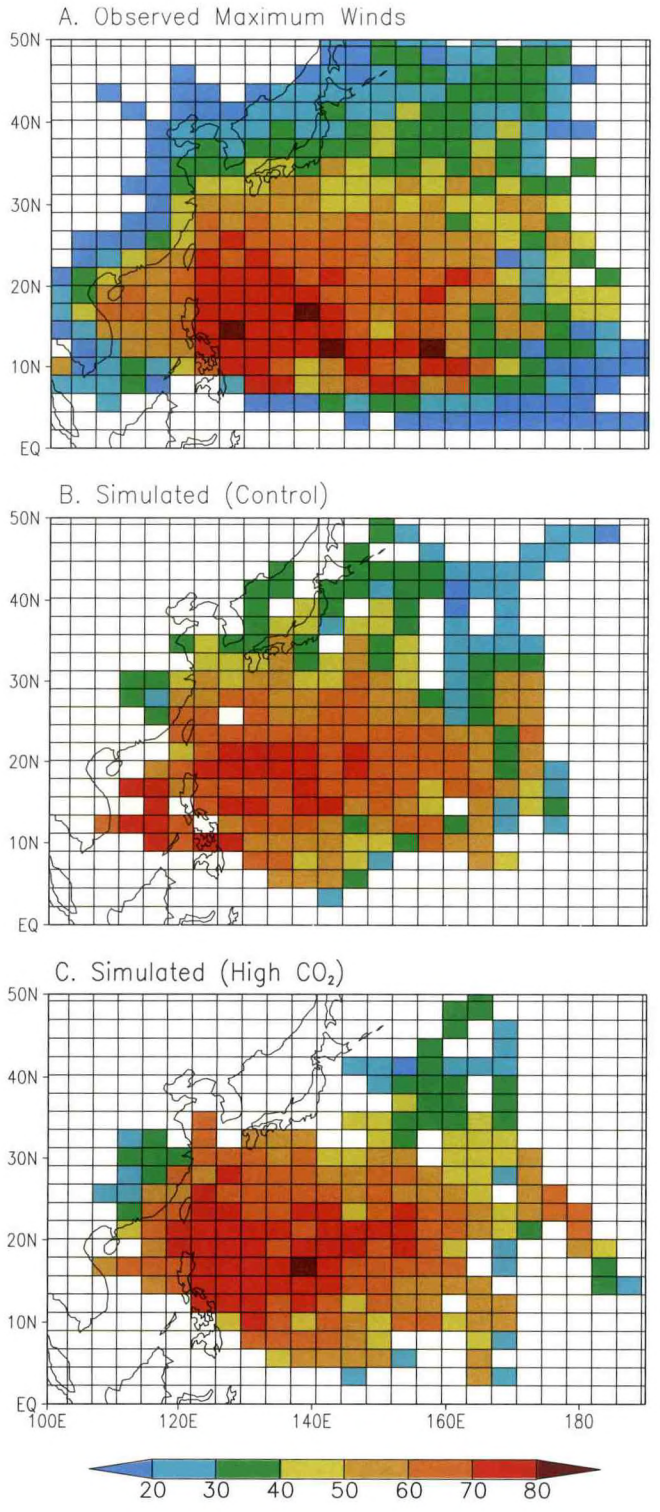

Fig. 6.2 Geographical distribution of the maximum surface wind speeds (m/s) observed during 1971-1992 (A) and simulated (B and C) for tropical storms in the northwest Pacific basin. Observations are from the Joint Typhoon Warning Center (Guam). Simulated distributions are based on 71 case studies each under control (B) and high CO_2 (C) conditions. Storms in the enhanced-CO_2 atmosphere are 5-12% stronger than in the control case.

about 3-7 m/sec (5%-12%) for surface wind speed and 7 to 23 hPa for central surface pressure. Near-storm precipitation simulated in the hurricane model is 28% greater in the high CO_2 sample. The storm tracks for the high CO_2 and control samples were quite similar.

Additional idealized experiments were also performed in which an initial storm disturbance was embedded in highly simplified flow fields using time mean temperature and moisture conditions from the global climate model. In another suite of idealized experiments, the sensitivity of the GFDL model storm intensity was tested for a wide range of SST and static stability (hc). These idealized experiments support the case study results and suggest that, in terms of thermodynamic influences, the results for the northwest Pacific basin should be qualitatively applicable to other tropical storm basins.

6.3.2 Tropical Cyclone-Ocean Interaction

*I. Ginis** *W. Shen**
M.A. Bender

**University of Rhode Island*

The sensitivity of storms intensity to the properties of the surface air near the storm center was investigated in relation to a feedback phenomenon between the ocean and the storm. Using a set of cases from the Atlantic basin, it was found that, while the surface pressure decrease between the storm's outer periphery and the storm center is well correlated with an increase in the equivalent potential temperature, the degree of interdependency differs from region to region and case to case. This suggests that the formation of the cold oceanic wake due to the storm-ocean coupling is an important factor, but not the only major factor controlling the storm intensity.

Evaluation of the impact of tropical cyclone-ocean interaction on the intensity forecasts of real storms was also performed for a number of Atlantic basin cases. On average, the intensity of the simulated storm was better with the storm-ocean coupled model, compared to the operational forecasts in which the sea surface temperature remained unchanged.

PLANS FY99

Additional methodologies for examining the hurricane intensity/climate change problem will be explored. Higher resolution GCM experiments or extended integrations of the regional hurricane model may be initiated. Work will continue to develop a future operational system using a tropical cyclone-ocean coupled model. A plan to extensively analyze storm behavior at landfall will be developed.

6.4 COMPARE PROJECT

ACTIVITIES FY98

M.A. Bender R.E. Tuleya
Y. Kurihara

Preparation of the dataset containing initial conditions for a case of a Western Pacific typhoon chosen for the third case of the COMPARE (Comparison Of Mesoscale Prediction And Research Experiment) project co-sponsored by the World Meteorological Organization was completed. Responding to a request from the COMPARE committee, the GFDL hurricane model initialization method was applied to global analyses performed at the Japan Meteorological Agency and NCEP. The GFDL scheme includes the solution of a balance equation to ensure the balance between the wind and mass fields. Problems were encountered in a very steep mountainous region, and were presumed to be caused by differences in the characteristics between the global model and hurricane model. The method by which the balance equation was applied was modified (6.5), yielding a quite reasonable solution.

6.5 MODEL IMPROVEMENT

ACTIVITIES FY98

M.A. Bender R.E. Tuleya
Y. Kurihara

In order to perform the initialization process for the COMPARE case (6.4), the reverse balance equation was reformulated to handle difficulties associated with steep topography. In the new formulation, once a wind field correction to the presumed balanced state is given, the mass field is adjusted to maintain balance. The new formula will be utilized in constructing an improved scheme of initial vortex specification (6.2.3).

Work on the improvement in the spatial resolution of the hurricane model was initiated in order to cope with the increase in the global model resolution (6.1.3), as well as to represent the hurricane structure more accurately.

PLANS FY99

Developmental work to improve the hurricane model initialization methodology will continue. An assessment will be made of possible methods for determining wind corrections by comparing the observed or analyzed wind against a presumed balanced state. Work to increase the grid resolution of the hurricane model will also proceed to improve simulation accuracy and enhance the capability of the model in both research and operational environments.

7. MESOSCALE DYNAMICS

GOALS

To produce accurate numerical simulations of storm-scale processes in order to understand the role that planetary and synoptic scale parameters play in their generation and evolution.

To understand the dynamics of synoptic and mesoscale phenomena and their interaction with larger and smaller scales.

To improve high-resolution model simulations of synoptic and smaller scale phenomena which can be used to guide parameterization development in coarser models.

7.1 ANALYSIS OF MIDLATITUDE CYCLONES AND STORM TRACKS

B. Gross *L. Polinsky*
I. Orlanski *J. Sheldon*

ACTIVITIES FY98

7.1.1 Observed Cyclone Evolution Along Winter Storm Tracks

The profound interactions between the cyclone scale and planetary scale have been examined in order to understand the nature of cyclone evolution along storm tracks. A study that focuses on the mechanisms controlling the evolution of the eastern ridge in the Pacific storm track has been completed (1572). This storm track originates in the vicinity of the stationary trough over the western Pacific and terminates near the stationary ridge over the west coast of North America. The analysis focuses primarily on the vertically averaged high frequency transients. Results show that forcing by the cyclone-scale eddies along the storm track is consistent with the poleward deflection of its axis and thus a positive feedback to the stationary circulation.

The results also clarify the role of high-frequency velocity correlations in the column averaged vorticity forcing. One contribution, associated with meridional momentum fluxes, has the well-known effect of intensifying the barotropic component of the zonal jet. An additional contribution, associated primarily with the meridional elongation and breaking of eddies, has heretofore not received a great deal of attention as a vorticity forcing. This contribution provides cyclonic and anticyclonic vorticity forcing northwest and northeast of the storm track, respectively, thereby enhancing the trough-ridge system associated with the stationary flow. The combined effects of the two contributions is to tilt the storm track axis into a southwest-northeast orientation. This effect is clearly identified in the observed stream function tendencies.

To interpret these results, one may assume for simplicity that the eddies are the only vorticity forcing in a zonal-mean flow. The expected response would be a trough downstream of the storm track entrance and a ridge slightly east of the termination, both of which are clearly seen in the observations. Once this stationary pattern has been established, strong positive feedback by the eddy forcing can, by itself, further enhance this pattern. At the beginning of the storm track, eddies grow by baroclinic processes, while near the middle of the storm track they grow at the expense of other eddies upstream, typical of downstream baroclinic development (1345). However, at the eastern termination point of the storm track, the eddies become meridionally elongated, at which point irreversible wave-breaking occurs and the ridge intensifies.

7.1.2 Seasonal Variability of Cyclone Activity in Storm Tracks

The aforementioned analysis clearly captures the seasonal life cycle of the eddy activity in the eastern Pacific, which increases during the early fall, reaches a maximum around the month of November, then decays for most of the winter months (1572). Month-to-month variations in eddy activity over the Pacific Ocean show that energy levels increase through November and decrease thereafter, reaching a winter minimum at the same time that the axis of the storm track is deflected poleward and the trough-ridge circulation pattern is intensifying. One of the more significant differences between November and December is that, in November, the storm track extends across the entire Pacific basin, whereas, in December, the eddy activity terminates short of the North American coast, at roughly 140°W. The forcing from the high-frequency eddies displays similar differences, with the activity pattern in November being elongated, due primarily to eddy momentum fluxes. In December, the effects of meridional elongation and wave-breaking become more prominent, resulting in increased forcing of the quasi-stationary trough-ridge pattern.

The transition from a fall to a winter circulation manifests itself in a number of ways. During the fall, upper-level eddies from Asia undergo additional development when they reach the relatively warm waters of the Pacific Ocean. Although wave breaking may occur, the eddy amplitudes in the lower levels are not particularly large, and the modest amounts of energy gained via baroclinic conversion are transferred to upper levels, where it is transferred downstream via ageostrophic geopotential fluxes (1345), extending the eddy activity over the entire ocean basin. But as the jet moves southward during the transition from fall to winter, eddies are partially blocked upstream by the Tibetan plateau. This blockage, combined with increased low-level cooling/stabilization over the Asian landmass, results in fewer (and weaker) eddies reaching the Pacific Ocean by early winter. By December, baroclinicity in the western Pacific has increased substantially, and low-level eddies are found to break by the time they reach the middle of the Pacific. With the upper-level eddies starting to break well before reaching the west coast of North America, the trough-ridge forcing is increased. This phenomenon has two negative feedbacks with respect to eddy activity. First, the intensification of the trough in the western Pacific accelerates the barotropic component of the zonal jet, reducing the residence time of the eddies in the baroclinic zone. Second, the intensification of the ridge in the eastern Pacific enhances the barotropic stretching deformation of the mean flow, adversely affecting the development of baroclinic eddies and making the termination of the storm track more abrupt. This process continues for the entire winter, reducing the kinetic energy of the transients.

All of these results are consistent with the fact that when the eastern Pacific ridge is weak (as during the warm ENSO phase), synoptic disturbances can more easily propagate through the eastern Pacific ridge and enter North America on the west coast of the U.S. However, in periods when the ridge is strong (as in the ENSO cold phase), transient eddies are blocked at these latitudes, with most of them suffering irreversible breaking or a deflection poleward. As a consequence, their entrance into North America is either blocked or is shifted northward into Canada and Alaska. These results thus suggest a positive feedback in which the presence of the ridge induces breaking of the transient eddies which, in turn, enhances the quasi-stationary ridge.

7.1.3 Interannual Variability of Cyclone Activity in Storm Tracks

The Pacific storm track also displays considerable interannual variability, shifting from a November-like state in which the eddy kinetic energy extends across the entire Pacific basin to a more December-like trough-ridge pattern (1572). This shift is particularly evident in connection with the ENSO cycle. The two regimes described above are observed to coincide with the warm and cold phases of the ENSO cycle, respectively. These phases are defined in the current study by the sea surface temperature (SST) anomalies in the tropical eastern Pacific. Over the Pacific Ocean, the eddy activity during the warm phase is slightly stronger, is more elongated, and lacks the southwest-northeast tilt (poleward deflection) present in the cold phase. It was also found that in the warm phase, the trajectories of the eddies are characterized by a regular eastward progression, while in the cold phase the signature characteristic of eddy termination is observed in the vicinity of the enhanced eastern Pacific ridge.

The extension of the storm track during warm events resembles that of fall conditions, and could conceivably be maintained for the entire winter, thanks to the enhanced source of low level baroclinicity which extends well into the eastern Pacific during this ENSO phase. The study suggests that it is this source of baroclinicity in the eastern Pacific that provides energy to the eddies, preventing the localization of any vorticity forcing by the high frequency eddies and thereby reducing the amplitude of the trough-ridge system and the associated upper-level jet diffluence in this region. Thus, the region in which the eddies can grow along the storm track is extended during the warm events and truncated during cold events.

PLANS FY99

Model simulations of storm tracks will continue to focus on the mechanisms responsible for the growth, maintenance, and dissipation of quasi-stationary features in idealized storm tracks. The analysis of storm tracks in the Northern Hemisphere are being extended to storm tracks in the Southern Hemisphere. A collaboration with CIMA (Centro de Investigaciones para el Mar y La Atmosfera, Buenos Aires, Argentina) has been initiated to performed this research.

7.2 THE EVOLUTION OF MIDLATITUDE CYCLONES

S. Garner *B. Gross*
I. Orlanski

ACTIVITIES FY98

7.2.1 The Evolution and Feedback of Cyclones in Storm Track Simulations

A series of numerical experiments employing the modified hydrostatic Zeta model (7.4.1) in spherical coordinates is being used to analyze the observed interaction between high-frequency eddies and the mean flow in idealized storm tracks. In these simulations, baroclinic eddies evolve within a baroclinic jet that is forcibly maintained within a small zonally confined region. Downstream of this region, distinct stationary features develop and dissipate. These include an isolated ridge that persists for over 100 model days. Preliminary analyses of the high frequency forcing show encouraging similarities between the velocity correlations that maintain the wintertime ridge in the eastern Pacific (7.1.1, 1572) and the isolated ridge in the model simulations.

Anticyclonic breaking of the upper level wave has been identified as the precursor of establishing this quasi-stationary ridge. For this reason, an effort has been made to clarify the mechanisms that predominate in the life cycle of eddies which eventually break in this way. One definition of wave breaking used for this purpose is the reversal of the meridional potential temperature gradient from its usually negative sign to a positive sign. This occurs when warm air is advected poleward and cold air is advected equatorward by the intensifying cyclone. This reversal usually occurs at the lower levels as the cold front associated with the cyclone occludes. It was found that this reversal occurs upstream and a few days earlier than the anticyclonic breaking in the upper levels.

A time-lag regression has been applied to the last 200 days of the model integrations in order to establish a composite view of the wave breaking process. The test condition in this regression is a reversal of the meridional potential temperature gradient in a region upstream of the position of the quasi-stationary ridge. This condition has been applied in order to separate the systems that break from those that do not. The latter mainly propagate downstream by means of geopotential fluxes (1053, 1125, 1345). An analysis of the cyclone environment at zero lag is shown in Fig. 7.1, in which isosurfaces of cyclonic relative vorticity are displayed, along with the surface potential temperature and wind vectors, and upper level energy fluxes.

On the upstream side of the central vortex (centered at 120° longitude) a growing eddy is observed within which baroclinicity generates the low-level vorticity. The upper level vorticity is tilted westward, a well-known feature of unstable baroclinic eddies. As this wave matures, the upper and lower relative vorticity centers undergo a rotation, during which the low level cyclone center moves poleward during its rollup, whereas the upper level center moves equatorward. These features are apparent in the central vortex, which shows features typical of a mature eddy, including the cold frontal structure behind warm (red) air advected from the south, and the associated cyclonic surface circulation. The open cone shape of the vorticity isosurface at 10 km indicates that the upper level vorticity has considerable meridional structure, with its center south of the surface center. As the low-level cyclonic

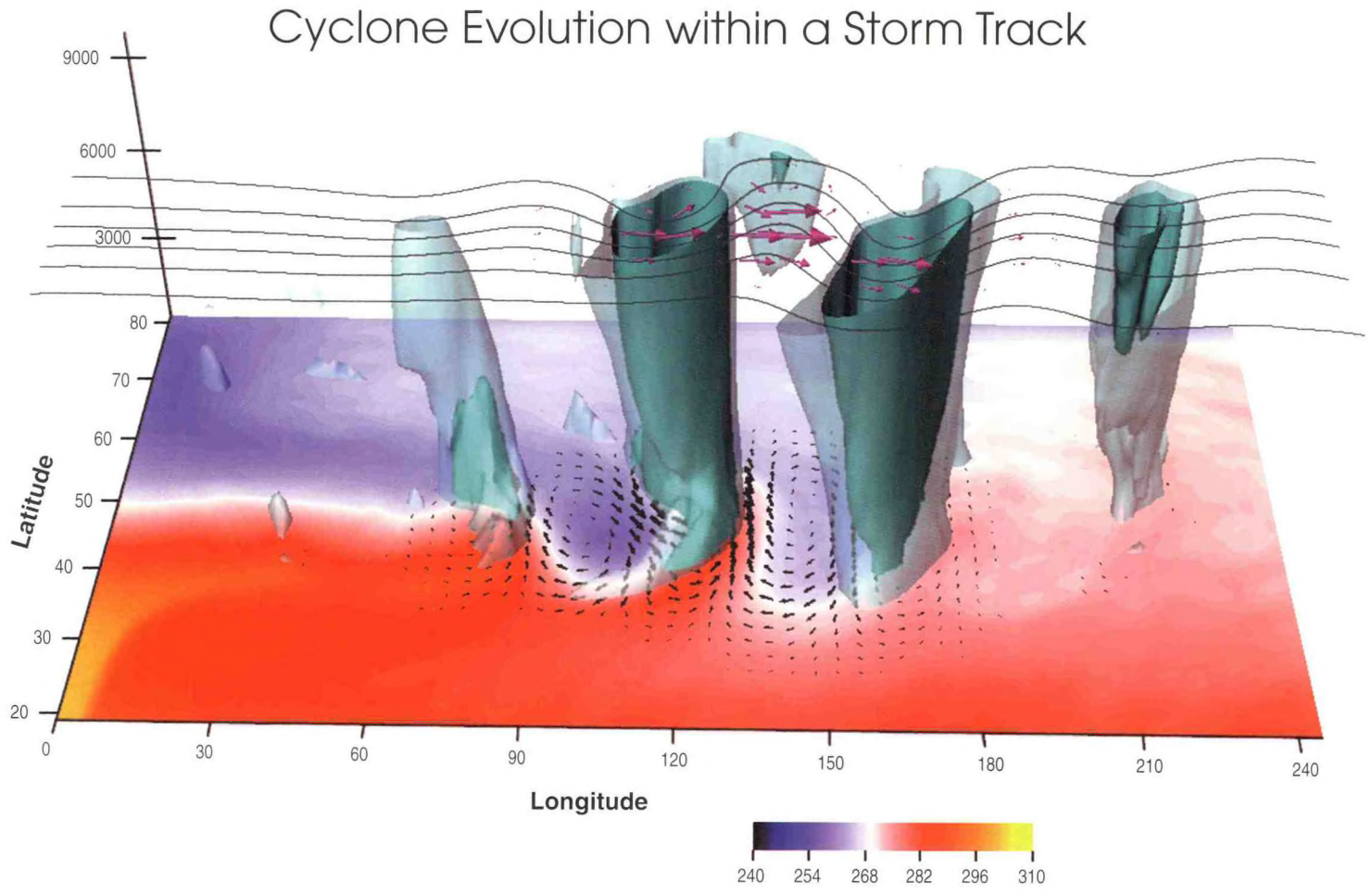

Fig. 7.1 Regression with 0 time lag of the relative vorticity (isosurfaces), surface potential temperature (color shading in °K), surface wind (black vectors), energy fluxes at 10 km (magenta vectors), and geopotential at 10 km (contours). The westernmost eddy has the westward tilt with height typical of developing cyclones. As this wave matures, the low level cyclone center moves poleward during its rollup and the upper level center moves equatorward. These features are apparent in the central vortex, which is typical of a mature eddy. Other features include a surface cold front behind warm air advected from the south, and the associated cyclonic surface circulation. Upper level energy fluxes are quite dispersive with a considerable equatorward component, which produces an upper level disturbance that tends to move equatorward, as shown in the third vorticity center. The anticyclonic shear on this side of the jet shreds the eddy, which breaks anticyclonically. Persistent breaking in the same location will generate a quasi-permanent ridge.

circulation rolls up the potential temperature field to produce the gradient reversal in the poleward flank, energy fluxes (magenta vectors) dominate at upper levels, consistent with the downstream development mechanism. These energy fluxes tend to be quite dispersive with a considerable equatorward component, which produces an upper level disturbance that tends to move equatorward, as in the third vorticity center. The anticyclonic shear on the equatorward side of the jet shreds the eddy, which breaks anticyclonically. Inspecting different time lags in the regression reveals that the upper wave downstream will decay without further regeneration, because by this point in the storm track surface baroclinicity has been severely depleted.

These results suggest that, aside from land-sea contrasts and orographic forcing, the characteristics of a storm track are strongly determined by the life cycle of the eddies, and the zonal distance at which they break. The eddies reinforce the quasi-stationary circulation by enhancing the trough at the entrance of the storm track and the region of diffluence associated with the ridge at the exit. This process is strongly interactive, since it is the trough-ridge system itself that limits the life cycle of the eddies.

7.2.2 Baroclinic Wave Equilibration in Zonal Flows

A study (1518) to determine whether baroclinic normal modes zonalize or organize into coherent structures at the end of their life cycles has focused on the distinction between long and short waves. At all stages of development, the long waves are dominated by poleward momentum flux, while the short waves show mainly equatorward flux. A positive feedback with the time-dependent zonal-mean wind then forces either cyclonic or anticyclonic breaking. The distinction between zonalizing and long-lived eddies lies in the amount of warm air that "secludes" during the growth phase. Cyclonic short waves develop relatively little warm temperature anomalies at low levels, and thereby become vulnerable to large-scale deformation.

PLANS FY99

The sensitivity of cyclone evolution to its position within the storm track will continue to be evaluated. In particular, the mechanisms responsible for the poleward progression of low-level eddies and the equatorward progression of upper-level eddies will be further analyzed. A clarification of the role that the structure of the high-frequency eddies play in determining the point when the temperature gradient reverses, and its relation to critical points in the flow, will be pursued. Mean-flow forcing by baroclinic waves of different zonal scale will be investigated by examining the growth of isolated (zonally asymmetric) unstable eddies within a linear-stochastic channel model, which will include non-zonal variations and parameterized time-dependence in the basic flow.

7.3 TOPOGRAPHIC INFLUENCES IN ATMOSPHERIC FLOWS

S. Garner *I. Orlanski*
B. Gross

ACTIVITIES FY98

7.3.1 Interaction of Fronts and Orography

The recently developed nonhydrostatic Zeta model (7.4.2) has been used to answer important questions related to the poor performance of current hydrostatic models in simulating the atmospheric circulation in the presence of orography. A series of experiments has been performed to assess a) the impact of small-scale terrain features, and b) the validity of the hydrostatic approximation in frontal passage over steep orography.

A control nonhydrostatic experiment with 10 km resolution has been used to simulate the passage of an idealized three-dimensional cold front, associated with a developing cyclone, over a smooth elongated mountain ridge with a half-width of 60 km and a height of 1500 m. The front is initially blocked by the ridge, but the cold postfrontal air eventually piles up to such a degree on the windward slope that it spills over the ridge top and flow down the lee slope as a gravity current. Lifting at the head of this gravity current in dramatically enhanced by a large-amplitude mountain wave, which then breaks backwards as a large horizontal roll oriented along the front. Hydrostatic simulations of this event are virtually identical to nonhydrostatic ones, as expected with these slopes.

The addition of random, small-scale (10 km) terrain features to the profile of the smooth ridge significantly delays the passage of the front into the lee, as indicated in Fig. 7.2 by the warm (red) potential temperature anomalies present along the entire length of the front leeward of the ridge. The most intense warm anomalies are located in the lee of the peaks, where the cold postfrontal air has failed to penetrate, but only weak anomalies appear directly downstream of the valleys. One possible explanation is that the front is blocked by the small-scale peaks, but is relatively unaffected by the small-scale valleys. It should be noted that the front would be completely blocked by this terrain if the valleys were filled (a technique analogous to using "envelope" orography). Another noteworthy feature is the acceleration of the front around the ends of the ridge with rough topography, indicated by the cold (blue) anomalies south of the ridge ends. Because the rough ridge blocks the front more than the smooth ridge, higher pressure builds on the windward slope, forcing faster flow around the ridge ends. Although further investigation is required to clarify the role of the small-scale terrain in such flows, these comparisons can be used to compare and verify various gravity-wave drag parameterizations required in coarser resolution simulations.

7.3.2 Gravity Wave Parameterizations over the Rockies

A combination of high-resolution numerical and analytical models have been used to test the feasibility of a proposed parameterization of total mountain drag due to unresolved terrain. The parameterization assumes steady, linear gravity waves and gradual horizontal variations of the basic flow. Given the low-level buoyancy frequency and topography, it yields a map of horizontal divergence due to the terrain. The total drag on the atmosphere can then be obtained by multiplying the divergent velocity by the vertical velocity due to the resolved horizontal surface wind.

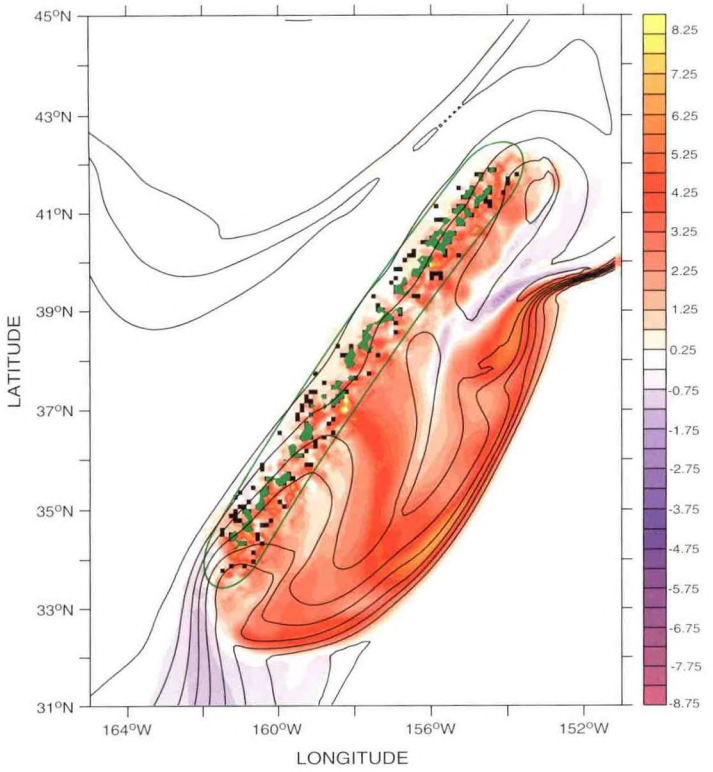

Fig. 7.2 Surface potential temperature in the solution with smooth topography (black contours, every 2°K) and the difference in the surface potential temperature (shaded °K) between the rough and the smooth solutions. The 500 m topography contour and small-scale topography higher than 1500 m are in green. Reddish shades indicate that the front in the solution with rough topography is delayed relative to that with the smooth ridge. The cold postfrontal air has difficulty penetrating into the lee of the small-scale peaks.

To avoid restrictions on the vertical structure of the atmosphere, the fully compressible ZETA model is used to generate comparable coarse- and fine-grain solutions for the same mountain range and same large-scale flow. The coarse-resolution experiments are conducted with so-called "silhouette" topography, which retains the maximum height of the terrain despite losing horizontal resolution. For summertime flow conditions, the fine-resolution runs indicate that most of the momentum flux reaching the stratosphere is due to linear, hydrostatic gravity waves launched by the smallest resolved terrain features. For the Rocky Mountains, this means primarily the upstream and downstream edges of the massif. The parameterized subgrid drag and divergent surface velocity from the coarse run are in good agreement with the high-resolution result, as shown in Fig. 7.3.

PLANS FY99

The physical mechanisms that cause delayed frontal propagation across a ridge with small-scale terrain features will be further investigated. Clarifying these mechanisms will aid in the continuing refinement of new gravity wave drag parameterizations. The linear model of total mountain drag will be tested within GCMs and by model simulations with very high resolutions and realistic temporal and spatial variations of the basic flow. The high-resolution simulations will also be used to assess the role of nonhydrostatic motion in orographic flows.

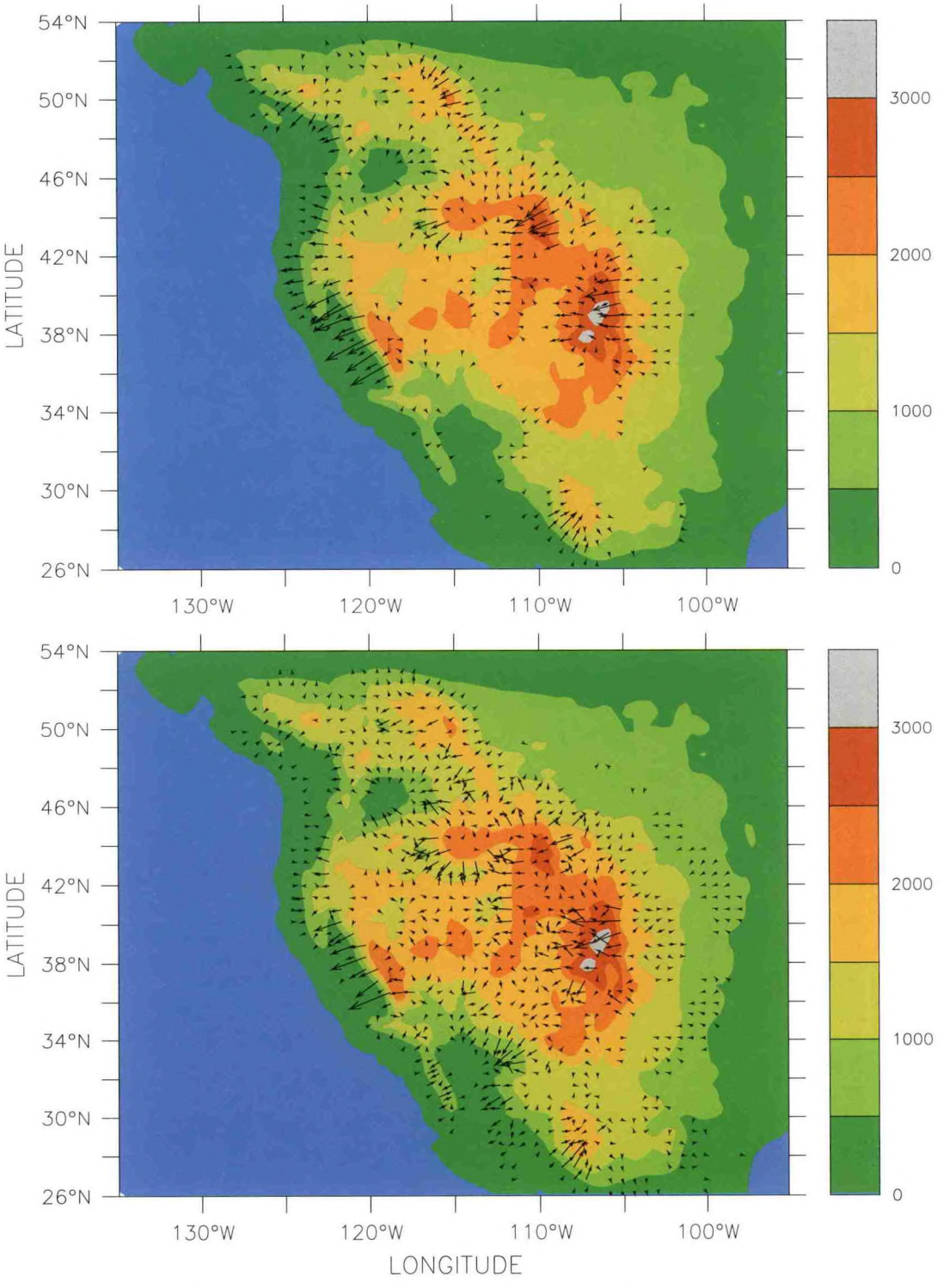

Fig. 7.3 Total topographic drag exerted on the atmosphere by the Rocky Mountains according to numerical model solutions for typical summertime flow conditions. Top: linear parameterization (7.3.2) of unresolved drag calculated for a coarse-resolution (120 km) numerical solution. Bottom: Explicit drag diagnosed from fine-resolution numerical solution (40 km). Topographic heights (in meters) are indicated by color shading. The parameterization appears to successfully capture the regions of significant drag over the Rocky Mountains.

7.4 MODEL DEVELOPMENT

S. Garner *I. Orlanski*
B. Gross *L. Polinsky*

ACTIVITIES FY98

7.4.1 Improvements to the Hydrostatic Zeta Model

In the current version of the hydrostatic ZETA model, the Boussinesq approximation is replaced by the anelastic approximation to account for more realistic atmospheric density profiles, and is expressed in spherical coordinates to more accurately simulate large-scale and synoptic-scale dynamics (7.2.1). This model can now run on Cray, SGI, and Sun platforms. This hydrostatic model was also used extensively in the ICTP (International Center for Theoretical Physics, Trieste, Italy) Summer Colloquium on the Physics of Weather and Climate entitled "The Effect of Topography on the Atmospheric Circulation". One outgrowth of this development is that the ZETA model is being used at a number of sites worldwide for investigating a wide variety of atmospheric flows.

7.4.2 Improvements to the Nonhydrostatic Compressible Zeta Model

The nonhydrostatic, fully compressible version of the hydrostatic Zeta model has been used to evaluate nonhydrostatic and terrain effects in mesoscale atmospheric circulations (7.3.1) and for developing physical parameterizations (7.3.2). The model currently runs on the Cray T90 and SGI workstations available at GFDL, and the code is currently being adapted to scalable architectures such as the Cray T3E.

In order to investigate a new gravity-wave drag parameterization (7.3.2), a radiative upper boundary condition, designed to make the upper boundary transparent to upward propagating internal gravity waves, has been added to the compressible ZETA model. This scheme treats linear, hydrostatic, non-rotating waves exactly in the case of Cartesian geometry and horizontally uniform background wind and static stability at the boundary. Some compensation for sphericity is incorporated by using geodesic distances to measure the influence from neighboring points on the latitude-longitude grid. The impact of planetary scales is objectively filtered for the sake of consistency. An option for open lateral boundaries has been added using a standard scheme which explicitly estimates the phase speed of waves leaving the domain.

PLANS FY99

Continuing idealized storm track simulations with the spherical-coordinate models should clarify the most important processes in the development, maintenance, and decay of these storm tracks. Sensitivity studies will be undertaken to clarify the features most important to cyclone evolution within them. Moist processes and boundary layer physics will continue to be incorporated into both the hydrostatic and nonhydrostatic Zeta models. The application of the ZETA vertical coordinate in a variety of numerical models is being pursued, as are efforts at parallelizing these codes.

8. TECHNICAL SUPPORT

GOALS

Provide a computational facility to support research conducted at GFDL with emphasis on supercomputing and networked desktop systems for developing, running, and analyzing results from numerical models.

Provide software tools for managing, manipulating, and visualizing large amounts of multi-dimensional data.

Maintain systems which provide documentation and time-sensitive information to users, create products for presentation and publication, and communicate GFDL's accomplishments to other agencies and to the public.

During FY98, a new Technical Support Group was created to consolidate most of the activities related to computerized functions throughout the Laboratory. First and foremost among these is the supercomputer center, housing two Cray T90's, a Cray T3E, and 240 terabytes of tape storage inhabiting 2 StorageTek silos. These large systems are tightly networked with a variety of desktop workstations and servers connected via a high-speed Ethernet network. The combined systems are administered by the Computer Systems Group, a subgroup within the Technical Support Group.

In addition to maintaining the computer hardware used for carrying out state-of-the-art numerical modeling of the atmosphere and ocean, the Technical Support Group provides the necessary software tools and personal assistance for managing the storage, manipulation, and visualization of the vast amounts of data such experiments generate.

The results of the Laboratory's research are generally disseminated via peer-reviewed journals, scientific conferences and briefings, and the Internet. The Technical Support Group provides assistance, through the Scientific Illustration Group, with the creation of visual materials for these products, as well as the preparation of digital documents for electronic publishing and submission to outside publishing organizations. Support is also provided for the creation of videotape presentations and digital media for communication via the world-wide-web, including web pages, images, animation sequences, and data interchange. Lastly, GFDL's information infrastructure includes a variety of digital and traditional library services.

8.1 COMPUTER SYSTEMS

T. Knutson *T. Taylor*
L. Lewis *R. White*
B. Ross *W. Yeager*
J. Sheldon

ACTIVITIES FY98

The Laboratory's main production system is a Cray T932 with 26 central processors, 512 megawords (MW) of central memory, 4 gigawords (GW) of solid state disk, 447 gigabytes (GB) of rotating disk storage, and 2 StorageTek silos with a tape capacity of up to 240 terabytes (TB). The reliability of this system degraded substantially following the February 1997 upgrade. System availability during the period from September through December 1997 was particularly poor but has improved since that time. A serious side-effect of the instability of the T932 is that workstation access to the multi-terabyte data archive is not possible when the T932 is down. Another area of concern has been the increased amount of input/output (I/O) wait time that has been observed on the T932 since the upgrade and particularly during early FY98. This increased system inefficiency has lead to a significant reduction in the number of usable CPU hours available for GFDL applications, even when system availability is relatively high.

GFDL staff worked with Cray Research personnel to address both the hardware reliability and the I/O wait time problems. Cray has devoted significant resources to improving the reliability of its large-chassis T90 hardware and some progress has been made. The I/O wait time problem received considerable attention, both from GFDL and on-site Cray personnel. While no definitive solution has been identified, several changes that were implemented have improved system efficiency by several percent.

In response to the poor system reliability, an engineering change to the final contract upgrade originally scheduled to occur by October 1998 was negotiated. Rather than installing 4-6 additional T932 processors, a separate T94 system was installed in August 1998. The T94 functions as the primary data server for the archive storage system. The new system, which is expected to be much more reliable than the T932, should provide increased stability to the GFDL computing environment by offering more reliable access to the data archive and serving as an effective interactive and analysis platform that should reduce the I/O workload on the T932. The T94 has 4 central processors, 128 MW of central memory, 512 MW of solid state disk, and 760 GB of rotating disk storage. A high-speed channel directly connects the T932 and T94.

The Laboratory's third high-performance computer system is a scalable 40-processor Cray T3E-900 system with 128 MB of local memory per processor, 148 GB of rotating disk storage, and high-speed channels that directly connect it to the T932 and T94. The T3E is an important development platform for redesigning GFDL models to a scalable architecture paradigm. The system has demonstrated outstanding reliability throughout the year and has provided significant production capability for several experiments.

During the past year, there were significant episodes of data loss from the GFDL archive. GFDL staff worked with StorageTek and Cray Research personnel to identify the

causes and to resolve the problems. StorageTek demonstrated that most of the problems were caused by faulty tape media and replaced all of the defective tape cartridges. Both companies made great efforts to recover data from faulty tapes. StorageTek also made design improvements in the tape drives and modified its maintenance procedures.

Table 8.1 shows the number of T932 and T3E user processor hours for each month and the accumulative amount of total archive data in trillions of bytes.

Table 8.1 Cray T932 and T3E User Processor Time and Total Archive Data

Month	T90 Hours	T3E Hours	Terabytes
Oct 97	14,330	15,717	31.4
Nov 97	15,986	15,045	33.8
Dec 97	14,954	19,012	36.2
Jan 98	17,619	21,898	38.4
Feb 98	14,382	18,732	40.0
Mar 98	17,397	21,192	42.2
Apr 98	17,076	20,252	44.7
May 98	15,967	20,416	46.2
Jun 98	16,850	20,623	48.0
Jul 98	16,627	21,829	48.7
Aug 98	15,181	23,089	50.2
Sep 98	15,738	21,006	51.9

In order to address the unprecedented increase in demand for GFDL research products and to take advantage of major new opportunities in climate and weather research, GFDL has submitted a budget initiative under the NOAA High Performance Computing and Communications (HPCC) Program to acquire a new enhanced system in FY2000 to replace the current GFDL computer system. Proposed is a comprehensive scalable computing system, including very large computing and storage capacities and the balanced analysis, visualization, and technical support required to make the most effective use of the available technology. This system would build on GFDL's impressive track record for leveraging its computational resources to reduce uncertainties in global warming projections, improve seasonal/interannual prediction capabilities, and improve hurricane track and other forecast products. A benefit/cost analysis and supporting IT architecture plan were submitted to NOAA, the Department of Commerce, and OMB as part of the FY2000 budget planning process. Activities associated with this procurement are proceeding, including an evaluation of the industry and the development of benchmarks and requirement specifications.

In addition to the three Cray systems, GFDL's computer facility includes three Silicon Graphics (SGI) servers, three Sun Microsystems servers, and a variety of text and graphics printers, one of which is a newly purchased Tektronix Phaser 560 color laser printer which will

provide improved quality (especially for publications) at reduced operating cost. Distributed throughout GFDL are 115 desktop workstations including 22 SGI Indigo2 R4400XZs (3 of which are refurbished machines purchased this year), 34 SGI Indigo R4000XZs, 10 SGI 4D/35s, 35 SGI 4D/25s, 5 Sun SPARCstation-1s, and 9 Sun 3/50s. The workstations are interconnected by eight Ethernet segments and a Network Systems Corporation (NSC) router. The servers, T932, T94, and T3E are interconnected by a Fiber Distributed Data Interface (FDDI) network which connects to the Ethernet network through the NSC router.

One of the Indigo2 workstations has been configured with extra memory and disk, and is connected directly to the FDDI network. This platform is being operated as a prototype "compute server", primarily to assess the potential utility to users of a platform with resources exceeding those afforded by their desktop workstation. Though this platform is still a single-CPU machine with no more processing speed than other Indigo2 desktops, it has received moderate to heavy use from scientists with less powerful desktops (and from some with Indigo2's of their own), indicating that a shared, powerful resource could provide valuable complementary capabilities to the desktop environment.

In order to provide improved throughput to each workstation, an upgrade of the shared 10 megabit/second (mbps) Ethernet network was begun in August 1998. The new network will be switched 10/100 mbps Fast Ethernet to each workstation with a 2000 mbps full-duplex Gigabit Ethernet backbone. The existing FDDI network will be connected to the new network.

During December 1997 the computer facility underwent a security assessment conducted by the National Security Agency at NOAA's request. The purpose of the assessment was to determine if adequate measures were in place to protect NOAA information and services from internal and external intrusion and to recommend measures to reduce or eliminate potential vulnerabilities. The final report commended GFDL on its information systems security posture and made several recommendations for improvement.

PLANS FY99

Most interactive sessions, analysis programs, and data-intensive tasks will be moved to the new T94 system, leaving the T932 primarily for running production models. This new operating strategy will continue to be refined during the year. The UNICOS operating system on the T932 will be upgraded to the same version running on the T94.

The network upgrade will be completed by November 1998. Network interface cards will be purchased for the SGI Indigo and Indigo2 workstations, improving their network throughput to 100 mbps. The GFDL administrative network will be upgraded and converted from Banyan Vines to Windows NT. A major upgrade of SGI operating system software will be installed on Indigo and Indigo2 workstations, making it possible to upgrade to newer and more powerful versions of several software applications and compilers. Replacement of the older Sun servers will be investigated. Pending availability of funds, older workstations will continue to be replaced with more advanced SGI graphics workstations. Candidate systems which might operate as a shared compute server/graphics workstation will be assessed.

The procurement process for the next high-performance computer system will proceed with a Request for Information (RFI) to vendors, development of the requirements document, formation of the procurement team, and preparation of a Statement of Need and benchmark codes. In view of the fact that the computer system that replaces the T932 will rely heavily on parallelism to produce acceptable performance, the Laboratory will accelerate the development of parallel versions of the major models and support applications to run in parallel on the T90 systems and the scalable T3E.

Because of their dramatically reduced operating cost, additional Tektronix Phaser 560 printers will replace the existing Calcomp printers, paying for themselves in approximately 18 months. Also, possible upgrades to GFDL's aging video-production station will be investigated.

8.2 DATA MANAGEMENT

V. Balaji *H. Vahlenkamp*
J. Sheldon

ACTIVITIES FY98

Virtually all of the principal models at GFDL now output data in Unidata's Network Common Data Format (netCDF). The benefits of using netCDF are manifold, chief among them the inherent benefit of having all of one's data in self-documented files that are readily interchangeable with other researchers. It also makes possible the use of many off-the-shelf data manipulation and visualization utilities, saving the development costs which had heretofore consumed much manpower. An in-house library of netCDF interface routines (NCIR) simplifies the creation of netCDF files, from the users standpoint. The latest release of the NCIR library was delayed somewhat, but is expected relatively soon, with the benefit of several additional features which address specific user needs.

Tests conducted with netCDF version 3.4 on the Cray T932 show approximately a 40% speedup for writes and a 15% speedup for reads, compared to netCDF release 2.4.2. Relative to the I/O speed of raw IEEE, netCDF 3.4 is about 10% faster for writes and about 40% slower for reads, though the latter figure is somewhat deceptive because both netCDF and IEEE reads are very fast (2-3 times faster than writes). NetCDF 3.4 will become the default version at GFDL shortly.

A collaborative project with the National Energy Research Scientific Computing Center (NERSC) has been initiated, with one goal being the development of a parallel I/O capability for netCDF on the Cray T3E. This will build on a special purpose library written for an earlier release of netCDF, but will use the latest parallel I/O tools available from Cray.

Over the past 6-7 years, many GFDL researchers stored their data in "GrADS" format, which is a flat binary file with an accompanying descriptor file. "GrADS" is a data manipulation and mapping tool that became popular because it was very easy to learn, which was a major consideration many years ago when the only other alternative was to custom code a plotting program. Since then, however, a variety of very useful off-the-shelf packages have become available, providing one's data is stored in netCDF. Rather than strand the rather sizable legacy of GrADS-formatted data, which is readable by very limited number of visualization packages

(*i.e.*, two), a utility has been written which converts GrADS-formatted data to netCDF. This will provide users with access to visualization capabilities such as 3-dimensional rendering, rapid data browsing, and other tools.

GFDL continues to participate in the development of conventions for storing netCDF data. While netCDF files are self-documenting and portable, there remains a need for agreement regarding exactly what documentary information is included in the file. GFDL currently adheres to the COARDS conventions, but is interacting with other researchers at the Hadley Centre and Lawrence Livermore National Laboratory to expand the COARDS conventions to accommodate more complex types of data (*e.g.*, averages) and handle the surprisingly complicated issue of calendar time.

PLANS FY99

GFDL will upgrade to netCDF 3.4, in concert with the release of a new version of the local NCIR library. The collaboration with NERSC is expected to continue, with testing on the GFDL and NERSC T3E's using the MOM3 ocean code. Additional netCDF file manipulation utilities will be developed as needed, and users will receive assistance when writing their own netCDF codes.

8.3 DATA VISUALIZATION

J. Sheldon *R. White*
H. Vahlenkamp

ACTIVITIES FY98

A relatively small number of changes were made to GFDL's suite of visualization tools, with the exception of GFDL's library of Explorer modules. The latest release of the modules represents a sizable expansion of the library's capabilities. Some of the most significant upgrades are listed below:

- A "special value" capability has been added to many modules, enabling them to handle fields with regions of missing data (*e.g.*, land points in an ocean temperature field).
- Map projections and multiple independent paths have been added to the particle trajectory display module.
- An external viewing window, disk buffering, and memory/speed optimization options were added to the module which animates images.
- Many new modules were added for manipulating pyramid data, displaying text and histogram-like bars, managing color palettes, and displaying particles.

These improvements were bundled into a new library and released to the Explorer user community via NAG's Iris Explorer Center. GFDL is, by far, the single largest contributor of modules to the Explorer repository, providing a valuable resource to the scientific visualization community.

A highly leveraged GFDL visualization activity in FY98 was the creation of an animation for the White House Conference on Climate Change at Georgetown University in October 1997. This animation illustrated the changes in surface air temperature that are expected to result from increasing levels of atmospheric carbon dioxide. The animation is available via the GFDL web page at "http://www.gfdl.gov/~gth/web_page/news.html".

PLANS FY99

An effort will be made to further exploit the very powerful Iris Explorer visualization package. This will entail a series of hands-on sessions with interested users, plus the development of some template modules that will facilitate the incorporation of user-developed subroutines as Explorer modules. New version of current packages will be obtained, tested, and installed. New packages will be examined as they become available, notably the new NCAR DataVision package.

8.4 INFORMATION AND PRESENTATION RESOURCES

G. Haller *H. Vahlenkamp*
C. Raphael *J. Varanyak*
J. Sheldon *R. White*
T. Taylor

ACTIVITIES FY98

Because the Macintosh platform is still the industry standard for graphic arts and document layout work, GFDL uses a MacIntosh computer to prepare digital graphics and documents for export to publishers, and for some internal purposes. The older PowerMac 7200 was replaced with a new PowerMac G3, providing a much needed increment in processing power. At the same time, the programs used to prepare documents and artwork were upgraded to the latest versions, so that this combined system is now up-to-date. While all of these together represent a very minor dollar expenditure, they comprise a critical resource needed for effectively relating the results of the laboratory's research to colleagues, other government agencies, and the public. The technical procedures for carrying out the necessary processing have been better defined and are in the process of being posted on-line for users who prefer to prepare their own artwork and documents, instead of relying on the Illustration Group.

GFDL's home page (http://www.gfdl.gov) has been upgraded to a more modern layout and to a form that downloads faster, both of which are important in getting GFDL's and NOAA's messages out to the public. In addition, both the formal seminars and the lunchtime seminar series are now posted on-line, providing a very useful information source for both GFDL and outside scientists wishing to participate in the exchange of the most up-to-the-minute research results.

The GFDL library manages on-line information services that target external as well as internal users. The library manages the electronic posting of the schedules for seminars and meetings held at GFDL. The on-line bibliography listing GFDL professional papers and abstracts from 1965 to present day has been updated. Users can access library holdings, new

acquisitions, and serial holdings from their workstations. The addition of on-line journals services and abstracting services aid GFDL researchers in obtaining information quickly.

PLANS FY99

A project will be initiated to merge the current "GFDL Computer Users Guide" with the independently developed "Scientific Visualization Guide" to the extent possible given that the former is strictly an internal document while the latter is intended to be useful to the entire visualization community.

Another project to be launched in the coming year is the development of a "Virtual Help Desk". Given a set of search terms, this web-based utility will perform searches through the various sources of information within the Laboratory (man pages, GFDL's "info" database, user guides, etc.) and return a set of prioritized "matches" that will address user questions.

8.5 PUBLIC INFORMATION DISSEMINATION

M. Crane *B. Ross*
G. Haller *J. Sheldon*
J.D. Mahlman *H. Vahlenkamp*

ACTIVITIES FY98

Fiscal year 1998 saw an unprecedented number of headlines related to science and technology issues. The successful prediction of a strong El Niño Event and the historic Kyoto Protocol on Climate Change served to focus global attention on two key areas of research conducted at GFDL. These headlines make clear the ever growing need for the dissemination of accurate and understandable scientific information to an expanding audience. Effort to meet this need has been directed toward increased media relations, educational enterprises, community relations, and continued enhancement of GFDL's web site. Some of the most significant activities are listed below:

- In October, movie clips showing surface temperature warming from the NOAA/GFDL climate model for projected doubling and quadrupling of atmospheric CO_2 were presented at the "White House Conference on Climate Change: The Challenge of Global Warming".
- Several GFDL color figures were placed on the White House web site under subtopic, "White House Conference on Climate Change: The Challenge of Global Warming".
- In November, Jerry Mahlman provided an evaluation of "Uncertainties in Projections of Human-Caused Climate Warming" in an invited SCIENCE article to assist in the worldwide preparation for the December Kyoto Protocol on Climate Change.
- In the months preceding and following the December Kyoto Conference, Jerry Mahlman provided numerous television and print interviews on the science of global warming. Especially significant were the interviews that led to educational articles with major media coverage. They include: The Washington Post, The New York Times, USA Today, The Philadelphia Inquirer, The Baltimore Sun, The Arizona Republic, The Christian Science Monitor, The Huntsville Times, National Geographic, Newsweek,

Environmental Media Services, National Public Radio, ABC Discovery Channel Live, and Discovery Channel Online.

- In March, a scientific colloquium was held to honor the remarkable climate achievements of Syukuro Manabe upon the occasion of his retirement from GFDL. The symposium, entitled "Understanding Climate Change" brought together many of the world's leading climate researchers. Reporters from several regional newspapers as well as The New York Times were in attendance. Numerous media articles resulted.
- The feature story in the May issue of National Geographic Magazine, entitled "Unlocking the Climate Puzzle", was made possible through close collaboration with GFDL scientists and also contains many illustrative GFDL graphical products describing climate change.
- In July, GFDL hosted The National Leadership Program for Teacher's Workshop. GFDL scientists presented teachers ranging from middle to high school level with the concepts of global warming and the mechanics of how this research is conducted at GFDL. With the continued guidance of GFDL scientists, the teachers then incorporated this information into the development of web sites designed to teach the concepts of global warming at various grade levels.
- In August, LIFE Magazine's cover feature story, entitled "Weather: What You Can Do About It" was partly made possible by contributions from GFDL.
- Over 100 outside seminars and lectures were presented to a wide variety of audiences by GFDL scientists in FY98. Of special note were 16 presentations on the science of global warming, four on ozone change, six on seasonal-interannual (El Niño) prediction, and nine on the GFDL hurricane prediction model (now the operational system at NOAA/NCEP and the U.S. Navy). The most active GFDL speakers on these informational topics were Jerry Mahlman, Hiram Levy II, Jeffrey Anderson, and Yoshio Kurihara.
- Numerous GFDL scientists volunteered to participate in educational outreach at schools (elementary school level to college), and with community groups throughout the year. These activities included classroom presentations, mentorships and tours of GFDL.
- Effort has been increased to alert the media of significant events and research results at GFDL, including advances in hurricane prediction, and the understanding of global climate change.
- A new educational page has been added to GFDL's web site. This page provides basic background material on the science of weather and climate (see http://www.gfdl.gov/Science_facts.html). In addition to GFDL research, this page provides links to a wide variety of sites with facts about climate change, hurricanes, El Niño, and other topics of interest to the public.

APPENDIX A

GFDL STAFF MEMBERS

and

AFFILIATED PERSONNEL

during

Fiscal Year 1998

PERSONNEL SUMMARY

September 30, 1998

GFDL/NOAA	
Full Time Permanent (FTP)	81
Part Time Permanent (PTP)	1
Part Time Temporary (PTT)	1
PRINCETON UNIVERSITY (PU)	
AOS Visiting Scientists	13
Graduate Students	8
Professors	3
Research Scholar	1
Senior Research Scholar	1
Research Scientists	1
Research Staff	6
Support Staff	3
Technical Staff	6
Visiting Senior Research Scientist	1
OTHER INSTITUTIONS	
U.S. Geological Survey (USGS)	2
University Corporation for Atmospheric Research (UCAR)	2
Massachusetts Institute of Technology (M.I.T.)	2
VENDORS	
Cray Research Inc. Computer Support Staff	4
IBM Research Staff	1
TOTAL	**137**

CLIMATE DYNAMICS

Held, Isaac M.	Senior Scientist at GFDL	FTP
Broccoli, Anthony J.	Meteorologist	FTP
Jackson, Charles	AOS Visiting Scientist	PU
Delworth, Thomas L.	Meteorologist	FTP
Dixon, Keith W.	Meteorologist	FTP
Emanuel, Kerry	Scientific Visitor	MIT
Hall, Alexander	Graduate Student	PU*
Hayashi, Yoshikazu	Meteorologist	FTP
Golder, Donald G.	Meteorologist	FTP
Knutson, Thomas R.	Meteorologist	FTP
Kushner, Paul	Physical Scientist	FTP
Milly, P.C.D.	Hydrologist	USGS**
Dunne, Krista	Physical Scientist	USGS**
Shmakin, Andrey	Scientific Visitor	UCAR
Pauluis, Olivier	Graduate Student	PU
Phillipps, Peter J.	Meteorologist	FTP
Schneider, Tapio	Graduate Student	PU
Stouffer, Ronald J.	Meteorologist	FTP
Spelman, Michael J.	Meteorologist	FTP
Vallis, Geoff	Senior Research Scholar	PU
Wetherald, Richard T.	Meteorologist	FTP
Williams, Gareth P.	Meteorologist	FTP
Zhang, Zhojun	AOS Visiting Scientist	PU*

*Affiliation terminated prior to September 30, 1998.
**United States Geological Survey (USGS), on detail to GFDL.

ATMOSPHERIC PROCESSES

Ramaswamy, V.	Physical Scientist	FTP
Cooke, William	AOS Visiting Scientist	PU
Donner, Leo J.	Physical Scientist	FTP
Andronache, Constantin	AOS Visiting Scientist	PU
Seman, Charles J.	Physical Scientist	FTP
Erlick, Carynelisa	AOS Visiting Scientist	PU
Freidenreich, Stuart	Meteorologist	FTP
Hamilton, Kevin P.	Meteorologist	FTP
Wilson, R. John	Meteorologist	FTP
Haywood, James	AOS Visiting Scientist	PU*
Hemler, Richard S.	Meteorologist	FTP
Klein, Steven	Meteorologist	FTP
Levy II, Hiram	Physical Scientist	FTP
Holloway, Teresa	Graduate Student	PU
Klonecki, Andrzej	Graduate Student	PU*
Moxim, Walter J.	Meteorologist	FTP
Wang, Sheng-Wei	AOS Visiting Scientist	PU
Perliski, Lori	Physical Scientist	FTP*
Ramachandran, S.	AOS Visiting Scientist	PU
Schwarzkopf, M. Daniel	Meteorologist	FTP

EXPERIMENTAL PREDICTION

Anderson, Jeffrey L.	Meteorologist	FTP
Gordon, C. Tony	Meteorologist	FTP
Griffies, Stephen M.	Physical Scientist	FTP
Ploshay, Jeffrey J.	Meteorologist	FTP
Rosati, Anthony J.	Physical Scientist	FTP
Gudgel, Richard G.	Meteorologist	FTP
Harrison, Matthew	Physical Scientist	FTP
Sirutis, Joseph J.	Meteorologist	FTP
Stern, William F.	Meteorologist	FTP
Smith, Robert G.	Computer Assistant	FTP
Vitart, Frederic	Graduate Student	PU
Wittenberg, Andrew	Graduate Student	PU
Wyman, Bruce L.	Meteorologist	FTP
Yang, Xiu-Qin	AOS Visiting Scientist	PU

*Affiliation terminated prior to September 30, 1998.

OCEANIC CIRCULATION

Toggweiler, J. R.	Oceanographer	FTP
Carson, Steven R.	Physical Scientist	FTP
Hallberg, Robert	Oceanographer	FTP
Hurlin, William J.	Meteorologist	FTP
Pacanowski, Ronald C.	Oceanographer	FTP
Samuels, Bonita L.	Oceanographer	FTP
Tziperman, Eli	AOS Visiting Scientist	PU
Winton, Michael	Oceanographer	FTP

CLIMATE DIAGNOSTICS

Lau, Ngar-Cheung	Meteorologist	FTP
Crane, Mark	Meteorologist	FTP
Lanzante, John	Meteorologist	FTP
Nath, Mary Jo	Meteorologist	FTP
Soden, Brian J.	Physical Scientist	FTP

HURRICANE DYNAMICS

Kurihara, Yoshio	Meteorologist	FTP
Bender, Morris A.	Meteorologist	FTP
Tuleya, Robert E.	Meteorologist	FTP
Zhang, Yunqing	Scientific Visitor	MIT

MESOSCALE DYNAMICS

Orlanski, Isidoro	Meteorologist	FTP
Garner, Stephen	Meteorologist	FTP
Gross, Brian	Physical Scientist	FTP
Polinsky, Larry	Meteorologist	FTP

MANAGEMENT FRAMEWORK

Administrative and Technical Structure

Mahlman, Jerry D.	Director	FTP
Ross, Bruce B.	Assistant Director	FTP
Balaji, V.	Applications Analyst	CRI
Byrne, James S.	Junior Technician	FTP
Kerr, Christopher L.	Scientific Visitor	IBM**
Marshall, Wendy H.	Secretary	FTP
Pege, Joan M.	Management Analyst	FTP
Shearn, William F.	Leader, COMPUTER OPERATIONS	FTP
Sheldon, John	Leader, TECHNICAL SUPPORT	FTP
Urbani, Elaine B.	Transportation Assistant	FTP
Uveges, Frank J.	Supervisory Computer Specialist	FTP*
Williams, Betty M.	Secretary	FTP

Scientific Structure

Mahlman, Jerry D.	Director	FTP
Anderson, Jeffrey L.	Leader, EXERIMENTAL PREDICTION	FTP
Held, Isaac M.	Leader, CLIMATE DYNAMICS	FTP
Kurihara, Yoshio	Leader, HURRICANE DYNAMICS	FTP
Lau, Ngar-Cheung	Leader, CLIMATE DIAGNOSTICS	FTP
Orlanski, Isidoro	Leader, MESOSCALE DYNAMICS	FTP
Ramaswamy, V.	Leader, ATMOSPHERIC PROCESSES	FTP
Toggweiler, J. R.	Leader, OCEANIC CIRCULATION	FTP

*Affiliation terminated prior to September 30, 1998.
**International Business Machines, on detail to GFDL.

TECHNICAL SUPPORT

Sheldon, John	Graphics Specialist/Meteorologist	FTP
Haller, Gail T.	Computer Assistant	FTP
Amend, Beatrice E.	Office Automation Clerk	PTT
Lewis, Lawrence J.	Computer Specialist	FTP
Rao, Ramesh	Applications Analyst	CRI*
Taylor III, Thomas E.	Computer Specialist	FTP
White, Robert K.	Computer Specialist	FTP
Yeager, William T.	Computer Specialist	FTP
Raphael, Catherine	Scientific Illustrator	PTP
Vahlenkamp, Hans	Scientific Visitor	UCAR
Varanyak, Jeffrey	Scientific Illustrator	FTP

COMPUTER OPERATIONS SUPPORT

Shearn, William F.	Operations Manager	FTP
Hopps, Frank K.	Supervisory Computer Operator	FTP
King, John T.	Lead Computer Operator	FTP
Duggins, Marsha	Computer Operator	FTP
Harrold, Renee M.	Computer Operator	FTP
Hand, Joseph S.	Supervisory Computer Operator	FTP
Cordwell, Clara L.	Lead Computer Operator	FTP
Ledden, Jay H.	Computer Operator	FTP
Lim, Jennifer J.	Computer Operator	PTP*
Yacovelli, Deborah	Peripheral Equipment Operator	FTP
Deuringer, James A.	Supervisory Computer Operator	FTP
Blakemore, Geneve	Computer Operator	FTP
Krueger, Scott R.	Lead Computer Operator	FTP
Mills, Tania	Computer Operator	FTP*
Henne, Ronald N.	Computer Assistant	FTP

*Affiliation terminated prior to September 30, 1998.

CRAY RESEARCH INCORPORATED

Siebers, Bernard	Analyst in Charge	CRI
Braunstein, Mark	Field Engineer	CRI
Balaji, V.	Applications Analyst	CRI
Rao, Ramesh	Applications Analyst	CRI*
Weiss, Ed	Engineer in Charge	CRI

*Affiliation terminated prior to September 30, 1998.

ATMOSPHERIC AND OCEANIC SCIENCES PROGRAM

Philander, S.G.H.	Professor, Program Director	PU
Bryan, Kirk	Visiting Senior Research Scientist	PU
Park, Young	AOS Visiting Scientist	PU
Callan, Johann V.	Technical Research Secretary	PU
Federov, Alexey	AOS Visiting Scientist	PU
Harper, Scott	Graduate Student	PU
Rossi, Laura	Program Manager	PU
Valerio, Anna	Technical Research Secretary	PU
Winter, Barbara	Technical Staff	PU
Mellor, George	Professor Emeritus	PU
Ezer, Tal	Research Staff	PU
Kim, Namsoug	Technical Staff	PU
Lee, Hyun-Chul	AOS Visiting Scienitst	PU
Oey, Lie-Yauw	Research Scholar	PU
Sarmiento, Jorge	Professor	PU
Armstrong, Robert	Research Staff	PU
Baker, David F.	Graduate Student	PU
Deutsch, Curtis	Graduate Student	PU
Fan, Song-Miao	Research Staff	PU
Gloor, Manuel	AOS Visiting Scientist	PU
Gnanadesikan, Anand	Research Staff	PU
Gruber, Nicholas	Research Staff	PU
Hughes, Tertia	Technical Staff	PU
Key, Robert M.	Research Scientist	PU
McDonald, Gerard	Technical Staff	PU
Rotter, Richard	Technical Staff	PU
Sabine, Christopher L.	Research Staff	PU
Slater, Richard D.	Technical Staff	PU
Yamanaka, Yasuhiro	AOS Visiting Scientist	PU

APPENDIX B

GFDL

BIBLIOGRAPHY

1995-1998

GFDL PUBLICATIONS

This is a partial listing of GFDL publications. A copy of the complete bibliography can be obtained by calling (609) 452-6502, or by writing to:

Director
Geophysical Fluid Dynamics Laboratory
Post Office Box 308
Princeton, New Jersey 08542

PUBLICATIONS PRIOR TO 1995 CITED IN THIS REPORT

(599) Oort, Abraham, *Global Atmospheric Circulation Statistics, 1958-1973*, NOAA Professional Paper No. 14, U.S. Printing Office, Washington, DC, 180 pp., 1983.

(885) Lipps, F.B., and R.S. Hemler, Numerical Modelling of a Line of Towering Cumulus on Day 226 of GATE, *Journal of the Atmospheric Sciences, 45(17)*, 2428-2444, 1988.

(1053) Orlanski, I., and J. Katzfey, The Life Cycle of a Cyclone Wave in the Southern Hemisphere, Part I: Eddy Energy Budget, *Journal of the Atmospheric Sciences, 48(17)*, 1972-1998, 1991.

* (1125) Chang, E.K.M., and I. Orlanski, On the Dynamics of a Storm Track, *Journal of the Atmospheric Sciences, 50(7)*, 999-1015, 1993.

PUBLICATIONS 1995-1998

(1274) Hamilton, K., R.J. Wilson, J.D. Mahlman, and L.J. Umscheid, Climatology of the SKYHI Troposphere-Stratosphere-Mesosphere General Circulation Model, *Journal of the Atmospheric Sciences, 52(1)*, 5-43, 1995.

(1275) Hamilton, K., Interannual Variability in the Northern Hemisphere Winter Middle Atmosphere in Control and Perturbed Experiments with the GFDL SKYHI General Circulation Model, *Journal of the Atmospheric Sciences, 52(1)*, 44-66, 1995.

* (1276) Yuan, L., and K. Hamilton, Equilibrium Dynamics in a Forced-Dissipative *f*-Plane Shallow-Water System, *Journal of Fluid Mechanics, 280*, 369-394, 1994.

* (1277) Branstator, G., and I.M. Held, Westward Propagating Normal Modes in the Presence of Stationary Background Waves, *Journal of the Atmospheric Sciences, 52(2)*, 247-262, 1995.

(1278) Garner, S.T., Permanent and Transient Upstream Effects in Nonlinear Stratified Flow over a Ridge, *Journal of the Atmospheric Sciences, 52(2)*, 227-246, 1995.

* (1279) Held, I.M., R.T. Pierrehumbert, S.T. Garner, and K.L. Swanson, Surface Quasi-Geostrophic Dynamics, *Journal of Fluid Mechanics, 282*, 1-20, 1995.

* (1280) Liu, Z., and S.P. Xie, Equatorward Propagation of Coupled Air-Sea Disturbances with Application to the Annual Cycle of the Eastern Tropical Pacific, *Journal of the Atmospheric Sciences, 51(24)*, 3807-3822, 1994.

* (1281) Ross, R.J., and Y. Kurihara, A Numerical Study on Influences of Hurricane Gloria (1985) on the Environment, *Monthly Weather Review, 123(2)*, 332-346, 1995.

* (1282) Xie, S.P., On the Genesis of the Equatorial Annual Cycle, *Journal of Climate, 7(12)*, 2008-2013, 1994.

*In collaboration with other organizations

* (1283) Burpee, R.W., J.L. Franklin, S.J. Lord, and R.E. Tuleya, The Performance of Hurricane Track Guidance Models With and Without Omega Dropwindsondes, in *Preprints 21st AMS Conference on Hurricanes and Tropical Meteorology*, pp. 6-8, 1995.

* (1284) Wu, C.-C., and K.A. Emanuel, Potential Vorticity Diagnostics of Hurricane Movement. Part I: A Case Study of Hurricane Bob (1991), *Monthly Weather Review, 123(1)*, 69-92, 1995.

* (1285) Wu, C.-C., and K.A. Emanuel, Potential Vorticity Diagnostics of Hurricane Movement. Part II: Tropical Storm Ana (1991) and Hurricane Andrew (1992), *Monthly Weather Review, 123(1)*, 93-109, 1995.

(1286) Manabe, S., R.J. Stouffer, and M.J. Spelman, Interaction Between Polar Climate and Global Warming, in *Preprints Fourth Conference on Polar Meteorology and Oceanography*, Dallas, TX, 15-20 January 1995, American Meteorological Society, Boston, MA, pp. 1-9, 1995.

(1287) Hamilton, K., Aspects of Mesospheric Simulation in a Comprehensive General Circulation Model, in *The Upper Mesosphere and Lower Thermosphere: A Review of Experiment and Theory*, Geophysical Monograph 87, American Geophysical Union, pp. 255-264, 1995.

* (1288) Sarmiento, J.L., C. LeQuéré, and S.W. Pacala, Limiting Future Atmospheric Carbon Dioxide, *Global Biogeochemical Cycles, 9(1)*, 121-137, 1995.

(1289) Lanzante, J.R., Circulation Response in GFDL Increased CO_2 Experiments and Comparison with Observed Data, *Proceedings of the Seventeenth Annual Climate Diagnostic Workshop*, Norman, OK, October 1992, pp. 248-253, 1993.

* (1290) Pierrehumbert, R.T., I.M. Held, and K.L. Swanson, Spectra of Local and NonLocal Two-Dimensional Turbulence, *Chaos, Solitons, and Fractals, 4(6)*, 1111-1116, 1994.

* (1291) Willems, R.C., S.M. Glenn, M.F. Crowley, P. Malanotte-Rizzoli, R.E. Young, T. Ezer, G.L. Mellor, H.G. Arango, A.R. Robinson, and C.-C.A. Lai, Experiment Evaluates Ocean Models and Data Assimilation in the Gulf Stream, *EOS, Transactions*, American Geophysical Union, *75(34)*, 385,391,394, 1994.

* (1292) Moody, J.L., S.J. Oltmans, H. Levy II, and J.T. Merrill, Transport Climatology of Tropospheric Ozone: Bermuda, 1988-1991, *Journal of Geophysical Research, 100(D4)*, 7179-7194, 1995.

* (1293) Gu, D., and S.G.H. Philander, Secular Changes of Annual and Interannual Variability in the Tropics During the Past Century, *Journal of Climate, 8(4)*, 864-876, 1995.

* (1294) Armstrong, R.A., J.L. Sarmiento, and R.D. Slater, Monitoring Ocean Productivity by Assimilating Satellite Chlorophyll into Ecosystem Models, in *Ecological Time Series*, edited by T.M. Powell and J.H. Steele, pp. 371-390, 1995.

(1295) Kurihara, Y., M.A. Bender, and R.E. Tuleya, Performance Evaluation of the GFDL Hurricane Prediction System in the 1994 Hurricane Season, in *Preprints 21st Conference on Hurricanes and Tropical Meteorology*, Miami, FL, 24-28 April 1995, American Meteorological Society, Boston, MA, pp. 41-43, 1995.

* (1296) Zhang, J., Effects of Latent Heating on Midlatitude Atmospheric General Circulation, Ph.D. Dissertation, Atmospheric and Oceanic Sciences Program, Princeton University, 1995.

(1297) Donner, L.J., Validating Cumulus Parameterizations using Cloud (System)-Resolving Models, in *Preprints 21st Conference on Hurricanes and Tropical Meteorology*, Miami, FL, 24-28 April 1995, American Meteorological Society, Boston, MA, pp. 564-566, 1995.

*In collaboration with other organizations

(1298) Bender, M.A., Numerical Study of the Asymmetric Structure in the Interior of Tropical Cyclones, in *Preprints 21st Conference on Hurricanes and Tropical Meteorology*, Miami, FL, 24-28 April 1995, American Meteorological Society, Boston, MA, pp. 600-602, 1995.

(1299) Hayashi, Y., and D.G. Golder, The Generation Mechanism of Tropical Transient Waves: Control Experiments and a Unified Theory with Moist Convective Adjustment, in *Preprints 10th Conference on Atmospheric and Oceanic Waves and Stability*, Big Sky, MT, 5-9 June 1995, American Meteorological Society, Boston, MA, pp. 7-8, 1995.

(1300) Stern, W.F., and K. Miyakoda, Feasibility of Seasonal Forecasts Inferred from Multiple GCM Simulations, *Journal of Climate, 8(5)*, 1071-1085, 1995.

(1301) Hamilton, K., Comment on "Global QBO in Circulation and Ozone. Part I: Reexamination of Observational Evidence," *Journal of the Atmospheric Sciences, 52(10)*, 1834-1838, 1995.

* (1302) Gleckler, P.J., D.A. Randall, G. Boer, R. Colman, M. Dix, V. Galin, M. Helfand, J. Kiehl, A. Kitoh, W. Lau, X.-Y. Liang, V. Lykossov, B. McAvaney, K. Miyakoda, S. Planton, and W. Stern, Cloud-Radiative Effects on Implied Oceanic Energy Transports as Simulated by Atmospheric General Circulation Models, *Geophysical Research Letters, 22(7)*, 791-794, 1995.

* (1303) Shine, K.P., Y. Fouquart, V. Ramaswamy, S. Solomon, and J. Srinivasan, Radiative Forcing, in *Climate Change 1994: Radiative Forcing of Climate Change*, Cambridge University Press, pp. 163-203, 1995.

* (1304) Shine, K.P., K. Labitzke, V. Ramaswamy, P. Simon, S. Solomon, W.-C. Wang, Radiative Forcing and Temperature Trends, in *Scientific Assessment of Stratospheric Ozone Depletion, 1994*, Global Ozone Research and Monitoring Project Report #37, WMO, pp. 8.1-8.26, 1995.

* (1305) Ginis, I., and G. Sutyrin, Hurricane-Generated Depth-Averaged Currents and Sea Surface Elevation, *Journal of Physical Oceanography, 25(6)*, 1218-1242, 1995.

* (1306) Zavatarelli, M., and G.L. Mellor, A Numerical Study of the Mediterranean Sea Circulation, *Journal of Physical Oceanography, 25(6)*, 1384-1414, 1995.

* (1307) Yienger, J.J., and H. Levy II, Empirical Model of Global Soil-Biogenic NO_x Emissions, *Journal of Geophysical Research, 100(D6)*, 11,447-11,464, 1995.

(1308) Rosati, A., R. Gudgel, and K. Miyakoda, Decadal Analysis Produced from an Ocean Data Assimilation System, *Monthly Weather Review, 123(7)*, 2206-2228, 1995.

(1309) Lau, N.-C., and M.W. Crane, A Satellite View of the Synoptic-Scale Organization of Cloud Properties in Midlatitude and Tropical Circulation Systems, *Monthly Weather Review, 123(7)*, 1984-2006, 1995.

* (1310) Chang, E.K.M., and I. Orlanski, On Energy Flux and Group Velocity of Waves in Baroclinic Flows, *Journal of the Atmospheric Sciences, 51(24)*, 3823-3828, 1994.

* (1311) Goddard, L., The Energetics of Interannual Variability in the Tropical Pacific Ocean, Ph.D. Dissertation, Atmospheric and Oceanic Sciences Program, Princeton University, 1995.

(1312) Mehta, V.M., and T.L. Delworth, Decadal Variability of the Tropical Atlantic Ocean Surface Temperature in Shipboard Measurements and in a Global Ocean-Atmosphere Model, *Journal of Climate, 8(2)*, 172-190, 1995.

(1313) Toggweiler, J.R., and B. Samuels, Effect of Drake Passage on the Global Thermohaline Circulation, *Deep-Sea Research, 42(4)*, 477-500, 1995.

*In collaboration with other organizations

(1314) Toggweiler, J.R., Anthropogenic CO_2 - The Natural Carbon Cycle Reclaims Center Stage, *Reviews of Geophysics, (Supplement)*, 1249-1252, 1995.

(1315) Toggweiler, J.R., and B. Samuels, Effect of Sea Ice on the Salinity of Antarctic Bottom Waters, *Journal of Physical Oceanography, 25(9)*, 1980-1997, 1995.

(1316) Lanzante, J.R., Analysis of Climate Data Using Resistant, Robust and Nonparametric Techniques: Some Examples and Some Applications to the Historical Radiosonde Record, *Proceedings of the Nineteenth Annual Climate Diagnostics Workshop*, College Park, MD, 14-18 November 1994, pp. 37-40, 1995.

(1317) Sarmiento, J.L., The Carbon Cycle and the Role of the Ocean in Climate, in *Ecological and Social Dimensions of Global Change*, edited by D.D. Caron, F.S. Chapin III, J. Donoghue, M. Firestone, J. Harte, L.E. Wells, and R. Stewardson, Institute of International Studies, University of California, Berkeley, CA, pp. 4-41, 1994.

(1318) Shaffer, G., and J.L. Sarmiento, Biogeochemical Cycling in the Global Ocean, I. A New, Analytical Model with Continuous Vertical Resolution and High Latitude Dynamics, *Journal of Geophysical Research, 100(C2)*, 2659-2672, 1995.

(1319) Joos, F., and J.L. Sarmiento, Der Anstieg des Atmospharischen Kohlendioxids, *Physikalische Blatter, 51(5)*, 405-411, 1995.

(1320) Sarmiento, J.L., R. Murnane, and C. LeQuéré, Air-Sea CO_2 Transfer and the Carbon Budget of the North Atlantic, *Philosophical Transactions of the Royal Society of London, B348*, 211-219, 1995.

(1321) Anderson, J.L., A Simulation of Atmospheric Blocking with a Forced Barotropic Model, *Journal of the Atmospheric Sciences, 52(15)*, 2593-2608, 1995.

* (1322) Lawrence, M.G., W.L. Chameides, P.S. Kasibhatla, H. Levy II, and W.J. Moxim, Lightning and Atmospheric Chemistry: The Rate of Atmospheric NO Production, in *Handbook of Atmospheric Electrodynamics*, edited by Hans Volland, CRC Press, pp. 189-202, 1995.

(1323) Lau, N.-C., The Antarctic Ozone Hole Story, *United Bulletin*, United College, Chinese University of Hong Kong, *49*, 49-53, 1992-93.

* (1324) Chen, C.-T., and V. Ramaswamy, Parameterization of the Solar Radiative Characteristics of Low Clouds and Studies with a General Circulation Model, *Journal of Geophysical Research, 100(D6)*, 11,611-11,622, 1995.

* (1325) Liu, Z., and S.G.H. Philander, How Different Wind Stress Patterns Affect the Tropical-Subtropical Circulations of the Upper Ocean, *Journal of Physical Oceanography, 25(4)*, 449-462, 1995.

* (1326) Sun, D.-Z., and A.H. Oort, Humidity-Temperature Relationships in the Tropical Troposphere, *Journal of Climate, 8(8)*, 1974-1987, 1995.

* (1327) Ezer, T., G.L. Mellor, and R.J. Greatbatch, On the Interpentadal Variability of the North Atlantic Ocean: Model Simulated Changes in Transport, Meridional Heat Flux and Coastal Sea Level Between 1955-1959 and 1970-1974, *Journal of Geophysical Research, 100(C6)*, 10,559-10,566, 1995.

* (1328) Chylek, P., and J. Li, Light Scattering by Small Particles in an Intermediate Region, in *Optics Communications, 117*, 389-394, 1995.

(1329) Kurihara, Y., M.A. Bender, R.E. Tuleya, and R.J. Ross, Improvements in the GFDL Hurricane Prediction System, *Monthly Weather Review, 123(9)*, 2791-2801, 1995.

(1330) Knutson, T.R., and S. Manabe, Time-mean Response over the Tropical Pacific to Increased CO_2 in a Coupled Ocean-Atmosphere Model, *Journal of Climate, 8(9)*, 2181-2199, 1995.

*In collaboration with other organizations

(1331) Freidenreich, S.M., and V. Ramaswamy, Stratospheric Temperature Response to Improved Solar CO_2 and H_2O Parameterizations, *Journal of Geophysical Research, 100(D8)*, 16,721-16,725, 1995.

(1332) Hamilton, K., Simulation of Vertically-Propagating Waves in Comprehensive General Circulation Models: Opportunities for Comparison with Observations, *Proceedings of the Workshop on Wind Observations in the Middle Atmosphere*, Centre National d'Etudes Spatiales, Paris, France, 15-18 November 1994, pp. 4.3-4.15, 1994.

(1333) Hamilton, K., Comprehensive Simulation of the Middle Atmospheric Climate: Some Recent Results, *Climate Dynamics, 11*, 223-241, 1995.

* (1334) Ramaswamy, V., R.J. Charlson, J.A. Coakley, J.L. Gras, Harshvardhan, G. Kukla, M.P. McCormick, D. Moller, E. Roeckner, L.L. Stowe, and J. Taylor, What are the Observed and Anticipated Meteorological and Climatic Responses to Aerosol Forcing?, in *Aerosol Forcing of Climate*, edited by R.J. Charlson and J. Heintzenberg, Wiley Interscience, pp. 386-399, 1995.

* (1335) Galloway, J.N., W.H. Schlesinger, H. Levy II, A. Michaels, and J.L. Schnoor, Nitrogen Fixation: Anthropogenic Enhancement-Environmental Response, *Global Biogeochemical Cycles, 9(2)*, 235-252, 1995.

* (1336) Shine, K.P., B.P. Briegleb, A.S. Grossman, D. Hauglustaine, H. Mao, V. Ramaswamy, M.D. Schwarzkopf, R. Van Dorland, and W.-C. Wang, Radiative Forcing Due to Changes in Ozone: A Comparison of Different Codes, in *Atmospheric Ozone as a Climate Gas*, edited by W.-C. Wang and I.S.A. Isaksen, NATO ASI Series I, Vol. 32, Springer-Verlag, pp. 373-396, 1995.

* (1337) Larichev, V.D., and I.M. Held, Eddy Amplitudes and Fluxes in a Homogeneous Model of Fully Developed Baroclinic Instability, *Journal of Physical Oceanography, 25(10)*, 2285-2297, 1995.

* (1338) Soden, B.J., and R. Fu, A Satellite Analysis of Deep Convection, Upper Tropospheric Humidity and the Greenhouse Effect, *Journal of Climate, 8(10)*, 2333-2351, 1995.

* (1339) Griffies, S.M., and E. Tziperman, A Linear Thermohaline Oscillator Driven by Stochastic Atmospheric Forcing, *Journal of Climate, 8(10)*, 2440-2453, 1995.

* (1340) Toggweiler, J.R., and S. Carson, What are Upwelling Systems Contributing to the Ocean's Carbon and Nutrient Budgets?, in *Upwelling in the Ocean: Modern Processes and Ancient Records*, edited by C.P. Summerhayes, K.-C. Emeis, M.V. Angel, R.I. Smith and B. Zeitzchel, John Wiley & Sons, Ltd., pp. 337-360, 1995.

* (1341) Hamilton, K., and R.A. Vincent, High-Resolution Radiosonde Data Offer New Prospects for Research, *EOS, Transactions*, American Geophysical Union, 76(49), 497, 506-507, 1995.

(1342) Manabe, S., and R.J. Stouffer, Simulation of Abrupt Climate Change Induced by Freshwater Input to the North Atlantic Ocean, *Nature, 378*, 165-167, 1995.

* (1343) Broccoli, A.J., S. Manabe, J.F.B. Mitchell, and L. Bengtsson, Comments on "Global Climate Change and Tropical Cyclones": Part II, *Bulletin of the American Meteorological Society, 76(11)*, 2243-2245, 1995.

* (1344) Jones, P.W., C.L. Kerr, and R.S. Hemler, Practical Considerations in Development of a Parallel SKYHI General Circulation Model, *Parallel Computing, 21*, 1677-1694, 1995.

(1345) Orlanski, I., and J. Sheldon, Stages in the Energetics of Baroclinic Systems, *Tellus, 47A*, 605-628, 1995.

*In collaboration with other organizations

(1346) Wetherald, R.T., Feedback Processes in the GFDL R30-14 Level General Circulation Model, in *Climate Sensitivity to Radiative Perturbations: Physical Mechanisms and Their Validation*, NATO ASI Series I, Vol. 34, 251-266, 1996.

* (1347) Lee, W.-J., and M. Mak, Dynamics of Storm Tracks: A Linear Instability Perspective, *Journal of the Atmospheric Sciences, 52(6)*, 697-723, 1995.

* (1348) Mak, M., Orthogonal Wavelet Analysis: Interannual Variability in the Sea Surface Temperature, *Bulletin of the American Meteorological Society, 76(11)*, 2179-2186, 1995.

* (1349) Donner, L.J., J. Warren, and J. Ström, Implementing Microphysics at Physically Appropriate Scales in GCMs, *Proceedings of the WCRP Workshop on Cloud Microphysics in GCMs*, Kananaskis, Alberta, Canada 23-25 May 1995, pp. 133-139,1995.

* (1350) Santer, B.D., K.E. Taylor, T.M.L. Wigley, P.D. Jones, D.J. Karoly, J.F.B. Mitchell, A.H. Oort, J.E. Penner, V. Ramaswamy, M.D. Schwarzkopf, R.J. Stouffer, and S. Tett, A Search for Human Influences on the Thermal Structure of the Atmosphere, *PCMDI Report, No. 27*, 26 pp., 1995.

(1351) Wyman, B.L., A Step-Mountain Coordinate General Circulation Model: Description and Validation of Medium-Range Forecasts, *Monthly Weather Review, 124(1)*, 102-121, 1996.

(1352) Wetherald, R.T., and S. Manabe, The Mechanisms of Summer Dryness Induced by Greenhouse Warming, *Journal of Climate, 8(12)*, 3096-3108, 1995.

(1353) Hamilton, K., Do Historical "Zero Depth" Hydrographic Data Contain Useful Information on Climate Trends? *Canadian Meteorological and Oceanographic Society Bulletin, 23(6)*, 6-8, 1995.

* (1354) Broccoli, A.J., and E.P. Marciniak, Comparing Simulated Glacial Climate and Paleodata: A Reexamination, *Paleoceanography, 11(1)*, 3-14, 1996.

(1355) Anderson, J.L., Selection of Initial Conditions for Ensemble Forecasts in a Simple Perfect Model Framework, *Journal of the Atmospheric Sciences, 53(1)*, 22-36, 1996.

(1356) Mahlman, J.D., Toward a Scientific Centered Climate Monitoring System, *Climatic Change, 31*, 223-230, 1995.

* (1357) Overland, J.E., P. Turet, and A.H. Oort, Regional Variations of Moist Static Energy Flux in the Arctic, *Journal of Climate, 9(1)*, 54-65, 1996.

* (1358) Oey, L.-Y., Simulation of Mesoscale Variability in the Gulf of Mexico: Sensitivity Studies, Comparison with Observations, and Trapped Wave Propagation, *Journal of Physical Oceanography, 26(2)*, 145-175, 1996.

(1359) Manabe, S., and R.J. Stouffer, Low Frequency Variability of Surface Air Temperature in a 1,000-Year Integration of a Coupled Atmosphere-Ocean-Land Surface Model, *Journal of Climate, 9(2)*, 376-393, 1996.

* (1360) Frey, R.A., S.A. Ackerman, and B.J. Soden, Climate Parameters from Satellite Spectral Measurements, Part I: Collocated AVHRR and HIRS/2 Observations of Spectral Greenhouse Parameter, *Journal of Climate, 9(2)*, 327-344, 1996.

* (1361) Milly, P.C.D., Effects of Thermal Vapor Diffusion on Seasonal Dynamics of Water in the Unsaturated Zone, *Water Resources Research, 32(3)*, 509-518, 1996.

* (1362) Held, I.M., and V.D. Larichev, A Scaling Theory for Horizontally Homogeneous, Baroclinically Unstable Flow on a Beta Plane, *Journal of the Atmospheric Sciences, 53(7)*, 946-952, 1996.

(1363) Hamilton, K., Tides, in *The Encyclopedia of Climate and Weather*, Oxford University Press, pp. 761-764, 1996.

*In collaboration with other organizations

* (1364) Li, J., and V. Ramaswamy, Four-Stream Spherical Harmonic Expansion Approximation for Solar Radiative Transfer, *Journal of the Atmospheric Sciences, 53(8)*, 1174-1186, 1996.

(1365) Anderson, J.L., and W.F. Stern, Evaluating the Potential Predictive Utility of Ensemble Forecasts, *Journal of Climate, 9(2)*, 260-269, 1996.

(1366) Lau, N.-C., Variability of the Midlatitude Atmospheric Circulation in Relation to Tropical and Extratropical Sea Surface Temperature Anomalies, in *From Atmospheric Circulation to Global Change*, Celebration of the 80th Birthday of Professor YE Duzheng, edited by The Institute of Atmospheric Physics, Chinese Academy of Sciences, Beijing, China, China Meteorological Press, pp. 549-572, 1996.

* (1367) Soden, B.J., and F.P. Bretherton, Interpretation of TOVS Water Vapor Radiances in Terms of Layer-Average Relative Humidities: Method and Climatology for the Upper, Middle, and Lower Troposphere, *Journal of Geophysical Research, 101(D5)*, 9333-9343, 1996.

* (1368) Sun, D.-Z., and I.M. Held, A Comparison of Modeled and Observed Relationships between Interannual Variations of Water Vapor and Temperature, *Journal of Climate, 9(4)*, 665-675, 1996.

* (1369) Pavan, V., and I.M. Held, The Diffusive Approximation for Eddy Fluxes in Baroclinically Unstable Jets, *Journal of the Atmospheric Sciences, 53(9)*, 1262-1272, 1996.

(1370) Wilson, R.J., and K. Hamilton, Comprehensive Model Simulation of Thermal Tides in the Martian Atmosphere, *Journal of the Atmospheric Sciences, 53(9)*, 1290-1326, 1996.

* (1371) Gnanadesikan, A., Modeling the Diurnal Cycle of Carbon Monoxide: Sensitivity to Physics, Chemistry, Biology, and Optics, *Journal of Geophysical Research, 101(C5)*, 12,177-12,191, 1996.

* (1372) Moxim, W.J., H. Levy II, and P.S. Kasibhatla, Simulated Global Tropospheric PAN: Its Transport and Impact on NO_x, *Journal of Geophysical Research, 101(D7)*, 12,621-12,638, 1996.

* (1373) Mellor, G.L., and T. Ezer, Sea Level Variations Induced by Heating and Cooling: An Evaluation of the Boussinesq Approximation in Ocean Models, *Journal of Geophysical Research, 100(C10)*, 20,565-20,577, 1995.

* (1374) Ezer, T., (Ed.), Proceedings from the Princeton Ocean Model (POM) Users Meeting, Princeton, NJ, 10-12 June 1996, Program in Atmospheric and Oceanic Sciences, Princeton University, 56 pp., 1996.

* (1375) Pinardi, N., A. Rosati, and R.C. Pacanowski, The Sea Surface Pressure Formulation of Rigid Lid Models. Implications for Altimetric Data Assimilation Studies, *Journal of Marine Systems, 6*, 109-119, 1995.

(1376) Hamilton, K., Comprehensive Meteorological Modelling of the Middle Atmosphere: A Tutorial Review, *Journal of Atmospheric and Terrestrial Physics, 58(14)*, 1591-1628, 1996.

* (1377) Hurtt, G.C., and R.A. Armstrong, A Pelagic Ecosystem Model Calibrated with BATS Data, *Deep-Sea Research, Part II, 43*, 653-683, 1996.

* (1378) Vinnikov, K.Ya., A. Robock, R.J. Stouffer, and S. Manabe, Vertical Patterns of Free and Forced Climate Variations, *Geophysical Research Letters, 23(14)*, 1801-1804, 1996.

(1379) Soden, B.J., and J.R. Lanzante, An Assessment of Satellite and Radiosonde Climatologies of Upper Tropospheric Water Vapor, *Journal of Climate, 9(6)*, 1235-1250, 1996.

* (1380) Dixon, K.W., J.L. Bullister, R.H. Gammon, and R.J. Stouffer, Examining a Coupled Climate Model using CFC-11 as an Ocean Tracer, *Geophysical Research Letters, 23(15)*, 1957-1960, 1996.

*In collaboration with other organizations

* (1381) Chen, C.-T., and V. Ramaswamy, Sensitivity of Simulated Global Climate to Perturbations in Low Cloud Microphysical Properties, Part I: Globally Uniform Perturbations, *Journal of Climate, 9(6)*, 1385-1402, 1996.

* (1382) Kushnir, Y., and I.M. Held, Equilibrium Atmospheric Response to North Atlantic SST Anomalies, *Journal of Climate, 9(6)*, 1208-1220, 1996.

* (1383) Masina, S., Tropical Instability Waves in the Pacific Ocean, Ph.D. Dissertation, Atmospheric and Oceanic Sciences Program, Princeton University, 1996.

* (1384) Santer, B., K. Taylor, T.M.L. Wigley, T.C. Johns, P.D. Jones, D.J. Karoly, J.F.B. Mitchell, A.H. Oort, J.E. Penner, V. Ramaswamy, M.D. Schwarzkopf, R.J. Stouffer, and S. Tett, A Search for Human Influences on the Thermal Structure of the Atmosphere, *Nature, 382*, 39-46, 1996.

* (1385) Mellor, G.L., and X.-H. Wang, Pressure Compensation and the Bottom Boundary Layer, *Journal of Physical Oceanography, 26(10)*, 2214-2222, 1996.

* (1386) Mellor, G.L., *Introduction to Physical Oceanography*, AIP Press, 260 pp., 1996.

* (1387) Toggweiler, J.R., E. Tziperman, Y. Feliks, K. Bryan, S.M. Griffies, and B. Samuels, Reply to Comment by S. Rahmstorf, *Journal of Physical Oceanography, 26(6)*, 1106-1110, 1996.

* (1388) Murnane, R.J., J.K. Cochran, K.O. Buesseler, and M.P. Bacon, Least Squares Estimates of Thorium, Particle, and Nutrient Cycling Rate Constants from the JGOFS North Atlantic Bloom Experiment, *Deep-Sea Research, 43(2)*, 239-258, 1996.

* (1389) Lee, S., and J.L. Anderson, A Simulation of Atmospheric Storm Tracks with a Forced Barotropic Model, *Journal of the Atmospheric Sciences, 53(15)*, 2113-2128, 1996.

(1390) Anderson, J.L., A Method for Producing and Evaluating Probabilistic Forecasts from Ensemble Model Integrations, *Journal of Climate, 9(7)*, 1518-1530, 1996.

* (1391) Hsieh, W.W., and K. Bryan, Redistribution of Sea Level Rise Associated with Enhanced Greenhouse Warming: A Simple Model Study, *Climate Dynamics, 12*, 535-544, 1996.

* (1392) Bryan, K., The Steric Component of Sea Level Rise Associated with Enhanced Greenhouse Warming: A Model Study, *Climate Dynamics, 12*, 545-555, 1996.

(1393) Lau, N.-C., and M.J. Nath, The Role of the "Atmospheric Bridge" in Linking Tropical Pacific ENSO Events to Extratropical SST Anomalies, *Journal of Climate* (Stan Hayes Special Issue), *9*(9), 2036-2057, 1996.

* (1394) Ramaswamy, V., M.D. Schwarzkopf, and W.J. Randel, Fingerprint of Ozone Depletion in the Spatial and Temporal Pattern of Recent Lower-Stratospheric Cooling, *Nature, 382*, 616-618, 1996.

* (1395) Slusser, J., K. Hammond, A. Kylling, K. Stamnes, L. Perliski, A. Dahlback, D. Anderson, and R. DeMajistre, Comparison of Air Mass Computations, *Journal of Geophysical Research, 101(D5)*, 9315-9321, 1996.

* (1396) Dunne, K.A., and C.J. Willmott, Global Distribution of Plant-Extractable Water Capacity of Soil, *International Journal of Climatology, 16*, 841-859, 1996.

* (1397) Raval, A., A.H. Oort, and J.R. Lanzante, A New Interpolation Routine ("ANAL95") for Obtaining Global Fields from Irregularly Spaced Meteorological Data, GFDL Web Pages, http://www.gfdl.gov/, 1996.

* (1398) Anderson, L., and J.L. Sarmiento, Global Ocean Phosphate and Oxygen Simulations, *Global Biogeochemical Cycles, 9(4)*, 621-636, 1995.

*In collaboration with other organizations

* (1399) Joos, F., M. Bruno, R. Fink, U. Siegenthaler, T.F. Stocker, C. LeQuéré, and J.L. Sarmiento, An Efficient and Accurate Representation of Complex Oceanic and Biospheric Models of Anthropogenic Carbon Uptake, *Tellus, 48B,* 397-417, 1996.

(1400) Williams, G.P., Jovian Dynamics. Part 1: Vortex Stability, Structure, and Genesis, *Journal of the Atmospheric Sciences, 53(18),* 2685-2734, 1996.

* (1401) Wu, C.-C., and Y. Kurihara, A Numerical Study of the Feedback Mechanisms of Hurricane-Environment Interaction on Hurricane Movement from the Potential Vorticity Perspective, *Journal of the Atmospheric Sciences, 53(15),* 2264-2282, 1996.

* (1402) Gnanadesikan, A., Mixing Driven by Vertically Variable Forcing: An Application to the Case of Langmuir Circulation, *Journal of Fluid Mechanics, 322,* 81-107, 1996.

(1403) Gordon, C.T., A. Rosati, and R. Gudgel, The Impact of Specified ISCCP Low Clouds in Coupled Model Integrations, in *Preprints 11th Conference on Numerical Weather Prediction,* 19-23 August 1996, Norfolk, VA, American Meteorological Society, Boston, MA, pp. 8-10, 1996.

(1404) Ramaswamy, V., Longwave Radiation, in *Encyclopedia of Climate and Weather,* edited by S.H. Schneider, Oxford University Press, pp. 478-481, 1996.

* (1405) Schimel, D., D. Alves, I. Enting, M. Heimann, F. Joos, D. Raynaud, T. Wigley, M. Prather, R. Derwent, D. Ehhalt, P. Fraser, E. Sanhueza, X. Zhou, P. Jonas, R. Charlson, H. Rodhe, S. Sadasivan, K.P. Shine, Y. Fouquart, V. Ramaswamy, S. Solomon, J. Srinivasan, D. Albritton, I. Isaksen, M. Lal, D. Wuebbles, Radiative Forcing of Climate Change, in *Climate Change 1995: The Science of Climate Change,* edited by J.T. Houghton et al., Cambridge University Press, pp. 69-131, 1996.

* (1406) Aikman, F., G.L. Mellor, T. Ezer, D. Sheinin, P. Chen, L. Breaker, K. Bosley, and D.B. Rao, Toward an Operational Nowcast/Forecast System for the U.S. East Coast, in *Modern Approaches to Data Assimilation in Ocean Modeling,* edited by P. Malanotte-Rizzoli, Elsevier Oceanography Service, pp. 347-376, 1996.

(1407) Oort, A.H., Angular Momentum Cycle in Planet Earth, Contribution to *Encyclopedia of Planetary Sciences,* pp. 13-19, 1997.

* (1408) Chen, C.-T., E. Roeckner, and B.J. Soden, A Comparison of Satellite Observations and Model Simulations of Column-Integrated Moisture and Upper Tropospheric Humidity, *Journal of Climate, 9(7),* 1561-1585, 1996.

* (1409) Galbraith, N.R., A. Gnanadesikan, W.M. Ostrom, E.A. Terray, B.S. Way, N.J. Williams, S.H. Hill, and E. Terrill, *Meteorological and Oceanographic Data During the ASREX III Field Experiment: Cruise and Data Report,* UOP Technical Report 96-1, Woods Hole Oceanographic Institution, Woods Hole, MA, 1996.

* (1410) Levy II, H., W.J. Moxim, and P.S. Kasibhatla, A Global Three-Dimensional Time-dependent Lightning Source of Tropospheric NO_x, *Journal of Geophysical Research, 101(D17),* 22,911-22,922, 1996.

(1411) Delworth, T.L., North Atlantic Interannual Variability in a Coupled Ocean-Atmosphere Model, *Journal of Climate, 9(10),* 2356-2375, 1996.

(1412) Lanzante, J.R., Lag Relationships Involving Tropical Sea Surface Temperatures, *Journal of Climate, 9(10),* 2568-2578, 1996.

* (1413) Suntharalingham, P., *Modeling the Global Oceanic Nitrous Oxide Distribution,* Ph.D. Dissertation, Atmospheric and Oceanic Sciences Program, Princeton University, 1997.

*In collaboration with other organizations

* (1414) Prospero, J.M., K. Barrett, T. Church, F. Dentener, R.A. Duce, J.N. Galloway, H. Levy II, J. Moody, and P. Quinn, Atmospheric Deposition of Nutrients to the North Atlantic Basin, *Biogeochemistry, 35*, 27-73, 1996.

* (1415) Ramaswamy, V., and J. Li, A Line-by-Line Investigation of Solar Radiative Effects in Vertically Inhomogeneous Low Clouds, *Quarterly Journal of the Royal Meteorological Society, 122*, 1873-1890, 1996.

* (1416) Chen, C.-T., and V. Ramaswamy, Sensitivity of Simulated Global Climate to Perturbations in Low Cloud Microphysical Properties, Part II: Spatially Localized Perturbations, *Journal of Climate, 9(11)*, 2788-2801, 1996.

* (1417) Lindberg, C., and A.J. Broccoli, Representation of Topography in Spectral Climate Models and its Effect on Simulated Precipitation, *Journal of Climate, 9(11)*, 2641-2659, 1996.

* (1418) Orris, R.L., *Ozone and Temperature: A Test of the Consistency of Models and Observations in the Middle Atmosphere*, Ph.D. Dissertation, Atmospheric and Oceanic Sciences Program, Princeton University, 1997.

(1419) Lanzante, J.R., Resistant, Robust and Nonparametric Techniques for the Analysis of Climate Data: Theory and Examples, Including Applications to Historical Radiosonde Station Data, *International Journal of Climatology, 16*, 1197-1226, 1996.

(1420) Gross, B.D., The Effect of Compressibility on Barotropic and Baroclinic Instability, *Journal of the Atmospheric Sciences, 54(1)*, 24-31, 1997.

* (1421) Kasibhatla, P.S., H. Levy II, A. Klonecki, and W.L. Chameides, Three-Dimensional View of the Large-Scale Tropospheric Ozone Distribution over the North Atlantic Ocean during Summer, *Journal of Geophysical Research, 101(D22)*, 29,305-29,316, 1996.

(1422) Wilson, R.J., A General Circulation Model Simulation of the Martian Polar Warming, *Geophysical Research Letters, 24(2)*, 123-126, 1997.

* (1423) Moody, J.L., J.C. Davenport, J.T. Merrill, S.J. Oltmans, D.D. Parrish, J.S. Holloway, H. Levy II, G.L. Forbes, M. Trainer, and M. Buhr, Meteorological Mechanisms for Transporting O_3 Over the Western North Atlantic Ocean: A Case Study for August 24-29, 1993, *Journal of Geophysical Research, 101(D22)*, 29,213-29,227, 1996.

* (1424) Oltmans, S.J., H. Levy II, J.M. Harris, J.T. Merrill, J.L. Moody, J.A. Lathrop, E. Cuevas, M. Trainer, M.S. O'Neill, J.M. Prospero, H. Vömel, and B.J. Johnson, Summer and Spring Ozone Profiles over the North Atlantic from Ozonesonde Measurements, *Journal of Geophysical Research, 101(D22)*, 29,179-29,200, 1996.

* (1425) Oort, A.H., and J.J. Yienger, Observed Long-term Variability in the Hadley Circulation and Its Connection to ENSO, *Journal of Climate, 9(11)*, 2751-2767, 1996.

* (1426) Peixoto, J.P., and A.H. Oort, The Climatology of Relative Humidity in the Atmosphere, *Journal of Climate, 9(12)*, 3443-3463, 1996.

(1427) Mahlman, J.D., A Scientist's Perspective on Integrated Observing and Long-Term Monitoring Systems, in *First Symposium on Integrated Observing Systems*, American Meteorological Society, pp. 76-78, 1997.

(1428) Delworth, T.L., S. Manabe, and R.J. Stouffer, Multidecadal Climate Variability in the Greenland Sea and Surrounding Regions: A Coupled Model Simulation, *Geophysical Research Letters, 24(3)*, 257-260, 1997.

* (1429) Griffies, S.M., and K. Bryan, Predictability of North Atlantic Multidecadal Climate Variability, *Science, 275*, 181-184, 1997.

* (1430) Winton, M., The Damping Effect of Bottom Topography on Internal Decadal-Scale Oscillations of the Thermohaline Circulation, *Journal of Physical Oceanography, 27(1)*, 203-208, 1997.

*In collaboration with other organizations

* (1431) Knutson, T.R., S. Manabe, and D. Gu, Simulated ENSO in a Global Coupled Ocean-Atmosphere Model: Multidecadal Amplitude Modulation and CO_2 Sensitivity, *Journal of Climate, 10(1)*, 138-161, 1997.

* (1432) Gu, D., and S.G.H. Philander, Interdecadal Climate Fluctuations that Depend on Exchanges Between the Tropics and Extratropics, *Science, 275*, 805-807, 1997.

(1433) Delworth, T.L., S. Manabe, and R.J. Stouffer, Interannual to Interdecadal Variability in a Coupled Ocean-Atmosphere Model, in *Proceedings of International Workshop on Numerical Prediction of Oceanic Conditions*, Tokyo, Japan, 7-11 March 1995, pp. 99-107, 1997.

(1434) Winton, M., The Effect of Cold Climates upon North Atlantic Deep Water Formation in a Simple Ocean-Atmosphere Model, *Journal of Climate, 10(1)*, 37-51, 1997.

(1435) Bender, M.A., The Effect of Relative Flow on the Asymmetric Structure in the Interior of Hurricanes, *Journal of the Atmospheric Sciences, 54(6)*, 703-724, 1997.

(1436) Manabe, S., Early Development in the Study of Greenhouse Warming: The Emergence of Climate Models, *Ambio* (Special volume commemorating 100th year anniversary of the publication of "Arrhenius" paper on Greenhouse Warming), *26(1)*, 47-51, 1997.

(1437) Lau, N.-C., Interactions Between Global SST Anomalies and the Midlatitude Atmospheric Circulation, *Bulletin of the American Meteorological Society, 78(1)*, 21-33, 1997.

* (1438) Ramaswamy, V., and C.-T. Chen, Linear Additivity of Climate Response for Combined Albedo and Greenhouse Perturbations, *Geophysical Research Letters, 24(5)*, 567-570, 1997.

* (1439) Balasubramanian, G., and S.T. Garner, The Role of Momentum Fluxes in Shaping the Life Cycle of a Baroclinic Wave, *Journal of the Atmospheric Sciences, 54(4)*, 510-533, 1997.

* (1440) Ramaswamy, V., and C.-T. Chen, Climate Forcing-Response Relationships for Greenhouse and Shortwave Radiative Perturbations, *Geophysical Research Letters, 24(6)*, 667-670, 1997.

(1441) Hamilton, K., The Role of Parameterized Drag in a Troposphere-Stratosphere-Mesosphere General Circulation Model, in *Gravity Waves Processes, Their Parameterization in Global Climate Models*, edited by K. Hamilton, Springer-Verlag, pp.337-350, 1997.

(1442) Donner, L.J., C.J. Seman, and J.P. Sheldon, Cloud-Radiative Interactions in High-Resolution Cloud-Resolving Models, in *Preprints 9th Conference on Atmospheric Radiation*, Long Beach, CA, 2-7 February 1997, American Meteorological Society, Boston, MA, pp. 47-48, 1997.

* (1443) Swanson, K.L., P.J. Kushner, and I.M. Held, Dynamics of Barotropic Storm Tracks, *Journal of the Atmospheric Sciences, 54(7)*, 791-810, 1997.

(1444) Manabe, S., and R.J. Stouffer, Coupled Ocean-Atmosphere Model Response to Freshwater Input: Comparison to Younger Dryas Event, *Paleoceanography, 12(2)*, 321-336, 1997.

* (1445) Levy II, H., P.S. Kasibhatla, W.J. Moxim, A.A. Klonecki, A.I. Hirsch, S.J. Oltmans, and W.L. Chameides, The Global Impact of Human Activity on Tropospheric Ozone, *Geophysical Research Letters, 24(7)*, 791-794, 1997.

* (1446) Zhang, Y., *On the Mechanisms for the Mid-winter Suppression of the Pacific Stormtrack*, Ph.D. Dissertation, Atmospheric and Oceanic Sciences Program, Princeton University, 1997.

*In collaboration with other organizations

* (1447) Treguier, A.M., I.M. Held, and V.D. Larichev, Parameterization of Quasigeostrophic Eddies in Primitive Equation Ocean Models, *Journal of Physical Oceanography, 27(4)*, 567-580, 1997.

* (1448) Lanzante, J.R., and G.E. Gahrs, Examination of Some Biases in Satellite and Radiosonde Measures of Upper Tropospheric Humidity using a Framework for the Comparison of Redundant Measurement Systems, in *Proceedings of the 21st Annual Climate Diagnostics and Prediction Workshop*, Huntsville, AL, October 1996, pp. 352-355, 1997.

(1449) Anderson, J.L., A. Rosati, and R.G. Gudgel, Potential Predictability in an Ensemble of Coupled Atmosphere-Ocean General Circulation Model Seasonal Forecasts, in *Proceedings of the 21st Annual Climate Diagnostics and Prediction Workshop*, Huntsville, AL, October 1996, pp. 18-21, 1997.

(1450) Anderson, J.L., and R.G. Gudgel, Impact of Atmospheric Initial Conditions on Seasonal Predictions with a Coupled Ocean-Atmosphere Model, in *Proceedings of the 21st Annual Climate Diagnostics and Prediction Workshop*, Huntsville, AL, October 1996, pp. 61-66, 1997.

* (1451) Peng, P., and N.-C. Lau, The Impact of the Monthly-Varying Global SST Anomalies on the Northern Hemisphere Circulation as Seen in an Ensemble of NCEP GCM Simulations, in *Proceedings of the 21st Annual Climate Diagnostics and Prediction Workshop*, Huntsville, AL, October 1996, pp. 102-105, 1997.

(1452) Hayashi, Y., and D.G. Golder, United Mechanisms for the Generation of Low- and High-Frequency Tropical Waves: Part I: Control Experiments with Moist Convective Adjustment, *Journal of the Atmospheric Sciences, 54(9)*, 1262-1276, 1997.

* (1453) Hall, A., and S. Manabe, Can Local Linear Stochastic Theory Explain Sea Surface Temperature and Salinity Variability?, *Climate Dynamics, (13)*, 167-180, 1997.

(1454) Williams, G.P., Planetary Vortices and Jupiter's Vertical Structure, *Journal of Geophysical Research, 102(E4)*, 9303-9308, 1997.

* (1455) Vitart, F., J.L. Anderson, W.F. Stern, Simulation of Interannual Variability of Tropical Storm Frequency in an Ensemble of GCM Integrations, *Journal of Climate, 10(4)*, 745-760, 1997.

* (1456) Jones, P.W., K. Hamilton, and R.J. Wilson, A Very High-Resolution General Circulation Model Simulation of the Global Circulation in Austral Winter, *Journal of the Atmospheric Sciences, 54(8)*, 1107-1116, 1997.

(1457) Rosati, A., K. Miyakoda, and R. Gudgel, The Impact of Ocean Initial Conditions on ENSO Forecasting with a Coupled Model, *Monthly Weather Review, 125(5)*, 754-772, 1997.

* (1458) Li, J., S.M. Freidenreich, and V. Ramaswamy, Solar Spectral Weight at Low Cloud Tops, *Journal of Geophysical Research, 102(D10)*, 11,139-11,143, 1997.

* (1459) Soden, B., Variations in the Tropical Greenhouse Effect during El Niño, *Journal of Climate, 10(5)*, 1050-1055, 1997.

* (1460) Li, X., P. Chang, and R.C. Pacanowski, A Wave-Induced Stirring Mechanism in the Mid-depth Equatorial Ocean, *Journal of Marine Research, 54*, 487-520, 1996.

(1461) Kurihara, Y., M.A. Bender, and R.E. Tuleya, For Hurricane Intensity Forecast: Formulation of a New Initialization Method for the GFDL Hurricane Prediction Model, in *Preprints 22nd Conference on Hurricanes and Tropical Meteorology*, Ft. Collins, CO, 19-23 May 1997, American Meteorological Society, Boston, MA, pp. 543-544, 1997.

*In collaboration with other organizations

(1462) Knutson, T., R. Tuleya, and Y. Kurihara, Exploring the Sensitivity of Hurricane Intensity to CO2-Induced Global Warming using the GFDL Hurricane Prediction System, in *Preprints 22nd Conference on Hurricanes and Tropical Meteorology*, Ft. Collins, CO, 19-23 May 1997, American Meteorological Society, Boston, MA, pp. 587-588, 1997.

* (1463) Bender, M.A., C.-C. Wu, M.A. Rennick, and Y. Kurihara, Comparison of the GFDL Hurricane Model Prediction in the Western Pacific using the NOGAPS and AVN Global Analysis, in *Preprints 22nd Conference on Hurricanes and Tropical Meteorology*, Ft. Collins, CO, 19-23 May 1997, American Meteorological Society, Boston, MA, pp. 615-616, 1997.

* (1464) Wacongne, S., and R.C. Pacanowski, Seasonal Heat Transport in a Primitive Equations Model of the Tropical Indian Ocean, *Journal of Physical Oceanography, 26(12)*, 2666-2699, 1996.

* (1465) Burpee, R.W., J.L. Franklin, S.J. Lord, R.E. Tuleya, and S.D. Aberson, The Impact of Omega Dropwindsondes on Operational Hurricane Track Forecast Models, *Bulletin of the American Meteorological Society, 77(5)*, 925-933, 1996.

* (1466) Milly, P.C.D., Sensitivity of Greenhouse Summer Dryness to Changes in Plant Rooting Characteristics, *Geophysical Research Letters, 24(3)*, 269-271, 1997.

* (1467) Li, T., S.G.H. Philander, On the Annual Cycle of the Eastern Equatorial Pacific, *Journal of Climate, 9(12)*, 2986-2998, 1996

* (1468) Philander, S.G.H., D. Gu, D. Halpern, G. Lambert, N.-C. Lau, T. Li, R.C. Pacanowski, Why the ITCZ is Mostly North of the Equator, *Journal of Climate, 9(12)*, 2958-2972, 1996.

(1469) Hamilton, K., Observation of an Ultraslow Large-Scale Wave Near the Tropical Tropopause, *Journal of Geophysical Research, 102(D12)*, 13,457-13,464, 1997

* (1470) Tuleya, R.E., and S.J. Lord, The Impact of Dropwindsonde Data on GFDL Hurricane Model Forecasts using Global Analyses, *Weather and Forecasting, 12(2)*, 307-323, 1997.

* (1471) Gnanadesikan, A., and R.C. Pacanowski, Improved Representation of Flow Around Topography in the GFDL Modular Ocean Model MOM2, *International WOCE Newsletter, 27*, 23-25, 1997.

(1472) Manabe, S., and R.J. Stouffer, Climate Variability of a Coupled Ocean-Atmosphere-Land Surface Model: Implication for the Detection of Global Warming, *Bulletin of the American Meteorological Society, 78(6)*, 1177-1185, 1997.

* (1473) Haywood, J.M., R.J. Stouffer, R.T. Wetherald, S. Manabe, and V. Ramaswamy, Transient Response of a Coupled Model to Estimated Changes in Greenhouse Gas and Sulfate Concentrations, *Geophysical Research Letters, 24(11)*, 1335-1338, 1997.

* (1474) Zhang, Y., K.R. Sperber, J.S. Boyle, M.R. Dix, L. Ferranti, A. Kitoh, K.M. Lau, K. Miyakoda, D. Randall, L. Takacs, and R. Wetherald, *GCM Simulated East Asian Winter Monsoon: Results from Eight AMIP Models*, PCMDI Report No. 39, 49 pp., 1997.

* (1475) Ezer, T., and G.L. Mellor, Data Assimilation in the Gulf Stream Region: How Useful are Satellite-Derived Surface Data for Nowcasting the Subsurface Fields?, *Journal of Atmospheric and Oceanic Technology, 14(6)*, 1379-1391, 1997.

* (1476) Ezer, T., and G.L. Mellor, Simulations of the Atlantic Ocean with a Free Surface Sigma Coordinate Ocean Model, *Journal of Geophysical Research, 102(C7)*, 15,647-15,657, 1997.

* (1477) Kelley, J.G.W., F. Aikman II, L.C. Breaker, and G.L. Mellor, Coastal Ocean Forecasts, *Sea Technology, 38(5)*, 10-17, 1997.

*In collaboration with other organizations

* (1478) Cess, R.D., M.-H. Zhang, G.L. Potter, V. Alekseev, H.W. Barker, S. Bony, R.A. Colman, D.A. Dazlich, A.D. Del Genio, M. Déqué, M.R. Dix, V. Dymnikov, M. Esch, L.D. Fowler, J.R. Fraser, V. Galin, W.L. Gates, J.J. Hack, W.J. Ingram, J.T. Kiehl, Y. Kim, H. LeTreut, X.-Z. Liang, B.J. McAvaney, V.P. Meleshko, J.-J. Morcrette, D.A. Randall, E. Roeckner, M.E. Schlesinger, P.V. Sporyshev, K.E. Taylor, B. Timbal, E.M. Volodin, W. Wang, W.-C. Wang, and R.T. Wetherald, Comparison of the Seasonal Change in Cloud-Radiative Forcing from Atmospheric General Circulation Models and Satellite Observations, *Journal of Geophysical Research, 102(D14)*, 16,593-16,603, 1997.

* (1479) Koster, R.D., and P.C.D. Milly, The Interplay between Transpiration and Runoff Formulations in Land Surface Schemes used with Atmospheric Models, *Journal of Climate, 10(7)*, 1578-1591, 1997.

* (1480) Chen, T.H., A. Henderson-Sellers, P.C.D. Milly, A.J. Pitman, A.C.M. Beljaars, J. Polcher, F. Abramopoulos, A. Boone, S. Chang, F. Chen, Y. Dai, C.E. Desborough, R.E. Dickinson, L. Dumenil, M. Ek, J.R. Garratt, N. Gedney, Y.M. Gusev, J. Kim, R. Koster, E.A. Kowalczyk, K. Laval, J. Lean, D. Lettenmaier, X. Liang, J.-F. Mahfouf, H.-T. Mengelkamp, K. Mitchell, O.N. Nasonova, J. Noilhan, A. Robock, C. Rosenzweig, J. Schaake, C.A. Schlosser, J.-P. Schulz, Y. Shao, A.B. Shmakin, D.L. Verseghy, P. Wetzel, E.F. Wood, Y. Xue, Z.-L. Yang, and Q. Zeng, Cabauw Experimental Results from the Project for Intercomparison of Land-surface Parameterization Schemes (PILPS), *Journal of Climate, 10(6)*, 1194-1215, 1997.

(1481) Mahlman, J.D., Dynamics of Transport Processes in the Upper Troposphere, *Science, 276*, 1079-1083, 1997.

* (1482) Hallberg, R., Stable Split Time Stepping Schemes for Large-Scale Ocean Modeling, *Journal of Computational Physics, 135*, 54-65, 1997.

* (1483) Haywood, J.M., V. Ramaswamy, and L.J. Donner, A Limited-Area-Model Case Study of the Effects of Sub-Grid Scale Variations in Relative Humidity and Cloud Upon the Direct Radiative Forcing of Sulfate Aerosol, *Geophysical Research Letters, 24(2)*, 143-146, 1997.

* (1484) Haywood, J.M., D.L. Roberts, A. Slingo, J.M. Edwards, and K.P. Shine, General Circulation Model Calculations of the Direct Radiative Forcing by Anthropogenic Sulfate and Fossil-Fuel Soot Aerosol, *Journal of Climate, 10(7)*, 1562-1577, 1997.

* (1485) Gruber, N., J.L. Sarmiento, and T.F. Stocker, An Improved Method for Detecting Anthropogenic CO_2 in the Oceans, *Global Biogeochemical Cycles, 10*, 809-837, 1996.

* (1486) Sarmiento, J.L., and C. LeQuéré, Oceanic CO_2 Uptake in a Model of Century-Scale Global Warming, *Science, 274*, 1346-1350, 1996.

* (1487) Key, R.M., WOCE Pacific Ocean Radiocarbon Program, *Radiocarbon, 38(3)*, 415-423, 1997.

* (1488) Key, R.M., and P.D. Quay, WOCE AMS Radiocarbon I: Pacific Ocean Results: P6, P16, and P17, *Radiocarbon, 38(3)*, 425-518, 1997.

* (1489) Stuiver, M., H.G. Ostlund, R.M. Key, and P.J. Reimer, Large Volume WOCE Radiocarbon Sampling in the Pacific Ocean, *Radiocarbon, 38(3)*, 519-561, 1997.

(1490) Hayashi, Y., and D.G. Golder, United Mechanisms for the Generation of Low- and High-Frequency Tropical Waves, Part II: Theoretical Interpretations, *Journal of the Meteorological Society of Japan, 75(4)*, 775-797, 1997.

*In collaboration with other organizations

(1491) Schwarzkopf, M.D., and V. Ramaswamy, Stratospheric Climatic Effects due to CH_4, N_2O, CFCs, and the H_2O Infrared Continuum: A GCM Experiment, in *IRS 96: Current Problems in Atmospheric Radiation*, International Radiation Symposium, Fairbanks, Alaska, 19-24 August 1996, pp. 336-339, 1997.

(1492) Donner, L.J., C.J. Seman, R.S. Hemler, and J.P. Sheldon, Radiative Transfer in a Three-Dimensional Cloud-System-Resolving Model, in *IRS 96: Current Problems in Atmospheric Radiation*, International Radiation Symposium, Fairbanks, Alaska, August 1996, pp. 109-112, 1997.

* (1493) Chen, C.-T., and V. Ramaswamy, Climate Sensitivity to Solar and Greenhouse Radiative Forcings, in *IRS 96: Current Problems in Atmospheric Radiation*, International Radiation Symposium, Fairbanks, Alaska, August 1996, pp. 279-281, 1997.

(1494) Ramaswamy, V., and S.M. Freidenreich, Absorption of Solar Radiation in Overcast Atmospheres, in *IRS 96: Current Problems in Atmospheric Radiation*, International Radiation Symposium, Fairbanks, Alaska, August 1996, pp. 125-127, 1997.

* (1496) Hurtt, G.C., *Ocean Ecosystem Models for Use in Studies of the Air-Sea Balance of Carbon Dioxide*, Ph.D. Dissertation, Department of Ecology and Evolutionary Biology, Princeton University, 1997.

(1497) Gruber, N., and J.L. Sarmiento, Global Patterns of Marine Nitrogen Fixation and Denitrification, *Global Biogeochemical Cycles, 11(2)*, 235-266, 1997.

* (1498) Michaels, A.F., D. Olson, J.L. Sarmiento, J.W. Ammerman, K. Fanning, R. Jahnke, A.H. Knap, F. Lipschultz, J.M. Prospero, Inputs, Losses and Transformations of Nitrogen and Phosphorus in the Pelagic North Atlantic Ocean, *Biogeochemistry, 35*, 181-226, 1997.

* (1499) Sabine, C.L., D.W.R. Wallace, and F.J. Millero, Survey of CO_2 in the Oceans Reveals Clues about Global Carbon Cycle, *EOS, 78(5)*, 49, 54-55, 1997.

* (1500) Hurtt, G.C., and R.A. Armstrong, A Pelagic Ecosystem Model Calibrated with BATS Data, *Deep-Sea Research, Part II, 43(2-3)*, 653-683, 1996.

* (1501) Klonecki, A., and H. Levy II, Tropospheric Chemical Ozone Tendencies in $CO\text{-}CH_4\text{-}NO_y\text{-}H_2O$ System: Their Sensitivity to Variations in Environmental Parameters and their Application to a Global Chemistry Transport Model Study, *Journal of Geophysical Research, 102(D17)*, 21,221-21,237, 1997.

* (1502) Donner, L.J., C.J. Seman, B.J. Soden, R.S. Hemler, J.C. Warren, J. Ström, and K.-N. Liou, Large-Scale Ice Clouds in the GFDL SKYHI General Circulation Model, *Journal of Geophysical Research, 102*(D18), 21,745-21,768, 1997.

* (1503) Nakamura, H., M. Nakamura, and J.L. Anderson, The Role of High- and Low-Frequency Dynamics in the Blocking Formation, *Monthly Weather Review, 125*(9), 2074-2093, 1997.

* (1504) Haywood, J.M., and K.P. Shine, Multi-Spectral Calculations of the Direct Radiative Forcing of Tropospheric Sulphate and Soot Aerosols using a Column Model, *Quarterly Journal of the Royal Meteorological Society, 123*, 1907-1930, 1997.

* (1505) Meehl, G.A., G.J. Boer, C. Covey, M. Latif, and R.J. Stouffer, Intercomparison Makes for a Better Climate Model, *EOS, Transactions, 78*(41), 445-446, 1997.

(1506) Christensen, N., J. Christy, R. Cooper, F. Culler, D. Hagen, R. Lindzen, J.D. Mahlman, L.D. Meeker, A. Robock, W. Schlesinger, H.H. Schmitt, M. Weidenbaum, and P. Wilcoxen, *Global Climate Change: Policy Making in the Context of Scientific and Economic Uncertainty*, The Annapolis Center, 15 pp., 1997.

* (1507) Griffies, S.M., and K. Bryan, A Predictability Study of Simulated North Atlantic Multidecadal Variability, *Climate Dynamics, 13*, 459-487, 1997.

*In collaboration with other organizations

* (1508) Spangenberg, D.A., G.G. Mace, T.P. Ackerman, N.L. Seaman, and B.J. Soden, Evaluation of Model-Simulated Upper Troposphere Humidity using 6.7 μm Satellite Observations, *Journal of Geophysical Research, 102*(D22), 25,737-25,749, 1997.

(1509) Anderson, J.L., The Impact of Dynamical Constraints on the Selection of Initial Conditions for Ensemble Predictions: Low-order Perfect Model Results, *Monthly Weather Review, 125*(11), 2969-2983, 1997.

* (1510) Haywood, J.M., K.P. Shine, and A. Slingo, Direct Radiative Forcing of Anthropogenic Sulfate and Soot Aerosol using a Flexible Radiation Code and a GCM, In *IRS '96: Current Problems in Atmospheric Radiation*, edited by William L. Smith and Knut Stamnes, A. Deepak Publishers, pp. 324-327, 1997.

* (1511) Klein, S., Synoptic Variability of Low-Cloud Properties and Meteorological Parameters in the Subtropical Trade Wind Boundary Layer, *Journal of Climate, 10*, 2018-2039, 1997.

* (1512) Hallberg, R., Localized Coupling Between Surface and Bottom-Intensified Flow Over Topography, *Journal of Physical Oceanography, 27*, 977-998, 1997.

(1513) Mahlman, J.D., Uncertainties in Projections of Human-Caused Climate Warming, *Science, 278*, 1416-1417, 1997.

(1514) Lau, N.-C., and M.W. Crane, Comparing Satellite and Surface Observations of Cloud Patterns in Synoptic-Scale Circulation Systems, *Monthly Weather Review, 125*(12), 3172-3189, 1997.

(1515) Hamilton, K., Meteorological Measurements on Ozonesonde Ascents: A Valuable Resource for Stratospheric Climatology, *SPARC Newsletter, 9*, 23, 1997.

* (1516) Forbes, J.M., M.E. Hagan, X. Zhang, and K. Hamilton, Upper Atmosphere Tidal Oscillations Due to Latent Heat Release in the Tropical Troposphere, *Annals Geophysicae, 15*, 1165-1175, 1997.

(1517) Miyakoda, K., J. Ploshay, and A. Rosati, Preliminary Study on SST Forecast Skill Associated with the 1982/83 El Niño Process using Coupled Model Data Assimilation, *Atmosphere-Ocean Special, XXXV* (No.1), 469-486, 1997.

* (1518) Balasubramanian, G., and S.T. Garner, The Equilibration of Short Baroclinic Waves, *Journal of the Atmospheric Sciences, 54*(24), 2850-2871, 1997.

* (1519) Ezer, T., and G.L. Mellor, Data Assimilation Experiments in the Gulf Stream Region: How Useful are Satellite-Derived Surface Data for Nowcasting the Subsurface Fields? *Journal of Atmospheric and Oceanic Technology, 14*(6), 1379-1391, 1997.

(1520) Broccoli, A.J., and S. Manabe, Mountains and Midlatitude Aridity, In *Tectonic Uplift and Climate Change*, edited by William F. Ruddiman, Plenum Press, pp. 89-121, 1997.

* (1521) Hayashi, Y., D.G. Golder, and P.W. Jones, Tropical Gravity Waves and Superclusters Simulated by High-Horizontal-Resolution SKYHI General Circulation Models, *Journal of the Meteorological Society of Japan, 75*(6), 1125-1139, 1997.

(1522) Hamilton, K., and R.S. Hemler, Appearance of a Super Typhoon in a Global Climate Model Simulation, *Bulletin of the American Meteorological Society, 78*(12), 2874-2876, 1997.

* (1523) Heintzenberg, J., R.J. Charlson, A.D. Clarke, C. Liousse, V. Ramaswamy, K.P. Shine, M. Wendisch, and G. Helas, Measurements and Modelling of Aerosol Single-Scattering Albedo: Progress, Problems and Prospects, *Contributions to Atmospheric Physics, 70*(4), 249-263, 1997.

(1524) Hamilton, K., "Gravity Currents in the Environment and the Laboratory", *EOS, Transactions, 79*, 71, 1998.

*In collaboration with other organizations

(1525) Knutson, T.R., and S. Manabe, Model Assessment of Decadal Variability and Trends in the Tropical Pacific Ocean, in *Preprints The Ninth Symposium on Global Change Studies and Namias Symposium on the Status and Prospects for Climate Prediction*, Phoenix, AZ, 11-16 January 1998, American Meteorological Society, Boston, MA, pp. 216-219, 1998.

(1526) Kurihara, Y., R.E. Tuleya, A Prospect of Improvement in the Forecast of Hurricane Landfall, in *Preprints 16th Conference on Weather Analysis and Forecasting and Symposium on The Research Foci of the U.S. Weather Research Program*, Phoenix AZ, 11-16 January 1998, American Meteorological Society, Boston, MA, pp. 524-525, 1998.

(1527) Knutson, T.R., R.E. Tuleya, and Y. Kurihara, Simulated Increase of Hurricane Intensities in a CO_2-Warmed Climate, *Science, 279*, 1018-1020, 1998.

(1528) Hamilton, K., Dynamics of the Tropical Middle Atmosphere, in *Proceedings of the Canadian Middle Atmosphere Project Summer School*, Cornwall, Ontario, Canada, 25-29 August 1997, edited by J.N. Koshyk and T.G. Shepherd, pp. 212-256, 1998.

* (1529) Haywood, J., and V. Ramaswamy, Global Sensitivity Studies of the Direct Radiative Forcing due to Anthropogenic Sulfate and Black Carbon Aerosols, *Journal of Geophysical Research, 103*(D6), 6043-6058, 1998.

* (1530) Holt, B., A.K. Liu, D.W. Wang, A. Gnanadesikan, and H.S. Chen, Tracking Storm-Generated Waves in the Northeast Pacific Ocean with ERS-1 Synthetic Aperture Radar Imagery and Buoys, *Journal of Geophysical Research, 103*(C4), 7917-7929, 1998.

* (1531) Hecht, A., T. Ezer, A. Huss, and A. Shapira, Wind Waves on the Dead Sea, in *The Dead Sea: The Lake and its Setting*, edited by T.M. Niemi, Z. Ben-Avraham and J.R. Gata, Monographs on Geology and Geophysics, No. 36, Oxford University Press, pp. 114-121, 1997.

* (1532) Goswami, B.N., Interannual Variations of Indian Summer Monsoon in a GCM: External Conditions versus Internal Feedbacks, *Journal of Climate, 11*, 501-522, 1998.

(1533) Kurihara, Y., R.E. Tuleya, and M.A. Bender, The GFDL Hurricane Prediction System and its Performance in the 1995 Hurricane Season, *Monthly Weather Review, 126*(5), 1306-1322, 1998.

(1534) Stouffer, R.J., and K.W. Dixon, Initialization of Coupled Models for Use in Climate Studies: A Review, in *Research Activities in Atmospheric and Oceanic Modelling*, Report No. 27, WMO/TD-No. 865, World Meteorological Organization, Geneva, Switzerland, pp. I.1-I.8, 1998.

* (1535) Griffies, S.M., A. Gnanadesikan, R.C. Pacanowski, V.D. Larichev, J.K. Dukowicz, and R.D. Smith, Isoneutral Diffusion in a Z-Coordinate Ocean Model, *Journal of Physical Oceanography, 28*(5), 805-830, 1998.

(1536) Griffies, S.M., The Gent-McWilliams Skew-Flux, *Journal of Physical Oceanography, 28*(5), 831-841, 1998.

* (1537) Andronache, C., L.J. Donner, V. Ramaswamy, C.J. Seman, and R.S. Hemler, The Effects of Atmospheric Sulfur on the Radiative Properties of Convective Clouds: A Limited Area Modeling Study, *Geophysical Research Letters, 25*(9), 1423-1426, 1998.

* (1538) Stephens, B.B., R.F. Keeling, M. Heimann, K.D. Six, R.J. Murnane, Testing Global Ocean Carbon Cycle Models using Measurements of Atmospheric O_2 and CO_2 Concentration, *Global Biogeochemical Cycles, 12*(2), 213-230, 1998.

(1539) Anderson, J.L., Impacts of Dynamically Constrained Initial Conditions on Ensemble Forecasts, in *Preprints 11th Numerical Weather Prediction Conference*, Norfolk, VA, 19-23 August 1996, American Meteorological Society, pp. 56-57, 1998.

*In collaboration with other organizations

(1540) Stern, W.F., and J.L. Anderson, Interannual Variability of Tropical Intraseasonal Oscillations in the GFDL/DERF GCM Inferred From an Ensemble of AMIP Integrations, in *Preprints 11th Numerical Weather Prediction Conference*, Norfolk, VA, 19-23 August 1996, American Meteorological Society, pp. 15-16, 1998.

(1541) Sirutis, J.J., and A. Rosati, The Impact of Cumulus Convection Parameterization in Coupled Air-Sea Models, in *Preprints 11th Numerical Weather Prediction Conference*, Norfolk, VA, 19-23 August 1996, American Meteorological Society, pp. 348-350, 1998.

(1542) Delworth, T.L., Interannual to Decadal Variability in the North Pacific of a Coupled Ocean-Atmosphere Model, in *Proceedings of the JCESS/CLIVAR Workshop on Decadal Climate Variability*, Columbia, MD, 22-24 April 1996, 1996.

* (1543) Donner, L.J., C. Andronache, and C.J. Seman, Chemistry and Radiation in Convective Cloud Systems: Transport, Transformation, and Climate Implications, *Abstracts of Papers Presented at the Rossby-100 Symposium*, Vol. 1, Department of Meteorology, University of Stockholm, Sweden, pp. 93-95, 1998.

* (1544) Gu, D., S.G.H. Philander, and M.J. McPhaden, The Seasonal Cycle and Its Modulation in the Eastern Tropical Pacific Ocean, *Journal of Physical Oceanography, 27*, 2209-2218, 1998.

* (1545) Trenberth, K.E., G.W. Branstator, D. Karoly, A. Kumar, N.-C. Lau, and C. Ropelewski, Progress During TOGA in Understanding and Modeling Global Teleconnection Associated with Tropical Sea Surface Temperatures, *Journal of Geophysical Research, 103*(C7), 14,291-14,324, 1998.

* (1546) D'Andrea, F., S. Tibaldi, M. Blackburn, G. Boer, M. Deque, M.R. Dix, B. Dugas, L. Ferranti, T. Iwasaki, A. Kitoh, V. Pope, D. Randall, E. Roeckner, D. Straus, W. Stern, H. van den Dool, and D. Williamson, Northern Hemisphere Atmospheric Blocking as Simulated by 15 Atmospheric General Circulation Models in the Period 1979-1988, *Climate Dynamics, 14*, 385-407, 1998.

(1547) Soden, B.J., and V. Ramaswamy, Variations in Atmosphere-Ocean Solar Absorption under Clear Skies: A Comparison of Observations and Models, *Geophysical Research Letters, 25*(12), 2149-2152, 1998.

* (1548) Mellor, G.L., L.-Y. Oey, and T. Ezer, Sigma Coordinate Pressure Gradient Errors and the Seamount Problem, *Journal of Atmospheric and Oceanic Technology, 15*(5), 1122-1131,1998.

* (1549) Bush, A., and S.G.H. Philander, The Role of Ocean-Atmosphere Interactions in Tropical Cooling During the Last Glacial Maximum, *Science, 279*, 1341-1344, 1998.

* (1550) Gu, D., and S.G.H. Philander, Interdecadal Climate Fluctuations that Depend on Exchanges Between the Tropics and Extratropics, *Science, 275*, 805-807, 1997.

* (1551) Gruber, N., Anthropogenic CO_2 in the Atlantic Ocean, *Global Biogeochemical Cycles, 12*(1), 165-191, 1998.

(1552) Hamilton, K., Effects of an Imposed Quasi-biennial Oscillation in a Comprehensive Troposphere-Stratosphere-Mesosphere General Circulation Model, *Journal of the Atmospheric Sciences, 55*(14), 2393-2418, 1998.

* (1553) Klonecki, A., *Model Study of the Tropospheric Chemistry of Ozone*, Ph.D. Dissertation, Atmospheric and Oceanic Sciences Program, Princeton University, Princeton, NJ, 1998.

(1554) Soden, B.J., Tracking Upper Tropospheric Water Vapor Radiances: A Satellite Perspective, *Journal of Geophysical Research, 103*(D14), 17,069-17,081, 1998.

*In collaboration with other organizations

* (1555) Haywood, J.M., M.D. Schwarzkopf, and V. Ramaswamy, Estimates of Radiative Forcing Due to Modeled Increases in Tropospheric Ozone, *Journal of Geophysical Research, 103*(D14), 16,999-17,007, 1998.

* (1556) Haywood, J.M., V. Ramaswamy, and L.J. Donner, A Limited-Area-Model Case Study of the Effects of Sub-Grid Scale Variations in Relative Humidity and Cloud Upon the Direct Radiative Forcing of Sulfate Aerosol, *Geophysical Research Letters, 24*(2), 143-146, 1997.

(1557) Ramaswamy, V., and M.D. Schwarzkopf, Stratospheric Temperature Trends: Observations and Model Simulations, in *Stratospheric Processes and Their Role in Climate (SPARC)*, Proceedings of the 1st SPARC Assembly, Melbourne, Australia, 2-6 December 1996, World Climate Research Program, pp. 149-152, 1997.

(1558) Klein, S.A., Comments on "Moist Convective Velocity and Buoyancy Scales", *Journal of Atmospheric Sciences, 54*, 2775-2777, 1997.

* (1559) Oltmans, S.J., A.S. Lefohn, H.E. Scheel, J.M. Harris, H. Levy II, I.E. Galbally, E.-G. Brunke, C.P. Meyer, J.A. Lathrop, B.J. Johnson, D.S. Shadwick, E. Cuevas, F.J. Schmidlin, D.W. Tarasick, H. Claude, J.B. Kerr, O. Uchino, and V. Mohnen, Trends of Ozone in the Troposphere, *Geophysical Research Letters, 25*(2), 139-142, 1998.

* (1560) Wielicki, B., B. Barkstrom, B. Baum, T. Charlock, R. Green, D. Kratz, R. Lee, P. Minnis, G. Smith, T. Wong, D. Young, R. Cess, J. Coakley, A.H. Crommelynck, L. Donner, R. Kandel, M. King, A. Miller, V. Ramanathan, D. Randall, L. Stowe, and R. Welch, Clouds and the Earth's Radiant Energy System (CERES): Algorithm Overview, *IEEE Transactions on Geoscience and Remote Sensing, 36*(4), 1127-1141, 1998.

* (1561) Sarmiento, J.L., T.M.C. Hughes, R.J. Stouffer, and S. Manabe, Simulated Response of the Ocean Carbon Cycle to Anthropogenic Climate Warming, *Nature, 393*, 245-249, 1998.

(1562) Toggweiler, J.R., and B. Samuels, On the Ocean's Large-Scale Circulation at the Limit of No Vertical Mixing, *Journal of Physical Oceanography, 28*(9), 1832-1852, 1998.

* (1563) Sabine, C.L., and R.M. Key, Controls on fCO_2 in the South Pacific, *Marine Chemistry, 60*, 95-110, 1998.

* (1564) Peng, T.-H., R.M. Key, and H.G. Ostlund, Temporal Variations of Bomb Radiocarbon Inventory in the Pacific Ocean, *Marine Chemistry, 60*, 3-1, 1998.

* (1565) Broecker, W.S., S.L. Peacock, S. Walker, R. Weiss, E. Fahrbach, M. Schroeder, U. Mikolajewicz, C. Heinze, R. Key, T.-H. Peng, and S. Rubin, How Much Deep Water is Formed in the Southern Ocean?, *Journal of Geophysical Research, 103*(C8), 15,833-15,843, 1998.

(1566) Hamilton, K., Observations of Tropical Stratospheric Winds Before World War II, *Bulletin of the American Meteorological Society, 79*(7), 1367-1371, 1998.

* (1567) Hall, A., *The Role of Water Vapor Feedback in Unperturbed Climate Variability and Global Warming*, Ph.D. Dissertation, Atmospheric and Oceanic Sciences Program, Princeton University, 1998.

(1568) Lau, N.-C., El Niño: Child of the Pacific, *Twenty First Century*, bimonthly published by Institute of Chinese Studies, Chinese University of Hong Kong, *46*, 101-111, 1998.

*In collaboration with other organizations

* (1569) Boucher, O., S.E. Schwartz, T.P. Ackerman, T.L. Anderson, B. Bergstrom, B. Bonnel, P. Chylek, A. Dahlback, Y. Fouquart, Q. Fu, R.N. Halthore, J.M. Haywood, T. Iversen, S. Kato, S. Kinne, A. Kirkevag, K.R. Knapp, A. Lacis, I. Laszlo, M.I. Mishchenko, S. Nemesure, V. Ramaswamy, D.L. Roberts, P. Russell, M.E. Schlesinger, G.L. Stephens, R. Wagener, M. Wang, J. Wong, and F. Yang, Intercomparison of Models Representing Direct Shortwave Radiative Forcing by Sulfate Aerosols, *Journal of Geophysical Research*, 103(D14), 16,979-16,998, 1998.

* (1570) Delworth, T.L., and V.M. Mehta, Simulated Interannual to Decadal Variability in the Tropical-Subtropical Atlantic, *Geophysical Research Letters*, *25*(15), 2825-2828, 1998.

* (1571) Latif, M., D. Anderson, T. Barnett, M. Cane, R. Kleeman, A. Leetmaa, J. O'Brien, A. Rosati, and E. Schneider, A Review of the Predictability and Prediction of ENSO, *Journal of Geophysical Research*, *103*(C7), 14,375-14,393, 1998.

(1572) Orlanski, I., Poleward Deflection of Storm Tracks, *Journal of the Atmospheric Sciences*, *55*(16), 2577-2602, 1998.

* (1573) Bryan, K., The Role of Mesoscale Eddies in the Poleward Transport of Heat by the Oceans, *Physica D.*, *98*(2-4), 249-257, 1996.

*In collaboration with other organizations

MANUSCRIPTS SUBMITTED FOR PUBLICATION

(bj) Held, I.M., Planetary Waves and Their Interaction with Smaller Scales, in *The Life Cycles of Extratropical Cyclones*, Bergen Symposium on Extratropical Cyclones, edited by M. Spapiro, American Meteorological Society, January 1996.

* (bk) Numaguti, A., and Y. Hayashi, Gravity-Wave Dynamics of the Hierarchical Structure of Super Cloud Clusters, *Journal of the Atmospheric Sciences*, January 1996.

* (cg) Bryan, K., and S. Griffies, North Atlantic Climate Variability on Decadal Time-Scales: Is it Predictable?, *Izvestia Atmospheric & Oceanic Physics*, June 1996.

* (cp) Ezer, T., On Decadal Variabilities of the Upper Layers of the Subtropical North Atlantic: An Ocean Model Study, *Journal of Physical Oceanography*, March 1996.

* (cw) Milly, P.C.D., Factors Determining the Partitioning of Precipitation into Evaporation and Runoff, in *Global Energy and Water Cycles*, edited by K. Browning and R. Gurney, August 1996.

* (cx) Jungclaus, J.H., and G.L. Mellor, A Three-Dimensional Model Study of the Mediterranean Outflow, *Journal of Marine Systems*, August 1996.

* (cz) Gnanadesikan, A., and E.A. Terray, Evidence for Wave-Stirred and Wall Layers in a Strongly Forced Mixed Layer, *Journal of Physical Oceanography*, August 1996.

* (dd) Swanson, K.L., Downstream Development and the Dynamics of Nonlinear Baroclinic Wave Packets, *Journal of the Atmospheric Sciences*, August 1996.

(ei) Wu, C.-C., M. Bender, and Y. Kurihara, Evaluation of the GFDL Hurricane Prediction System in the Western North Pacific in 1995, *Weather and Forecasting*, January 1997.

(el) Garner, S.T., Blocking and Frontogenesis by Two-Dimensional Terrain in Baroclinic Flow, *Journal of the Atmospheric Sciences*, January 1997.

(ep) Sirutis, J., K. Miyakoda, and J. Lanzante, Eastward Propagation of Southern Oscillation Signals, *Tellus*, February 1997.

* (eq) Park, Y.-G., The Stability of Thermohaline Circulation in a Two-Box Model, *Journal of Physical Oceanography*, March 1997.

* (et) Winton, M., R. Hallberg, and A. Gnanadesikan, Simulation of Density-Driven Frictional Downslope Flow in Z-Coordinate Ocean Models, *Journal of Physical Oceanography*, April 1997.

* (ey) Toggweiler, J.R., B. Samuels, and R.M. Key, Why is the Deep Water Around Antarctica so Old?, Tracer Oceanography Monograph, American Geophysical Union, May 1997.

* (ez) Gnanadesikan, A., Representing the Bottom Boundary Layer in the GFDL Ocean Model: Model Framework, Dynamical Impacts, and Parameter Sensitivity, *Journal of Physical Oceanography*, May 1997.

* (fd) Pacanowski, R.C., and A. Gnanadesikan, Transient and Mean Response in a Z-level Ocean Model with Resolved Topography, *Journal of Geophysical Research*, June 1997.

(fe) Broccoli, A.J., N.-C. Lau, and M.J. Nath, The Cold Ocean-Warm Land Pattern: Model Simulation and Relevance to Climate Change Detection, *Journal of Climate*, June 1997.

* (fh) Yang, X.-Q., J.L. Anderson, and W.F. Stern, Reproducible Forced Modes in AGCM Ensemble Integrations and Potential Predictability of Atmospheric Seasonal Variations in the Extratropics, *Journal of Climate*, August 1997.

*In collaboration with other organizations

* (fi) Bender, M.A., and I. Ginis, Real Case Simulations of Hurricane-Ocean Interaction using a High Resolution Coupled Model: Effects on Hurricane Intensity, *Monthly Weather Review*, August 1997.

* (fj) Kushner, P.J., and I.M. Held, Potential-Vorticity-Thickness Fluxes and Wave-Mean-Flow Interaction, *Journal of the Atmospheric Sciences*, August 1997.

(fl) Hayashi, Y., and D.G. Golder, Sensitivity of Tropical Intraseasonal Oscillations to the Near-Surface Mean Wind: Idealized Model Experiments, *Journal of the Atmospheric Sciences*, September 1997.

* (fn) Murnane, R.J., J.L. Sarmiento, and C. LeQuéré, The Spatial Distribution of Air Sea-CO_2 Fluxes and the Interhemispheric Transport of Carbon by the Oceans, *Global Biogeochemical Cycles*, September 1997.

* (fp) Armstrong, R.A., J.L. Sarmiento, G.C. Hurtt, and S.W. Pacala, Food Web Models for Ocean Biogeochemistry, in *Marine Food Webs*, edited by A. Solow and D. DeAngelis, September 1997.

* (fq) Hurtt, G.C., and R.A. Armstrong, A Pelagic Ecosystem Model Calibrated with BATS and OWSI Data, *Deep-Sea Research*, September 1997.

* (fr) Ortiz, J.D., A.C. Mix, P. Wheeler, and R.M. Key, An Estimate of the Anthropogenic Offset of Oceanic $\delta^{13}C_{dic}$ Based on the Ventilation of the California Current at 42N, *Global Biogeochemical Cycles*, September 1997.

* (fs) Milly, P.C.D., and K.A. Dunne, Non-Detectability of 20th Century Trends in River Discharge from Large Basins--Observational and Model-Based Results, in *Proceedings of the 9th Symposium Global Change Studies*, October 1997.

* (fv) Klein, S.A., B.J. Soden, and N.-C. Lau, Remote Sea Surface Temperature Variations During ENSO: Evidence for a Tropical Atmospheric Bridge, *Journal of Climate*, October 1997.

(fy) Donner, L.J., C.J. Seman, and R.S. Hemler, Three-Dimensional Cloud System Modeling of GATE Convection, *Journal of the Atmospheric Sciences*, October 1997.

* (fz) Hall, A., and S. Manabe, Role of Water Vapor Feedback in Natural Variability and Global Warming: A Coupled Model Study, *Journal of Climate*, November 1997.

(ga) Ramaswamy, V., and S.M. Freidenreich, A High-Spectral Resolution Study of the Near-Infrared Solar Flux Disposition in Clear and Overcast Atmospheres, *Journal of Geophysical Research*, November 1997.

(gb) Milly, P.C.D., and K.A. Dunne, Upward Trend in River Flow Attributable to Smoke Aerosols from Tropical Biomass Burning, *Nature*, November 1997.

* (ge) Gnanadesikan, A., and R.W. Hallberg, Deficiencies of Traditional Form Drag and Sverdrupian Explanations for the Strength of the Circumpolar Current, *Journal of Physical Oceanography*, December 1997.

* (gf) Harshvardhan, W. Ridgway, V. Ramaswamy, S.M. Freidenreich, M. Batey, Spectral Characteristics of Solar Near-Infrared Absorption in Cloudy Atmospheres, *Journal of Geophysical Research*, December 1997.

(gg) Stouffer, R.J., and S. Manabe, Response of a Coupled Ocean-Atmosphere Model to Increasing Atmospheric Carbon Dioxide: Sensitivity to the Rate of Increase, *Journal of Climate*, December 1997.

* (gh) Gnanadesikan, A., Numerical Issues for Coupling Biological Models with Isopycnal Mixing Schemes, *Journal of Marine Research*, December 1997.

*In collaboration with other organizations

(gk) Delworth, T.L., S. Manabe, and R.J. Stouffer, Simulations of Natural and Forced Variability in the North Atlantic, in *Proceedings of the Atlantic Climate Change Program Meeting*, Lamont-Doherty Earth Observatory, Palisades, NY, September 1997.

(gl) Hamilton, K., Dynamical Coupling of the Lower and Middle Atmosphere: Historical Background to Current Research, *Journal of Atmospheric and Terrestrial Physics*, January 1998.

* (gm) Held, I.M., and T. Schneider, The Surface Branch of the Zonally Averaged Mass Transport Circulation in the Troposphere, *Journal of the Atmospheric Sciences*, January 1998.

(gn) Delworth, T.L., J.D. Mahlman, and T.R. Knutson, Changes in Heat Index Associated with CO_2-induced Global Warming, *Climatic Change*, January 1998.

* (go) Yienger, J.J., A.A. Klonecki, H. Levy II, W.J. Moxim, and G.R. Carmichael, An Evaluation of Chemistry's Role in the Winter-Spring Ozone Maximum Found in the Northern Mid-Latitude Free Troposphere, *Journal of Geophysical Research*, February 1998.

* (gq) Wittenberg, A.T., and J.L. Anderson, Dynamical Implications of Forcing a Model with Prescribed Components, *Journal of Climate*, February 1998.

* (gr) Zhang, Y., and I.M. Held, A Linear Stochastic Model of a GCM's Midlatitude Stormtracks, *Journal of the Atmospheric Sciences*, February 1998.

* (gs) Sarmiento, J.L., T.M.C. Hughes, R.J. Stouffer, and S. Manabe, Response of the Ocean Carbon Cycle to Anthropogenic Climate Warming, *Nature*, February 1998.

(gt) Hamilton, K., Dynamics of the Tropical Middle Atmosphere: A Tutorial Review, *Atmosphere-Ocean Special Issue*, February 1998.

* (gv) Gnanadesikan, A., A Global Model of Silica: Sensitivity to Eddy Parameterization and Remineralization, *Global Biogeochemical Cycles*, March 1998.

* (gw) Larson, K., D.L. Hartmann, and S.A. Klein, On the Role of Clouds, Water Vapor, Circulation and Boundary Layer Structure in the Sensitivity of the Tropical Climate, *Journal of Climate*, March 1998.

* (gx) Jakob, C., and S.A. Klein, The Role of Vertically Varying Cloud Fraction in the Parameterization of Microphysical Processes in the ECMWF Model, *Quarterly Journal of the Royal Meteorological Society*, March 1998.

* (gy) Park, Y.-G., and K. Bryan, Intercomparison of Thermally Driven Circulation from a Depth Coordinate Model and an Isopycnal Layer Model, Part I. A Scaling - the Sensitivity to the Vertical Diffusivity, *Journal of Physical Oceanography*, April 1998.

(hb) Mahlman, J.D., Science and Non-Science Concerning Human-Caused Climate Warming, *Annual Review of Energy and the Environment*, April 1998.

* (hc) Shen, W., R.E. Tuleya, and I. Ginis, A Sensitivity Study of Atmospheric Static Stability on GFDL Model Hurricane Intensity: Implications for Global Warming, *Journal of Climate*, April 1998.

* (hd) Wallace, J.M., D.W.J. Thompson, G.C. Hegerl, A.J. Broccoli, and N.-C. Lau, Contribution of the Arctic Oscillation to Recent Wintertime Surface Air Temperature Trends, *Science*, April, 1998.

* (he) Anderson, J., H. van den Dool, A. Barnston, W. Chen, W. Stern, and J. Ploshay, Present Day Capabilities of Numerical and Statistical Models for Atmospheric Extratropical Seasonal Prediction, *Bulletin of the American Meteorological Society*, May 1998.

(hf) Hemler, R.S., Key Elements of the User-Friendly GFDL SKYHI General Circulation Model, 2nd International Workshop on Software Engineering and Code Design in Parallel Meteorological and Oceanographic Applications, Scottsdale, AZ, June 1998.

*In collaboration with other organizations

* (hg) Jungclaus, J.H., A Three-Dimensional Simulation of the Formation Anticyclonic Lenses (Meddies) by the Instability of an Intermediate Depth Boundary current, *Journal of Physical Oceanography*, May 1998.

* (hi) Ezer, T., Sensitivity Studies with the North Atlantic Princeton Ocean Model, *Deep-Sea Research*, May 1998.

* (hj) Ezer, T., and G.L. Mellor, Mesoscale Variability in the North Atlantic Ocean: Model Simulations and Assimilation of Three Years of Topex/Poseidon Altimeter Data, *Deep-Sea Research*, May 1998.

(hk) Winton, M., Polar Water Column Stability, *Journal of Physical Oceanography*, May 1998.

* (hl) Rodin, A.V., R.T. Clancy, R.J. Wilson, M.J. Wolff, and M.I. Richardson, Thermal Feedback Between Dust and Water Ice Clouds in the Mars Atmosphere: Implications for the Aphelion Climate, *Icarus*, May 1998.

* (hm) Norris, J.R., and S.A. Klein, Low Cloud Type Over the Ocean from Surface Observations, Part III: Relationship to Vertical Motion and the Regional Surface Synoptic Environment, *Journal of Climate*, June 1998.

* (hn) Stouffer, R.J., G. Hegerl, and S. Tett, A Comparison of Surface Air Temperature Variability in Three 1000-Year Coupled Ocean-Atmosphere Model Integrations, *Journal of Climate*, May 1998.

* (ho) Klein, S.A., and C. Jakob, Validation and Sensitivities of Frontal Clouds, *Monthly Weather Review*, June 1998.

* (hp) Andronache, C., L.J. Donner, C.J. Seman, V. Ramaswamy, and R.S. Hemler, Atmospheric Sulfur and Deep Convective Clouds in the Tropical Pacific: A Model Study, *Journal of Geophysical Research*, June 1998.

(hq) Manabe, S., and R.J. Stouffer, Are Two Modes of Thermohaline Circulation Stable?, *Tellus*, June 1998.

(hr) Wetherald, R.T., and S. Manabe, Detectability of Summer Dryness Caused by Greenhouse Warming, *Climate Change*, June 1998.

* (hs) Vitart, F., J.L. Anderson, and W.F. Stern, Impact of Large Scale Circulation on Tropical Storm Frequency, Intensity, and Location Simulated by an Ensemble of GCM Integrations, *Journal of Climate*, June 1998.

* (ht) Milly, P.C.D., Comment on "Antiphasing Between Rainfall in Africa's Rift Valley and North America's Great Basin", *Quaternary Research*, June 1998.

* (hu) Kushner, P.J., and I.M. Held, A Direct Test, using Atmospheric Data, of a Method for Estimating Oceanic Eddy Diffusivity, *Geophysical Research Letters*, June 1998.

* (hv) Waliser, D.E., Z. Shi, J.R. Lanzante, and A.H. Oort, The Hadley Circulation: Comparing Reanalysis and Sparse In-Situ Estimates, *Climate Dynamics*, June 1998.

(hw) Soden, B.J., The Sensitivity of the Tropical Hydrological Cycle to ENSO, *Journal of Climate*, June 1998.

* (hx) Pincus, R., S.A. McFarlane, and S.A. Klein, Albedo Bias and the Horizontal Variability of Clouds in Subtropical Marine Boundary Layers: Observations from Ships and Satellites, *Journal of Geophysical Research*, July 1998.

(hy) Knutson, T.R., and S. Manabe, Model Assessment of Decadal Variability and Trends in the Tropical Pacific Ocean, *Journal of Climate*, April 1997.

(hz) Knutson, T.R., and R.E. Tuleya, Increased Hurricane Intensities with CO_2-Induced Warming as Simulated using the GFDL Hurricane Prediction System, *Climate Dynamics*, July 1998.

*In collaboration with other organizations

(ia) Held, I.M., The Macroturbulence of the Troposphere, *Tellus*, July 1998.

* (ib) Goddard, L., and S.G.H. Philander, On the Energetics of ENSO, *Journal of Climate*, July 1998.

(ic) Manabe, S., and R.J. Stouffer, A Study of Abrupt Climate Change by a Coupled Ocean-Atmosphere Model, *Quaternary Science Review*, July 1998.

* (id) Gnanadesikan, A., and J.R. Toggweiler, Constraints Placed by Silica Cycling on Oceanic Vertical Exchange, *Science*, July 1998.

(ie) Hallberg, R., Time Integration of Diapycnal Diffusion and Richardson Number Dependent Mixing in Isopycnal Coordinate Ocean Models, *Monthly Weather Review*, July 1998.

* (if) Toggweiler, J.R., I. Held, B. Samuels, and H. Ho, Effect of Drake Passage on Temperature Differences Between the Northern and Southern Hemispheres, *Nature*, July 1998.

* (ig) Denning, A.S., M. Holzer, K.R. Gurney, M. Heimann, R.M. Law, P.J. Rayner, I.Y. Fung, S-M. Fan, S. Taguchi, P. Friedlingstein, Y. Balkanski, M. Maiss, and I. Levin, Three-Dimensional Transport and Concentration of SF6: A Model Intercomparison Study (TransCom 2), *Tellus*, December 1997.

* (ih) Fan, S., M. Gloor, J. Mahlman, S. Pacala, J. Sarmiento, T. Takahashi, and P. Tans, Atmospheric and Oceanic CO_2 Data and Models Imply a Large Terrestrial Carbon Sink in North America, *Science*, May 1998.

* (ii) Fan, S-M., T.L. Blaine, and J.L. Sarmiento, Terrestrial Carbon Sink in the Northern Hemisphere Since 1959, *Tellus*, July 1998.

* (ij) Armstrong, R.A., Stable Food Web Structures for Pelagic Ecosystem Models with Multiple Phytoplankton Taxa, *Journal of Plankton Research*, December 1997.

* (ik) Armstrong, R.A., A Model of Iron-Ammonium-Light CO-Limitation of Nitrate Uptake and Phytoplankton Growth, *Limnology and Oceanography*, June 1998.

(il) Schwarzkopf, M.D., and V. Ramaswamy, Radiative Effects of CH_4, N_2O, Halocarbons and the Foreign-Broadened H_2O Continuum: A GCM Experiment, *Journal of Geophysical Research*, July 1998.

* (im) Mashiotta, T.A., D.W. Lea, and J.R. Toggweiler, Planktic Cd Indicates Lower Nutrients in the Glacial Subantarctic, *Paleoceanography*, June 1998.

* (in) Joussaume, S., K.E. Taylor, P. Braconnot, J.F.B. Mitchell, J. Kutzbach, S.P. Harrison, I.C. Prentice, A.J. Broccoli, A. Abe-Ouchi, P.J. Bartlein, C. Bonfils, B. Dong, J. Guiot, K. Herterich, C.D. Hewitt, D. Jolly, J.W. Kim, A. Kislov, A. Kitoh, V. Masson, B. McAvaney, N. McFarlane, N. de Noblet, W.R. Peltier, J.Y. Peterschmitt, D. Pollard, D. Rind, J.F. Royer, M.E. Schlesinger, J. Syktus, S. Thompson, P. Valdes, G. Vettoretti, R.S. Webb, and U. Wyputta, Monsoon Changes for 6000 Years Ago: Results of 18 Simulations from the Paleoclimate Modeling Intercomparison Project (PMIP), *Science*, August 1998.

* (io) Andronache, C., L.J. Donner, V. Ramaswamy, C.J. Seman, and R.S. Hemler, Possible Impact of Atmospheric Sulfur Increase on Tropical Convective Systems: A TOGA COARE Case, COARE 98 Extended Abstract Volume, in *Proceedings of the COARE 98 Conference*, Boulder, CO, July 1998.

* (ip) Mellor, G., S. Hakkinen, and T. Ezer, *A Generalization of a Sigma Coordinate Ocean Model and an Intercomparison of Model Vertical Grids, Ocean Forecasting: Theory and Practice*, Springer Publishing, edited by N. Pinardi, August 1998.

(iq) Donner, L.J., and C.J. Seman, The Role of Ice Sedimentation in the Microphysical and Radiative Budgets of COARE Convective Systems, in *Proceedings of the COARE 98 Conference*, Boulder, CO, July 1998.

*In collaboration with other organizations

* (ir) Harper, S., Thermocline Ventilation and Pathways of Tropical-Subtropical Water Mass Exchange, *Tellus*, August 1998.

(is) Lau, N.-C., and M.J. Nath, Observed and GCM-Simulated Westward-Propagating, Planetary-Scale Fluctuations with ~3-week Periods, *Monthly Weather Review*, August 1998.

(it) Hamilton, K., R.J. Wilson, and R.S. Hemler, Climatology of the Middle Atmosphere Simulated with High Vertical and Horizontal Resolution Versions of a General Circulation Model: Improvements in the Cold Pole Bias and Generation of a QBO-Like Oscillation in the Tropics, *Journal of the Atmospheric Sciences*, August 1998.

* (iu) Koshyk, J., and K. Hamilton, Mesoscale Spectral Regime Simulated in a Global Climate Model, *Science*, August 1998.

* (iv) Schneider, T., and S.M. Griffies, A Conceptual Framework for Predictability Studies, *Journal of Climate*, September 1998.

*In collaboration with other organizations

BIBLIOGRAPHY
1995-1998
CROSS REFERENCE BY AUTHOR

APPENDIX C

Seminars Given at GFDL

During Fiscal Year 1998

7 October 1997	Driving Northern Hemisphere Climate Change from the Southern Hemisphere, by Dr. J.R. Toggweiler, Mrs. Bonnie Samuels, and Mr. Matthew Harrison, Geophysical Fluid Dynamics Laboratory, Princeton, NJ
8 October 1997	Double Hemisphere Thermohaline Flows: How Big, How Many and When?, by Dr. Barry Klinger, Nova Southeastern University, Fort Lauderdale, FL
9 October 1997	Comparison of Elastic-Viscous-Plastic and Viscous-Plastic Sea Ice Dynamics Models, by Dr. Elizabeth Hunke, Theoretical Division, Los Alamos National Laboratory, Los Alamos, NM
14 October 1997	Towards "Predicted" Cloud Distributions in SKYHI GCM Simulations, by Dr. V. Ramaswamy, Geophysical Fluid Dynamics Laboratory, Princeton, NJ
17 October 1997	Dynamical Implications of Forcing a Model with a Prescribed Boundary, by Andrew Wittenberg, Atmospheric and Oceanic Sciences Program, Princeton University, Princeton, NJ
21 October 1997	The Sensitivity of Thermally Driven Circulation in MOM and HIM, by Drs. Young-Gyu Park and Kirk Bryan, Atmospheric and Oceanic Sciences Program, Princeton University, Princeton, NJ
23 October 1997	Mixing in the Ocean, by Dr. James Ledwell, Woods Hole Oceanographic Institution, Woods Hole, MA
27 October 1997	Modeling of the East Sea (Japan Sea) using MOM-Separation of the Western Boundary Current and the Deep Current in the East Sea, by Dr. Cheoi-Ho Kim, Korea Ocean Research and Development, Seoul, Korea
30 October 1997	Aerosols in the Marine Boundary Layer: Tracking Mixed Particle Growth and using Particles to Track Mixing, by Prof. Lynn M. Russell, School of Engineering and Applied Science, Princeton University, Princeton, NJ
31 October 1997	A New Multiple Band Solar Radiative Parameterization, by Stuart Freidenreich and Dr. V. Ramaswamy, Geophysical Fluid Dynamics Laboratory, Princeton, NJ
4 November 1997	Recent Developments in the Longwave Radiative Transfer Parameterization, by M. Daniel Schwarzkopf, Geophysical Fluid Dynamics Laboratory, Princeton, NJ
6 November 1997	Modeling Equatorial/Subtropical Exchange for the Pacific Ocean, by Dr. Keith Rodgers, Lamont-Doherty Earth Observatory, Palisades, NY
7 November 1997	Ensemble Transformation and Adaptive Observations, by Dr. Craig Bishop, Pennsylvania State University, University Park, PA
13 November 1997	Assessment of Interfacial Stress Parameterizations for OGCMs, by Dr. Jun She, Center for Coastal Physical Oceanography, Old Dominion University, Norfolk, VA

18 November 1997	The Thermohaline Circulation in the Limit of Small Diapycnal Diffusion, by Dr. Robert Hallberg, Geophysical Fluid Dynamics Laboratory, Princeton, NJ
20 November 1997	Decadal Climate Variability in the North Atlantic Sector: An Oceanographic Perspective, by Dr. Martin Visbeck, Lamont-Doherty Earth Observatory, Palisades, NY
25 November 1997	Radiative Effects of Aerosols and Tropospheric Ozone, by Dr. James Haywood, Atmospheric and Oceanic Sciences Program, Princeton University, Princeton, NJ
1 December 1997	Atmospheric Convection-Diffusion with Checkerboard Surface Conditions, by Prof. John R. Philip, CSIRO, Canberra, Australia
2 December 1997	A Numerical Study of the Yellow Sea and the East China Sea, by Dr. Hyun-Chul Lee, Atmospheric and Oceanic Sciences Program, Princeton University, Princeton, NJ
4 December 1997	Absorption of Solar Radiation by a Cloudy Atmosphere: Interpretation from Co-Located Aircraft Measurements, by Dr. Robert Cess, Institute for Terrestrial and Planetary Atmosphere, Marine Sciences Research Center, State University of New York, Stony Brook, NY
5 December 1997	A Comparison of the Role of Water Vapor Feedback in Natural Variability and Global Warming using a Coupled Ocean-Atmosphere Model, by Dr. Alex Hall, Atmospheric and Oceanic Sciences Program, Princeton University, Princeton, NJ
10 December 1997	The Vertical Structure of Turbulence in the Ocean Surface Layer, by Dr. Gene Terray, Woods Hole Oceanographic Institution, Woods Hole, MA
15 December 1997	Near-Global Ocean Simulation with the Miami Isopycnic Coordinate Ocean Model, by Dr. Shan Sun, University of Miami, Miami, FL
18 December 1997	The Anomalous 1990s: Implications for ENSO Prediction, by Dr. Ming Ji, National Center for Environmental Prediction, Camp Springs, MD
8 January 1998	Dynamics and Variability of a Zonal Averaged Coupled Climate Model, by Dr. Halldor Bjornsson, McGill University, Montreal, Canada
29 January 1998	A Perspective on Remote Sensing Observing Systems for the Climate Sciences, by Dr. Graeme L. Stephens, Department of Atmospheric Sciences, Colorado State University, Fort Collins, CO
30 January 1998	An Evaluation of the NCEP RSM for Regional Climate Modeling, by Dr. Song-You Hong, Environmental Modeling Center, National Centers for Environmental Prediction, Camp Springs, MD
11 February 1998	Aerosol Properties and Radiative Effects in the U.S. East Coast Haze Plume, by Dr. Philip B. Russell, NASA/Ames Research Center, Moffett Field, CA

11 February 1998	ENSO 97/98: Its Impact on the Long Lead U.S. Seasonal Temperature and Precipitation Predictions, by Dr. Huug van den Dool, National Centers for Environmental Prediction, Camp Springs, MD
12 February 1998	Ensemble Forecasting of Tropical Cyclones and Adaptive Observations, by Dr. Sim D. Aberson, Hurricane Research, Atlantic Oceanographic and Meteorological Laboratories, Miami, FL
20 February 1998	Computationally Efficient Modeling of Atmospheric Processes, by Dr. Herschel A. Rabitz, Chemistry Department, Princeton University, Princeton, NJ
10 March 1998	Comparison of ECMWF Frontal Clouds to ISCCP Satellite Observations, by Dr. Steven Klein, Geophysical Fluid Dynamics Laboratory, Princeton, NJ
17 March 1998	Effects of Stability in Tropical Storm Intensity: Global Warming Implications, by Robert Tuleya, Geophysical Fluid Dynamics Laboratory, Princeton, NJ, and Weixing Shen and Isaac Ginis, Graduate School of Oceanography, University of Rhode Island, Narragansett, RI
24 March 1998	Resurrecting the Polar Nutrient Hypothesis for Glacial-Interglacial CO_2, by Dr. J. R. Toggweiler, Geophysical Fluid Dynamics Laboratory, Princeton, NJ
26 March 1998	Ice Shelf - Ocean Interaction, by Dr. David Holland, Lamont-Doherty Earth Observatory, Palisades, NY
30 March 1998	Intensification of Tropical-Cyclone-Like Vortices in Zonal Flows, by Dr. Klaus Dengler, Department of Earth and Atmospheric Sciences, State University of New York, Albany, NY
31 March 1998	Simulated Increase of Hurricane Intensities in a CO_2-Warmed Climate, by Thomas Knutson, Robert Tuleya, and Dr. Y. Kurihara, Geophysical Fluid Dynamics Laboratory, Princeton, NJ
3 April 1998	Trends in the Development of Parallel Ocean Models, by Dr. Matthew T O'Keefe, Department of Electrical and Computer Engineering, University of Minnesota, Minneapolis, MN
6 April 1998	The Influence of Cloud-Aerosol Interactions on Cloud Properties and Possible Implications to Climate, by Dr. Tamir G. Reisin, Department of Geophysics and Planetary Sciences, Tel Aviv University, Tel Aviv, Israel
8 April 1998	The Lake Victoria - Lake Lohantan Oscillation, by Dr. Wallace S. Broecker, Lamont-Doherty Earth Observatory, Palisades, NY
9 April 1998	The Transient Behavior of Baroclinic Waves Near Orography, by Dr. Christopher Davis, National Center for Atmospheric Research, Boulder, CO
13 April 1998	The Global Climate Change Signal in the Co-variability of Global SSTs and U.S. Climate Division Temperatures, by Dr. Robert E. Livezey, Climate Prediciton Center/NCEP, Camp Springs, MD

14 April 1998	A Case Study of Quasi-Isentropic Transport Processes in Mid- and High-Latitudes, by Dr. Christian Marquardt, Institute for Meteorology, Free University of Berlin, Berlin, Germany
14 April 1998	The Sensitivity of the Tropical Hydrological Cycle to ENSO, by Dr. Brian Soden, Geophysical Fluid Dynamics Laboratory, Princeton, NJ
20 April 1998	Nonlinear ENSO Response to Greenhouse Warming, by Dr. Axel Timmermann, Max-Planck Institute of Meteorology, Hamburg, Germany
21 April 1998	Sensitivity of Tropical Intraseasonal Oscillations to Cloud and Evaporation Feedback, by Dr. Y. Hayashi and Mr. Donald Golder, Geophysical Fluid Dynamics Laboratory, Princeton, NJ
22 April 1998	The Equatorial MLT Region: Intraseasonal, Planetary, and Gravity Waves and their Relationship to Interannual Variability in the Tropical Pacific, by Dr. Robert Vincent, Department of Physics, University of Adelaide, Adelaide, Australia
23 April 1998	Mid-latitude Seasonal Predictability and Intraseasonal Dynamics from the Dynamical Seasonal Predictability Project, by Dr. David Strauss, Center for Ocean-Land-Atmosphere Studies, Calverton, MD
27 April 1998	Prototypes for Ocean-Atmosphere Interaction at Midlatitudes, by Prof. David Neelin, University of California, Los Angeles, CA
27 April 1998	The Accuracy of a Tangent Linear Model with Moist Physics, by Dr. Ronald Errico, National Center for Atmospheric Research, Boulder, CO
28 April 1998	Entrainment in Convectively Driven PBLs: An Assessment of Errors and Uncertainties in Numerical Modeling Studies, by Dr. Bjorn Stevens, National Center for Atmospheric Research, Boulder, CO
29 April 1998	Drizzle, Martine Stratocumulus and Aerosol Indirect Effects, by Dr. Bjorn Stevens, National Center for Atmospheric Research, Boulder, CO
29 April 1998	Impacts of Double-Diffusive Processes on the Thermohaline Circulation, by Mr. Jubao Zhang, MIT/Woods Hole Joint Program, Massachusetts Institute of Technology, Cambridge, MA
30 April 1998	Modeling of Soil Dust Aerosols, by Dr. Ina Tegen, Department of Applied Physics, Columbia University, NASA/Goddard Institute for Space Studies, New York, NY
5 May 1998	Correction of Systematic Errors in Coupled GCM Forecasts, by Dr. Xiu-Qun Yang, Atmospheric and Oceanic Sciences Program, Princeton University, Princeton, NJ
6 May 1998	On the Sensitivity of the Ocean's Circulations to High-Latitude Surface Conditions, by Prof. Achim Stoessel, Department of Oceanography, Texas A & M University, College Station, TX

7 May 1998	Interfacing Field Experimental Data with GCM Parameterizations: Methodology and Application to CCM3, by Prof. Minghua Zhang, State University of New York, Stony Brook, NY
8 May 1998	Horizontal Spectra in the High-Resolution SKYHI Simulations, by Dr. John Koshyk, Department of Physics, University of Toronto, Toronto, Canada
12 May 1998	The Role of Water Vapor Feedback in Natural and Anthropogenic Variations of the Global Hydrologic Cycle, by Alexander Hall, Atmospheric and Oceanic Sciences Program, Princeton University, Princeton, NJ
13 May 1998	Modeling Sea-Ice as a Granula Material, by Dr. Bruno Tremblay, Lamont-Doherty Earth Observatory, Palisades, NY
14 May 1998	Semi-Lagrangian and Finite-Element Methods in Ocean Modeling, by Dr. Daniel Le Roux, McGill University, Montreal, Canada
19 May 1998	Climate Drift and Initialization Issues Related to Coupled Climate Models, by Mr. Keith Dixon, Geophysical Fluid Dynamics Laboratory, Princeton, NJ
28 May 1998	Atmosphere-Ocean Interactions in the Tropical Pacific and Atlantic, by Prof. Carlos R. Mechoso, Department of Atmospheric Sciences, University of California, Los Angeles, CA
29 May 1998	Vortex Intensification by Convectively Forced Rossby Waves, by Dr. Michael Montgomery, Department of Atmospheric Science, Colorado State University, Fort Collins, CO
2 June 1998	A Test, Using Atmospheric Data, of a Method for Estimating Oceanic Eddy Diffusivities, by Dr. Paul Kushner, Atmospheric and Oceanic Sciences Program, Princeton University, Princeton, NJ
4 June 1998	A Possible Negative Feedback Mechanism for ENSO Transition, by Dr. Bin Wang, Department of Meteorology, University of Hawaii, Honolulu, HI
8 June 1998	Effect of Sulfate Aerosols on Cloud Microphysics: A Case Study, by Dr. Harshvardhan, Department of Earth and Atmospheric Sciences, Purdue University, West Lafayette, IN
8 June 1998	Mechanisms of Variability in Mode Water Formation, by Dr. Wilco Hazeleger, KNMI Oceanographic Research, The Netherlands
9 June 1998	Stratospheric Data Assimilation, by Dr. Richard Swinbank, Universities Space Research Association, Seabrook, MD
16 June 1998	Monte Carlo Prediction and Data Assimilation: How Lucky Can You Get?, Dr. Jeffrey Anderson, Geophysical Fluid Dynamics Laboratory, Princeton, NJ
23 June 1998	Horizontal Inhomogeneity in Cirrus Clouds Observed During FIRE, by Samantha Smith, NASA/Goddard Institute for Space Studies, New York, NY

7 July 1998	Tropical Dynamics Near the Stratopause: The 2-Day Wave and its Relatives, by V. Limpasuvan, University of Washington, Seattle, WA
14 July 1998	Energizing the Ocean's Circulation for Climate Change ("Water-Planet" Model), by J.R. Toggweiler and Bonnie Samuels, Geophysical Fluid Dynamics Laboratory, Princeton, NJ
15 July 1998	Parameterizing Mesoscale Eddy Transport in Ocean Circulation Models, by Dr. Richard Greatbatch, Dalhousie University, Halifax, Nova Scotia, Canada
28 July 1998	Introduction to MPP, by Dr. V. Balaji, Cray Computer at Geophysical Fluid Dynamics Laboratory, Princeton, NJ
3 August 1998	Parallel Supercomputing 1992-2002, by Horst D. Simon, Director, National Energy Research Scientific Computing (NERSC) Division, Lawrence Berkeley National Laboratory/DOE, Berkeley, CA
4 August 1998	MOM3 Reviewed, by S. Griffies and R. Pacanowski, Geophysical Fluid Dynamics Laboratory, Princeton, NJ
3 September 1998	Dynamics of the Mediterranean Salinity Tongue, by James Stephens, Department of Meteorology, University of Reading, Reading, United Kingdom
15 September 1998	Sensitivity Studies with an Adjoint OGCM, by Dr. Ralf Giering, Massachusetts Institute of Technology, Cambridge, MA
16 September 1998	Constructing the Adjoint of A/OGCMs: Finite Difference of Adjoint or Adjoint of Finite Difference?, by Dr. Ziv Sirkes, Center for Ocean and Atmospheric Modeling, Institute of Marine Sciences, University of Southern Mississippi, Stennis Space Center, MS
16 September 1998	An Analysis of the Mechanisms for the QBO in Ozone in the Tropical and Subtropical Stratosphere, by Dr. Dylan Jones, Department of Earth and Planetary Sciences, Harvard University, Cambridge, MA

APPENDIX D

Talks, Seminars, and Papers Presented Outside GFDL

During Fiscal Year 1998

6 October 1997	Dr. Charles T. Gordon "Tropical Sensitivity to Specified ISCCP Low Clouds in a Coupled Model", 22nd Annual Climate Diagnostics and Prediction Workshop, Berkeley, CA
6 October 1997	Dr. Jeffrey L. Anderson "Seasonal-Interannual Predictions from an Ensemble of Fully-Coupled Ocean-Atmosphere GCM Integrations", 22nd Annual Climate Diagnostics and Prediction Workshop, Berkeley, CA
7 October 1997	Mr. Thomas R. Knutson "Simulated Increase of Hurricane Intensities in a CO_2-Warmed Climate", EPA Climate Change and Extreme Events Workshop, Washington, DC
16 October 1997	Mr. Anthony J. Rosati "Status of GFDL Seasonal/Interannual Prediction", IRI Modeling and Prediction Workshop, Palisades, NY
16 October 1997	Dr. Jeffrey Anderson "Seasonal Interannual Prediction at GFDL", IRI Modeling and Prediction Workshop, Palisades, NY
18 October 1997	Dr. Yoshio Kurihara "Interaction of Typhoons with the Ocean and the Land", Yonsei University, Seoul, Korea
20 October 1997	Dr. Yoshio Kurihara "Outlook for Improvement of Typhoon Prediction", Korea Meteorological Administration, Seoul, Korea
21 October 1997	Dr. Yoshio Kurihara "Scale Interaction in Typhoon Dynamics", Seoul National University, Seoul, Korea
21 October 1997	Dr. Brian D. Gross "A Comparison of Hydrostatic and Non-hydrostatic Trajectories over Topography with the New GFDL Mesoscale Models", 2nd Meeting of NOAA Mesoscale Modelers, Boulder, CO
22 October 1997	Dr. John R. Toggweiler "Driving Northern Hemisphere Climate Change from the Southern Hemisphere", Harvard University, Cambridge, MA
23 October 1997	Dr. Yoshio Kurihara "Typhoon Forecast Using the GFDL Prediction System", Korea Meteorological Society Meeting, Seoul, Korea
31 October 1997	Dr. Hiram Levy II "Tropospheric Ozone: The Natural Background, the Impact of Human Activity, and the Different Roles of Chemistry", University of Michigan, Ann Arbor, MI

31 October 1997	Dr. Jeffrey Anderson "Seasonal Prediction with Coupled Models", University of Maryland, College Park, MD
5 November 1997	Dr. Jerry D. Mahlman "Climate Change: Science and Policy", Woodrow Wilson School for Public Policy, Princeton University, Princeton, NJ
6 November 1997	Dr. Bruce B. Ross "Status and Plans for NOAA/HPCC High Performance Computing", NOAA HPCC Council Meeting, Silver Spring, MD
6 November 1997	Dr. Hiram Levy II "Asian Emissions and their Impact on Tropospheric Ozone", China MAP Meeting, Atlanta, GA
12 November 1997	Dr. Robert W. Hallberg "The Ocean's Thermohaline Circulation in the Limit of Weak Diapycnal Diffusion", Massachusetts Institute of Technology, Cambridge, MA
12 November 1997	Dr. Brian Soden "Impact of GOES Winds on GFDL Hurricane Model Forecasts", Workshop of GOES and Numerical Weather Prediction, Camp Springs, MD
13 November 1997	Dr. Jeffrey Anderson "Predictability of SSTs and Implications for DSP", DSP/PROVOST Seasonal Prediction Workshop, European Centre for Medium Range Weather Forecasts, Reading, United Kingdom
14 November 1997	Dr. John R. Toggweiler "Driving Northern Hemisphere Climate Change from the Southern Hemisphere", Lamont-Doherty Earth Observatory, Palisades, NY
17 November 1997	Dr. Jeffrey Anderson "Use of Ensembles in DERF", World Meteorological Organization Workshop on Dynamical Extended Range Forecasting, Toulouse, France
17 November 1997	Dr. V. Ramaswamy "Updates on Stratospheric Temperature Trends Analyses", Scientific Steering Group Meeting of SPARC, Port Jefferson, NY
17 November 1977	Dr. Kevin P. Hamilton "Gravity Wave Processes and Parameterization", Scientific Steering Group Meeting of SPARC, Port Jefferson, NY
19 November 1997	Dr. Robert Hallberg "The Ocean's Thermohaline Circulation in the Limit of Small Diapycnal Diffusion", Courant Institute, New York, NY

23 November 1997	Dr. Thomas L. Delworth "Simulation of Natural and Forced Variability in the North Atlantic", North Atlantic Ocean Modeling for Climate Studies Workshop, Goddard Institute for Space Studies, New York, NY
24 November 1997	Dr. Hiram Levy II "A Global Study of Human Impact on Tropospheric Ozone and its Chemistry", Atmospheric Environmental Research, Inc., Cambridge, MA
24 November 1997	Dr. Stephen Griffies "North Atlantic Predictability and Ocean Modeling", North Atlantic Ocean Modeling for Climate Studies Workshop, Goddard Institute for Space Studies, New York, NY
8 December 1997	Mr. R. John Wilson "Comparison of GCM Results with Viking and Mariner 9 Data and Implications for the Interpretation of MGS Atmospheric Temperature Data", 1997 American Geophysical Union Fall Meeting, San Francisco, CA
8 December 1997	Dr. Jeffrey Anderson "Seasonal/Interannual Prediction with Coupled Models", University of Utah, Salt Lake City, UT
8 December 1997	Dr. Hiram Levy "Simulation and Quantification of Human Impact on Tropospheric Ozone over the North Atlantic", 1997 American Geophysical Union Fall Meeting, San Francisco, CA
9 December 1997	Mr. Anthony J. Broccoli "Simulated Spatial Variability of Glacial Cooling: Implications for the Reconstruction of Past Climates", 1997 American Geophysical Union Fall Meeting, San Francisco, CA
11 December 1997	Dr. Thomas L. Delworth "Decadal to Centennial Variability in the North Atlantic as Simulated by a Coupled Ocean-Atmosphere Model", 1997 American Geophysical Union Fall Meeting, San Francisco, CA
15 December 1997	Dr. Kevin P. Hamilton "Stratospheric Chemistry/Transport Experiments in a General Circulation Model", Canadian Middle Atmosphere Model Annual Scientific Workshop, Toronto, Canada
12 January 1998	Dr. Isaac M. Held "The Strength of the Hadley Cell and Partitioning of Heat Transport Between Atmosphere and Ocean", American Meteorological Society's Ninth Conference on Global Change Studies, Phoenix, AZ
13 January 1998	Dr. Yoshio Kurihara "A Prospect of Improvement in the Forecast of Hurricane Landfall", American Meteorological Society's Ninth Conference on Global Change Studies, Phoenix, AZ

13 January 1998	Mr. Robert E. Tuleya "Improvements to the GFDL Hurricane Forecast System", American Meteorological Society's Ninth Conference on Global Change Studies, Phoenix, AZ
13 January 1998	Mr. Anthony J. Broccoli "The Cold Ocean-Warm Land Pattern: Model Simulation and Relevance to Climate Change Detection", American Meteorological Society's Ninth Conference on Global Change Studies, Phoenix, AZ
13 January 1998	Mr. Thomas R. Knutson "Model Assessment of Decadal Variability and Trends in the Tropical Pacific Ocean", American Meteorological Society's Ninth Conference on Global Change Studies, Phoenix, AZ
14 January 1998	Mr. William Stern "Behavior of Tropical Intraseasonal Oscillations in a Atmosphere-Ocean Coupled GCM", American Meteorological Society's Ninth Conference on Interaction of Sea and Atmosphere, Phoenix, AZ
14 January 1998	Dr. Charles T. Gordon "Tropical Sensitivity to Low Clouds in a Coupled Model", American Meteorological Society's Ninth Conference on Interaction of Sea and Atmosphere, Phoenix, AZ
14 January 1998	Mr. Matthew Harrison "An Analysis of Ocean Surface Boundary Conditions from Models and Observations: Implications for Coupled Modeling", American Meteorological Society's Ninth Conference on Interaction of Sea and Atmosphere, Phoenix, AZ
15 January 1998	Dr. Jeffrey L. Anderson "Predictability and Potential Predictability in an Ensemble of Fully Coupled GCM Integrations", American Meteorological Society's Ninth Conference on Interaction of Sea and Atmosphere, Phoenix, AZ
15 January 1998	Dr. Jeffrey L. Anderson "A Fully Nonlinear Filter and Monte Carlo Techniques for Atmospheric Data Assimilation", American Meteorological Society's 14th Conference on Probability and Statistics in the Atmospheric Sciences, Phoenix, AZ
20 January 1998	Dr. Jerry D. Mahlman "Greenhouse Warming: Implications for Future Energy Sources", Princeton Plasma Physics Laboratory, Princeton University, Princeton, NJ
26 January 1998	Mr. Morris A. Bender "Improvements to the GFDL Hurricane Forecast System", 52nd Interdepartmental Hurricane Conference, Clearwater Beach, FL

28 January 1998	Dr. Jerry D. Mahlman "Human-Caused Climate Change: Implications for Practically Everything", United States Catholic Conference, Domestic and International Policy Committees, Washington, DC
4 February 1998	Dr. Leo J. Donner "Large-Scale Ice Clouds and the Atmospheric General Circulation", State University of New York, Stony Brook, NY
4 February 1998	Dr. Stephen Griffies "North Atlantic Predictability - Some Fundamental Issues", Weizmann Institute, Rehovat, Israel
10 February 1998	Dr. Robert W. Hallberg "The Ocean's Density Structure and Thermohaline Circulation with Weak Diapycnal Diffusion", American Geophysical Union Ocean Sciences Meeting, San Diego, CA
11 February 1998	Mr. William Hurlin "Response of the Labrador Basin to Freshening Events", American Geophysical Union Ocean Sciences Meeting, San Diego, CA
11 February 1998	Dr. Jerry D. Mahlman "The Coupled Climate System: Modeling and Observations", NOAA Environmental Assessment and Prediction Constituent's Workshop, Washington, DC
12 February 1998	Dr. Jerry D. Mahlman "Global Warming: Emerging Scientific Challenges and Policy Issues", University of Maryland, College Park, MD
18 February 1998	Dr. V. Ramaswamy "The NOAA Modeling Program: Effect of Aerosol Spatial and Temporal Variability on Radiative Forcing and Climate Response", NOAA Climate and Global Change Review Panel Meeting, Philadelphia, PA
20 February 1998	Dr. Jerry Mahlman "The Science of Global Warming", Center for Economic Policy Studies, Economic Forum, Princeton University, Princeton, NJ
27 February 1998	Dr. Stephen A. Klein "Comparison of ECMWF Frontal Clouds to ISCCP Satellite Observations", NASA/Goddard Institute for Space Studies, New York, NY
3 March 1998	Dr. Kevin P. Hamilton 1. "Recent Results with a Very High-Resolution Version of the GFDL SKYHI Model", 2. "Modeling Stratospheric Influence on the Troposphere", SPARC General Circulation Model Intercomparison Workshop, Greenbelt, MD
4 March 1998	Mr. Robert J. Wilson "Stratosphere GCM Intercomparison of Tropical Oscillations and Waves", GRIPS Stratosphere Model Intercomparison, Greenbelt, MD

5 March 1998	Dr. Yoshio Kurihara "Hurricanes in Weather Forecasts and in the Simulated Warm Climate", University of Maryland, College Park, MD
9 March 1998	Dr. V. Ramaswamy "Modeling the Effect of Stratospheric Ozone on Climate", Euro CLIVAR Workshop - Attribution Beyond Discernible, Hadley Center, Bracknell, United Kingdom
10 March 1998	Dr. Kevin P. Hamilton "Quasi-biennial Oscillation Effects in General Circulation Models", SPARC Workshop on the Quasi-biennial Oscillation and Its Climate Effects, La Jolla, CA
1 April 1998	Dr. V. Ramaswamy "Radiative Forcing by Trace Species", IPCC Workshop on Rapid Nonlinear Climate Change, Noorwijkerhaub, The Netherlands
1 April 1998	Dr. John R. Toggweiler "Energizing the Ocean's Large-Scale Circulation", School of Oceanography, University of Washington, Seattle, WA
3 April 1998	Dr. Isaac M. Held "The Strength of the Hadley Cell", NOAA Atlantic Working Group Meeting, University of Washington, Seattle, WA
8 April 1998	Dr. Jeffrey Anderson "Monte Carlo Implementation of a Nonlinear Filter for Atmospheric Prediction", Metron Inc., Reston, VA
8 April 1998	Dr. Isaac M. Held "Dynamics of Global Warming", Physics Department, Rutgers University, New Brunswick, NJ
14 April 1998	Dr. Jerry D. Mahlman "The Science of Climate Change", Sierra Club of S.E. Pennsylvania and The Environmental Working Group of the Religious Society of Friends, Arch Street Meeting House, Philadelphia, PA
21 April 1998	Dr. Leo J. Donner "Sensitivity of Cloud Radiation and Microphysics to Ice Sedimentation", CERES Science Team Meeting, Hampton, VA
22 April 1998	Mr. Keith Dixon "Initialization and Climate Drift Issues Found in Coupled Climate Model Integrations", 23rd General Assembly of the European Geophysical Society, Nice, France
23 April 1998	Dr. Leo J. Donner "Anvil-Ice Sedimentation: Implication for Cloud-Radiative Interactions", NASA/ Langley, Hampton, VA

23 April 1998	Mr. Richard Wetherald "Global Warming: Past, Present, and Future", Princeton Plasma Physics Laboratory, Princeton University, Princeton, NJ
27 April 1998	Dr. Yoshikazu Hayashi "Generation Mechanisms for Tropical Intraseasonal Oscillations Simulated by a Realistic GCM", Nitta Symposium, University of Tokyo, Tokyo, Japan
29 April 1998	Dr. Thomas L. Delworth "Simulated Interannual to Multidecadal Variability in the North Atlantic", Climate System Research Program, Texas A & M University, College Station, TX
29 April 1998	Dr. Robert Hallberg "The Ocean's Overturning Circulation in the Limit of Weak Diapycnal Diffusion", Applied Physics Department, Columbia University, New York, NY
30 April 1998	Dr. Jerry Dr. Mahlman "Global Climate Change: What are the Facts? What are the Realities", Bucknell University, Lewisburg, PA
1 May 1998	Dr. Ngar-Cheung Lau "Interactions Between Global Sea Surface Temperature Anomalies and the Atmospheric Circulation", Earth Science Colloquium, Lamont-Doherty Earth Observatory, Palisades, NY
12 May 1998	Dr. Thomas L. Delworth "Simulated Multidecadal Variability in the North Atlantic Excited by Ocean Atmosphere Flluxes", Workshop on the Role of the Atlantic Ocean in Climate Variability, Florence, Italy
13 May 1998	Dr. Yoshio Kurihara "Will Typhoons Become Stronger", Institute for Global Change, Tokyo, Japan
13 May 1998	Dr. Leo J. Donner "Cumulus Parameterization, Microphysics, and Radiation in General Circulation Models", Hadley Centre, Bracknell, United Kingdom
15 May 1998	Dr. Yoshio Kurihara "How Accurately Can We Predict Typhoons?", Kyushu University, Fukuoka, Japan
16 May 1998	Dr. V. Ramaswamy "Stratospheric Temperature Trends", Baseline Surface Radiation Network Workshop, sponsored by the World Climate Research Programme, Budapest, Hungary
18 May 1998	Dr. Leo J. Donner "Large-Scale Ice Clouds and the Atmospheric General Circulation", Reading University, Reading, United Kingdom

22 May 1998	Dr. Leo J. Donner "Three-Dimensional, High-Resolution Modeling of Tropical Convective Systems", Hadley Centre, Bracknell, United Kingdom
26 May 1998	Dr. Kevin P. Hamilton "Simulation of the Ozone Quasi-biennial Oscillation in a Comprehensive GCM", American Geophysical Union Spring Meeting, Boston, MA
26 May 1998	Dr. John R. Toggweiler "A New Mechanism for Cooling the Tropics and Warming the Poles", 1998 American Geophysical Union Spring Meeting, Boston, MA
26 May 1998	Dr. Brian Soden 1. "A Lagrangian Study of Upper Tropospheric Water Vapor", 2. "Impact of GOES Wind Observations on GFDL Hurricane Model Forecasts", American Meteorological Society's Satellite Meteorology Conference, Paris, France
26 May 1998	Mr. Anthony J. Broccoli "Extratropical Influences on Tropical Paleoclimates", 1998 American Geophysical Union Spring Meeting, Boston, MA
29 May 1998	Dr. Jerry D. Mahlman "The Global Warming Controversy: Scientific Aspects", Association of Princeton Graduate Alumni, Princeton University, Princeton, NJ
31 May 1998	Dr. Ngar-Cheung Lau "Interactions Between Global SST Anomalies and the Midlatitude Atmospheric Circulation", 32nd Congress of the Canadian Meteorological and Oceanographic Society, Dartmouth, New Brunswick, Canada
1 June 1998	Dr. V. Ramaswamy "Stratospheric Temperature Trends", 1998 World Meteorological Organization, Ozone Assessment Peer Review Meeting, Les Diablerets, Switzerland
1 June 1998	Dr. John R. Toggweiler "What GCMs Tell Us About Bottom-Water Formation and the Circulation of Antarctic Bottom Water", Lamont-Doherty Earth Observatory, Palisades, NY
2 June 1998	Mr. Anthony J. Broccoli "Detection and Monitoring of Climate Changes and Trends", Commercial Refrigerator Manufacturers Association Meeting, Washington, DC
2 June 1998	Dr. Brian Soden "Results of the GVaP UTH Transmittance Model Comparison", GVaP UTH Intercomparison Workshop, Darmstadt, Germany
8 June 1998	Dr. Isaac M. Held "The Macro Turbulence of the Troposphere", Rossby-100 Symposium, Stockholm, Sweden

8 June 1998	Dr. Leo J. Donner "Chemistry and Radiation in Convective Cloud Systems: Transport, Transformation and Climate Implications", Rossby-100 Symposium, Stockholm, Sweden
9 June 1998	Dr. Isidoro Orlanski "Storm Tracks Shaping the Quasi-Stationary Circulation", Colloquium - The Role of Large Topography in Weather and Climate, International Center for Theoretical Physics, Trieste, Italy
11 June 1998	Dr. Bruce B. Ross "NOAA/GFDL FY2000 Budget Initiative", NOAA IT Review Board for GFDL FY2000 Budget Initiative, Silver Spring, MD
12 June 1998	Dr. Kevin P. Hamilton "Meteorological Modeling of the Middle Atmosphere", CEDAR/GEM Workshop on Models for the New Millennium, Boulder, CO
15 June 1998	Mr. Richard Hemler "Key Elements of the User-Friendly SKYHI Model", Second International Workshop on Software Engineering and Code Design in Parallel Meteorological and Oceanographic Applications, Scottsdale, AZ
15 June 1998	Dr. V. Ramaswamy "High-Spectral Resolution Modeling of the Shortwave Flux Disposition in the Atmosphere-Surface System", Gordon Conference on Solar Radiation and Climate, Plymouth State College, Plymouth, NH
15 June 1998	Dr. Brian Soden "Variations in Atmosphere-Ocean Solar Absorption under Clear Skies", Gordon Conference on Solar Radiation and Climate, Plymouth State College, Plymouth, NH
15 June 1998	Mr. Anthony J. Broccoli "Extratropical Influences on Tropical Paleoclimates", American Geophysical Union Chapman Conference: Mechanisms of Millenial-Scale Global Climate Change, Snowbird, UT
15 June 1998	Dr. Kevin P. Hamilton "The SPARC Field Experiment - Current Status and Plans", Second Planning Meeting for the SPARC Tropical Field Experiment, Boulder, CO
15 June 1998	Dr. Jerry D. Mahlman "Model-Based Climate-change Scenarios for Impact Researchers", National Research Council Board on Atmospheric Sciences and Climate, Washington, DC
19 June 1998	Dr. Jerry D. Mahlman "Attacking Frontier Challenges in Weather and Climate Modeling", U.S. Department of Commerce, Washington, DC

23 June 1998	Dr. Stephen T. Garner "Comparison Between High-Resolution Linear and Nonlinear Wave Drag Over Realistic Topography", International Center for Theoretical Physics, Trieste, Italy
23 June 1998	Dr. Brian D. Gross "Frontal Interactions with Orography in Hydrostatic and Non-Hydrostatic Models", International Center for Theoretical Physics, Trieste, Italy
1 July 1998	Dr. Isaac M. Held "Model Development at GFDL", USGCRP/JASON Workshop on Climate Prediction, La Jolla, CA
7 July 1998	Dr. Matthew Harrison "Warm Pool Physics in Model Simulation Comparisons to Observations", COARE 98 Conference, Boulder, CO
7 July 1998	Mr. Anthony J. Rosati 1. "Warm Pool Dynamics", 2. "Simulation of the Western Pacific Warm Pool using a CGCM", COARE 98 Conference, Boulder, CO
7 July 1998	Dr. Leo J. Donner "The Role of Ice Sedimentation in the Microphysical and Radiative Budgets of COARE Convective Systems", UCAR Board of Trustees Meeting, Boulder, CO
9 July 1998	Dr. Jerry D. Mahlman "Attacking Frontier Challenges in Climate and Weather Modeling", Commerce IT Review Board Meeting, Washington, DC
9 July 1998	Dr. Bruce B. Ross "Attacking Frontier Challenges in Climate and Weather Modeling - NOAA/ GFDL FY2000, HPCC Budget Initiative", Commerce IT Review Board Meeting, Washington, DC
14 July 1998	Mr. Robert E. Tuleya "Modeling Hurricane Motion", NCAR's Summer Colloquium Program on Hurricanes at Landfall, Boulder, CO
21 July 1998	Mr. Robert E. Tuleya "Increased Hurricane Intensities with CO_2 Induced Warming as Simulated using the GFDL Hurricane Prediction System", Climate Change and Extreme Events, Miami, FL
10 August 1998	Mr. Thomas Knutson "Simulated Increase of Hurricane Intensities in a CO_2-Warmed Climate", Climate Extremes: Changes, Impacts, and Projections, Aspen Global Change Institute, Aspen, CO
18 August 1998	Dr. Stephen Klein "Comparison of ECMWF Frontal Clouds to Satellite Observations", American Meteorological Society's Conference on Cloud Physics, Everett, WA

20 August 1998	Dr. Jerry D. Mahlman "The Science of Human-Caused Climate Change", Environmental Council of the States ECOS Climate Change Workshop, Madison, WI
24 August 1998	Dr. John R. Toggweiler "Energizing the Ocean's Large-Scale Circulation for Climate Change", Sixth International Conference on Paleoceanography, Lisbon, Portugal
24 August 1998	Dr. Jeffrey Anderson "A Monte Carlo Implementation of a Non-Linear Filter for Ensemble Data Assimilation and Prediction", NCAR, Boulder, CO
25 August 1998	Dr. Brian Soden "Monitoring Tropospheric/Stratospheric Moisture Transport from Geostationary Satellites", SPARC Workshop on Stratospheric and Upper Tropospheric Water Vapor, Boulder, CO
25 August 1998	Dr. Isidoro Orlanski "Recent Progress in the Analysis and Forecasting of the ENSO Cycle", Workshop on the Effect of the ENSO Cycle over South America - MERCOSUR, Buenos Aires, Argentina
1 September 1998	Dr. V. Ramaswamy 1. "Aerosol Radiation Research", 2. "Cloud-Radiation Interactions in GCMs", WCRP-GEWEX Radiation Panel Meeting, St. Andrews, Scotland, United Kingdom
15 September 1998	Dr. Leo J. Donner "Surface and TOA Radiative Fluxes in TOGA-COARE: Cloud-System Model Studies", CERES Science Team Meeting, Stony Brook, NY
15 September 1998	Dr. Jerry D. Mahlman "Human-Caused Global Warming: Implications for Practically Everything", Environmental Protection Agency, Washington, DC
22 September 1998	Dr. Thomas L. Delworth "Multidecadal Variability of the Thermohaline Circulation in the North Atlantic Excited by Stochastic Surface Flux Forcing", NASA Workshop on Decadal Climate Variability, Williamsburg, VA
30 September 1998	Dr. Ngar-Cheung Lau "The Atmospheric Bridge Linking Tropical Pacific ENSO Events to World-Wide SST Anomalies", Institute for Terrestrial and Planetary Atmospheres, State University of New York, Stony Brook, NY

APPENDIX E

ACRONYMS

ACRONYMS

AASE	Arctic Airborne Stratospheric Experiment
ABLE	Atmospheric Boundary Layer Experiment
AEROCE	Air Ocean Chemistry Experiment
AGCM	Atmospheric General Circulation Model
AMEX	Australian Monsoon Experiment
AMIP	Atmospheric Model Intercomparison Project
AOML	Atlantic Oceanographic and Meteorological Laboratory/NOAA
AOU	Apparent Oxygen Utilization
ARL	Atmospheric Research Laboratory/NOAA
A96/P97	GFDL Activities FY96, Plans FY97
BC	Barnett and Corney
CCN	Cloud Condensation Nuclei
CEM	Cumulus Ensemble Model
CFC	Chlorofluorocarbon
CHAMMP	Computer Hardware, Advanced Mathematics and Model Physics project
CIRA	COSPAR International Reference Atmosphere
CLIPER	A simple model combining CLImatology and PERsistence used in hurricane prediction.
CMC	Carbon Modeling Consortium
CMDL	Climate Monitoring and Diagnostics Laboratory/NOAA
COADS	Comprehensive Ocean-Atmosphere Data Set
COARE	Coupled Ocean-Atmosphere Response Experiment
COSPAR	Congress for Space Research
CRAY	Cray Research, Inc.
CSIRO	Commonwealth Scientific & Industrial Research Organization
DAMEE	Data Assimilation and Model Evaluation Experiments
DJF	December, January, February (winter)
DU	Dobson units
E	A physical parametrization package in use at GFDL. E physics includes a high-order closure scheme for subgrid turbulence.
ECMWF	European Centre for Medium-Range Weather Forecasts

E"n"	Horizontal model resolution corresponding to "n" points between a pole and the equator on the E-grid.
ENSO	El Niño - Southern Oscillation
EOF	Empirical Orthogonal Function
EPOCS	Equatorial Pacific Ocean Climate Studies
ERBE	Earth Radiation Budget Experiment
FDDI	Fiber Distributed Data Interface
FDH	Fixed Dynamic Heating model
FIRE	First ISCCP Regional Experiment
FY"yy"	Fiscal Year "yy" where "yy" are the last two digits of the year.
GARP	Global Atmospheric Research Program
GATE	GARP Atlantic Tropical Experiment
GCM	General Circulation Model
GCTM	Global Chemical Transport Model
GEOSAT	Geodetic Satellite
GFD	Geophysical Fluid Dynamics
GFDL	Geophysical Fluid Dynamics Laboratory/NOAA
GMT	Greenwich Mean Time
GOES	Geostationary Operational Environmental Satellite
GTE	Global Tropospheric Experiment
HIBU	Federal Hydrological Institute and Belgrade University
HPCC	High Performance Computing and Communications
HRD	Hurricane Research Division/AOML
ICRCCM	InterComparison of Radiation Codes in Climate Models
IGBP/PAGES	International Geosphere-Biosphere Project/Past Global Changes
I/O	Input/Output
ICTP	Intenational Center for Theoretical Physics, Trieste, Italy
IPCC	Intergovernmental Panel on Climate Change
ISCCP	International Satellite Cloud Climatology Project
IT	Information Technology
ITCZ	Intertropical Convergence Zone
JGOFS	Joint Global Ocean Flux Study
JJA	June, July, August (summer)

JPL	Jet Propulsion Laboratory
KPP	K-Profile Parameterization
LAHM	Limited Area HIBU Model
LAN	Limited Area Nonhydrostatic
LBL	Line By Line
LIMS	Limb Infrared Monitor of the Stratosphere
L"n"	Vertical model resolution of "n" levels.
LWP	Liquid Water Path
MLS	Microwave Limb Sounder
MMM	Multiply-nested Movable Mesh
MOM	Modular Ocean Model
MOM2	Modular Ocean Model, Version 2
MOODS	Master Oceanographic Observations Data Set
MPP	Massively Parallel Processor
NABE	North Atlantic Bloom Experiment
NADW	North Atlantic Deep Water
NARE	North Atlantic Regional Experiment
NASA	National Aeronautics and Space Administration
NCAR	National Center for Atmospheric Research
NCDC	National Climate Data Center/NOAA
NH	Northern Hemisphere
NMC	National Meteorological Center/NOAA
NOAA	National Oceanic and Atmospheric Administration
NODC	National Oceanographic Data Center/NOAA
ODA	Ocean Data Assimilation
OLR	Outgoing Longwave Radiation
OTL	Ocean Tracers Laboratory/Princeton University
PCMDI	Program for Climate Model Diagnosis and Intercomparison
PFC	Perfluorocarbon
PILPS	Project for Intercomparison of Land-Surface Parameterization Schemes
PMEL	Pacific Marine Environmental Laboratory
PMIP	Paleoclimate Model Intercomparison Project

PNA	Pacific-North American
POM	Princeton Ocean Model
PSCs	Polar Stratospheric Clouds
QBO	Quasi-Biennial Oscillation
QG	Quasi-Geostrophic
RAS	Relaxed Arakawa-Schubert
RFP	Request for Proposal
R"n"	Horizontal resolution of spectral model with rhomboidal truncation at wavenumber "n".
SAGE	Stratospheric Aerosol and Gases Experiment
SAMS	Stratospheric Aerosol Measurement System
SAVE	South Atlantic Ventilation Experiment
SBUV	Solar Backscatter Ultraviolet (satellite)
SGI	Silicon Graphics, Inc.
SH	Southern Hemisphere
SiB	Simple Biosphere
SKYHI	The GFDL Troposphere-Stratosphere-Mesosphere GCM
SME	Solar Mesosphere Explorer
SOI	Southern Oscillation Index
SPCZ	South Pacific Convergence Zone
SPECTRE	Spectral Radiation Experiment
SST	Sea Surface Temperature
SUN	Sun Microsystems, Inc.
THC	Thermohaline Circulation
TIO	Tropical Intraseasonal Oscillations
T"n"	Horizontal resolution of spectral model with triangular truncation at wavenumber "n".
TOGA	Tropical Ocean and Global Atmosphere project
TOGA/TAO	Tropical Ocean Global Atmosphere/Tropical Atmosphere Ocean
TOMS	Total Ozone Mapping Spectrometer
TOPEX	Topographic Experiment
TOVS	Tiros Operational Vertical Sounder
TTO	Transient Tracers in the Oceans

UARS	Upper Atmosphere Research Satellite
WGNE	Working Group on Numerical Experimentation
WMO	World Meteorological Organization
WOCE/HP	World Ocean Circulation Experiment/Hydrographic Program
XBT	Expendable Bathythermograph
ZODIAC	Gridpoint Climate Model